Myofibroblasts and the Pathogenesis of Dupuytren's Disease

Liaquat Suleman Verjee

A thesis submitted for the degree of Doctor of Philosophy

2010

The Division of Muscuoloskeletal Surgery and The Kennedy Institute of Rheumatology Division

Imperial College London
Faculty of Medicine

ABSTRACT

Dupuytren's disease is defined in Green's Operative Hand Surgery as a condition of the hand characterised by the development of new tissue in the form of nodules and cords. Hand function can be significantly impaired and whilst the mainstay of treatment is surgery, recurrence has been reported in approximately 40-50% of patients. Myofibroblasts are central to the pathogenesis of Dupuytren's disease although what regulates the myofibroblast phenotype during Dupuytren's disease remains unclear.

This thesis set out to test the hypothesis that the myofibroblast phenotype in Dupuytren's disease is regulated by dermal fibroblasts and inflammatory mediators, specifically advanced glycation end products (AGEs) and TNF-α.

I aimed to (1) systematically characterise the distribution of myofibroblasts (α-smooth muscle actin positive cells (α-SMA)) throughout excised Dupuytren's tissue in relation to clinical disease activity (fixed flexion deformity and recurrence); (2) establish an *in vitro* contraction model to examine Dupuytren's myofibroblasts and (3) use this model to examine how myofibroblast phenotype may be regulated by dermal fibroblasts and inflammatory mediators.

I examined 103 Dupuytren's cords and correlated the histological findings with the patient's clinical flexion contracture and disease severity. Histological nodules, defined as a focal condensation of α−SMA positive cells, were seen in two-thirds of excised digital cord samples. These nodules were found in the vicinity of the proximal interphalangeal joints of the fingers. Nodules were more frequently observed in digits with less severe contractures and more active disease, whereas non-nodular cords were significantly associated with advanced digital contracture, reflecting end stage disease. Based on our current understanding of how myofibroblasts thrive on tension and contract against resistance, a mechanism for digital contraction has been proposed: nodules containing highly contractile myofibroblasts are present in active Dupuytren's disease where digital flexion and extension of the interphalangeal joints is still possible and these nodules involute in end-stage disease,

where severe contractures limit digital movement.

In order to further study Dupuytren's myofibroblasts, I also compared cell contraction in stress-released collagen gels with that in restrained gels using a culture force monitor (CFM). With the latter I was able to reliably measure cell-generated forces within restrained collagen gels. By using genetically matched sets of cells from patients, I also correlated cell contractility with α-SMA expression. Unlike control skin cells that initially contract and then plateau, Dupuytren's myofibroblasts show continually increasing contractile force. Furthermore, increased contractility of Dupuytren's myofibroblasts was reflected by higher α-SMA protein content and alignment of the α-SMA to stress fibres. Interestingly mRNA levels of α-SMA were similar in all matched cells, reflecting post-translational regulation of protein levels in myofibroblasts.

Based on the observation that recurrence is significantly reduced following dermofasciectomy, I also tested whether dermal fibroblasts down-regulate the contractile Dupuytren's myofibroblast. I co-cultured Dupuytren's myofibroblasts and dermal fibroblasts and found that contractility of Dupuytren's cells is not influenced by dermal cells. Therefore, reduced recurrence rate following dermofasciectomy may be due to other factors, such as more complete excision of affected tissue combined with reduced tension following application of full thickness skin grafts. Finally, recent studies have suggested that inflammatory mediators and AGE-RAGE interaction play a role in the development of the myofibroblast phenotype. I therefore used the CFM to examine the effect of AGEs and TNF-α on myofibroblast contractility. No difference in contractility of dermal fibroblasts was observed with AGEs, although a two-fold increase was seen with TNF-α.

Overall, I have characterised the distribution of myofibroblasts in Dupuytren's tissue and these data have led to interesting insights into disease pathogenesis. I have also established a reliable *in vitro* model for assessing Dupuytren's myofibroblast phenotype and used this to demonstrate that whilst dermal fibroblasts do not downregulate myofibroblast activity, pro-inflammatory mediators may play a key role in modulating myofibroblast phenotype in this disease.

ACKNOWLEDGEMENTS

I am extremely grateful to Professor Jagdeep Nanchahal for the privilege and the opportunity to study under his clinical and academic supervison. He is a great mentor and has provided me with continuous support and guidance throughout my PhD.

Equally, I have been very fortunate to have Dr. Kim Midwood supervise this project and invest time and effort in trying to make a surgeon understand science. I am very grateful for her patience, educational guidance and encouragement.

Professor Mark Eastwood has been a key collaborator and his expertise and support have been invaluable. Much of this study would also not have been possible without the constant supply of patient samples from Scotland, for which I am extremely grateful to both the patients and to Ms. Dominique Davidson.

I would like to thank Professor Hideaki Nagase for giving me the opportunity to study in his lab and both Dr. Ann Sandison and David Essex for providing technical support and advice with histological techniques. I would also like to express my appreciation to the many colleagues with whom I have worked over the past four years. In particular I would like to thank them for the fond memories I have of my time in the lab. I would also like to thank Graeme, Matt and James for contributing to these memories and to Abhi and Loz for paving the way.

I am very grateful to the The Healing Foundation in association with the British Society for Surgery of the Hand, the Hammersmith Hospitals Trustees' Research Committee and the Kennedy Institute of Rheumatology Trustees, Imperial College London. This work was funded by their generous grant awards.

Finally, I am very fortunate to have been blessed with such a loving and supportive family. Without them so much of what I have achieved would not have been possible – thank you.

DECLARATION

This thesis represents my original work. Collaborators that I would like to acknowledge include David Essex from the Deparment of Histopathology at Charing Cross Hospital (prepared the immunohistochemistry sections), Dr. Ann Sandison (consultant histopathologist provided advice on analysis of immunohistochemistry), Professor Mark Eastwood, Universtiy of Westminster (provided the culture force monitor) and Ms Dominique Davidson, St. John's Hospital, Scotland (provided Dupuytren's tissue specimens and relevant clinical data). Professor Jagdeep Nanchahal also provided tissue specimens and both he and Dr Kim Midwood provided me with guidance through the course of my study towards completing this thesis.

Liaquat Suleman Verjee

September 2010

LIST OF ABBREVIATIONS

2D	Two dimensional
3D	Three dimensional
α-SMA	alpha smooth muscle actin
Ab	Antibody
ADAMTS	A disintegrin and metalloproteinase with thrombospondin motifs
AGE	Advanced glycation end products
AP	Alkaline phosphatase
bFGF	basic fibroblast growth factor
BSA	Bovine serum albumin
$CaCl_2$	Calcium chloride
CD3	T cell receptor
CD4	T cell receptor
CD45	Leucocyte common antigen
CD68	C68 positive macrophage
cDNA	complementary DNA
CFM	Culture force monitor
CO_2	Carbon dioxide
CTGF	Connective tissue growth factor
d	days
dATP	2´-deoxyadenosine 5´-triphosphate
dCTP	2´-deoxycytidine 5´-triphosphate
dGTP	2´-deoxyguanosine 5´-triphosphate
dTTP	2´-deoxythymidine 5´-triphosphate
DAPI	4'-6-Diamidino-2-phenylindole
DIPJ	Distal interphalangeal joint
DMEM	Dulbecco's modified eagles medium
DMSO	Dimethyl sulfoxide
DNA	Deoxyribonucleic acid
ECL	Enhanced chemiluminescence
ECM	Extracellullar matrix
EDTA	Ethylenediaminetetraacetic acid

EGF	Epidermal growth factor
FA	Focal adhesion
FACS	Fluorescence activated cell sorting
FAK	Focal adhesion kinase
FBS	Fetal bovine serum
FCS	Fetal calf serum
FN	Fibronectin
FN EDA	Fibronectin ED-A
FN EDB	Fibronectin ED-B
FPCL	Fibroblast populated collagen lattice
GAPDH	Glyceraldehyde-3-phosphate dehydrogenase
GFP	Green fluorescent protein
h	hours
H&E	Haematoxylin and Eosin
HIV	Human immunodeficiency virus
HMGB1	High mobility group protein B1
HRP	Horse Radish Peroxidase
HUVEC	Human umbilical vein endothelial cells
IF	Immunofluorescence
IFN-γ	Interferon-gamma
IgG	Immunoglobulin
IHC	Immunohistochemistry
IL-1, -6,	Interleukin-1, -6
kDa	Kilodaltons
KO	Knockout
MAb	Monoclonal antibody
MCPJ	metacarpophalangeal joint
MFI	Mean fluorescence intensity
$MgCl_2$	Magnesium chloride
min	minutes
MLC	Myosin light-chain
MLCK	Myosin light-chain kinase
MMP	Matrix metalloproteinase

mRNA	messenger ribonucleic acid
MT1-MMP	Membrane type 1-matrix metalloproteinase
MTT	3-(4,5-dimethylthiazol-2-yl)-2,5-diphenyltetrazolium bromide
MW	Molecular weight
NaCl	Sodium chloride
NaOH	Sodium hydroxide
nm	nanometer
O.D.	Optical density
PAb	Polyclonal antibody
PBS	Phosphate buffered saline
PCR	Polymerase chain reaction
PDGF	Platelet derived growth factor
PGE_2	Prostaglandin E_2
PIPJ	Proximal interphalangeal joint
PVDF	Polyvinylidene difluoride
RAGE	Receptor for advanced glycation end products
RMT	Residual matrix tension
RNA	Ribonucleic acid
ROCK	Rho kinase
RPLPO	Ribosomal protein control
RT-PCR	Reverse transcriptase-polymerase chain reaction
SA	Surface area
SDS	Sodium dodecyl sulphate
SDS-PAGE	Sodium dodecyl sulphate-polyacrylamide gel electrophoresis
SEM	Standard error of the mean
SMCs	Smooth muscle cells
TGF-β	Transforming growth factor-beta
TIMPs	Tissue inhibitors of metalloproteinases
TNF-α	Tumor necrosis factor-alpha

TABLE OF CONTENTS

Abstract ii
Acknowledgements iv
Declaration v
Abbreviations vi

CHAPTER ONE 1

Introduction

1.1 Dupuytren's disease 2

1.2 Epidemiology 3

1.3 Aetiology 4
1.3.1 Genetics 4

1.4 Palmar fascia anatomy 6

1.5 Clinical presentation 9
1.5.1 Dermatopathology 9
1.5.2 Nodules 11
1.5.3 Cord 13
1.5.4 Disease progression and diathesis 15
1.5.5 Ectopic Dupuytren's disease 15

1.6 Histology of Dupuytren's tissue 16
1.61 Other histological observations 23

1.7 Treatment 24
1.7.1 Surgical treatment 24
1.7.2 Minimally invasive procedures, surgical adjuncts and non-operative treatment 28

1.8 Recurrence following surgery 31

1.9 Myofibroblasts 33

1.10 Cytoskeletal and cell surface markers 34

1.11 Origin of myofibroblasts 37

1.12 Contractility 39

1.13 Extracellular matrix components 44

1.14 AGEs and RAGE 48

1.15 Growth factors and cytokines 50

1.16 Matrix cell adhesions and stress perception 54

1.17 The mechanical environment of myofibroblasts 56

1.18 Apoptosis 58

1.19 Summary of key steps in myofibroblast differentiation **60**

1.20 Hypothesis **61**

1.21 Aims and objectives of study **62**

CHAPTER TWO **63**

Material and Methods

2.1 Reagents **64**

2.1.1 General reagents 64
2.1.2 Tissue culture reagents 64
2.1.3 SDS-PAGE reagents 65
2.1.4 Western blotting reagents 65
2.1.5 General indirect immunofluorescence staining reagents 65
2.1.6 FACS analysis reagents 66
2.1.7 RT-PCR reagents 66

2.2 Antibodies **67**

2.3 Surgical model and sample collection **68**

2.4 Cell isolation and tissue culture **69**

2.4.1 Preparation of surgical samples 69
2.4.2 Cell isolation from matched tissue samples 69
2.4.3 Cell culture 70
2.4.4 Dupuytren's nodule-derived cell line (sourced from Japan) 71
2.4.5 Cell counting 71
2.4.6 Cell viability 71
2.4.7 Freezing and thawing cells 72

2.5 Immunohistochemistry **73**

2.6 Isotonic force contraction **74**

2.7 Isometric force contraction –culture force monitor **76**

2.8 Immunofluorescence **78**

2.8.1 Immunofluorescent staining of cells in monolayer 78
2.8.2 Immunofluorescent staining of FPCLs 79

2.9 Western blotting **79**

2.9.1 Sample preparation 79
2.9.2 Tricine SDS-PAGE 80
2.9.3 Transfer of proteins to PVDF membrane 80

2.10 Reverse transcription polymerase chain reaction **82**

2.10.1 mRNA isolation 82
2.10.2 RT-PCR 83
2.10.3 Real time PCR 85

2.11 Fluorescence activated cell sorting (FACS) **85**

2.12 Cell tracing studies **86**

2.13 MTT assay **87**

2.14 Statistical analyses **87**

CHAPTER THREE **89**

Characterisation of myofibroblast distribution in cords

3.1 Introduction **90**

3.2 Results **91**

3.2.1 Patients and samples 91
3.2.2 Immunohistochemistry 96
3.2.3 Histological nodularity 98
3.2.4 Relationship between α-SMA rich nodules and the PIPJ 101
3.2.5 Analysis of α-SMA distribution throughout Dupuytren's tissue 103
3.2.6 Histological nodularity correlated with digital contracture 108
3.2.7 Histological nodularity correlated with primary or recurrent disease 111

3.3 Discussion **114**

CHAPTER FOUR **120**

Establishing an *in vitro* model to study Dupuytren's disease

4.1 Introduction **121**

4.2 Results **123**

4.2.1 Human myofibroblast cell lines 123
4.2.2 Cells from Dupuytren's patient samples 126
4.2.3 Cells derived from whole Dupuytren's cord 126
4.2.4 Nodule-derived *versus* non-nodular fibroblasts 127
4.2.5 Cell passage 131
4.2.6 FPCL contraction 132
4.2.6.1 Isotonic contractionof FPCLs 132
4.2.6.2 Isometric contraction of FPCLs 134
4.2.7 Post-transcriptional regulation of α-SMA drives myofibroblast Contractility 140
4.2.8 Dermal fibroblasts co-cultured with nodule-derived cells show no difference in isometric force contraction 142

4.3 Discussion **148**

CHAPTER FIVE **157**

Inflammatory mediators and Dupuytren's disease

5.1 Introduction **158**

5.2 Results **161**

5.2.1 Inflammatory cells in Dupuytren's tissue are distributed predominantly within nodules 161

5.2.1.1 Nodules 163

5.2.1.2 Cord tissue distal from the nodule 165

5.2.1.3 Non-nodular cord 167

5.2.1.4 Quantofication of inflammatory cells in Dupuytren's tissue 169

5.2.2 RAGE expression is observed predominantly in α-SMA rich Dupuytren's nodules 170

5.2.2.1 Nodules 172

5.2.2.2 Peri-nodular cord tissue 173

5.2.2.3 Cord tissue distal from the nodule 174

5.2.2.4 Non-nodular cord tissue 175

5.2.3 Cell surface RAGE expression in nodule-derived cells, non-nodular cells, palmar skin fibroblasts and non-palmar skin fibroblasts 176

5.2.4 Contractility of palmar fibroblasts with TNF-α and AGEs 180

5.3 Discussion **183**

CHAPTER SIX **189**

Concluding discussion

6.1 Concluding discussion and future plans **190**

6.2 Conclusion **200**

BIBLIOGRAPHY **201**

References **202**

APPENDIX **229**

Publications and presentations arising from this work

LIST OF FIGURES

CHAPTER ONE

Figure 1.1.	Dupuytren's contracture affecting the little and ring fingers.	2
Figure 1.2.	Normal anatomical structures and palmar fascia of the left hand.	7
Figure 1.3.	Normal anatomical structures of the distal palmar fascia and digital fascia of the hand.	8
Figure 1.4.	Dupuytren's contracture with clinical nodule and palmar skin pit.	10
Figure 1.5.	Clinical nodules.	12
Figure 1.6.	Dupuytren's cord.	13
Figure 1.7.	Open fasciotomy to correct digital contracture.	25
Figure 1.8.	Limited fasciectomy to correct digital contracture.	26
Figure 1.9.	Dermofasciectomy to correct digital contracture resulting. from recurrent disease	27
Figure 1.10.	Three dimensional collagen lattice models.	40
Figure 1.11.	Summary model of key steps in myofibroblast differentiation.	60

CHAPTER TWO

Figure 2.1.	The co-culture construct.	75

CHAPTER THREE

Figure 3.1.	Dupuytren's clinical proforma used to prospectively collect patient data on diathesis, previous surgery and pre-operative flexion contracture.	93
Figure 3.2.	Immunohistochemical analysis of Dupuytren's tissue.	97
Figure 3.3.	Quantification of histological nodules in excised digital cords.	99
Figure 3.4.	Relationship between α-SMA rich nodules and the PIPJ	102
Figure 3.5.	Systematic regional analysis of histological sections of nodular and non-nodular cord.	104
Figure 3.6.	α-SMA distribution in Dupuytren's tissue.	107
Figure 3.7.	Dupuytren's tissue nodularity correlated with flexion contracture.	109
Figure 3.8.	Nodule and cord surface area compared with flexion deformity.	110

CHAPTER FOUR

Figure 4.1.	α-SMA distibution in Dupuytren's nodule-derived cell lines.	125
Figure 4.2.	α-SMA distribution in cells from whole Dupuytren's tissue and dermal fibroblasts.	127
Figure 4.3.	Methodology used to isolate Dupuytren's cells from nodular *versus* non-nodular cord.	128
Figure 4.4.	Quantification of α-SMA localisation to stress fibres in dermal fibroblasts, Dupuytren's nodule-derived and non-nodular cells.	130
Figure 4.5.	The effect of cell passage on α-SMA stress fibres in Dupuytren's nodule-derived cells and dermal fibroblasts.	131
Figure 4.6.	Isotonic contraction of collagen gels by dermal fibroblasts and Dupuytren's nodule-derived cells.	133
Figure 4.7.	The culture force monitor (CFM).	134
Figure 4.8.	Isometric contraction of collagen gels by dermal fibroblasts and Dupuytren's nodule-derived cells.	135
Figure 4.9.	Isometric force generated by PIPJ nodular and non-nodular cells.	136
Figure 4.10.	Isometric contraction in FPCLs from 5 nodular and 3 non-nodular matched patient samples.	137
Figure 4.11.	Isometric force contraction in collagen gels seeded with decreasing numbers of Dupuytren's nodule-derived cells.	138
Figure 4.12.	The effect of cell passage on the contractility of Dupuytren's nodule-derived cells and dermal fibroblasts.	139
Figure 4.13.	Contractility of Dupuytren's nodule-derived cells is regulated by post-transcriptional changes in α-SMA.	141
Figure 4.14.	Isotonic contraction of stress released FPCLs using matched cells isolated from 4 patients.	143
Figure 4.15.	Isometric contraction of collagen gels seeded with co-cultures of dermal fibroblasts and Dupuytren's nodule-derived cells.	145
Figure 4.16.	Five day co-culture proliferation studies and cell viability assay.	146
Figure 4.17.	Rate of contraction and maximum isometric force contraction with different FPCL aspect-ratios.	147

CHAPTER FIVE

Figure 5.1.	Immunohistochemistry staining controls for inflammatory cells	162
Figure 5.2.	Immunohistochemistry staining for inflammatory cells in Dupuytren's nodule.	164
Figure 5.3.	Immunohistochemistry staining for inflammatory cells in Dupuytren's cord distal to nodule.	166
Figure 5.4.	Immunohistochemistry staining for inflammatory cells in non-nodular Dupuytren's cord.	168
Figure 5.5.	Immunohistochemistry staining controls for RAGE	171
Figure 5.6.	RAGE co-localises with α-SMA distribution in Dupuytren's nodule.	172
Figure 5.7.	RAGE and α-SMA distribution in Dupuytren's peri-nodular region.	173
Figure 5.8.	RAGE expression and α-SMA distribution in Dupuytren's cord distal from nodule.	174
Figure 5.9.	RAGE expression and α-SMA distribution in non-nodular Dupuytren's cord.	175
Figure 5.10.	Nodule-derived cells express higher levels of cell surface RAGE than matched dermal fibroblasts.	177
Figure 5.11.	RAGE cell surface expression is greater in palmar than non-palmar fibroblasts.	179
Figure 5.12.	Contractility of palmar skin fibroblasts is augmented by TNF-α and TGF-β1.	182

LIST OF TABLES

CHAPTER ONE

Table 1.1	Summary of pathological cords in Dupuytren's disease, their anatomical origins and clinical implications.	14

CHAPTER TWO

Table 2.1.	Summary of antibodies used in this study.	67
Table 2.2.	Steps involved in RT-PCR.	83
Table 2.3.	Primer sequences.	84

CHAPTER THREE

Table 3.1.	Differences in diathesis and pre-operative contractures are compared in samples from Edinburgh and London. Samples were grouped by either primary disease or recurrence (following previous surgical procedure as indicated).	95
Table 3.2.	Examples of cell counts in excised Dupuytren's tissue.	106
Table 3.3.	Nodular and non-nodular cords grouped by primary procedure or secondary procedure (for recurrent disease). Mean nodule surface areas (SA) for primary and recurrent disease are also included.	112

CHAPTER FIVE

Table 5.1	Quantification of total cell number, α-SMA positive cells, CD3 positive T cells, CD4 positive T cells, CD68 positive macrophages, and cells positive for mast cell tryptase and neutrophil elastase throughout excised Dupuytren's cord. Nodules, cord distal to nodule and non-nodular cord were analysed (presented as mean count (±SDEV) per mm^2) Six fields of view were counted within each region	169
Table 5.2.	FACS analysis to determine RAGE cell surface expression (Δ mean fluorescence intensity) in 4 nodular and 4 non-nodular matched patient samples. Cells isolated from Dupuytren's nodule co-located with the PIPJ, non-nodular PIPJ, non-palmar skin (NPS) and palmar skin (PS).	178

CHAPTER ONE

Introduction

1.1 Dupuytren's disease

Dupuytren's disease is a condition of the hand characterized by thickening and contraction of the fascia of the palm and fingers. It is a fibroproliferative disorder that results in progressive deformities through physical shortening of the diseased fascia. It may lead to significant digital contractures (Fig 1.1) and impairment of hand function to the extent that patients with severe flexion contractures may require amputation.



Figure 1.1. Dupuytren's contracture affecting the little and ring fingers.

This condition bears the name of Baron Guillaume Dupuytren, the chief surgeon at the Hotel Dieu in Paris (1831), who described the treatment of this condition in front of an audience and then without anaesthetic performed a simple release of the fascia (reviewed in Elliot, 1999).

1.2 Epidemiology

Epidemiological studies have consistently shown that Dupuytren's disease affects 4-6% of all Caucasians, although it is commoner in individuals of Northern European extraction (reviewed in Ross, 1999). A Scottish study showed more than 25% of males and 17% of females over the age of 65 years have signs of Dupuytren's disease (Ling, 1963). An extensive population study in Iceland of 2165 randomly selected individuals reported Dupuytren's disease in 7.2% between the age of 45 and 49 and up to 39.5% between age of 70 and 74 (Gudmundsson et al., 2000). All patients in this study were examined by the same medical practitioner. Dupuytren's disease is commoner in men than women, with approximately 5.9:1 male-to-female ratio aged 45 -55 years (Hindocha et al., 2009). The difference in prevalence seen with gender has been shown to be age dependent. Men tend to present in their fifth decade whereas women present a decade later. By the eighth and ninth decades of life the ratio of men to women being affected by Dupuytren's disease is nearer 1.5:1 (Mikkelsen et al., 1999). Dupuytren's disease has also been reported in children, although is rare (Urban et al., 1996).

Dupuytren's disease is less common in individuals from non-caucasian backgrounds. A 10-year retrospective study of 9,938 patients from the Department of Veterans Affairs computer system (USA) was conducted to determine the racial distribution of this disorder. The estimated prevalence was reported as 734 per 100,000 in Caucasians, 130 per 100,000 in Afro-Carribeans, 237 per 100,000 in Hispanics, 144 per 100,000 in native Americans, and 67 per 100,000 in Asians. Although Dupuytren's disease is rarely seen in people from African or Asian descent, it is interesting that Indian patients living in the UK are now developing the

disease (Srivastava et al., 1989). A high prevalence of Dupuytren's disease is also seen in Japan. However, 90% of these cases are reported to have no contracture, suggesting that the disease may show a different phenotype in Japan (Egawa, 1985).

Finally, large epidemiological studies have suggested that patients with Dupuytren's contracture followed up over 15 years show increased mortality from malignancy (Gudmundsson et al., 2000; Mikkelsen et al., 1999; Wilbrand et al., 2000). Although this observation was maintained when adjusted for age, smoking and occupation, other significant risk factors also need to be considered and further more detailed analysis is required.

1.3 Aetiology

The cause of Dupuytren's disease remains uncertain and has been linked to different aetiologies. These include alcohol, smoking, occupation and trauma, epilepsy, diabetes and rheumatoid arthritis. Different theories have been proposed to account for each of their roles in the pathogenesis of Dupuytren's disease although some remain controversial (Hindocha et al., 2009; Yi et al., 1999).

1.3.1 Genetics

Dupuytren's disease is often familial. A detailed study conducted in Edinburgh examined fifty patients with Dupuytren's disease and reported 16% familial incidence as documented from the patient's history. However, in the same study the incidence rose to 68% when up to third degree relatives were examined (Ling, 1963). Despite this genetic link, the inheritance pattern remains unclear. Autosomal dominance with variable penetrance has

been proposed as a likely mode of inheritance, although to date no single gene has been identified and many sporadic cases have also been reported (Burge, 1999; Hu et al., 2005).

Dupuytren's disease may be a complex oligogenic condition and discordance of Dupuytren's disease in pairs of monozygotic twins, whereby only one partner of each was reported to have Dupuytren's disease, has also implied a role for environmental factors (Lyall, 1993). It is possible that an inherited susceptibility may influence tissue sensitivity to the effects of environmental exposures. This may explain why Dupuytren's disease should start at a particular age or even at different times in two hands.

Many studies have used DNA microarray technology to compare gene expression profiles using both explants and cells isolated from Dupuytren's fascia and control carpal ligament, in an attempt to identify susceptible genes and identify novel therapeutic targets (Lee et al., 2006; Pan et al., 2003; Satish et al., 2008). Results have varied and have included genes previously shown to be involved in Dupuytren's disease such as fibronectin, tenascin-C, all three transforming growth factor (TGF)-β isoforms and type III, IV and VI collagens. Not surprisingly, many genes expressed are involved in extracellular matrix (ECM) organisation and more recent studies found genes for a disintegrin and metalloproteinase domain (ADAM-12), Periostin, proteoglycan-4 also to be upregulated (Lee et al., 2006; Pan et al., 2003; Satish et al., 2008). Novel gene candidates reported to be highly expressed in Dupuytren's nodular tissue include MafB (musculoaponeurotic fibrosarcoma oncogene homolog B) (Lee et al., 2006), aldehyde dehydrogenase 1 family member (ALDH1A1), and Iroquois homeobox protein 6 (IRX6) (Shih et al., 2009a; Shih et al., 2009b). This latest study examined differential gene expression in Dupuytren's fascia, non-diseased transverse

palmar fascia, palmar skin overlying nodule, palmar fat and compared to control carpal ligament tissue. They found increased ADAM12, ALDH1A1, and IRX6 expression levels in Dupuytren's disease fat compared to control tissue (Shih et al., 2009a). In all these studies a consistent pattern of candidate genes has not been reported and therapeutic strategies based on the genes identified have yet to be developed.

Furthermore, no association has been shown between naturally occurring gene polymorphisms and Dupuytren's disease. Specifically a lack association with TGF-β1, TGF-β2 and TGFβ receptors has been documented in Dupuytren's disease (Bayat et al., 2002a; Bayat et al., 2002b; Bayat et al., 2003). However, these findings do not necessarily exclude direct or indirect involvement of other relevant gene polymorphisms in the pathogenesis of Dupuytren's disease.

1.4 Palmar fascia anatomy

The hand has a precise ordered three-dimensional system of subcutaneous fascial fibres (fibrous tissue) that makes up the palmar and digital fascia. This fascia lies between the skin and deeper structures of the hand. It is essentially a framework that forms the soft tissue skeleton of the hand. It also supports the palmar skin and protects the hand against shear and compressive forces. The normal fascia consists of both longitudinal and transverse components (Fig. 1.2). As fascial fibres traverse the palm towards the digits, they condense to form "bands" or ligaments. These palmar fascial fibres become involved in those individuals that develop Dupuytren's disease to form cords.

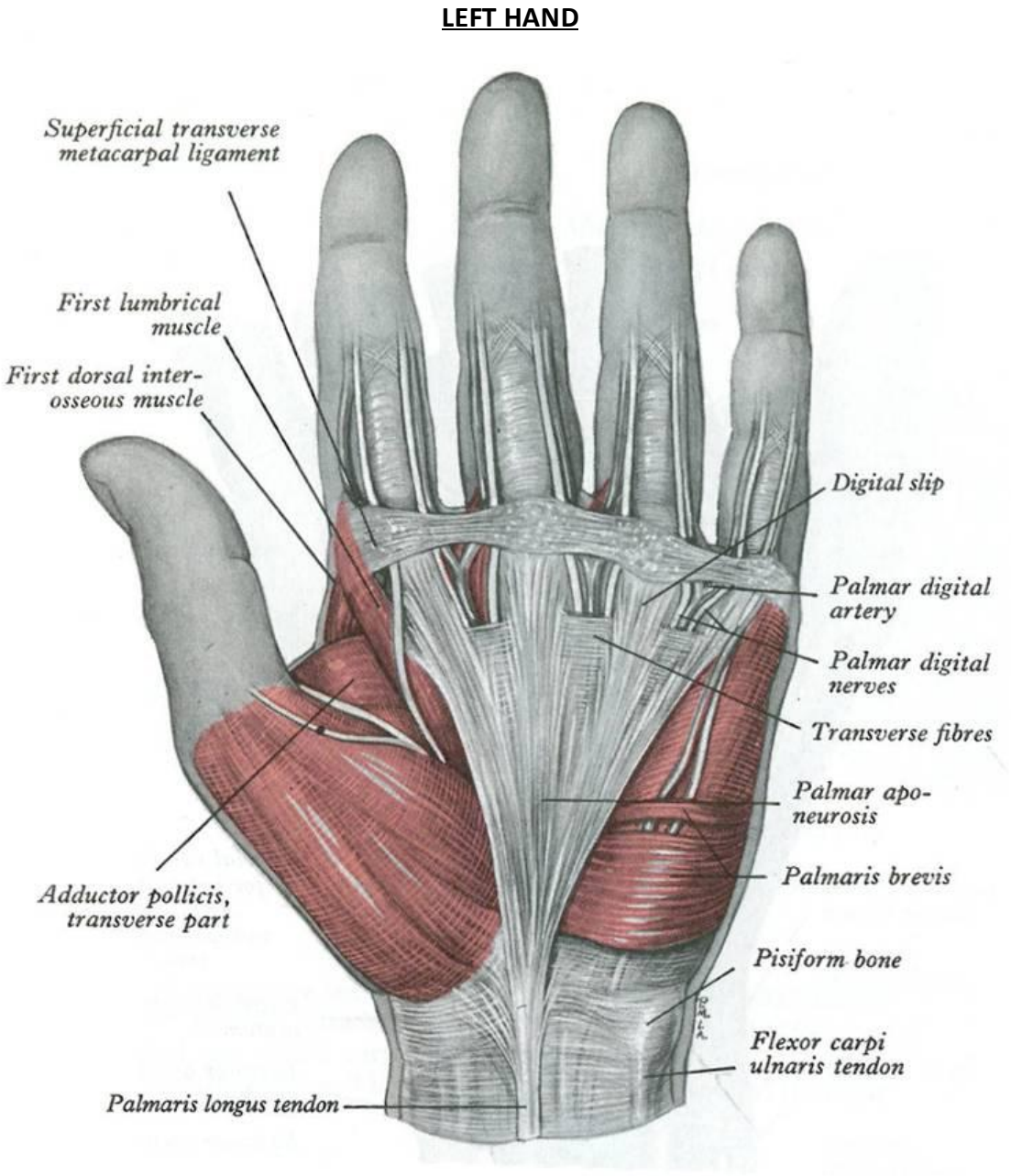


Figure 1.2. Normal anatomical structures and palmar fascia of the left hand. Illustration adapted from Gray's Anatomy (37th Edition).

In contrast to the palmar fascia, the digital fascia is a more complex structure. It is tubular and envelopes the flexors and extensor tendons with a fine meshwork of transverse, oblique and horizontal fibres. Various constituents of this fascia condense to form bands (Fig. 1.3) and which can become involved in the disease process.

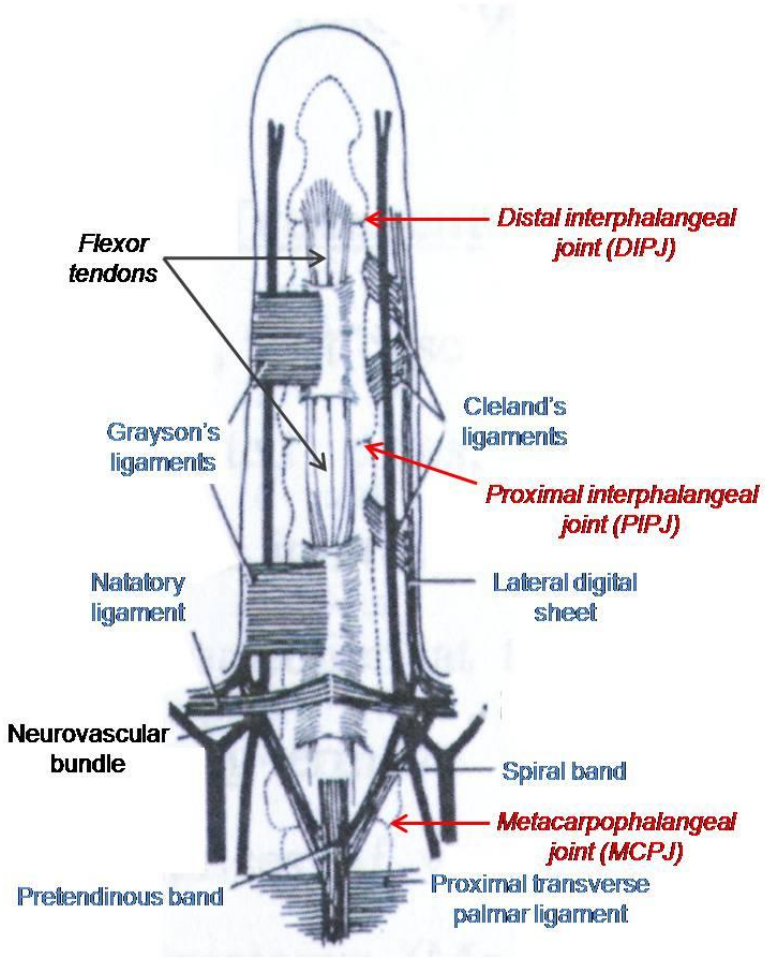


Figure 1.3. Normal anatomical structures of the distal palmar fascia and digital fascia of the hand. The main anatomical structural elements of the normal bands and ligaments are labelled for a single digit in the hand. Normal bands and ligaments (blue) are shown in relation to neurovascular bundles (black), flexor tendons (black arrows), and interphalangeal joints (red arrows) (adapted from McFarlane, Journal of Plastic & Reconstructive Surgery, 1974).

1.5 Clinical presentation

In Dupuytren's disease, changes in palmar skin and the formation of palmar nodules have classically been described as the first signs of Dupuytren's disease. Subsequent cord formation leads to gradual contraction and digital deformity. Dupuytren's lesions occur along precise fascial fibres that have a predominantly longitudinal orientation along lines of tension in the hand. Therefore, certain components of the palmar fascia, such as the transverse fibres (Fig. 1.2), are never involved, except in the first web space. This difference may be due to the fact that mechanical stress may be involved in the aetiology of Dupuytren's disease: the thumb, unlike the fingers, applies stress in both the longitudinal and transverse axes (McGrouther, 2005).

1.5.1 Dermatopathology

Skin changes can be the earliest manifestation of Dupuytren's disease and skin pits caused by deep full thickness skin retraction into the subcutaneous tissue by the diseased fibres which insert into the dermis may be observed (McGrouther, 1982) (Fig. 1.4). Fibrotic replacement of the subcutaneous fat in the deeper layer of the fat has also been described (reviewed in Rayan, 1999) and as a result of these changes, the thickened palmar skin becomes tethered and loses its normal mobility. Based on these observations, Heuston initially suggested that Dupuytren's disease pathogenesis may to some extent be influenced by the overlying skin (Hueston, 1985; Hueston, 1963; Maccallum and Hueston, 1962).

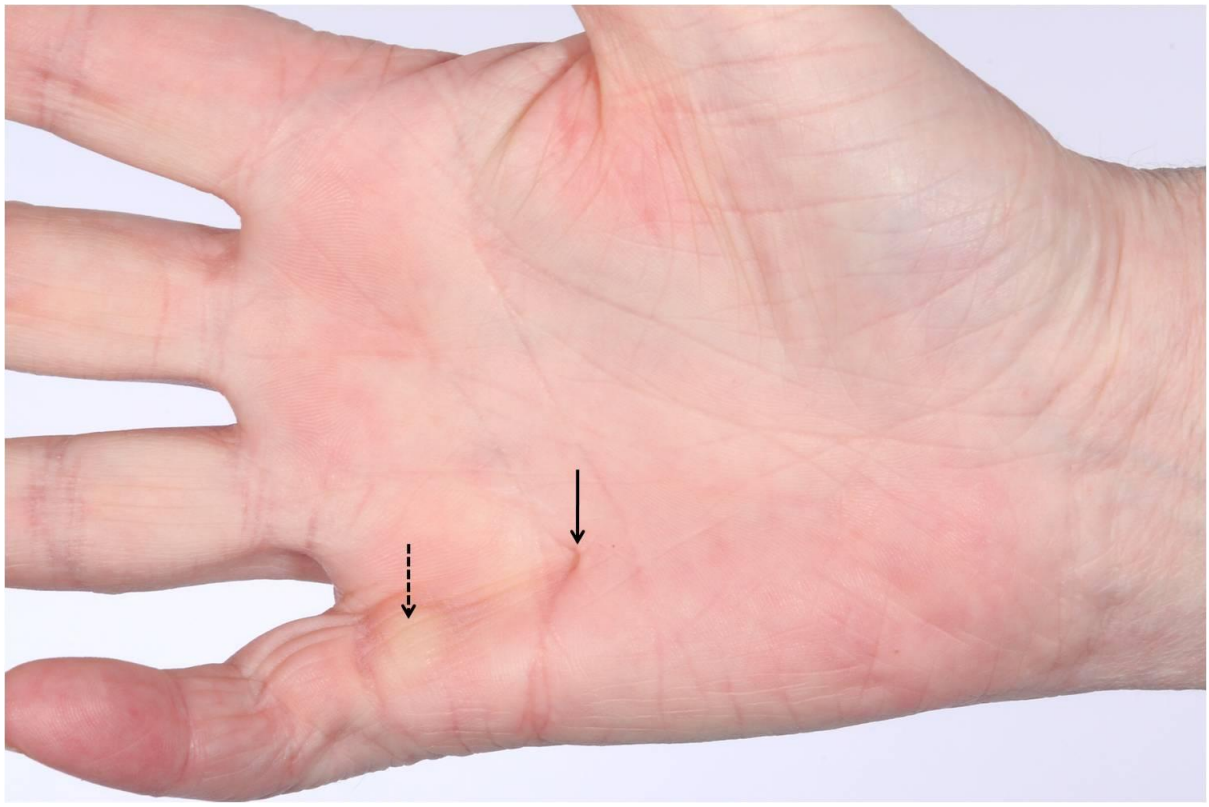


Figure 1.4. Dupuytren's contracture with a clinical nodule and a palmar skin pit. Dupuytren's disease affecting the little finger with a clinical nodule (dotted arrow) and a more proximally based skin pit (black arrow) is seen in the palm.

1.5.2 Nodule

The palmar nodule has been described as one of the earliest signs of Dupuytren's disease (Maccallum and Hueston, 1962). A clinical nodule is defined as a palpable subcutaneous lump (McGrouther in Green's operative hand surgery, 2005) and anatomical descriptions suggest nodules originate amongst the longitudinal fibres extending in to the dermis and within the superficial components of the palmar and digital fascia (McGrouther, 1982). Whilst clinical nodules may result from cell proliferation and extracellular matrix synthesis pushing upward on the skin, bunching up of the skin caused by contraction of the underlying fascia may also appear as a clinical nodule {McGrouther, 1982 #86; McGrouther, 2005)(Fig. 1.5).

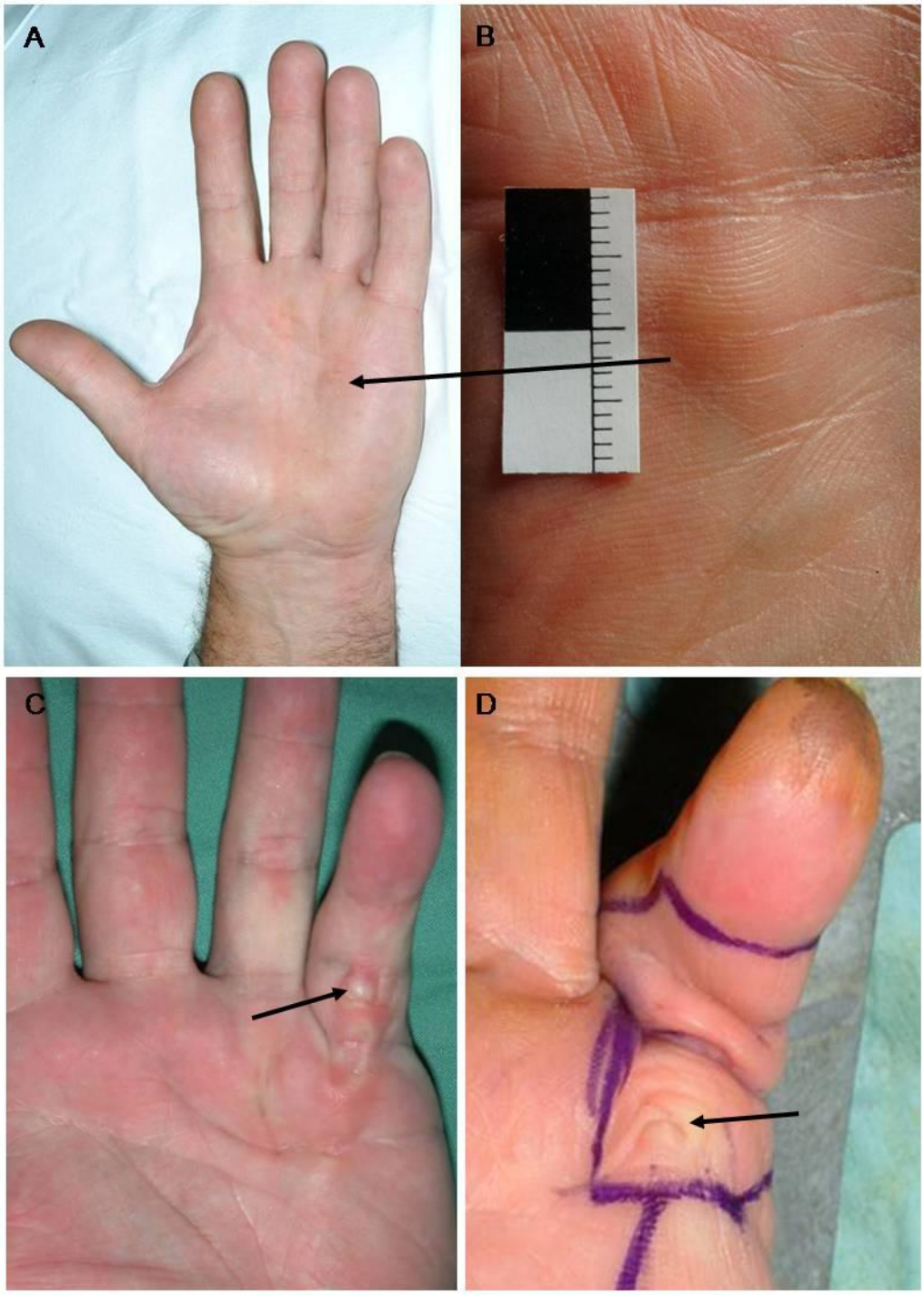


Figure 1.5. Clinical nodules. (A) Palpable clinical nodule in the palm with no digital contracture. (B) Same nodule seen magnified with a scale bar. (C) Dupuytren's contracture presenting with a clinical nodule (back arrow) and cord. The nodule is co-located with the proximal interphalangeal joint (PIPJ) and the prominent tendon-like cord can be seen extending proximally into the palm. (D) Dupuytren's contracture with a clinical nodule seen here as bunching of the palmar skin (black arrow).

1.5.3 Cord

Luck viewed the nodule as a "powerhouse" that matures as the disease progresses to form cord (Luck, 1959). However, whilst this may in part account for cord formation, it has also been suggested that normal bands in the hand hypertrophy and thicken in response to increased tension. These bands are precursors to pathological cords that become prominent and clinically acquire the consistency and appearance of tendon (Fig. 1.6) (McFarlane, 1974; McGrouther, 2005). Cords develop gradually and maturation may take place in the presence or absence of clinical nodules.

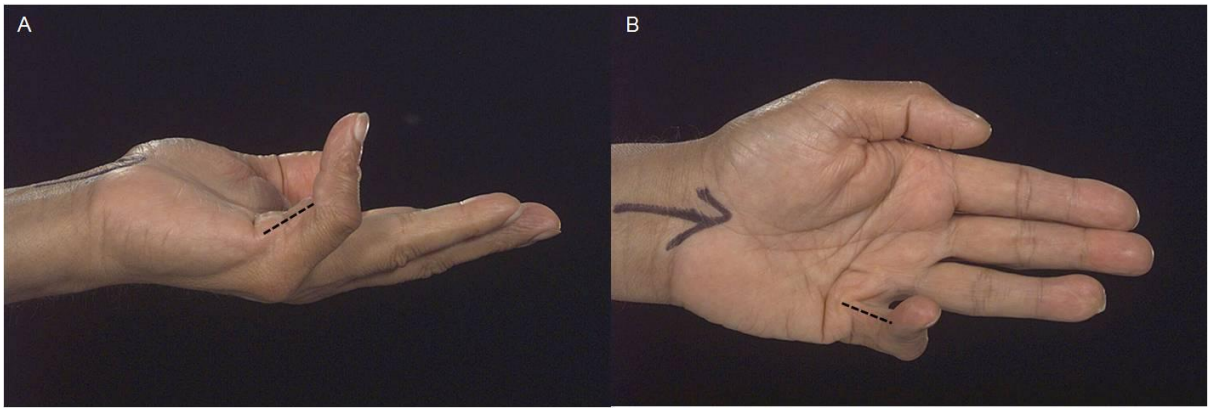


Figure 1.6. Dupuytren's cord. (A) Lateral view of Dupuytren's contracture affecting the left little finger and the prominent cord is highlighted with a dotted black line. (B) Antero-posterior view of the same hand (note the black arrow at the wrist denotes routine pre-operative marking for purposes of identification).

The various types of palmar and digital cords, the normal bands from which they arise, and the clinical significance of the diseased cords are summarised in Table 1.1.

Table 1.1 Summary of pathological cords in Dupuytren's disease, their anatomical origins and clinical implications (adapted from R.B. Shaw, PRS, 2006)

Diseased cord	Origin (band)	Clinical implication
Pretendinous cord	Pretendinous band	MCPJ contracture
Vertical cord	Vertical fibres/ septa	Triggering
Spiral cord	Pretendinous band, Spiral bands, Lateral digital sheet, Grayson's ligament and Retrovascular band	MCPJ, PIPJ contractures and displacement of neurovascular bundle
Natatory cord	Natatory ligament	Decreased digital abduction
Central cord	Pretendinous cord	PIPJ contracture
Retrovascular cord	Retrovascular band	PIPJ, DIPJ contractures
Lateral cord	Lateral digital sheet	PIPJ, DIPJ contractures and displaces neurovascular bundle
Abductor cord	Abductor digiti minimi tendon	PIPJ contracture
Thumb proximal commissural cord	Proximal commissural ligament	1st web contracture
Thumb distal commissural cord	Distal commissural ligament	1st web contracture
Thumb pretendinous cord	Pretendinous band	MCPJ contracture

MCPJ (metacarpophalangeal joint); PIPJ (proximal interphalangeal joint); DIPJ (distal interphalangeal joint)

1.5.4 Disease progression and diathesis

The course and progression of Dupuytren's disease is unpredictable as disease may remain confined to the palm and not progress to cause digital flexion deformity. It is in cases which progress to digital contractures that surgical intervention may be considered. Palmar involvement usually precedes disease extension into the digits, but the disease may begin or remain confined to the digit.

Dupuytren's disease often occurs bilaterally. The ring finger is most commonly affected, followed closely by the small finger. The thumb, middle finger and the index finger (ie. radial side of the hand) are less frequently involved as compared with the ulnar two digits (Rayan, 1999).

Some patients have a stronger predisposition to getting the disease and are said to have a strong "diathesis" (Hueston, 1963). The initial description of Dupuytren's disease diathesis by Heuston has been modified and recognised diathesis factors now include a positive family history (1^{st} degee relatives), bilateral disease, ectopic lesions (thickened knuckle pads or Garrod's pads), male gender and age at onset of younger than 50 years (Hindocha et al., 2006). Radial sided disease has also been suggested as an additional factor (Abe et al., 2004c).

1.5.5 Ectopic Dupuytren's disease

Although Dupuytren's disease refers to involvement of the palmar surface of the hand, a proportion of patients have extra palmar disease. This includes Garrod's pads (or thickened knuckle pads over the proximal interphalangeal joint (PIPJ)), which have been reported in

approximately 50% of patients. Proportionally, the index finger is more frequently affected by Garrod's pads and it is almost twice as common in patients with bilateral compared to unilateral disease (Caroli et al., 1991). Whilst a spectrum of knuckle changes have been described varying from loss of PIPJ skin wrinkles to knuckle pads (Rayan, 1999), it has also been reported that the cell type and extracellular matrix of Garrod's pads and Dupuytren's nodules were identical when examined at an ultrastructural level (Caroli et al., 1991).

A smaller proportion of patients also present with distant ectopic disease. These include plantar fibromatosis (Lederhose disease, 6-31%) that involves the soles of the feet, and often does not lead to contractures (Classen and Hurst, 1992). Patients may also present with contraction of the penile fascia (Peyronie's disease, 2-8%), resulting in penile deformity and erectile dysfunction (Gholami and Lue, 2002). Ectopic disease, in particular Garrod's pads is associated with more aggressive disease pattern in the hand (Abe et al., 2004b; Hindocha et al., 2006)

1.6 Histology of Dupuytren's tissue

Studies of Dupuytren's disease progressed using histology to examine tissue excised from patients. This revealed the presence of what have been described as histopathological nodules. Luck first described the histological nodule as a focus of fibroblasts which resembles a fibroma or as a focal fibroplasia (Luck, 1959). Histological textbook descriptions now define a histopatholoigcal nodule as collection of cells in a whorled pattern (Reviewed by McGrouther in Green's Operative Hand Surgery, 2005).

Both Luck (Luck, 1959) and Chiu and McFarlane (Chiu and McFarlane, 1978) described clinical nodules at various locations in the palm and digits of the hand. Luck viewed the initial and essential lesion in Dupuytren's contracture as the focus of proliferating fibroblasts. He states "that while grossly, a focus may exist as a solitary lesion in the palmar fascia, multiple foci are the rule. In most instances, the fibroblastic focus creates a palapable nodule". Chiu and McFarlane (Chiu and McFarlane, 1978) also describe many areas of cellular activity in diseased Dupuytren's tissue. In line with Luck's findings, this study reported histological nodules to vary significantly in size from tiny foci of cells to larger well defined nodules. However, Chiu stated that "some [nodules] were large enough to be palpated clinically, but most were microscopic in size". Therefore, it seems that clinical nodules do not always necessarily correlate with histological nodules. Hence when using the term 'nodule' it is important to distinguish between the two different types. Throughout this thesis I use the term 'clinical nodule' to describe a palpable subcutaneous lump and the term 'nodule' to describe a histological nodule defined as a collection of cells in a whorled pattern (McGrouther in Green's Operative Hand Surgery, 2005).

Following Luck's histological description of Dupuytren's nodules other studies have also examined Dupuytren's tissue using light microscopy. Gabbiani and Majno also noted the presence of histological nodules and observed that in these highly cellular areas, cells often had two characteristic features, namely intracellular fibrils and cross banded nuclei (Gabbiani and Majno, 1972). Samples of skin and underlying cord obtained at dermofasciectomy from 20 patients have also been examined by light microscopy. Varying amounts of hypercellular and collagenous tissue were reported. Hypercellular foci demonstrated very variable cellularity. In these areas swollen and rounded cell nuclei were

noted compared to largely acellular regions which were characterised by very long elongated thin nuclei (McCann et al., 1993). This study also showed that Dupuytren's tissue extended into the dermis and in three cases reached the epidermis.

Numerous studies have attempted to classify different stages of Dupuytren's disease based on histology using light microscopy. These studies have most often interpreted their findings within a histological framework defined by Luck: proliferation, involution and the residual phase (Luck, 1959). Luck described the proliferative phase to comprise a focal fibroplasia where cells are arranged in no purposeful arrangement in a histological nodule. As nodules involute fibroblasts align themselves predominantly in a longitudinal direction along stress lines passing through the nodule. In the final residual phase the nodule disappears, leaving fibrous cord which is almost acellular and tendon-like. This is reflected in the three histological stages of Dupuytren's disease proposed by Rombouts and Ballaguer: (1) a proliferative stage with high cellularity and the presence of mitotic figures, (2) a fibrocellular stage characterised by high cellularity but no mitotic figures and the presence of reticulin network, and finally (3) a fibrous stage with few cells separated by broad bundles of collagen fibres (Balaguer et al., 2009; Rombouts et al., 1989). Chiu's classification also broadly fits this theme: nodules in early disease have been described as composed of proliferating perivascular spindle-shaped cells with no increased collagen deposition. These become more closely packed in active disease with little intervening collagen, and in advanced disease less numerous elongated cells are described separated by broad parallel bands of collagen (Chiu and McFarlane, 1978). Histological texts also suggest that microscopic findings depend on the age of the nodule starting with cellular proliferation of plump, immature appearing spindle-shaped fibroblasts, some mitotic

activity and minimal collagen deposition. Nodules that have been present for a long time are less cellular and contain markedly increased amounts of dense birefringent collagen. Here fibroblasts are smaller and more slender. Cords between nodules are composed of dense fibrocollagnous tissue which resembles tendons (Weiss and Goldblum, 2008).

Histological staging determined by light microscopy studies has also been correlated with recurrence of following fasciectomy. These studies demonstrate that highly cellular and proliferative Dupuytren's tissue seen in primary disease correlates with higher disease recurrence rate (71%) when compared to the recurrence rate of less cellular fibrous tissue samples (18%) (Rombouts et al., 1989). Similar findings were confirmed in a larger series of 139 Dupuytren's samples, although histological staging was found to be independent of Dupuytren's diathesis (Balaguer et al., 2009).

Electron microscopy techniques have also been used to further examine Dupuytren's tissue to try and better determine the cell type that comprises each stage of disease. Myofibroblasts are modified fibroblasts with smooth muscle-like features that were first observed in granulation tissue of healing wounds by electron microscopy (Gabbiani et al., 1971). This led to the suggestion of a contractile role for these cells in wound healing. Subsequently, myofibroblasts were observed in Dupuytren's nodules; cells composing histological nodules were described to have three ultrastructural features: a fibrillar system similar to smooth muscle cells, nuclear deformations as found on contracted cells, and cell-to-cell and cell-to-stroma attachments (Gabbiani and Majno, 1972). Similarly, in a study of 21 Dupuytren's tissue samples, myofibroblasts were observed in clinical nodules, whereas proximal cord tissue was found to have longitudinally aligned collagen fibres with elongated

mature fibroblasts (Badalamente et al., 1983). Finally, in a study that examined the ultrastructural relationship of skin to nodule and cord, myofibroblasts were not seen at the skin/cord interface, although they were reported in specimens from skin/nodule interface (Rudolph and Vande Berg, 1991; VandeBerg et al., 1982).

The presence of myofibroblasts in Dupuytren's tissue has been assessed at different disease stages by electron microscopy. Dupuytren's fascia from 38 patient samples was examined and the findings correlated with the duration of disease activity in each case. Early disease was defined as a nodule in the palm without contracture. The authors reported that "early" nodules were composed of proliferated perivascular fibroblasts. "Active" disease was defined as palmar nodules with contracture for less than 3 years and in these samples the predominant cell seen in nodules was the myofibroblast. Diffuse thickening of the palmar fascia with joint contracture for more than 3 years was defined as "advanced" disease and although myofibroblasts and fibroblasts were also reported in these samples, they were present in much reduced numbers (Chiu and McFarlane, 1978). However, a study that examined 43 patient samples by electron microscopy found that proliferative stage nodules were chiefly composed of myofibroblasts with a small number of immature fibroblasts. The involutional stage consisted of nodules and some fibrous tissue extending from them and scar-like tissue was reported in the residual stage with few fibrocytes sparsely poplated amongst the collagenous matrix (Iwasaki et al., 1984). Similarly, proliferative phase nodules have been reported to be composed of myofibroblasts with a few fibroblasts whereas involutional nodules were described as being essentially composed of myofibroblasts. Nodules in the residual phase were described as hypocellular with slender cells aligned with thick bands of collagen giving them a tendon-like appearance (Schurch et al., 1990). Finally,

a study that examined 24 Dupuytren's patient samples by electron microscopy reported that clinical recurrence is not related to patient age at onset, duration, or severity of disease. Instead, recurrence was related to the presence of myofibroblasts in nodules (Gelberman et al., 1980; Rudolph and Vande Berg, 1991).

Immunohistochemical studies of histopathological nodules revealed more about the distribution of myofibroblasts in Dupuytren's tissue. Myofibroblasts have been shown to characteristically express α-smooth muscle actin (α-SMA) which is the actin isoform typical of vascular smooth muscle cells (Skalli et al., 1986). Unlike in granulation tissue where the expression of α-SMA is transient, increasing over time during wound closure and gradually disappearing during scar formation (Darby et al., 1990), α-SMA expression in Dupuytren's disease appears to be more sustained, with large numbers of α-SMA rich cells observed in diseased tissue. α-SMA expression was initially described to exhibit positive staining in Dupuytren's nodule tissue by immunofluorescence (Benzonana et al., 1988). In a key study, it was demonstrated by immunofluorescence that some of the cells from Dupuytren's nodules and hypertrophic scars express α-SMA in addition to vimentin, whereas cells from normally healing granulation tissue, eschars and normally healed scars only expressed vimentin. Furthermore, using gel electrophoresis β and γ actin was demonstrated in dermis and normal scar, whereas hypertrophic scars and palmar fibromatosis also contained α-SMA (Skalli et al., 1989). Subsequently, skin and cord samples from 20 patients undergoing dermofasciectomy were stained for α-SMA with the skin/ cord tissue orientation maintained. They reported diffusely distributed α-SMA positive cells in the dermis of eight samples. This study also noted foci of hypercellular Dupuytren's tissue staining positive for

α-SMA and the pattern of staining observed was variable, from very intensely stained foci to weakly stained and dispersed patches (McCann et al., 1993).

In another study, immunohistochemical analysis of excised Dupuytren's cord samples from 8 patients has shown hypercellular zones within nodules comprised up to 40% α-SMA positive cells, compared to 20% in less cellular regions of the same specimen (Hindman et al., 2003). Considerable variation in cellularity was reported between patient samples. Other studies have quantified the number of α-SMA positive cells within Dupuytren's nodules. Using immunofluoresent staining studies have found that between 1-26% of cells isolated from clinical nodules and 1-9% of control flexor retincaulum cells stained positive for α-SMA (Tomasek and Rayan, 1995). Similarly in a more recent study 9.7% of cells derived from a clinical nodule, 2.7% from cord tissue and 1.3% from control flexor retinaculum cells stained positive for α-SMA (Bisson et al., 2003). Finally, high levels of α-SMA protein have also been shown to be expressed in nodule-derived cells compared to cord cells and control dermal fibroblasts by western blotting (Dave, 2001 #35}.

The expression of α-SMA in Dupuytren's disease therefore appears to be more sustained than in the wound. These data suggest that aberrant regulation of α-SMA expression is occurring in Dupuytren's myofibroblasts compared to wound myofibroblasts. A better understanding of what drives α-SMA expression may be gained from studies examining the promoter of α-SMA and the environmental factors within Dupuytren's disease that contribute to the sustained expression of this protein. Some studies report lower numbers of myofibroblasts in late stage Dupuytren's disease (Chiu and McFarlane, 1978; Iwasaki et al., 1984; Schurch et al., 1990), suggesting that α-SMA expression may be induced early in

disease but down regulated later in disease. Serial biopsies from the same patients or an animal model of Dupuytren's disease would be helpful in understanding the kinetics of α-SMA expression through different stages of disease but neither of these options are available.

1.61 Other histological observations

Dupuytren's nodules have also been examined by electron microscopy for vascular changes. Within histological nodules and around the periphery of these nodules it has been shown that the majority of microvessels were occluded due to bulging of the endothelial cells into the lumen. These microvessels were surrounded by extensive layers of basal laminae and the histological nodules were described as essentially avascular (Kischer and Speer, 1984).

Several investigators have also identified inflammatory cells in Dupuytren's tissue. In particular, macrophages have been shown in cellular nodules clustered specifically around new blood vessels and a correlation between the numbers of macrophages and the presence of myofibroblasts has been reported (Andrew et al., 1991). Increased mast cells in excised Dupuytren's's tissue compared to control carpal ligament has also been reported (Schubert et al., 2006). Further studies have examined biopsies taken from the interface between palmar skin and excised Dupuytren's tissue for inflammatory cells using light and electron microscopy. Large numbers of macrophages were reported in samples taken from the palmar skin/clinical nodule interface compared to palmar skin/cord (VandeBerg et al., 1982). Increased numbers of Langerhans cells and CD45 positive cells have also been reported in histological nodules and at the dermo-epidermal junction in the overlying palmar skin (Qureshi et al., 2001). These studies have all examined Dupuytren's tissue

excised from patients with contractures and hence tissue samples will inevitably reflect active or advanced Dupuytren's disease. Nodules of both proliferative and involutional stages have been reported to contain small foci of perivascular haemorrhage with macrophages, some lymphocytes and mast cells (Iwasaki et al., 1984).

1.7 Treatment

Many different treatment types, both operative and non-operative have been trialled in the management of Dupuytren's disease. Currently surgery is the mainstay of treatment for patients with significant digital contractures resulting from Dupuytren's disease. However, increasingly in selected cases, minimally invasive techniques such as collagenase injections are being trialled.

1.7.1 Surgical treatment

Surgery is indicated in patients with functional disability or progressive digital contracture with PIPJ and MCPJ contractures of 30 degrees or more. Over time a number of different operative techniques have been used and can be broadly classified as fasciotomy, fasciectomy and dermofasciectomy (McGrouther, 2005).

Fasciotomy is simple division of the cord and was described by Baron Guillaume Dupuytren and Sir Astley Cooper (Fig. 1.7) (Elliot, 1999). It can be performed as an open or percutaneous procedure (needle fasciotomy). It is principally used to treat isolated pretendinous cords in the palm and is useful in selected cases, for example elderly patients with significant co-morbidity.

Fasciotomy can be carried out at multiple levels and it has also been indicated for initial correction of joint contracture as part of a staged procedure (Bryan and Ghorbal, 1988).

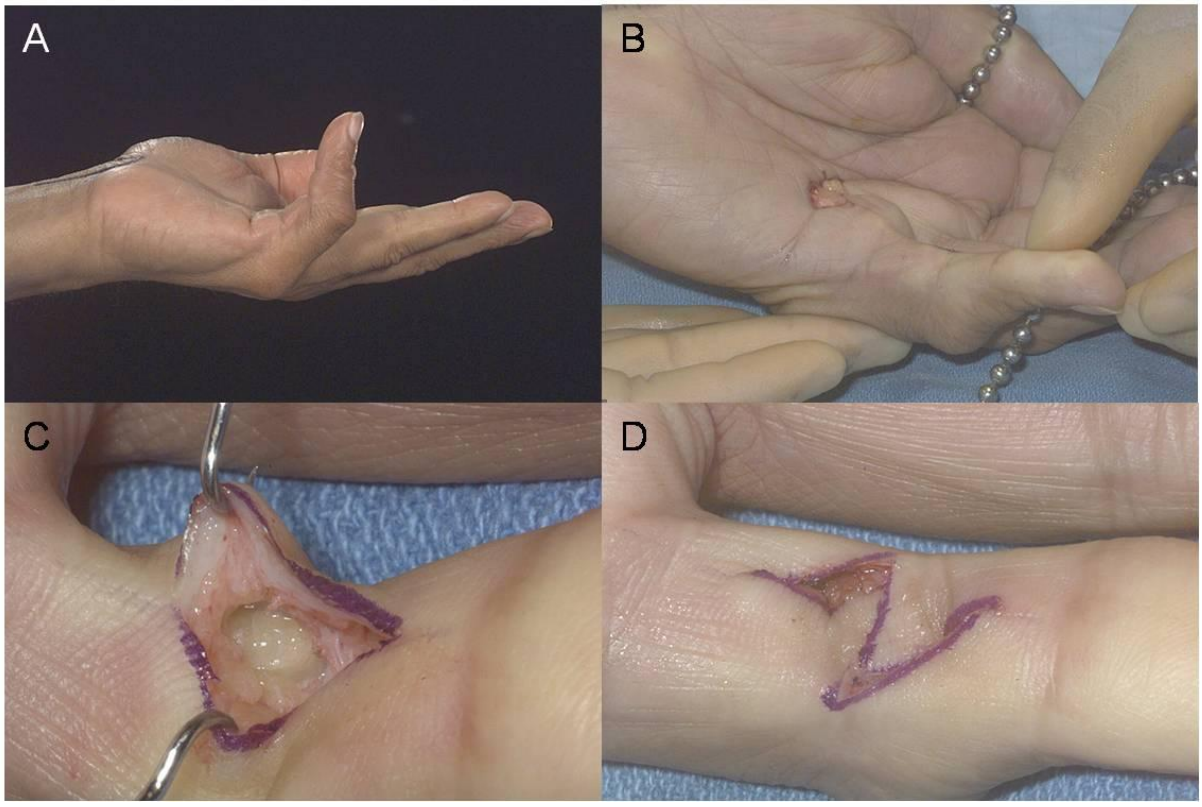


Figure 1.7. Open fasciotomy to correct digital contracture. (A) Primary Dupuytren's contracture. (B) Fasciotomy release carried out at the level of the metacarpophalangeal joint (MCPJ) and note residual contracture at the proximal interphalangeal joint (PIPJ). (C) Segmental fasciectomy at the PIPJ with, (D) correction of the PIPJ flexion deformity and subsequent closure with a z-plasty.

Limited *fasciectomy* is the most common procedure and involves surgical excision of the affected fascia (Fig. 1.8) (Hueston, 1961). Fasciectomy involves varying degrees of resection of Dupuytren's tissue. Whilst limited fasciectomy removes macroscopically diseased fascia within the surgical field, a segmental fasciecotomy involves excision of up to 1cm of diseased fascia and achieves a similar result to fasciotomy (Andrew and Kay, 1991; Moermans, 1991).

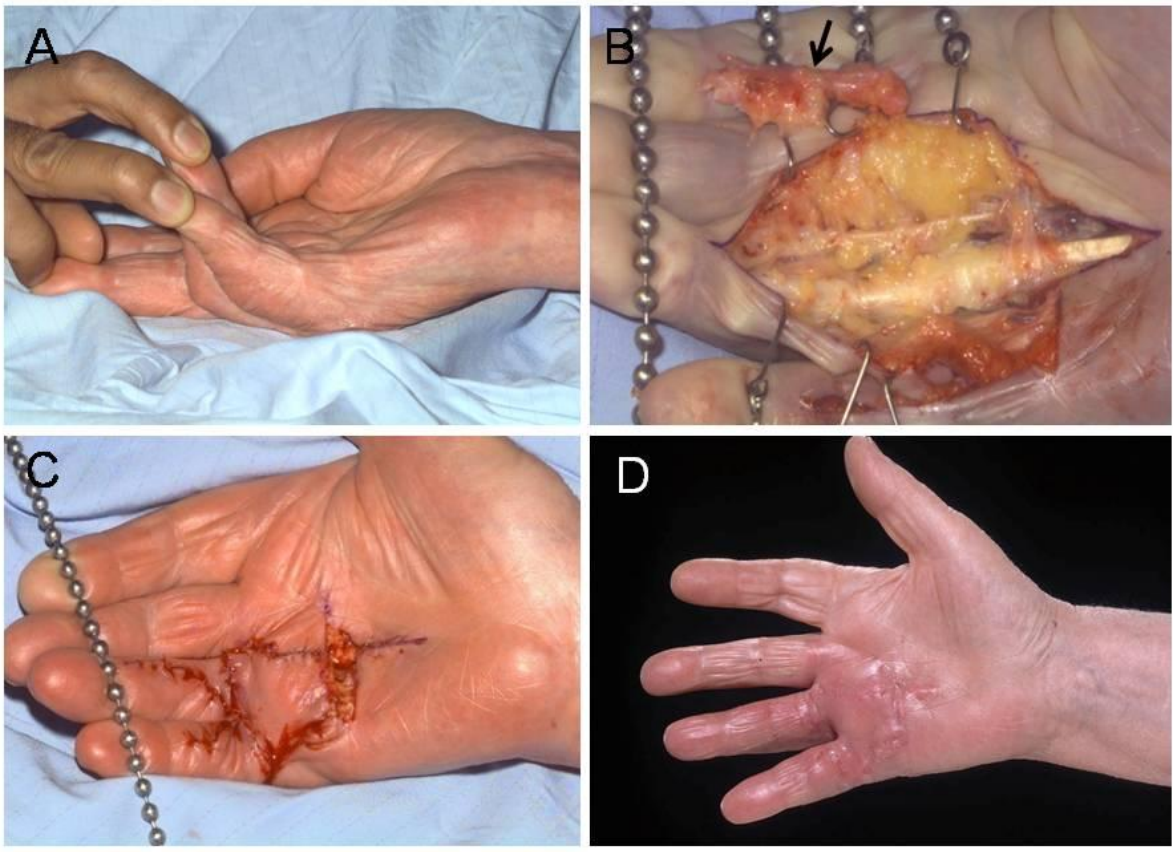


Figure 1.8. Limited fasciectomy to correct digital contracture. (A) Primary Dupuytren's contracture. (B) Dupuytren's diseased fascia (highlighted with the black arrow) is excised through a longitudinal incision. Flexor tendons and subcutaneous fat can be soon at the base of the operating field. (C) Wound closure with z-plasty with incision over distal palmar crease left open. (D) Outcome 3 weeks following fasciectomy, with no residual flexion contracture.

Radical fasciectomy entails extensive removal of the palmar and digital fascia in an attempt to remove all longitudinal fibres to the digits. However, complications from this procedure are more common without reduced disease recurrence rates (McIndoe and Beare, 1958).

Dermofasciectomy is surgical excision of the diseased fascia combined with replacement of the overlying palmar skin with full thickness non-palmar skin grafts (McGrouther, 2005) (Fig. 1.9). Typically dermofasciectomy is used in cases of recurrence or very aggressive primary disease, where there is significant skin involvement. Based on the observation that

Dupuytren's disease does not recur beneath skin grafts, a "firebreak" dermofasciectomy has also been advocated with strategic placement of full thickness skin grafts at a flexion crease that would act as firebreak in areas of potential flare-up of recurrent disease (Hueston, 1984).

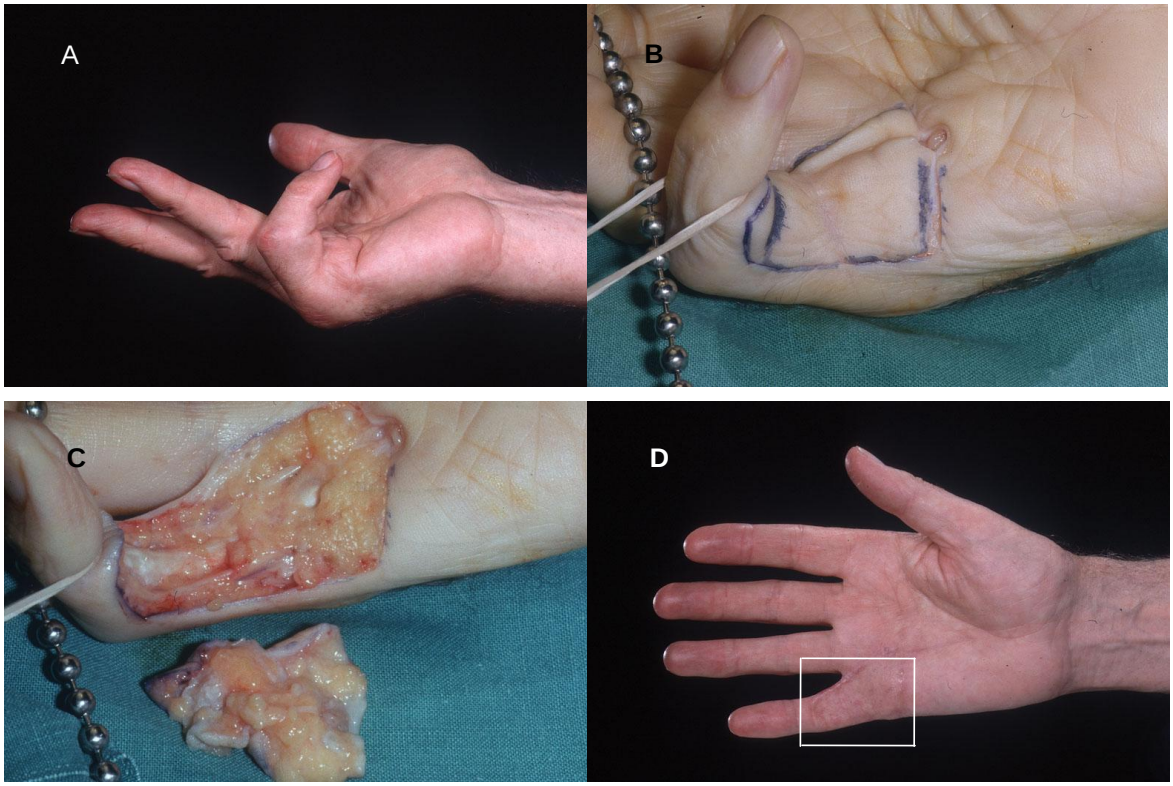


Figure 1.9. Dermofasciectomy to correct digital contracture resulting from recurrent disease. (A) Recurrent Dupuytren's contracture, (B) Outline for skin excision (C) Post excision of palmar skin and contracted fascia (D) Outcome at 1 year following resurfacing of cutaneous defect with non-palmar full-thickness skin graft from the groin skin, showing no recurrence of Dupuytren's contracture

Unfortunately, surgery may also be associated with complications, including inadvertent injury to the tendon (0.2%), digital nerve (1.7-7.8%) or artery (1.9-9.7%) with the potential loss of a digit. Other potential complications include infection (1-10.6%), reduced grip strength, complex regional pain syndrome, delayed wound-healing (very common) and recurrence of contracture (Bulstrode et al., 2005; Dias and Braybrooke, 2006; Foucher et al., 2003; Honner et al., 1971; Loos et al., 2007; Sennwald, 1990).

1.7.2 Minimally invasive procedures, surgical adjuncts and non-operative treatment

Enzymatic fasciotomy using collagenase injections augmented by mechanical stress and splinting has been trialled in a few studies (Badalamente and Hurst, 2007; Hurst et al., 2009; McCarthy, 1992; Starkweather et al., 1996; Watt et al., 2010). A recent phase III randomized placebo-controlled trial in the USA showed that collagenase (clostridium histolyticum) treatment significantly improved outcomes (Hurst et al., 2009). In total 308 patients with joint contractures of 20 degrees or more were enrolled (mean MCPJ (55°) and PIPJ (45°)). Primary MCPJ or PIPJ cord contractures were randomly assigned to receive up to three injections of collagenase or placebo at 30-day intervals. Significantly more digits (64%) treated with collagenase than cords injected with placebo (6.8%) were reduced to within less than 5 degrees of full extension. However, 77% of MCPJ and only 40% of PIPJ treated contractures treated with collagenase met this end point at 30 days. Serious complications included two tendon ruptures in digits with PIPJ contractures and one case of complex regional pain syndrome was reported. Other than superficial bruising and swelling, there were no significant changes in flexion or grip strength, no systemic allergic reactions and no nerve injuries were observed. Based on this study, it appears that enzymatic fasciotomy has a role in treating early contractures, although treatment outcomes for MCPJ contractures appear to be better than for PIPJ contractures.

Early splinting is also often used, either in isolation or more commonly, as an adjunct to enzymatic fasciotomy and surgery. However, for splints to be effective in isolation without surgery, they need to be worn continuously and this in itself is an unacceptable impairment (Abbott et al., 1987). A recent systematic review of post-operative splinting in Dupuytren's

disease suggested that splints are widely used and supported mainly by clinical reasoning and anecdotal evidence. The difficulty the reviewers found was that the multiple studies did not control for variables, including the use of different types of splints, duration of treatment and patient compliance (Larson and Jerosch-Herold, 2008).

Slow continuous elongation of Dupuytren's contracture by an external fixator has been shown to result in remodelling of the contractile fascia and gradual extension of the digit. However, following discontinuation of traction digital contracture rapidly recurred (Citron and Messina, 1998; Messina and Messina, 1993). Based on these observations, the Digit Widget ™ has been proposed to provide a period of continuous elongation followed by definitive treatment by limited fasciectomy (Hand Biomechanics Lab, USA). Proponents claim that in more advanced cases, gradual release of the joint contractures leads to improved functional outcomes. However, this has yet to be verified.

Local radiotherapy for Dupuytren's disease has been used with some success in patients with early disease and limited contractures (Betz et al., 2010; Keilholz et al., 1996; Seegenschmiedt et al., 2001). However, a study with median 7 year follow-up suggested no benefit from radiotherapy (Weinzierl et al., 1993). Although data are now available at 13 years follow up, there remains the potential for slow wound healing in patients treated with radiotherapy who might subsequently undergo surgery and the optimal radiotherapy dose remains uncertain (Betz et al., 2010). Furthermore, there are potential issues with treating a benign disorder with radiotherapy.

A prospective randomised controlled trial using intra-operative topical treatment with 5-fluorouracil was performed in an attempt to control fibroblast proliferation in Dupuytren's

disease (Bulstrode et al., 2004). This was based on data from the same group that suggested an anti-proliferative effect of 5-fluorouracil in cultured Dupuytren's fibroblasts (Jemec et al., 2000). However, in the clinical trial, there was no significant difference in recurrent contracture at 18 months between control and 5-fluorouracil treated digits.

Steroids have also been used with variable success in Dupuytren's disease (Ketchum and Donahue, 2000). None of the 75 hands treated in this study had MCPJ contractures of more than a 15° and none had PIPJ contractures at the outset of treatment with triamcinolone injections. Although temporary resolution of the nodules was observed following intralesional triamcinolone injection, improvement of the joint contracture was not seen. Furthermore, increased tendon rupture was also reported with frequent steroid injections (Ketchum and Donahue, 2000). It has been proposed that the therapeutic benefit of steroids in early disease is due to their anti-inflammatory role (Meek et al., 1999; Meek et al., 2002).

Finally, other non-operative therapies have been trialled for Dupuytren's disease, albeit with limited success. Treatment with oral vitamin E (Richards, 1952), allopurinol (Hurst and Badalamente, 1999; Murrell, 1991), ultrasound therapy (Stiles, 1966) and dimethyl sulphoxide (DMSO) (Hurst and Badalamente, 1999) have all been used and have demonstrated no clinical effect.

1.8 Recurrence following surgery

Recurrence rates following surgery for Dupuytren's contracture can vary significantly, depending on the type of procedure. True recurrence or recurrent contracture are defined as the appearance of a new lesion (Dupuytren's tissue) or resulting fixed flexion deformity due to Dupuytren's disease tissue (and not scar tissue), in a previously operated field. In contrast, disease extension refers to new lesions outside the previously operated area but within the same hand.

Following open or percutaneous fasciotomy, recurrence rates have been reported between 40-70% as soon as 2 years following surgery (Bryan and Ghorbal, 1988; Foucher et al., 2003; Rodrigo et al., 1976; van Rijssen and Werker, 2006). The recent phase III trial of 308 patients treated with collagenase has only reported on 30 day outcomes (Hurst et al., 2009). Results from the earlier phase of this trial suggests that the recurrence rates were approximately 8% in patients with MCPJ contractures and 57% with PIPJ contractures at 2 years follow-up (Badalamente and Hurst, 2007). Increased recurrence following fasciotomy for PIPJ contractures compared to MCPJ contractures has also been reported in other studies (Bryan and Ghorbal, 1988; Foucher et al., 2003).

Recurrence rates following fasciectomy are approximately 40-50% at 5 years (Foucher et al., 1992; Hueston, 1961; Tonkin et al., 1984). However, recurrence rates have been reported as high as 71% at 10 years (Norotte et al., 1988) and 100% at 20 years follow-up (McGrouther, 2005).

In comparison, recurrence following dermofasciectomy is quoted at 1-8% between 2-12 years follow-up (Brotherston et al., 1994; Hall et al., 1997; Tonkin et al., 1984). One study reported that in 46 patients following dermofasciectomy, no recurrence and no recurrent contracture greater than 15 degrees was found after 6-12 years follow-up (Brotherston et al., 1994). Heuston through his observation that Dupuytren's contracture did not recur beneath skin grafts, advocated their strategic placement at a flexion crease would act as 'firebreak' between areas of potential flare-up of recurrent disease (Hueston, 1984). A recent study of 79 patients with PIPJ contracture randomised patients to either a firebreak skin graft or fasciectomy. At 36 months follow-up no difference was observed in recurrence rate following either firebreak dermosfasciectomy or fasciectomy (Ullah et al., 2009).

Recurrence of Dupuytren's contracture has been correlated with various factors, including increased expression levels of several matrix metalloproteinases (MMPs) and a disintegrin and metalloproteinase with thrombospondin motifs (ADAMTSs) (Johnston et al., 2008), histological staging (Balaguer et al., 2009; Rombouts et al., 1989) and Dupuytren's diathesis (Hindocha et al., 2006). Histological findings suggest that highly cellular and proliferative Dupuytren's tissue seen in primary disease correlates with higher disease recurrence rate (71%) when compared to the recurrence rate of less cellular fibrous tissue samples (18%) (Rombouts et al., 1989). Although similar findings were confirmed in a larger series of 139 Dupuytren's samples, histological staging was found to be independent of Dupuytren's diathesis (Balaguer et al., 2009). In a study that examined 24 Dupuytren's patient samples by electron microscopy reported that clinical recurrence is not related to patient age at onset, duration, or severity of disease. Instead, recurrence was related to the presence of myofibroblasts in the nodules (Gelberman et al., 1980; Rudolph and Vande Berg, 1991). The

authors demonstrated that myofibroblast presence may help to predict recurrence of disease and based on this suggested that palmar skin should be excised when adherent to disease nodules.

Dupuytren's diathesis is also considered important in predicting recurrent disease following surgery. The presence of all diathesis factors is associated with a higher risk of recurrent Dupuytren's disease (71%) compared with a baseline risk of 23% in patients with Dupuytren's disease but none of the diathesis factors (Hindocha et al., 2006). This was shown in a study conducted on 322 patients in Northwest England, where patients with Dupuytren's disease were assessed for diathesis based on clinical history and examination. Odds ratios of developing recurrent disease were calculated using logistic regression. Interestingly, in the largest series of 73 fasciectomy cases in Japan, the reported recurrence was only 14% at 4 years follow-up and the significant diathesis factors only included radial side disease, ectopic lesions and an early onset of disease (Abe et al., 2004a). The authors suggested that low recurrence rates reflected the relatively shorter follow-up period, although a less aggressive Dupuytren's disease phenotype amongst Japanese people should also be considered.

1.9 Myofibroblasts

The cells that primarily contribute to the pathogenesis of Dupuytren's disease are myofibroblasts. Myofibroblasts were first defined by Gabbiani as cells showing three ultrastructural features: a fibrillar system similar to smooth muscle cells, nuclear deformations (the severest recognisable by light microscopy as cross banded nuclei) and

cell-to-cell and cell-to-stroma attahments (Gabbiani et al., 1971). Myofibroblasts can be distinguished from fibroblasts by the presence of bundles of intracellular contractile microfilaments, extensive cell-to-matrix attachment sites (fibronexi) and intercellular adherens and gap junctions (Eyden, 2005; Schurch et al., 2006).

The presence of myofibroblasts represents a key event during normal wound healing and tissue repair. These highly contractile cells are normally seen in the gravid uterus and transiently during wound healing. Typically, myofibroblasts disappear as the scar matures or when tissue remodelling is complete. However, myofibroblasts can also be detrimental for tissue function when they persist and become excessive. Examples of this are seen in hypertrophic scars (Ehrlich et al., 1994), keloid scar (Eyden, 2003; Shoukrey and Tabbara, 1993), burn scar tissue (Eddy et al., 1988), contracture of capsules around breast implants (Hwang et al., 2010) and Dupuytren's contracture (Schurch et al., 1990).

1.10 Cytoskeletal and cell surface markers

Myofibroblasts characteristically express α-SMA which is the actin isoform typical of vascular smooth muscle cells (Skalli et al., 1986), in addition to the β- and γ-cytoplasmic actins that are traditionally found in fibroblasts. Fibroblast to myofibroblast differentiation is proposed to be a two-step process whereby in response to changes in compostion of the matrix, fibroblasts develop de novo contractile bundles or stress fibres that are composed of β- and γ-cytoplasmic actins (Hinz, 2007). These are termed "proto-myofibroblasts" and are different from quiescent fibroblasts that in vivo have no contractile apparatus (Tomasek et al., 2002). With increasing stress in the remodelled ECM proto-myofibroblasts start expressing de novo α-SMA and only develop into "differentiated myofibroblasts" when this

α-SMA is incorporated in to stress fibres (Goffin et al., 2006). Although this process has been divided into two stages, there exists a stage in between the proto-myofibroblast and the differentiated myofibroblast where α-SMA is found transitorially in the cytoplasm but is not incorporated into stress fibers (Hinz, 2006). This process is regulated by a number of different factors which are summarized in Figure 1.12 and which I review below.

To date, α-SMA is the most commonly used and the most reliable myofibroblast marker (Hinz, 2007). However, whilst α-SMA has been reported to distinguish myofibroblasts from fibroblasts, it cannot be used in isolation to reliably distinguish between myofibroblasts and vascular SMCs (Christen et al., 2001). This is especially true in Dupuytren's nodules, where mixed populations exist. Therefore, other cytoskeletal and cell surface markers have been examined to try and distinguish between these cell populations.

Intermediate filaments vimentin and desmin are cytoskeletal proteins that play a role in maintaining cell architecture and have been studied in fibroblasts, myofibroblasts and SMCs. Fibroblasts, myofibroblasts and SMCs all express vimentin (Gabbiani et al., 1981). Myofibroblasts from granulation tissue also only express vimentin but not desmin (Skalli et al., 1989), whereas vascular SMCs express vimentin and desmin. However, in Dupuytren's disease, whilst nodules are often composed of myofibroblasts (Iwasaki et al., 1984; Schurch et al., 1990), up to 20% cells present around capillaries and blood vessels in proliferating nodules have also been shown by immunohistochemistry to express desmin (Schurch et al., 1990; Shum and McFarlane, 1988). Furthermore, the use of desmin as a marker for SMCs is limited as it is lost from these cells when placed in culture, as is caldesmon smooth muscle myosin heavy chain (Christen et al., 2001; Serini and Gabbiani, 1999).

Other myofibroblast markers, including smoothelin (Chambers et al., 2003) and the 41g isoform of the stress fibre protein paladin (Chambers et al., 2003; Mykkanen et al., 2001) have been considered. However, neither is exclusively expressed in smooth muscle cells or myofibroblasts when analysed by gene expression profiling or western blot analysis respectively.

Myofibroblasts cell surface markers have also been investigated. The expression of specific trans-membrane cell-cell adhesion proteins that are linked to the intracellular actin cytoskeleton (cadherins) has been proposed as a potential marker for differentiated myofibroblasts. Fibroblasts in normal dermis express almost none, if any, of the cadherin protein family. N-cadherin (A-cell adhesion molecule (A-CAM)) is expressed in early granulation tissue and in cultured fibroblasts. However, in TGF-β1 treated cells that express α-SMA or in differentiated myofibroblasts in granulation tissue, N-cadherins become replaced by OB-cadherin (Hinz et al., 2004). This transition has also been described in prostate cancer stromal fibroblasts (Tomita et al., 2000). Although OB cadherin is not expressed in SMCs, it has been shown in other cells of mesenchymal origin, and therefore, cannot be used as an exclusive myofibroblast marker.

Thy-1 is a cell surface glycoprotein that has been described in fibroblasts from several organs (Dudas et al., 2007; Koumas et al., 2003) and reported to be absent in myofibroblasts. Furthermore, it has been suggested that only Thy-1 positive cells have the potential to undergo myofibroblastic differentiation as compared to Thy-1 negative cells, which cannot. Thy-1 expression has not been examined in cells derived from Dupuytren's disease.

1.11 Origin of myofibroblasts

In Dupuytren's disease the origin of the myofibroblasts remains unknown. Two theories have dominated thinking about the origin of Dupuytren's contracture and, therefore, the source for myofibroblasts in Dupuytren's disease. The ``extrinsic'' theory suggests that initial changes are observed in the overlying palmar dermis (Hueston, 1985; Hueston, 1963), whereas the ``intrinsic'' theory argues that the disease process originates within the palmar fascia (McFarlane, 1974). Neither of these theories has been proven and there is speculation that massive cellular proliferation starts following rupture of palmar fascial fibres (Yi et al., 1999). Examination of fibroblasts from normal palmar fascia and normal dermal fibroblasts has suggested that cells from both sources have the potential to develop in to myofibroblasts (Rayan and Tomasek, 1994; Tomasek et al., 2002). Both cell types develop stress fibres when placed in culture on rigid substrates or in 3D collagen matrices and in the presence of TGF-β1 they further develop α-SMA positive stress fibres (Bisson et al., 2003; Desmouliere et al., 1993; Wong and Mudera, 2006).

Pericytes and smooth muscle cells from the vasculature have also been implicated as a source for myofibroblasts in Dupuytren's disease (Kischer and Speer, 1984). Desmin is present in parenchymal smooth muscle cells and some vascular smooth muscle cells. In Dupuytren's disease nodules, the presence of desmin-positive cells around blood vessels in a stellate pattern has also led to the hypothesis that Dupuytren's myofibroblasts may arise from migrating perivascular smooth muscle cells (Shum and McFarlane, 1988). Pericytes and vascular smooth muscle cells have also been implicated in scleroderma (Rajkumar et al., 2005) as well as in liver and glomerular fibrosis (Desmouliere et al., 2003).

It is recognised that myofibroblasts often arise from resident cell populations within the organ system involved. In dermal wound healing it is thought that fibroblasts are recruited locally from sites adjacent to the injury and differentiate into myofibroblasts in the wound bed (Desmouliere et al., 2005). In pulmonary fibrosis most myofibroblasts have been shown to arise from locally residing fibroblasts, in the liver hepatic stellate cells are the main contributor for liver fibrosis and media smooth muscle cells are the main contributor to atheromatous plaques (Hinz, 2007).

However, it is also known that myofibroblasts may arise from fibrocytes, which are a sub-population of bone marrow derived leucocytes with fibroblast characteristics (Abe et al., 2001). Fibrocytes derived from bone marrow are possibly a significant source of myofibroblasts. This has been shown in studies by transplanting bone marrow from male to irradiated female mice (Direkze et al., 2003) and identifying the Y chromosome by *in situ* hybridisation and also by transplanting bone marrow from transgenic green fluorescent mice to irradiated wild-type animals (Hashimoto et al., 2004). These studies have shown that up to 30-50% of wound myofibroblasts are potentially derived from fibrocyte progenitors and this has been demonstrated in hepatic, renal and pulmonary fibrotic conditions (Direkze et al., 2003; Forbes et al., 2004; Hashimoto et al., 2004). However, it remains unclear whether myofibroblasts precursors in fibrotic conditions, and indeed Dupuytren's disease, are recruited from several different sources.

1.12 Contractility

Cells exist *in vivo* within a dynamic environment whereby mechanical tension and load determine cell morphology and function. Fibroblasts in 3D collagen matrices acquire a similar bipolar phenotype to that seen *in vivo*, unlike fibroblasts cultured in monolayer (Elsdale and Bard, 1972). Initial experiments using fibroblast populated collagen lattices (FPCLs) demonstrated contraction of the lattices, which led to the use of this model in the study of wound contraction (Bell et al., 1979; Grinnell, 1994). Subsequently, studies have demonstrated dose-dependent FPCL contraction with fetal calf serum (FCS) (Brown et al., 2002; Rayan and Tomasek, 1994; Tomasek et al., 1992) and that contraction was related to final FPCL collagen concentration (Bell et al., 1979).

Whilst alternative models of cell contractility have been developed, such as wrinkling of two dimensional silicone substrates (Harris et al., 1980; Harris et al., 1981), three dimensional FPCL contraction models are most commonly employed (Grinnell and Petroll, 2010). These various inter-related FPCL models have been used to study collagen matrix contraction (Grinnell, 2003; Grinnell and Petroll, 2010; Tomasek et al., 2002) and include free-floating and restrained matrices. Contraction of restrained matrices has been used to measure both isotonic contraction following stress-release and also to quantify real-time isometric force contraction using the culture force monitor (Fig. 1.10).

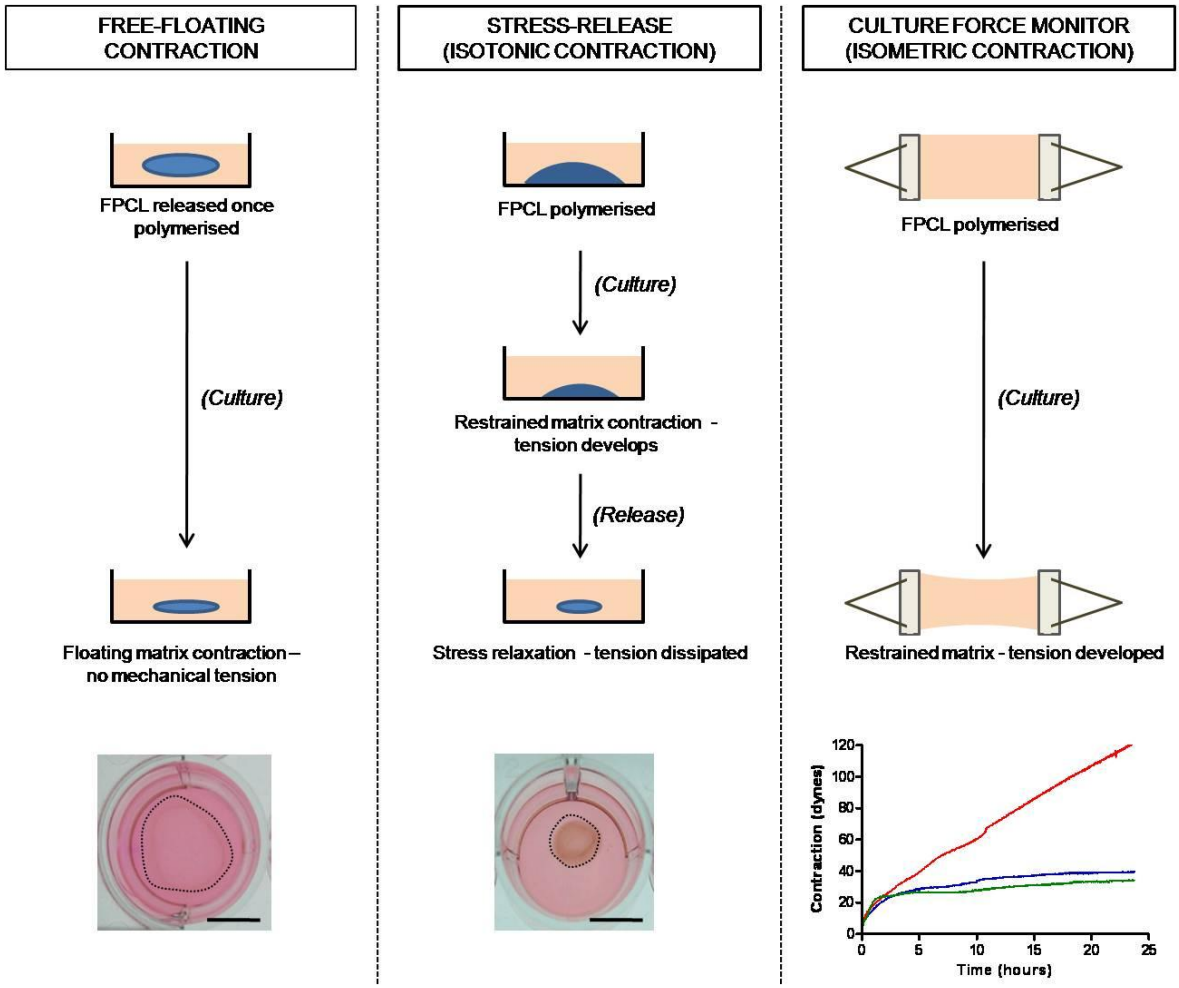


Figure 1.10. Three dimensional collagen lattice models. Free-floating matrix contraction occurs when FPCLs are released from surfaces of the culture dish soon after matrix polymerization and placed in culture media. Mechanical tension cannot develop in free-floating lattices and fibroblasts exert tractional forces, resulting in slow compaction of the lattice. Restrained matrix contraction occurs when cells are incubated with matrices that remain attached to the surfaces of the culture dish. Stress-relaxation then occurs upon release of restrained FPCLs which previously developed tension, therefore resulting in isotonic contraction. FPCL contraction and stress-relaxation can be quantified by measuring the change in matrix diameter (scale bar shown = 7mm). Without detaching FPCLs from culture, real-time quantification of uniaxial isometric force generated in restrained FPCLs can be quantified using the culture force monitor (CFM). Using this model, FPCLs (pink) are cast and floated in medium, tethered between two flotation bars (light grey) one of which is held stationary whilst the other is attached to a force transducer. As force develops, FPCLs acquire an hour glass shape.

Floating matrix contraction occurs when FPCLs are released from the culture surfaces soon after matrix polymerization and is considered a low cell-matrix tension state. During and

after contraction, the cells exhibit few α-SMA stress fibres. Restrained matrix contraction occurs when FPCLs remain attached to the culture surfaces. This results in isometric contraction, where cell contraction is opposed by an equal load that prevents cell shortening. Cells develop prominent α-SMA stress fibres and this is considered a high cell-matrix tension state (Arora and McCulloch, 1994; Hinz et al., 2001a). Stress-relaxation upon release of restrained FPCLs that have developed tension results in isotonic contraction as the cells shorten in an attempt to maintain tension. The loss of tension during stress-relaxation has been shown to result in rapid disassembly of stress fibres (Hinz et al., 2001b). More specifically, following FPCL stress-relaxation, degradation of α-SMA is observed within 2 minutes and after 10 minutes almost all stress fibres have disappeared (Tomasek et al., 1992). Furthermore, fibronectin matrix and fibronexus junctions are disrupted and cells and collagen lose their aligned orientation. FPCL contraction and stress-relaxation are frequently quantified by measuring the change in matrix diameter.

Many groups have examined cell contractility using isotonic contraction models. Increased contractility has been shown with rat lung fibroblasts expressing high levels of α-SMA, compared to rat subcutaneous fibroblasts expressing low levels of α-SMA (Hinz et al., 2001a). However, in Dupuytren's disease studies using isotonic contraction to compare nodule, cord and carpal ligament-derived cells have reported inconsistent findings. Whilst some groups reported no differences in contraction (Rayan and Tomasek, 1994; Tarpila et al., 1996), others have reported increased contraction only with early passage (passage 4) but not with late passage (passage 8) nodule-derived cells (Moyer et al., 2002), or in nodule-derived cells expressing higher levels of α-SMA as determined by immunofluorescence (Tomasek and Rayan, 1995). More recently, isometric contractile forces within restrained

FPCLs have been studied using a culture force monitor (CFM). FPCLs were cast and floated in medium, tethered between two flotation bars, one of which is held stationary whilst the other is attached to a force transducer (Eastwood et al., 1994; Eastwood et al., 1996). This allows real-time quantification of uniaxial isometric forces generated by cells within 3D collagen matrices. FPCLs with a high aspect-ratio (ratio of length/ width/ thickness) have been shown to produce increased strain gradients, resulting in longitudinal fibroblast alignment within the collagen lattice (Eastwood et al., 1998). This best reflects cell morphology in Dupuytren's cord, where fibroblasts are longitudinally aligned amongst collagen fibres along the major axis of the cord (Luck, 1959).

Using this model, dermal fibroblasts seeded in FPCLs contracted and reached a plateau (Brown et al., 1998). This study measured forces generated by dermal fibroblasts in response to changes in applied load using a tensional CFM. Increased external loading was followed immediately by a reduction in cell-mediated contraction, whilst decreased external loading elicited increased contraction. In contrast, Dupuytren's nodules and cord-derived cells up to cell passage five did not reach plateau and generated significantly greater isometric contractile force than control carpal ligament fibroblasts over a 20 hour test period (Bisson et al., 2004).

Myofibroblasts contract and do not reach a plateau. The mechanism for their contraction is not entirely understood. Myofibroblasts can sustain a contractile force over long periods of time and this force is generated by contractile stress fibres which are composed of actin microfilaments and associated with non-muscle myosin and other actin-binding proteins (Burridge and Chrzanowska-Wodnicka, 1996; Serini and Gabbiani, 1999; Tomasek et al.,

2002). Previously it has been demonstrated that contraction in myofibroblasts is regulated by myosin light-chain (MLC) phosphorylation and is mediated via the Rho/Rho-kinase pathway. In contrast, SMC rely on intracellular calcium influx for immediate and rapid increases in force generation (Kamm and Stull, 1989), whereas elevation of intracellular calcium has been shown not to promote contraction of myofibroblasts within collagen lattices or granulation tissue (Parizi et al., 2000; Tomasek et al., 2006). Furthermore, differentiated myofibroblasts in wound granulation tissue do not contract in response to an agonist when treated with the Rho kinase inhibitor Y27632 (Tomasek et al., 2006). However, others have reported that myofibroblast contraction is regulated by changes in intracellular calcium concentration and MLC kinase (MLCK) (Goto et al., 1998; Levinson et al., 2004; Raizman et al., 2007). This difference in regulation of SMC and myofibroblast contraction may relate to their functional differences. SMCs contract and relax in response to their environment, whereas myofibroblasts need to generate continuous force over long periods of time and contraction might result in irreversible tissue contractures (Tomasek et al., 2002).

A recent study has examined how spontaneous changes in the intracellular calcium concentration contribute to myofibroblast contraction. Contractile events were assessed by tracking stress-fibre-linked microbeads and by atomic force microscopy (Castella et al., 2010). Myofibroblasts exhibit periodic calcium oscillations that control small and weak contractions. Whilst depletion of intracellular calcium reduced these micro-contractions, cell isometric tension was unaffected as assessed by growing cells on deformable substrates. Inhibition of Rho- and ROCK-mediated calcium-independent contraction demonstrated no effect on micro-contractions, but abolished cell tension. The authors proposed that Rho-

and ROCK dependent isometric tension generates slack in extracellular matrix fibrils, which are then accessible for the low-amplitude and high frequency contractions mediated by intracellular calcium. This study used atomic force microscopy to investigate isometric force generation in a non-3D environment and, whilst it may provide an explanation for contraction, the findings do not account for how contraction is further propagated once individual cells are fully contracted and the matrix has been remodelled (Castella et al., 2010).

1.13 Extracellular matrix components

The ECM is a complex 3D environment composed of a structural network of connective tissue fibres that provides support and protection for cells. The ECM is dynamic, with constant turnover of its various components including collagen and elastin contained within a ground substance of various proteins, proteoglycans and hyaluronates (Alberts et al., 2002). Myofibroblasts significantly contribute to synthesis of the constituents of the ECM.

Collagen is a major component of the ECM and the most prevalent and ubiquitous is type I collagen (Prockop and Kivirikko, 1995). Types I, III, IV, V and VI collagen have been reported to be the most common myofibroblast products (Naugle et al., 2006; Schurch et al., 2006). In Dupuytren's disease fascia there is an elevated level of total collagen and an alteration in the collagen III/I ratio according to the phase of the disorder (Brickley-Parsons et al., 1981). This study reported that initially more collagen type III was produced compared to type I and that the balance normalises as the tissues mature. However, the increased type III/I collagen ratio has also been explained by reduced type I collagen production in cell cultures of Dupuytren's disease fibroblasts compared to age and sex matched control carpal

ligament-derived fibroblasts (Murrell et al., 1991). Type-III collagen, which is virtually absent from normal adult palmar fascia, has been shown to comprise up to 40% of total collagen in Dupuytren's tissue. Interestingly, type-III collagen was also abundant in clinically 'normal' fascia of patients with established Dupuytren's disease, suggesting that the disease is widespread throughout the fascia (Brickley-Parsons et al., 1981).

Myofibroblasts are highly active in ECM synthesis and in Dupuytren's disease as in many other fibrotic diseases, matrix metalloproteinases (MMPs), a related family of MMPs, a disintegrin and metalloproteinase domain with thrombospondin motif (ADAMTSs) and their tissue inhibitors of metalloproteinases (TIMPs) play an important role. Normal ECM turn-over depends on a balance between proteinase and inhibitor activities, whereby an imbalance of proteolysis may lead to fibrosis (Brinckerhoff and Matrisian, 2002). An interest in the role of MMPs in Dupuytren's disease began in the 1980s following reports that the use of broad-spectrum MMP inhibitor (Marimastat) in clinical trials to reduce local cancer invasion and distant metastasis, was associated with the development of Dupuytren's disease and frozen shoulder (Hutchinson et al., 1998).

Several studies have looked at various MMPs and TIMPs in Dupuytren's disease. MMP-1, -2, -9 and TIMP-1 and -2 levels were measured in the sera of patients with Dupuytren's disease and compared to those who had carpal tunnel release. Significantly higher levels of TIMP-1 were found in Dupuytren's patients (Ulrich et al., 2003). Microarray analysis of gene expression in Dupuytren's disease and Peyronie's disease demonstrated increased expression of MMP-2 and -9 in the diseased tissues compared with normal palmar fascia and tunica albuginea (Qian et al., 2004). In contrast, a comparison of Dupuytren's tissue

with frozen shoulder and control shoulder tissue showed that MMP-1, -2, -9 and TIMP-1 was expressed in all tissues and MMP-3 was absent from Dupuytren's tissue, whilst MT1-MMP was increased in Dupuytren's tissue compared with control normal shoulder tissue (Bunker et al., 2000). Interestingly, increased MMP-1, -2 and -9 expression has been reported in Dupuytren's tissue in response to mechanical load using an external fixator (Bailey et al., 1994; Tarlton et al., 1998) and this was accompanied by an increase in newly synthesised collagen following tissue extension and remodelling. More recently a complete expression profile of MMPs in Dupuytren's nodules compared to normal palmar fascia taken from patients who had carpal tunnel release was been performed using real-time reverse-transcription polymerase chain reaction (RT-PCR). MMP-1, -7, -13, MT1-MMP, ADAMTS-14 and TIMP-1 were all significantly increased in Dupuytren's nodules compared to control tissue (Johnston et al., 2007). The same authors subsequently reported significant correlation between several MMPs and ADAMTSs and recurrent fixed flexion deformity over a 14 month follow-up period (Johnston et al., 2008).

Recent studies have also analysed the effects of a broad spectrum MMP inhibitor (ilomastat) on isotonic contraction of FPCLs seeded with Dupuytren's nodule-derived cells, cord cells and compared to control cells from control carpal ligament. Treatment of FPCLs with MMP inhibitor (100μM ilomastat) significantly reduced isotonic contraction and led to concomitant suppression of MMP-1 and -2 as determined by western blot analysis and gelatin zymography (Townley et al., 2008). The same authors also demonstrated reduced isometric force contraction in the CFM using cells derived from the same tissues (Townley et al., 2009).

This group also examined the differences in residual matrix tension (RMT) following the addition of cytochalasin D to FPCLs following 48 hours contraction in the CFM (Townley et al., 2009). Cytochalasin D inhibits actin-dependent processes and, therefore, uncouples fibroblast force generation from the collagen matrix. They found significantly greater RMT in nodule-derived cells compared to control cells following treatment with cytochalasin D. However, in FPCLs treated with ilomastat no significant difference in RMT was observed following addition of cytochalasin D, suggesting that isometric force generation is in part determined by MMP associated matrix remodelling and in part by the cell contraction.

An essential component and a reliable marker of the myofibroblast ECM is fibronectin (FN). Increased FN production, and in particular the expression of fibronectin ED-A splice variant, has been shown to play a role in cell migration, adhesion, cell morphology and myofibroblast differentiation (Hynes, 1990). In Dupuytren's tissue, fibronectin ED-A and ED-B expression has been demonstrated using indirect immunofluorescence, immunohistochemistry and by PCR (Berndt et al., 1995; Halliday and Tomasek, 1995; Kosmehl et al., 1995). More recent studies have shown that fibronectin ED-A contains cryptic domains that unfold upon cell traction and is required for TGF-β1 induced myofibroblast differentiation (Serini et al., 1998; Vogel and Sheetz, 2006). It has, therefore, been proposed that tension within the ECM may promote myofibroblast differentiation by revealing cryptic epitopes in ECM proteins under stress.

Tenascin-C, another glycoprotein, is also a component of the myofibroblast ECM which is associated with tissue repair (Chiquet-Ehrismann and Chiquet, 2003). It has been shown to be upregulated in Dupuytren's nodules (Berndt et al., 1995) and in Dupuytren's cord tissue

compared to control palmar fascia (Kuhn et al., 2002; Lee et al., 2006; Shih et al., 2009b). It is also upregulated in other fibrotic diseases, including keloid and hypertrophic scars (Dalkowski et al., 1999; Kaarteenaho-Wiik et al., 2000). Retinoids appear to downregulate the tension of fibroblasts in FPCLs by the induction of tenascin-C (Yamada et al., 1999). Conversely, tenascin-C stimulates migration, differentiation and contractility of cardiac myofibroblasts derived from tenascin-C null mice show reduced myofibroblast development after cardiac injury. Therefore, the effects of tenascin-C remain unclear and this multi-domain hexameric molecule may have different effects in different systems.

Periostin is an ECM component of many collagen-rich connective tissues that are subjected to mechanical stress-tension (Norris et al., 2007) and periostin mRNA levels are highly up-regulated in Dupuytren's nodule and cord tissue relative to normal palmar fascia (Shih et al., 2009b). A recent study on the effects of periostin on fibroblasts derived from whole Dupuytren's cord compared to normal fascia has suggested that perisotin treatment may promote the myofibroblast phenotype through increased α-SMA expression by western blot analysis and increased isotonic contraction of FPCLs seeded with Dupuytren's's cells compared to normal fascia (Vi et al., 2009).

1.14 AGEs and RAGE

Recently studies have suggested that advanced glycation end-products (AGEs) and the receptor for advanced glycation end-products (RAGE) are implicated in cell dysfunction, fibrosis (Li et al., 2004; Oldfield et al., 2001) and mechanisms of inflammatory disease (van Beijnum et al., 2008). RAGE is a multiligand receptor that has also specifically been implicated in driving sterile inflammation (Sims et al., 2010). There is widespread expression

of RAGE on vascular endothelial cells, neutrophils, monocytes/macrophages, lymphocytes (Brett et al., 1993) and dermal fibroblasts (Niu et al., 2008). RAGE expression is amplified in circumstances when ligands, such as AGEs, and inflammatory mediators accumulate (Schmidt et al., 1993). Activation of RAGE had been shown to mediate signalling pathways upstream of pro-inflammatory mediators such as TNF-α (Vlassara et al., 1988) thus prompting the hypothesis that this receptor may be key to the initiation of inflammation. The RAGE promoter contains multiple functional NF-κB and SP-1 transcription factor–binding sites (Huttunen et al., 1999; Li et al., 1998), and therefore, ligands and proinflammatory cytokines can also further promote the expression of RAGE.

AGE-modified proteins are the final products formed from the irreversible non-enzymatic glycation between reducing sugars and polypeptides (Vlassara et al., 1994) and have been shown to exert their influence by forming protein cross links that alter ECM structure and function as well as interacting with cell surface receptors (Neeper et al., 1992). AGEs are found in the plasma and accumulate in various tissues during ageing (Brett et al., 1993) and occur at higher levels in diabetes (Makita et al., 1991; Makita et al., 1992). The interaction between AGEs and their binding proteins also activates multiple signal transduction pathways, leading to the secretion of inflammatory cytokines, up-regulation of adhesion molecules and the production of cytokines, including TGF-β1 and platelet derived growth factor (PDGF) (Throckmorton et al., 1995), tumour necrosis factor alpha (TNF-α) and interleukin-1 (IL-1) (Vlassara et al., 1988).

The interaction of AGE with RAGE has also been shown to induce a TGF-β1 dependent epithelial-myofibroblast transdifferentiation in a proximal renal tubule cell line (Li et al.,

2004; Oldfield et al., 2001) and has also been suggested to induce the myofibroblast phenotype in peritoneal fibrosis (De Vriese et al., 2006). It has been demonstrated that specific binding of ^{125}I-AGE-BSA to cell membranes in a rat proximal tubule cell line showed the binding site was RAGE. Furthermore, AGE exposure induced dose-dependent myofibroblast differentiation determined by morphological changes and de novo α-SMA expression, and these effects were blocked with antibodies against RAGE of TGF-β1 (Oldfield et al., 2001). This group further confirmed de novo α-SMA expression by immunocytochemistry, mRNA and protein levels (Li et al., 2004). This study also demonstrated that AGEs activate the RAGE-ERK1/2 MAP kinase pathway to mediate the early myofibroblast differentiation process. When these findings are considered in combination with the previously reported association between diabetes and Dupuytren's contracture (Arkkila et al., 1996), they suggest a possible role for AGE dependent differentiation of myofibroblasts in Dupuytren's disease.

1.15 Growth factors and cytokines

There is now considerable evidence demonstrating raised levels of various cytokines and growth factors in Dupuytren's disease. These include Interleukin-1 (IL-1), basic fibroblasts growth factor (bFGF), TGF-β1, TGF-β2, epidermal growth factor (EGF), platelet-derived growth factor (PDGF) and connective tissue growth factor (CTGF) (Baird et al., 1993; Bunker et al., 2000; Igarashi et al., 1996; Kuhn et al., 2001; Terek et al., 1995). This has led to studies of their role in Dupuytren's disease in stimulating cell proliferation, contraction and ECM production.

PDGF expression is higher in Dupuytren's tissue compared to normal fascia as determined by southern blotting and immunohistochemistry (Terek et al., 1995). It has also been shown that PDGF is highly expressed in myofibroblast-rich nodules (Badalamente et al., 1992). Cells from Dupuytren's tissue and control normal palmar fascia exposed to PDGF and bFGF also demonstrated increased proliferation rates and increased collagen synthesis. An early study on 12 Dupuytren's disease cords and 12 normal palmar fascia controls found significantly increased expression of IL-1α, IL-1β, TGF-β1 and bFGF by RT-PCR. However, no siginificant difference in PDGF-α or -β were found (Baird et al., 1993).

Using RNA in situ hybridisation and immunhistochemistry, it has been demonstrated that TGF-β1, TGF-β2, bFGF and fibronectin ED-A and B are localised in proliferating α-SMA positive nodules. Furthermore, the expression of TGF-β1, 3 and bFGF in peri-nodular tissues was also increased, implying a role for these growth factors in recruitment of quiescent fibroblasts (Berndt et al., 1995). TGF-β1 is recognised as the major growth factor promoting myofibroblast differentiation by inducing expression of α-SMA (Desmouliere et al., 1993) as well as ECM proteins, including collagen (Alioto et al., 1994; Werner and Grose, 2003), integrins (Riikonen et al., 1995) and a number of cytoskeletal proteins that make up the myofibroblast contractile apparatus (Malmstrom et al., 2004). The TGF-β family exerts its effects mainly through Smad signal transduction pathways to regulate α-SMA expression (Derynck and Zhang, 2003).

Upregulation of all three isoforms of TGF-β is seen on immunohistochemical staining of Dupuytren's specimens (Badalamente et al., 1996) and also by DNA microarray analysis in Dupuytren's cord and para-cord fascia when compared to normal control palmar fascia. In

this study there was a 10-20 fold increase in TGF-β2 expression in cord tissue as assessed by RT-PCR (Lee et al., 2006). Three forms of TGF-β receptor (I, II and III) have also been demonstrated in Dupuytren's fibroblasts compared to normal adult skin fibroblast controls (Kloen et al., 1995). TGF-β1 and 2 are potent stimulators for cell proliferation in Dupuytren's disease (Badalamente et al., 1996) and in FPCLs seeded with Dupuytren's nodule-derived fibroblasts, both have also been shown to be associated with greater isotonic and isometric force contraction as compared to FPCLs with fibroblasts from normal fascia when treated with TGF-β1 (Bisson et al., 2009; Brown et al., 2002; Kuhn et al., 2002; Wong and Mudera, 2006). Whilst these studies show dose dependent contractile differences between these cell types, increased contractility of FPCLs in response to TGF-β1 were found in all cell types and have also been reported by many authors using normal dermal fibroblasts (Arora et al., 1999; Grinnell and Ho, 2002; Liu et al., 2001; Vaughan et al., 2000).

TGF-β1 has also been shown to act synergistically with other cytokines, including EGF and connective tissue growth factor (CTGF) (Folger et al., 2001; Kloen et al., 1995). CTGF potentiates the profibrotic action of TGF-β1 and also induces fibroblast proliferation, but does not substitute for the action of TGFβ-1 as α-SMA remains unchanged after the addition of CTGF to cultures of corneal fibroblast (Folger et al., 2001).

Certain soluble factors have also been shown to antagonise TGF-β1 and hence reduce myofibroblast differentiation. The inflammatory mediator, IL-1 has been shown to inhibit TGF-β1 induced α-SMA expression in cultured dermal fibroblasts when added as a recombinant protein. Controlled secretion of IL-1 alpha and beta by keratinocytes when co-cultured with fibroblasts may be a mechanism for suppressing myofibroblast differentiation

in early wounds (Shephard et al., 2004). IL-1 beta has been shown to be abundantly expressed in Dupuytren's fascia (Baird et al., 1993). IFN-γ, a cytokine produced by T cells, has also been shown to reduce α-SMA mRNA and protein expression in cultured rat subcutaneous fibroblasts (Desmouliere et al., 1992) and Dupuytren's myofibroblasts (Tanaka et al., 2007). In an earlier clinical trial, IFN-γ was injected into hypertrophic scars and Dupuytren's contracture of 14 patients and demonstrated some therapeutic effects with a decrease in size of the lesions, although not complete resolution. Using immunofluorescence techniques, the authors also showed that IFN-γ qualitatively decreased α-SMA expression level in these contractile lesions (Pittet et al., 1994).

TNF-α is another potent inflammatory cytokine and high levels of TNF-α mRNA have been reported in Dupuytren's cord tissue compared to tissue from frozen shoulder and control shoulder tissue (Bunker et al., 2000). TNF-α has been shown to inhibit TGF-β1 induced expression of α-SMA and collagen 1A, via inhibition of Smad3 phosphorylation of JNK pathway in human dermal fibroblasts using both western blot analysis and RT-PCR. Cells in this study were derived from normal adult skin. Furthermore, this study demonstrated a decrease in collagen matrix stiffness and isotonic contraction after 5 days in culture (Goldberg et al., 2007). Similar findings have also been reported using myofibroblasts derived from human hip joint tissue (Mattyasovszky et al., 2010). Although in this study TNF-α demonstrated a suppressive effect on myofibroblasts derived from hip joint capsule, it was also found to promote cell proliferation and viability in the same study. Furthermore, increased proliferation of human dermal microvascular endothelial cells with TNF-α has also been reported, suggesting that TNF-α may play a role in myofibroblast induction (Chaudhuri et al., 2007).

Finally, significant time-dependent upregulation of vasoactive prostaglandin E_2 (PGE_2) synthesis has been shown in myofibroblast rich tissue (Mattyasovszky et al., 2010). Vasoactive prostaglandins including PGE_2 have previously been shown by immunohistochemistry to localise to myofibroblast-rich Dupuytren's nodules and the increased expression of PGE_2 in Dupuytren's nodules compared to control normal fascia has been previously demonstrated by radioimmunoassay (Badalamente et al., 1988). The consequences of PGE_2 in Dupuytren's disease have not been further examined.

1.16 Matrix cell Adhesions and stress perception

Ultrastructural analysis of myofibroblasts in Dupuytren's disease, granulation tissue and other fibrotic conditions has shown extensive cell-matrix attachment sites, called fibronexi (Dugina et al., 2001; Tomasek et al., 1987; Tomasek and Haaksma, 1991). Fibronexi are specialised adhesion complexes that use transmembrane integrins to link intracellular actin with extracellular fibronectin fibrils and can help distinguish myofibroblasts from fibroblasts and SMCs (Eyden, 2005; Tomasek et al., 1999). Actin bundles terminate at the myofibroblast surface at these fibronexi and functionally provide a mechano-transduction system, whereby force generated by stress fibres can be transmitted to the surrounding extracellular matrix and, equally, stress within the matrix can be perceived by myofibroblasts.

In vitro, myofibroblasts develop specialised "supermature" focal adhesions (FAs), so called because they are significantly longer (8-30 µm) (Dugina et al., 2001), compared to "classical" FAs (2-6 µm) of α-SMA negative fibroblasts (Geiger et al., 2001). What also marks out these supermature FAs in myofibroblasts is that they co-express high levels of vinculin, paxillin,

tensin, αvβ3 and α5β1 integrins, unlike classical FAs of fibroblasts which do not express tensin and α5β1 integrin (Dugina et al., 2001; Hinz et al., 2003). Separately, fibrillar adhesions express tensin and and α5β1 integrin, but not vinculin, paxillin and αvβ3 integrin (Geiger et al., 2001).

Establishing these supermature FAs depends on the intracellular contractility generated by α-SMA and on stress resistance provided by the ECM (Hinz, 2006). When myofibroblasts are cultured on soft substrates and in newly polymerised collagen gels, they convert supermature FAs into smaller classical FAs (Goffin et al., 2006; Hinz, 2006). Specifically, it has been shown that myofibroblasts cultured on less than 6μm adhesion islets rapidly lose α-SMA, whereas dynamically enlarging these islets to 8.1μm islets on extendable membranes was shown to result in reincorporation of α-SMA in to stress fibres (Goffin et al., 2006). In this key study, arrays of fibronectin islets were created on glass by microcontact printing whereas non-printed regions were chemically modified against cell attachment. Furthermore, resizing classical to supermature FAs was shown to allow application of approximately 4 fold greater stress (Goffin et al., 2006), making myofibroblasts very adhesive to the ECM (Hinz et al., 2003). These findings suggest that α-SMA is a mechanosensitive protein that is recruited to stress fibres under high tension and that myofibroblasts sense the mechanical environment of the ECM by assessing tension in stress fibres, which in turn is determined by the size of their matrix adhesions. However, it remains uncertain whether the primary event is α-SMA stress fibre generated tension or FA supermaturation. Regardless, effective myofibroblast contraction only occurs when the ECM has been sufficiently remodelled.

1.17 The mechanical environment and myofibroblasts

The myofibroblast phenotype is critically influenced by the mechanical microenvironment. In particular the organisation and stiffness of the ECM plays a key role in differentitation of fibroblasts into myofibroblasts (reviewed in Hinz, 2007). Resident or quiescent fibroblasts in intact tissues are considered to be "stress-shielded" by the ECM and lack the contractile stress fibres observed in myofibroblasts but instead have actin microfilaments organised predominantly in to a cortical meshwork (reviewed in Tomasek et al., 2002). When the protective mechanical microenvironment of the ECM is altered or lost through injury, fibroblasts try and re-establish matrix tension by increased ECM remodelling (Marenzana et al., 2006) and In mechanically restrained gels tension gradually increases and first induces the formation of α-SMA negative stress fibres (Marenzana et al., 2006; Tamariz and Grinnell, 2002). Quiescent fibroblasts respond to changes in ECM organisation, composition and mechanical properties following tissue damage (Hinz and Gabbiani, 2003) and acquire a migratory phenotype by developing de novo contractile bundles or stress fibres that are composed of cytoplasmic actins and capable of generating small tractional forces (Hinz et al., 2001b). These activated fibroblasts have been given the term "proto-myofibroblasts", distinguishing them from quiescent fibroblasts that lack these stress fibres (Tomasek et al., 2002). Increasing matrix stiffness due to remodelling by proto-myofibroblasts, leads to myofibroblast differentiation and de novo expression of α-SMA which organises transitorily in the cytoplasm, and only once a significant intracellular threshold tension has been reached is α-SMA incorporated to stress fibres (Goffin et al., 2006; Hinz, 2006). In vivo the appearance of proto-myofibroblasts has been shown in 5 to 6 day old granulation tissue and after 8-9 days in wounds in a rat model (Hinz et al., 2001b).

Whilst myofibroblast differentiation is precisely regulated by TGF-B1 (Desmouliere et al., 1993) and FN ED-A (Serini and Gabbiani, 1999), the mechanical environment is also crucial as α-SMA is a mechanosensitive protein that is recruited to stress fibres only under significant mechanical load (Goffin et al., 2006). Increasing the matrix rigidity using collagen or polyacryamide gel substrates of varying stiffness led to increased α-SMA expression in cultured fibroblasts (Arora et al., 1999; Hinz et al., 2003), whereas reducing stress fibre tension by reducing substrate stiffness has been shown to lead to disassembly of α-SMA from stress fibres and accumulates in cytosolic aggregates that resemble short rods (Goffin et al., 2006). Similarly *in vivo,* preventing wound closure by mechanically splinting the edges of experimental wounds accelerates expression of α-SMA compared with normally healing wounds and stress release by removing these mechanical splints leads to a reduction in α-SMA expression (Hinz et al., 2001b).

Threshold stiffness for incorporation of α-SMA in stress fibres has also been examined in contractile wound granulation tissue and in myofibroblasts cultured on elastic substrates and shown to be around 20,000Pa (Goffin et al., 2006). For comparison matrix stiffness measured in granulation tissue towards the end of wound healing and has been shown to be greater than 50,000Pa (Goffin et al., 2006), whereas the stiffness of provisional ECM wounds has been shown to be comparable to newly polymerised gels and approximately 10-100Pa (Kaufman et al., 2005).

In Dupuytren's disease, it has been observed clinically that after simple division of Dupuytren's tissue (fasciotomy), cords which are no longer under tension, soften and temporarily disappear (Hueston, 1992). Reducing skin tension following fasciotomy by a

single Z-plasty has also shown a significant reduction in recurrence at 2 years (Citron and Hearnden, 2003). Using the CFM to measure isometric force generated by FPCLs, nodule-derived cells reacted to initial mechanical overloading with increased force development, instead of the relaxation seen with control carpal ligament cells. The failure of nodule-derived cells to reach 'tensional homeostasis' suggests that Dupuytren's myofibroblasts favour a higher baseline level of matrix stress for tensional homeostasis, or that the phenomenon of tensional homeostasis may be absent in Dupuytren's nodule-derived cells (Bisson et al., 2004). It may be that Dupuytren's nodule-derived cells are unable to appropriately detect the level of extracellular load and subsequently over-estimate actual stress which in turn results in over contraction. It was subsequently shown that the addition of TGF-β1, resulted in significant increase in force from all cell types seen particularly during the early phase of fibroblast attachment and with an overall increased rate of FPCL contraction in response to overloading (Bisson et al., 2009).

The differences in isometric force contraction between Dupuytren's myofibroblasts and control fibroblasts lend further support to the notion that myofibroblasts are influenced by their mechanical environment, although these observations have not been correlated with levels of α-SMA expression using this model.

1.18 Apoptosis

It has been shown that myofibroblasts are abundant in Dupuytren's nodules, especially during active disease (Chiu and McFarlane, 1978) and the proliferative and involutional phase of disease (Schurch et al., 1990). In contrast, reduced numbers of fibroblasts and myofibroblasts have been reported in advanced disease (Chiu and McFarlane, 1978),

whereas residual phase nodules have been described as hypocellular with mature fibroblasts (fibrocytes) present (Schurch., et al. 1990). The fate of the numerous myofibroblasts remains unclear.

In vitro, several studies have tried to reverse differentiated myofibroblasts in an attempt to develop therapeutic targets to inhibit their formation. Down-regulation of α-SMA has been shown in response to TGF-β1 antagonists, various growth factors, cell density and matrix compliance (Hinz, 2007).

However, *in vivo*, reversal of the myofibroblast phenotype is not seen and instead during wound healing, massive apoptosis occurs following re-epithelialisation (Desmouliere et al., 1995). Whilst the process that leads to apoptosis remains unclear, it has been proposed that at the end of physiological tissue repair, cell release from stress or increased formation of cell-cell contacts may account for this 'group' myofibroblast disappearance. Once fully repaired, the ECM regains its original mechanical properties and 'stress-shields' the resident fibroblasts. In a rat model, where the wound was splinted with a sutured metal template, thereby preventing tension release, myofibroblast apoptosis was inhibited and subsequent splint removal was followed by a reduction in myofibroblast numbers (Carlson et al., 2003).

Myofibroblast apoptosis has also been shown *in vitro* by relaxing stressed FPCLs seeded with human foreskin derived fibroblasts (Grinnell et al., 1999). These authors found that approximately 15% of cells apoptosed within 3 to 6 hours and reached a plateau by 24 hours. Although the pathways linking stress and apoptosis remain unclear, it is likely to involve cell matrix junctions and similar stress perception mechanisms used in the transition from fibroblast to myofibroblast (Reddig and Juliano, 2005; Stupack and Cheresh, 2002).

1.19 Summary model of key steps in myofibroblast differentiation.

Figure 1.11 below summarises key relations between matrix stiffness, adhesion maturation, α-SMA expression during differentiation of a fibroblast to proto-myofibroblast and finally in to a fully differentiated myofibroblast.

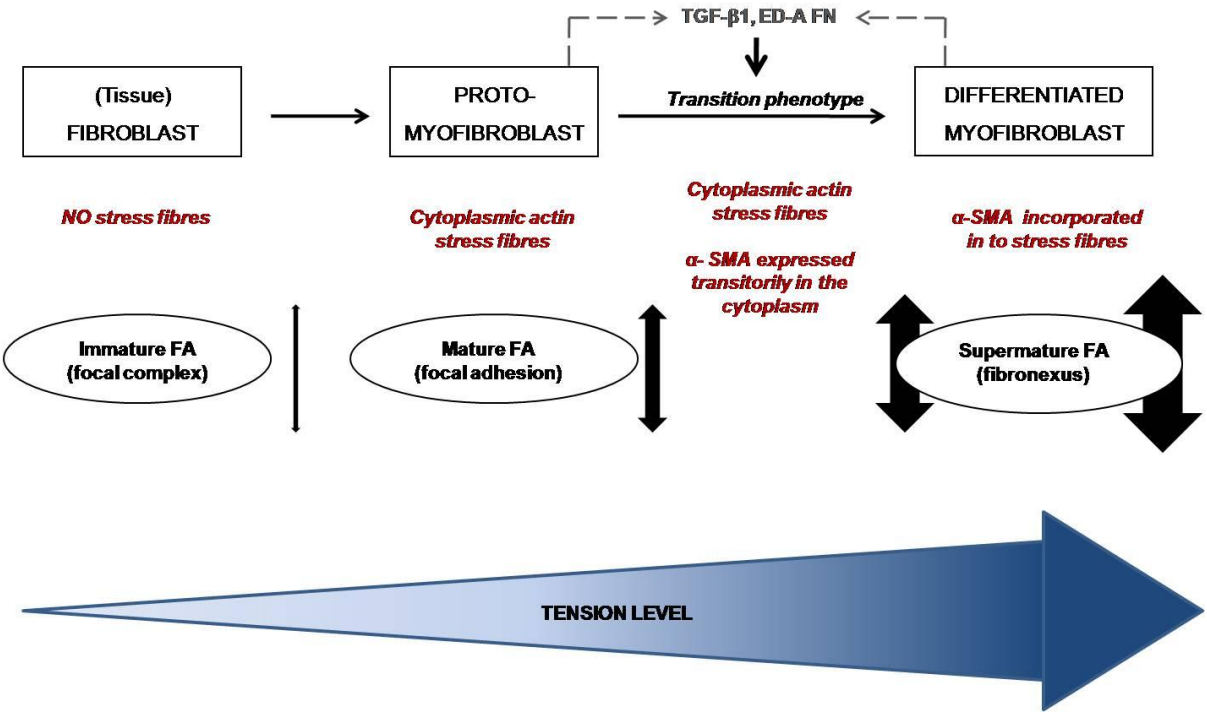


Figure 1.11. Summary model of fibroblast to myofibroblast differentiation. In most normal tissues and on compliant substrates, fibroblasts express immature if any cell-matrix contacts and have no stress fibres. These small complexes (immature FAs) are sufficient to initiate local cell remodelling activity that leads to gradual increase in matrix stiffness and tension development. The formation of the proto-myofibroblast phenotype is dependent on this increasing matrix tension and is characterised by the development of mature focal adhesions (FA) and contractile stress fibres that are composed of only cytoplasmic actins. These stress fibres exert further contractile force and in turn further increase matrix tension, leading to the maturation of FAs. The co-ordinated action of tension, TGF-β1 and ED-A FN induce de novo expression of α-SMA which organises transitorily in cytoplasmic rod-like structures. As adhesions grow to the size of supermature FAs, intracellular tension reaches a critical level that allows incorporation of α-SMA in to the pre-existing stress fibres. This defines myofibroblast differentiation and results in further contractile force generation (adapted from Hinz B, European Jouran of Cell Biology, 2006).

1.20 Hypothesis

This thesis sets out to test the hypothesis that in Dupuytren's disease the myofibroblast phenotype is regulated by dermal fibroblasts and inflammatory mediators, specifically advanced glycation end products (AGEs) and TNF-α.

1.21 Aims and objectives of this study

1. I aim to systematically characterise the distribution of α-SMA positive cells throughout excised Dupuytren's tissue and examine if the presence of α-SMA rich nodules correlates with fixed flexion deformity and primary or recurrent disease.

2. I aim to establish a reliable *in vitro* model of Dupuytren's disease by comparing the isotonic and isometric contractile profiles of matched cells isolated from Dupuytren's nodules, non-palmar and palmar skin samples within 3D collagen lattices. Using this model I will compare α-SMA expression in Dupuytren's cells and dermal fibroblasts and based on the observation that recurrence is significantly reduced following dermofasciectomy, I will examine whether dermal fibroblasts can modulate Dupuytren's myofibroblast contractility.

3. Inflammatory mediators play a role in the pathogenesis of Dupuytren's disease and there is recent data that AGE-RAGE interaction may induce the myofibroblast phenotype in various cell types. The effects of both TNF-α and AGEs have not been examined in Dupuytren's disease. I aim to examine Dupuytren's tissue for inflammatory cells and RAGE expression, and based on the observation that early signs of Dupuytren's disease are often seen in the palmar skin, determine if AGEs or TNF-α can modulate the contractile phenotype of palmar skin fibroblasts.

CHAPTER TWO

Materials and methods

2.1 Reagents

2.1.1 General reagents

General reagents were purchased from the following sources: 10×phosphate buffered saline (PBS), sodium carbonate, sodium chloride, sodium hydroxide, methanol, isopropanol and acetic acid from VWR International GmbH (Darmstadt, Germany); sulphuric acid from BDH (VWR International); Trizma base (minimum 99.9% titration), glycine, ehtylenediaminetetraacetic acid (EDTA), Tween-20, bovine serum albumin (BSA), sodium *n*-dodecyl sulphate (SDS) and 38% paraformaldehyde (BioChemika) from Sigma-Aldrich (Dorset, UK).

2.1.2 Tissue culture reagents

All reagents used were of tissue culture grade and sterile. Reagents were purchased from the following sources: Dulbecco's modified Eagle's medium (DMEM) with high Glucose 4.5 g/l, L-Glutamine and Sodium Pyruvate, Ham's F-12 medium with L-glutamine, 1xRPMI-1640 with L-Glutamine, 100 X penicillin and streptomyocin (1000 U/ml penicillin and 10 mg/ml streptomycin), amphoterecin (250 µg/ml) and 1xTrypsin-EDTA solution from PAA Laboratories Ltd. (Somerset, UK); 10xRPMI-1640 medium, sterile dimethyl sulphoxide (DMSO) from Sigma-Aldrich Ltd (Dorset, UK); Heat Inactivated Foetal Bovine Serum (FBS) from Gibco (Invitrogen, Paisley, UK); Type I collagen (rat tail acid extracted) from First Link (UK); Glass slides from Menzel-Glaser (Braunschweig, Germany); Glass coverslips from VWR International; all plastic-ware for tissue culture from Invitrogen (Paisley, UK), BD Biosciences (Oxford, UK) and Corning BV (Amsterdam, The Netherlands), Trypan Blue Solution from Sigma-Aldrich (Dorset, UK).

2.1.3 SDS-PAGE reagents

Reagents were purchased from the following sources: bromophenyl blue, glycerol, N, N, N', N' Tetramethylethylenediamine (TEMED) from Merck Biosciences (UK); 30% (w/v) acrylamide/bis-acrylamide from Severn Biotech Ltd.; ammonium persulfate (APS) from Acros Organics; dithiothreitol (DTT) from AXXORA, Nottingham, UK; Prestained Precision Plus Protein standards from Bio-Rad Laboratories, Hemel Hempstead, UK.

2.1.4 Western blotting reagents

Reagents were purchased from the following sources: Dot blotting filter paper from Bio-Rad Laboratories, Hemel Hempstead, UK; nitrocellulose from GE Healthcare, Buckinghamshire, UK; polyvinylidene difluoride (PVDF) membrane, ECL substrate and Hyperfilm™ from Amersham Pharmacia Biotech, Little Chalfont, UK; Re-Blot Plus Strong Solution (10x) from Chemicon International (USA); dried skimmed milk from Tescos (UK).

2.1.5 General indirect immunofluorescence staining reagents

Reagents were purchased from the following sources: Alexa Fluor-488 phalloidin (A12379), Alexa Fluor-568 phalloidin (A12380) and Prolong Gold Antifade reagent from Invitrogen (Paisley, UK); DAPI staining for cell nuclei and 3.8% paraformaldehyde from Sigma-Aldrich (Dorset, UK); Triton X-100 from BDH (VWR International GmbH, Darmstadt, Germany).

2.1.6 FACS analysis reagents

Reagents were purchased from the following sources: goat serum (Sigma UK), normal human AB heat inactivated serum (PAA laboratories Ltd., Somerset, UK) and normal rabbit IgG (Santa Cruz Biotechnology, Inc., USA).

2.1.7 RT-PCR reagents

Reagents were purchased from the following sources: puReTaq Ready-To-Go PCR beads from GE Healthcare (UK); dATP, dCTP, dTTP, dGTP, random primers and UltraPure™ agarose from Invitrogen, Paisley, UK; Stratascript buffer, RNAse block, Stratascript reverse transcriptase from Stratagene, UK; ethidium bromide from BDH, (VWR International GmbH, Darmstadt, Germany); Loading sample buffer, 500 bp and 1 kb DNA ladders from Bio-Rad, Hemel Hempstead, UK. For real-time PCR, TaqMan Universal PCR Master Mix was purchased from AppliedBiosystems (UK).

2.2 Antibodies

Table 2.1. Summary of antibodies used in this study

Antigen	Specificity	Antibody type	Use	Dilutions	Raised in	Company, # no., (clone)
α-SMA	Human	MAb	IF	400	Mouse	Sigma, A-2547 (clone 1A4)
α-SMA	Hu, rabbit, mouse, chicken, goat	MAb	IHC	2000	Mouse	Sigma, A-5228 (Clone 1A4)
			WB	600		
			IF	400		
Desmin	Human	MAb	IHC	200	Mouse	DAKO, M0760 (Clone D33)
RAGE	Hu, mouse	PAb	IHC	2000	Goat	Abcam, ab7764
RAGE	Hu, mouse, rat, cow	PAb	IF	200	Rabbit	Abcam, ab37647
			WB	1000		
			FACs	100		
Vimentin	Hu, chicken, goat, mouse, rat	MAb	WB	1000	Mouse	Abcam, ab8978 (Clone RV202)
CD3	Human	MAb	IHC	300	Mouse	Vision Biosystems, NCL-CD3PS1 (clone PS1)
CD4	Human	MAb	IHC	50	Mouse	Vision Biosystems, NCL-CD4IF6 (Clone IF6)
CD68	Human	MAb	IHC	250	Mouse	DAKO, M0876 (Clone PGMI)
Mast cell tryptase	Human	MAb	IHC	400	Mouse	Vision Biosystems, NCL-MCT428 (Clone 10D11)
Neutrophil elastase	Human	MAb	IHC	200	Mouse	DAKO, M0752 (Clone NP57)
Alexa Fluor-488 anti-rabbit	Rabbit	PAb	IF	1000	Goat	Invitrogen, A11034
			FACs	1000		
Alexa Fluor-568 anti-mouse	Mouse	PAb	IF	1000	Goat	Invitrogen, A11031
HRP conjugated anti-rabbit	Rabbit	PAb	WB	3000	Donkey	GE Healthcare, NA9340V
HRP conjugated anti-mouse	Mouse	PAb	WB	3000	Sheep	GE Healthcare, NA9310V

AP, alkaline phosphatase; HRP, hydrogen peroxide; MAb, monoclonal antibody; PAb, polyclonal antibody; WB, Western blot; IF, immunofluorescence; IHC, immunohistochemistry; FACS, fluorescence activated cell sorting

2.3 Surgical model and sample collection

Dupuytren's tissue samples were obtained from patients undergoing elective surgery for either fasciectomy of dermofasciectomy for Dupuytren's disease between September 2006 and 2008 with informed consent (COREC no. 06/Q0403/95). The samples were collected from patients operated on by either Professor Jagdeep Nanchahal at Charing Cross hospital or by Ms. Dominique Davidson at St John's hospital in Livingston, Scotland. Both surgeons agreed and adopted a standardised method for the surgery. The procedure and implications of tissue donation were discussed with all patients and they were given an information sheet to read. Either myself or the clinicians mentioned above were present to answer any questions. Tissue samples were harvested and transported to London by overnight courier in sterile containers containing 20ml DMEM, 1x penicillin-streptomycin and 10% FBS. The samples were processed the following morning upon arrival. All samples were anonymised as per local ethics protocols and assigned a number, prefixed "SM" (Charing Cross hospital, London) or "ED" (St. Johns hospital, Edinburgh). Clinical details on disease progression were also collected for each patient using a standard Dupuytren's proforma and are also kept anonymised (Fig. 3.1).

For dermofasciectomy samples, three types of tissue were obtained from each patient: Dupuytren's tissue, palmar skin (uninvolved skin overlying Dupuytren's tissue) and non-palmar skin (full-thickness skin harvested from the groin). All palmar skin and Dupuytren's tissue samples were orientated with a distal marking suture. In Dupuytren's tissue samples the corresponding level of the proximal interphalangeal joint was also marked with a suture.

Note, the cells that I isolated were from surgical samples received from Charing Cross hospital or St John's hospital in Edinburgh (prefixed "SM" or "ED" as outlined in the previous section). However, also available for use in this project were Dupuytren's matched cells from Australia. These cells were isolated from patient samples obtained by Professor Nanchahal while he was based in Sydney (2006). These were anonymised and prefixed with the letter "D".

2.4 Cell isolation and tissue culture

2.4.1 Preparation of surgical samples

Dupuytren's tissue samples were processed in the lab and washed in sterile DMEM and cleaned of surrounding fatty and loose connective tissue. Skin samples were also washed and defatted up to the level of the dermis. In total 103 excised digital cord samples were processed for use in this study. Out of these, the latter 53 samples were marked intra-operatively with a distal marking suture and also a PIPJ marking suture. Cord tissue samples were either processed for histology and cell culture.

2.4.2 Cell isolation from matched tissue samples

Non-palmar and palmar dermal fibroblasts were isolated from whole skin samples. Matched Dupuytren's tissue (nodule or cord), palmar and non-palmar skin samples were thoroughly dissected into small pieces with sterile scissors, scalpel and forceps. The resultant finely "diced" tissue was digested in 20ml DMEM containing 5% FBS, 2mg/ml of type I collagenase (Worthington), and 0.15 mg/ml of DNase I (Roche) per 0.5g tissue for up to 3 hours at 37°C. Supernatant from the digested tissue was pipetted into a sterile falcon tube. Cell pellets

were obtained from the resultant suspension by centrifugation and then re-suspended in 20 ml DMEM with 10% FBS and plated in 175 cm^2 culture flasks for 24 hours. Cells were reviewed daily, with media changes every 3 to 4 days until they reached confluence. At this point cells were either harvested for experiments or frozen down for later use.

2.4.3 Cell culture

Unless stated otherwise, all cells were cultured in DMEM supplemented with penicillin-streptomycin (1x) and 10% FBS, in a 37˚C humidified incubator supplied with 5% CO_2. The fibroblasts were passaged upon ~80% confluence by trypsinisation. Cells between passages 1 and 5 were used for the experiments except where stated otherwise.

For indirect immunofluorescence studies, RT-PCR and western blotting, fibroblasts were plated in 24 well plates at a density of $4x10^5$/ml (unless stated otherwise), on sterilised 13 mm diameter glass coverslips and cultured in DMEM supplemented with 10% FBS and penicillin-streptomycin (1x) and incubated at 37˚C, 5% CO_2. In experiments carried out to assess the effects of TGF-β1, TNF-α or AGE-BSA on palmar skin fibroblasts over time, DMEM was supplemented with 2% FBS and penicillin-streptomycin (1x). In these experiments, cells were incubated for 2 hours before TGF-β1, TNF-α, AGE-BSA or BSA (buffer volume) was added directly to the media at the specified concentration and incubated for the required time period. The dishes were then removed from incubation and examined under x10 magnification on a light microscope (Olympus ULWCD 0.30, Japan) and changes in cell shape or confluence were noted before processing further.

2.4.4 Dupuytren's nodule-derived cell line (sourced from Japan)

Three myofibroblast cell lines sourced from Japan and derived from Dupuytren's nodules were also available for use in this study. These cells were described in the literature as having been derived by sub-culturing Dupuytren's nodule-derived cells over 2 years and to comprise a homogenous population of myofibroblasts (Tanaka et al., 2007; Yuba et al., 2007). I therefore set up collaboration with Dr Tanaka (Kinki University School of Medicine, Osaka, Japan) and was supplied with these cell lines for use in this project. All three cell lines were cultured in MEM (with Earle's Salts and L-Glutamine), penicillin-streptomycin (1x) and 20% FCS, and incubated at 37˚C, 5% CO_2. The culture media and conditions used were exactly as advised by the collaborators.

2.4.5 Cell Counting

Cells were counted using a haemocytometer (Improved Neubaur by Hawksley) prior to use in experiments. The number of cells counted in the sixteen-square area of the haemocytometer was multiplied by $1x10^4$ to give the total number of cells per ml. This figure was then multiplied by the volume (ml) in the culture to give the total number of cells.

2.4.6 Cell viability

Cell viability was checked using Trypan Blue Solution exclusion studies. Trypan Blue Solution is a dye excluded from viable cells but taken up by those that are not. Uptake of Trypan Blue Solution in to cells is verified by studying cells under the microscope (Olympus ULWCD 0.30, Japan) . Cells were diluted 1:1 with Trypan Blue Solution and placed in a haemocytometer

for counting. The final count calculated was multiplied by 2 to allow for dilution in Trypan Blue Solution.

2.4.7 Freezing and thawing cells

Cells were frozen in FBS supplemented with 10% DMSO in 1ml cryovials. Approximately 1-3 $x10^6$ cells per ml were frozen in cyrovials and placed in a NALGENETM Cryo 1°C Freezing Container (containing Iso-propylalcohol) at -70°C for 24 hours. After 24 hours cryovials were transferred to long term liquid nitrogen stores. To thaw, cells were warmed up rapidly in a 37°C waterbath and washed in culture media to remove DMSO as soon as possible to prevent DMSO toxicity to cells as they warmed up. Cells were counted and viability checked using Trypan Blue Solution.

2.5 Immunohistochemistry

Immunohistochemistry staining was used to analyse α-SMA, desmin, RAGE, CD3, CD4, CD68, mast cell tryptase and neutrophil elastase expression in the Dupuytren's cord, palmar and non-palmar skin.

Dupuytren's tissue samples were longitudinally bisected, fixed in 10% neutral buffered formalin (Cellstor, Cellpath, Powys, UK), embedded in paraffin wax and 7 µm sections from the cut surface processed for immunohistochemistry. Palmar and non-palmar skin samples were cut in cross-section, and similarly fixed in 10% neutral buffered formalin, embedded in paraffin wax and 7 µm sections from the cut surface processed for immunohistochemistry.

Sequential sections were stained with Haematoxylin and Eosin (H&E) and also with the panel of antibodies outlined in Table 2. Outlined in this table are also methods used for antibody detection and retrieval. Species appropriate serum was used at the same protein concentration as the antibody solutions for negative controls. Tissue blocks were processed by David Essex according to standard Charing Cross hospital departmental protocols.

Specific methodology employed to analyse processed histological section and details of relevant controls used are outlined in detail in chapters three and five where immunohistochemistry results are presented.

2.6 Isotonic force contraction

Cells were cultured within stabilised collagen lattices and FPCL contraction assessed using a stress-release model (Grinnell, 1994, 2003; Tomasek et al., 1992). Collagen gel was prepared by mixing 10 volumes of ice-cold Collagen Type I (Cellmatrix type I-A, Kyowa Chemical Products, Japan) supplemented with 1 volume 10xRPMI, and titrated with 1M NaOH to adjust the solution to a neutral pH. Mixing was done rapidly on ice. Following trypsinisation, 1 x 10^5 cells were seeded in 250µl of neutralised collagen (FirstLink). FPCLs were allowed to polymerise at 37°C for 30 minutes in 24-well tissue culture plates and then cultured with 1ml DMEM (with 10% FBS) at 37°C in 5% CO_2 for 24 hours. Gels were cultured for 24 hours with 1ml DMEM supplemented with 10% FCS and penicillin-streptomycin (1x). At 24 hours, constructs were mechanically released from the plate using a sterile needle and lattice contraction was digitally recorded at regular time intervals over 48 hours. Gel contraction was quantified by measuring changes in lattice surface area using Openlab (Openlab Software, Massachusetts, USA).

With co-culture experiments, FPCLs seeded with Dupuytren's cells were allowed to polymerise and then overlaid with 1 x 10^5 dermal fibroblasts in 1ml of DMEM with 10% FBS, from either palmar skin or non-palmar skin. Constructs was then cultured at 37°C in 5% CO2 for 24 hours. At 24 hours, the constructs were mechanically released from the plate using a sterile needle and lattice contraction was digitally recorded at regular time intervals over 48 hours (Fig. 2.1). Gel contraction was quantified by measuring changes in lattice surface area. Standardised photographic images were recorded using a digital camera (SONY Cybershot DSC-T30, SONY, Japan).

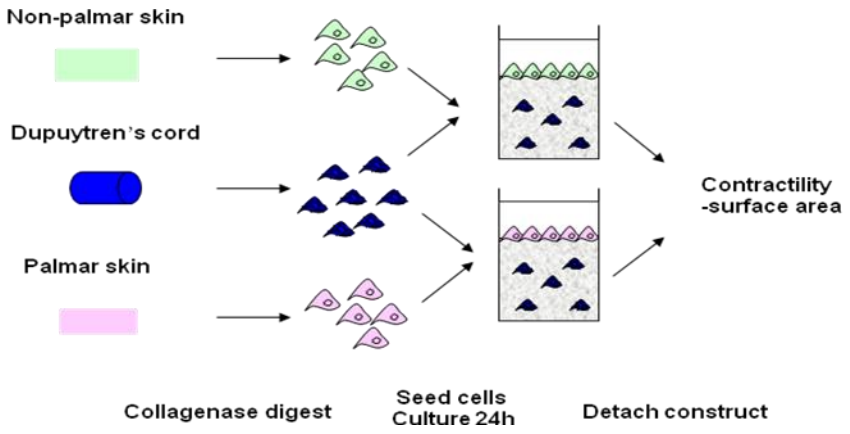


Figure 2.1. The co-culture construct. Cells are isolated from surgical samples by collagenase digestion. Myofibroblasts are seeded into a type I collagen gel. This construct is overlaid with dermal fibroblasts either from palmar skin or non-glabrous skin and cultured for 24h. Gel contraction is assessed by measuring the surface areas

The images were then quantified using OPENLAB software analysis through tracing the diameter of each magnified image and measuring the surface area in mm^2. A standard internal diameter of 15 mm for each 24 well culture dish was used to calibrate each image, and the decreasing surface area of each gel was expressed as a percentage of total gel contraction over time. The formula used to calculate percentage gel contraction was:

$$\% \text{ contraction} = 100 - \left(\frac{\text{gel surface area}}{\text{Well surface area}} \times 100 \right)$$

2.7 Isometric force contraction – culture force monitor (CFM)

Measurement of the contractile forces generated by FPCLs was performed as previously described (Eastwood et al., 1996; Tomasek et al., 2002). This project had access to a 4 channel CFM through collaboration with Professor Mark Eastwood at The University of Westminster, London (Eastwood et al., 1996). Separate 4 cell chambers (moulds) for CFM based cell culture were manufactured from ertacetal C copolymer (Engineering & Design plates UK Ltd). Circular disc shaped ertacetal C blocks were cut from a cylinder bar stock (disc size: 6.1 cm diameter, 1.2 mm thickness) and a central rectangular mould of dimension 20 x 40 x 10mm was drilled out using a mill (Bridgeport Vertical Mills, UK). Ertacetal C is hydrophobic and hence inhibited cell attachment. Attachment bars to connect the CFM gages to the polymerised FPCL were made from hydrophillic microsporous Vyon (Porvair Ltd, Kings Lynn, Norfolk, U.K.). Stock sheets were 5 mm thick and were cut into strips of 5 x 10 mm bars. These bars were sterilised by autoclaving at 120^{o}C for 20 minutes. This also removed any volatile residues. The hydrophillic nature of the vyon and the hydrophobic nature of the cell channel encouraged cell and substrate attachment only to the vyon attachment bars. Attachment bars were connected to the CFM strain gages through two "A" frames of stainless steel suture wire (0.35mm diameter). The "A frame" was configured with a loop at one end to provide a hook to attach to the CFM strain gage. The stainless steel wires were easily inserted into the vyon attachment bars and these were sufficiently buoyant to support the mass of the wire "A" frames.

Collagen gel was prepared by mixing ice-cold Type I Collagen with 1 volume 10xRPMI, which was then neutralised drop-wise with 1M NaOH to adjust the solution to a neutral pH.

Mixing was done rapidly on ice. In total, either $1.5x10^6$ nodule-derived cells, palmar or non-palmar fibroblasts were re-suspended in 0.5 ml DMEM with 10% FBS per gel. Cells were then seeded in 2 ml of neutralised collagen (final volume 2.5 ml, final concentration 1.8 mg/ml) and poured between the A frames within each mould. Each mould was then placed in the incubator for 5 mins to allow for the FPCL to gel. The long axis of the FPCL was then detached using a sterile needle and 3 ml DMEM (with 10% FBS) was gently added on top of the FPCLs. Each CFM mould was covered with a plastic petri dish lid and they were then placed into the humidified CFM incubator at 37°C. The A frames were attached to the CFM strain gages and force measurements were begun after 15 minutes to allow the incubator temperature to normalise. The floating FPCLs and attachment bars provided an almost friction-free bearing surface and allowed the system to reliably measure force generated. Therefore once set up in the CFM, FPCLs were tethered between two flotation bars and held stationary at one end whilst the other end attached to a force transducer contracted against a "fixed" point. FPCL generated tensional forces were continuously measured and data logged every 15 seconds (Dynes: 1 x 10-5N) (Eastwood et al., 1994).

FPCLs attached to the CFM were also stimulated for 24 hours with control BSA (150µg/ml) or AGE-BSA (150µg/ml) (gift from Professor Vlassara, Mount Sinai Hospital, USA); TNF-α (1ng/ml) or TGF-β1(10ng/ml) (both from Pepro Tech, UK). The final concentration of these products was added to the media in which the FPCLs were floating. Separately, palmar skin fibrobalsts were also cultured in the presence of AGE-BSA (150µg/ml) for 5 days prior to trypsinisation and seeding in to FPCLs in the CFM.

2.8 Immunofluorescence

2.8.1 Immunofluorescent staining of cells in monolayer

For monolayer studies 10,000 nodule-derived cells, non-palmar fibroblasts or palmar fibroblasts were cultured on glass coverslips in DMEM and 10% FBS for 24 hours. After 24 hours in culture, cells were washed once in 1xPBS and then fixed for 15 minutes with 3% paraformaldehyde in PBS and permeabilised with 0.2% Triton X-100 (Sigma) for 5 minutes. Cells were then washed three times, 5 minutes per wash in 1xPBS and then incubated with mouse monoclonal α-SMA or rabbit polyclonal RAGE primary antibodies diluted in 2% BSA-PBS for 1 hour. Cells were washed a further three times, 10 minutes per wash in 1xPBS followed by incubation with appropriate secondary Alexa Fluor 568-conjugated anti-mouse or anti-rabbit antibodies. F-actin was probed with Phalloidin-Alexa Fluor 488 and DNA with DAPI diluted in 2% BSA-PBS for a further 1 hour, and followed by a final set of three washes, 10 minutes per wash in 1xPBS. Coverlips were mounted onto glass slides with ProLong Gold Antifade Reagent. Slides were imaged under a fluorescent microscope at x40 or x60 magnification (Nikon TE2000-E light/fluorescent microscope (Nikon Co., Japan)). All immunofluorescent staining was carried out at room temperature. Secondary antibodies alone were used as an immunolabelling control.

2.8.2 Immunofluorescent staining of FPCLs following contraction in the CFM

Following 24 hour contraction in the CFM, FPCLs were fixed whilst under tension for 30 minutes in 3% paraformaldehyde, washed three times in 1xPBS for 10 minutes per wash. FPCLs were then bisected and embedded in paraffin wax. Slides with 10 µm cut sections were then "ring-fenced" with a PAP pen (DAKO) to create a hydrophobic ring around the section and retain staining solutions. Next immunofluorescent staining was performed as described above for monolayer. Sections were embedded in ProLong Gold Antifade Reagent protected with a glass coverslip and images were acquired using oil immersion objectives. Images were processed using the Volocity® 3D Imaging Software (Invitrogen, Paisley, UK). Microscopes used were Nikon TE2000-E light/fluorescent microscope (Nikon Co., Japan) with a Hamamatsu camera (Hertfordshire, UK) and Ultraview Nipkow scanning disc Nikon TE2000-U confocal microscope (Nikon Co., Japan).

2.9 Western blotting

2.9.1 Sample preparation

Nodule-derived cells, palmar and non-palmar fibroblasts were cultured in monolayer for 24 hours. In total $1x10^5$ cells were plated per well in a 24 well culture plate. Cell extracts were prepared with 150µl SDS sample buffer and boiled for 3 minutes at 95ºC. Equal volumes of cell lysates were separated on 7.5% or 10% SDS-PAGE gel.

Protein was also extracted from fibroblasts within 3-D collagen matrices following 24 hours contraction. FPCLs were harvested, washed in sterile 1xPBS and sheared using a sterile 21

gauge needle. Proteins were then extracted with 500 µl SDS sample buffer, boiled for 3 minutes at 95ºC and processed as outlined above for monolayer studies.

2.9.2 Tris-glycine sodium dodecyl sulphate polyacrylamide gel electrophoresis (sds-page)

For gel recipes, please see section 18.53 of Molecular Cloning (Sambrook et al., 1989). Proteins were separated by 7.5% or 10% Tris-glycine SDS-PAGE dependent on the size of the protein band being investigated. Samples were added to 2xSDS loading sample buffer with 0.2 M dithiothreitol (DTT) in a 1:1 ratio with sample and boiled for 5 min before loading. 5 µl Prestained Precision Plus Protein standards were loaded alongside the samples to allow determination of protein band sizes. Gels were run in protein gel tanks (Mighty Small II, Amersham) in 1x tris-glycine running buffer for approximately 1 hour at 150 mV.

2x loading sample buffer
1.7 % (w/v) SDS
42.52 % (v/v) upper gel buffer
8.5 % (v/v) bromophenol blue (0.1%)
34.01 % (v/v) glycerol
0.25 M EDTA

10x Tris-glycine running buffer
0.06 M Tris base
0.48 M glycine
1 % (w/v) SDS

2.9.3 Transfer of proteins to PVDF membrane

After electrophoresis, the separated proteins were transferred onto a polyvinylidene difluoride membrane (PVDF) (Amersham Biosciences, Bucks, UK) in transfer buffer using the

X cell II blot module (Invitrogen, Paisley, UK) at 25 V for 90 minutes. Membranes were blocked at room temperature for 1 hour in 10% milk for HRP.

Blocking solution was removed and primary antibody solution applied directly. The primary antibody was diluted in 10% milk for HRP, and incubated at room temperature for 1 hour. The membranes were washed for 3 x 15 minutes in wash buffer. Diluted secondary antibody was then applied to the membrane. Appropriate horse radish peroxidase (HRP) conjugated secondary antibodies were diluted in 10% milk and incubated at room temperature for 1 hour.

The membranes were washed in wash buffer for 3 x 15 minutes and enhanced chemiluminescence (ECL) substrate (Amersham) was applied and bands detected by film. A shaker was used to ensure optimal antibody coverage and membrane washing. Semi-quantitative analysis of protein expression was performed using densitometry analysis software (Phoretics International).

Transfer buffer
0.72% (w/v) glycine
0.15% (w/v) Trizma base
20% (v/v) methanol
Water up to 1 litre

Wash buffer
0.25 M Tris pH7.5
1.5 M NaCl
1% Tween-20

2.10 Reverse transcription polymerase chain reaction

2.10.1 mRNA isolation

The QIAmp RNA blood mini kit (QIAGEN, Crawley, UK) was used – see kit manual for full details. Cells were cultured in monolayer as described earlier in the chapter. Conditioned medium was aspirated off and cells were lysed with lysis buffer RLT containing β-mercaptoethanol (QIAGEN, Crawley, UK). The lysate was either frozen at -80°C for processing later or it was processed using the QIAmp RNA blood mini kit to isolate mRNA according to the manufacturer's instructions (QIAGEN, Crawley, UK). The RNA was then stored immediately at -80°C or underwent a reverse transcriptase reaction. The quality of the isolated RNA was determined by measuring the OD of a 3:7 dilution of the RNA at 230, 260, 280 and 320 nm. By determining the 260/280 ratio > 1.8, this ensures low protein contamination and 260/280 >2 indicates pure RNA isolation. 230 nm and 320 nm readings measure small peptide contamination and hence should be low.

Following 24 hours contraction in the CFM, mRNA was also isolated from FPCLs. Cells within 3D Collagen lattices were lysed using a 1:1 volume ratio of RLT buffer to collagen gel. The lysate was then processed as per the remaining steps as outlined above for monolayer cultures.

2.10.2 RT-PCR

The reverse transcriptase reaction was performed as described in Table 3. The dNTP mix was made by mixing dATP, dCTP, dTTP and dGTP to a total concentration of 100 mM.

Table 2.2. Steps involved in RT-PCR

Step	Reagent	Volume (µl)
Incubate at 65°C for 5 min then cool at RT for 10 min	0.5 µg RNA	X
	300 ng random primers	3
	Autoclaved H_2O	50-(X+3)
Heat in 42°C for 1 h then heat in 100°C heatblock for 5 min.	Stratascript buffer (10x)	5
	RNAse block (40U/µl)	1
	dNTP mix	2
	Stratascript reverse transcriptase (50U/µl)	1
Aliquot and store at -20°C		

The RNA was then used in PCR reactions with primers specific for the GAPDH house-keeping gene and primers designed specifically against α-SMA (Table 4). For PCR, puReTaq Ready-To-Go PCR beads (Amersham Pharmacia Biotech, Little Chalfont, UK) were used. Beads were reconstituted in 21 µl water, 1 µl of the forward primer, 1 µl of the reverse primer and

2 µl of cDNA template or water (negative control) or cDNA from isolated from Dupuytren's cord explants (positive control). 5 µl aliquots of each PCR product was then loaded in loading sample buffer and resolved on 1% agarose gels containing ethidium bromide. 500 bp and 1 kb DNA ladders were included on each gel.

Primers were designed specific for the GAPDH housekeeping gene and human α-SMA gene. For each primer set, the optimum annealing temperature was determined by a temperature gradient reaction for 40 cycles. The optimum cycle number was determined by a cycle curve to ensure the reaction occurs within the linear range of the PCR: the GAPDH primer required 26 cycles and the α-SMA primer required 30 cycles for optimal amplification within the linear range.

Table 2.3. Primer sequences

Primer	Sequence	PCR product size (bp)
GAPDH forward primer	catggagaaggctggggctc	672
GAPDH reverse primer	atgaggtccaccaccctgtt	
α-SMA forward primer	ttctacaatgagcttcgtgttgcc	478
α-SMA reverse primer	ggtgatcacttgcccatcag	

2.10.3 Real time PCR

Levels of α-SMA and RAGE mRNA were also analysed by quantitative real-time PCR. These experiments were performed using a Corbett Rotor-gene 6000 machine (Corbett Research Ltd, Cambridgeshire, UK) and analysed using Corbett Rotogene 6000 software. TaqMan® PreAmp Master Mix (Applied Biosystems) and ABI TaqMan probes specific for α-SMA (Hs00426835-g1) (Applied Biosystems) were used as per the manufacturer's instructions. Reactions were carried out in triplicate, each in 10 µl volumes. Thermocycling conditions were as follows: 10 minutes at 95°C; then 10 seconds at 95°C and 35 seconds at 60°C for 45 cycles. The Ct values of both the gene of interest and the house-keeping gene were converted into concentrations according to their respective standard curve. α-SMA expression levels were normalised to levels of ribosomal protein control RPLPO (Taq man probe set 4310879E) and to the level of gene expression in unrelated non-palmar skin fibroblasts which were assigned the value of 1 (ΔΔCT method).

2.11 Fluorescence activated cell sorting (FACS)

In total $1x10^5$ cells from each matched nodule-derived cells, non-palmar and palmar fibroblasts were used to examine RAGE expression on the cell surface. Cells were blocked with 2% normal human serum in 100µl FACS buffer (1% FBS in PBS) for 10 minutes at room temperature before incubated with either FACS buffer alone, control 1% rabbit IgG or 1 µg/ml RAGE antibody for 1 hour at 4°C. Afterwards cells were washed once in FACS buffer before re-suspended in 100 µl FACS buffer containing 2% goat serum for 10 minutes at 4°C. After blocking with goat serum, cells were incubated with Alexa Fluor-488 anti-rabbit secondary antibody for 30 minutes at 4°C. Finally, cells were washed twice in FACS buffer to

remove excessive antibody and re-suspended in 200µl FACS buffer before analysed on a BD FACSCanto Flow Cytometer (BD Biosciences, Oxford, UK). Routinely 10,000 events were acquired.

2.12 Cell tracing studies

Monolayer experiments with 2,500 cells cultured on coverslips were performed with fluorescently labelled nodule-derived cells and stained with DAPI to determine proliferation rates of cells when in co-culture with either non-palmar or palmar fibroblasts. A stock solution 0.5 mM fluorescent probe (Vybrant CFDA SE Cell Tracer Kit, Invitrogen, UK) was prepared in dimethyl sulphoxide (DMSO). Nodule-derived cells were trypsinised, washed and re-suspended in 1xPBS containing probe and incubated for 15 minutes at 37°C. These cells were then washed in pre-warmed DMEM with 10% FBS and incubated for a further 30 minutes prior to re-suspending. Experiments were performed to optimize labelling and dye concentration for 5 days in culture. Nodule-derived cells, non-palmar and palmar fibroblasts were then counted and in total $2.5x10^3$ cells plated per glass coverslip either as individual cells types alone or co-cultures at different ratios for 5 days. After 5 days, cells were fixed, labelled with DAPI and examined under a fluorescence microscope. In each construct, the overall proportion of cells with positive fluorescent dye after 5 days was compared to the relative ratios of nodule-derived cells, palmar and non-palmar fibroblasts plated at the start of the experiment.

2.13 MTT assay ((3-(4,5-dimethylthiazol-2-yl)-2,5-diphenyl tetrazolium bromide)

To assess cell viability in co-cultures, nodule-derived cells, non-palmar and palmar fibroblasts were plated at $1x10^4$/ml in a 96 well culture dish for 24 hours and for 5 days. Cells were either cultured alone or in co-cultures with nodule-derived cells and either palmar or non-palmar skin fibroblasts. After the required period of incubation at 37°C, 5% CO_2, conditioned medium was aspirated and 100 µl fresh serum-free medium containing 0.5 mg/ml MTT (Sigma-Aldrich) was applied and cells incubated for 2 hours before addition of 100 µl MTT stop solution and incubation overnight at 37°C. Plates were then read at 574 nm on a Labsystems plate reader (Multiskan BIOCHROMATIC, UK)

MTT stop solution

10% SDS

0.01M HCl

2.14 Statistical analysis

Histological nodularity was compared with total flexion deformity in all samples, and within subgroups of primary and recurrent disease, geographical site and gender. These analyses were done using either a Mann-Whitney non-parametric test, or an unpaired t-test depending on Gaussian distribution (determined by the Kolmogorov-Smirnov test). Analysis of single variance was performed when comparing nodule surface area with fasciectomy or dermofasciectomy, further divided by primary or recurrent disease. The association

between total flexion deformity and total nodular or cord surface area were assessed using Spearman correlation.

The rate of FPCL contraction (dynes/ hr) was calculated by measuring the average gradient of the curve between 6 -24 hours. Contraction gradients and different aspect-ratio FPCLs were compared using unpaired t-tests. Analysis of single variance was used for comparisons of matched set contraction profiles and percentage stress fibres, and also for comparisons of co-cultures.

Finally, analysis of single variance was used for comparisons of RAGE expression levels between matched sets. A paired t-test was used to compare RAGE expression levels between palmar and non-palmar skin. Analysis of single variance was performed using a Dunnett multiple comparison test to compare contractility of control untreated FPCLs and FPCLS stimulated with TNF-α or AGE-BSA, or both in combination or with TGF-β1.

All statistical analyses were performed using software (Prism; GraphPad Software, San Diego, CA). Significance was achieved if $p<0.05$.

CHAPTER THREE

Characterisation of myofibroblast distribution in Dupuytren's cords

3.1 INTRODUCTION

Histologically, Dupuytren's contracture has classically been described as comprising hypercellular nodules, which mature as the disease progresses to form almost acellular tendon-like cords (Luck, 1959). Disease recurrence following fasciectomy has been correlated with increased tissue cellularity as shown by light microscopy (Balaguer et al., 2009; Rombouts et al., 1989).

The cell that primarily contributes to digital contraction is thought to be the myofibroblast. Dupuytren's tissue has been analysed for the presence of myofibroblasts by electron microscopy (Chiu and McFarlane, 1978; Gabbiani and Majno, 1972; Iwasaki et al., 1984). Disease recurrence following fasciectomy has also been correlated myofibroblasts identified ultrastructurally in histological nodules (Gelberman et al., 1980; Rudolph and Vande Berg, 1991).

The most frequently employed marker that characterises myofibroblasts is α-smooth muscle actin (α-SMA) (reviewed in Hinz, 2007) and the distribution of α-SMA in Dupuytren's tissue has also been examined by immunohistochemistry (Hindman et al., 2003; McCann et al., 1993). However, clinical data of disease activity in terms of pre-operative digital contracture have not been correlated with α-SMA expression or myofibroblast distribution throughout Dupuytren's tissue. It would also be interesting to compare any differences in the presence of myofibroblasts in samples following surgery for both primary and recurrent contracture.

The first aim of this part of the study was to systematically characterise the distribution of α-SMA positive cells throughout excised Dupuytren's tissue. The next objective was to determine whether there was a correlation between the presence of α-SMA positive myofibroblasts and the degree of pre-operative flexion contracture and finally, to determine any differences between the presence of myofibroblasts in samples from primary or recurrent disease**.**

3.2 RESULTS

3.2.1 Patients and samples

In total, 103 digital cords were excised from 80 patients. The surgery was performed between 2006 and 2008. Patients were recruited to the study after providing written consent (SMREC06/Q0403/95). Specimens were collected from 2 sites: London and Edinburgh. Fasciectomy samples accounted for 70% (n=72) and dermofasciectomy 30% (n=31). All samples were from active or advanced disease with digital contracture. No early disease palmar nodules without digital contracture were available for analysis in this study. The majority of samples were from Edinburgh (n=74) and the remainder from London (n=29). The mean age in both groups was 64 years (range, 33–88), with an overall ratio of men to women of 3:1. Digital cords were mainly from ulnar-sided disease (62– little finger, 30– ring finger, 7– middle finger, 2– index finger, and 2 from the thumb).

Overall, 53 patients were treated for both MCP and PIP joint contractures in the same digit, 11 patients for isolated metacarpophalangeal (MCP) joint contracture and 29 for isolated proximal interphalangeal (PIP) joint contracture. Combined MCP, PIP and distal

interphalangeal (DIP) joint contractures in the same digit affected 5 patients and both PIP joint and DIP joint contractures in the same digit were seen in 5 patients.

The indications for surgery included functional disability, PIPJ contracture >30 degrees and progression of contracture. The same surgical selection criteria and operative protocols were used by both surgeons. Of the 103 excised digital cords, the PIPJ was identified intra-operatively and marked in the later 53 samples. Marking the cord at the level of the PIPJ was done intra-operatively prior to excision of the affected fascia whilst the digit was still flexed. The MCPJ was similarly identified and marked intra-operatively in only 2 cases and the DIPJ in only one sample. Clinical data for each patient were recorded concurrently using the clinical proforma shown overleaf (Fig. 3.1). The data collected using this proforma are presented for each site to compare differences between the two groups in terms of diathesis (as defined by (Hindocha et al., 2006)), previous surgery and pre-operative flexion contracture (Table 3.1).

DUPUYTREN'S CLINICAL PROFORMA

Hospital no. _____
Sample no. _____
DOB _____

Diathesis

Gender	Male / Female	
Bilateral disease	Yes / No	
Early onset (<50 yrs)	Yes / No	
Garrods pads	Yes / No	
FHx (1st degree relatives):	Yes / No	details:

Relevant past surgical history

Past Dupuytren's surgery	Yes / No	details:
		Dates:
Recurrence	Yes / No	details:
Extension	Yes / No	details:

Pre-operative range of movement (degrees)

LEFT

	Thumb	Index	Middle	Ring	Little
MCPJ					
PIPJ					
DIPJ					

RIGHT

	Thumb	Index	Middle	Ring	Little
MCPJ					
PIPJ					
DIPJ					

Operation (date)

Details:

Scar tissue from previous operation:

Other:

Figure 3.1. Dupuytren's clinical proforma used to prospectively collect patient data on diathesis, previous surgery and pre-operative flexion contracture.

Comparing Dupuytren's samples from Edinburgh and London highlighted differences between patients from the 2 sites (Table 3.1). The majority of patients were from Edinburgh (n=74) and the remainder from London (n=29). In London, 90% of patients were male, the digits tended to be less flexed (mean flexion deformity: 63±26°) and the majority of patients presented with primary disease (76%). Most of the patients (26/29) were treated by fasciectomy and the remaining 3 by dermofasciectomy. In comparison, 70% of patients in Edinburgh were male and the overall mean flexion deformity amongst Edinburgh patients was significantly greater (mean flexion deformity: 93±40°) (p= 0.01). There were comparatively more female patients in the Edinburgh cohort and they presented with a significantly greater mean flexion deformity than men (female mean flexion deformity: 111±38°; male mean flexion deformity: 84±39°) (p=0.02). This may reflect delayed presentation in female patients, rather than selection bias. Approximately one-third of samples from Edinburgh were obtained from patients with recurrence following previous surgery and half of these were following previous fasciotomy. Although previous fasciectomy accounted for most of the remaining recurrences, both sites had 1 recurrence following a firebreak dermofasciectomy. There was no difference in digital distribution between Edinburgh and London and the diathesis was similar. Recurrence was seen in the ring and little fingers but not in the middle finger, index finger or thumb.

Table 3.1. Differences in diathesis and pre-operative contractures are compared in samples from Edinburgh and London. Samples were grouped by either primary disease or recurrence (following previous surgical procedure as indicated).

	Edinburgh	London	Combined
Diathesis (% incidence)			
Male	70	90	76
Family history (1st degree relative)	38	28	34
Early onset <50 yrs	46	41	44
Bilateral disease	75	83	78
Garrod's pads	38	44	40
Pre-operative flexion deformity (degrees)			
Mean MCPJ	40 ± 19	39 ± 18	40 ± 18
Mean PIPJ	65 ± 27	55 ± 15	62 ± 24
Mean DIPJ	33 ± 16	18 ± 0	32 ± 16
Mean total flexion deformity	93 ± 41	63 ± 26	83 ± 39
Fasciectomy (sample nos.)	**46**	**26**	**72**
Primary	36	22	58
Secondary, following previous:	10	4	14
Fasciotomy	7	0	7
Fasciectomy	3	4	7
Dermofasciectomy	**28**	**3**	**31**
Primary	13	0	13
Secondary, following previous:	15	3	18
Fasciotomy	6	0	6
Fasciectomy	6	2	8
Dermofasciectomy – scar	2	0	2
Dermofasciectomy – firebreak	1	1	2
Total no. samples	**74**	**29**	**103**

3.2.2 Immunohistochemistry

Excised digital cord samples were longitudinally bisected, fixed in formalin, embedded in paraffin wax and 7µm sections from the cut surface processed for immunohistochemistry (Fig. 3.2). Sequential sections were stained with Haematoxylin and Eosin (H&E), mouse monoclonal anti α-SMA antibody (Sigma, A2547), mouse monoclonal anti-desmin (DAKO, M0760) antibody and mouse serum (Sigma, M5905). As both myofibroblasts and smooth muscle cells in blood vessels stain positive for α-SMA, desmin was used to help distinguish α-SMA positive vascular areas especially within the histological nodules. Mouse serum at the same protein concentration as the monoclonal antibody solutions was used as a negative control.

In serial sections stained for α-SMA, desmin and mouse serum control the same area of tissue (highlighted by the black box in Figure 3.2B) has been magnified from each of the sections. Figure 3.2C shows α-SMA staining of this area, figure 3.2D shows desmin staining of the same area and figure 3.2E depicts staining of this area when using the mouse serum control. In areas where there were few or no α-SMA positive fibroblasts α-SMA staining in blood vessel walls was used as an internal positive control. An example of an area with few α-SMA positive cells within the cord, but with a highly stained vascular area is depicted in the red box in Figure 3.2 and magnified in figure 3.2F.

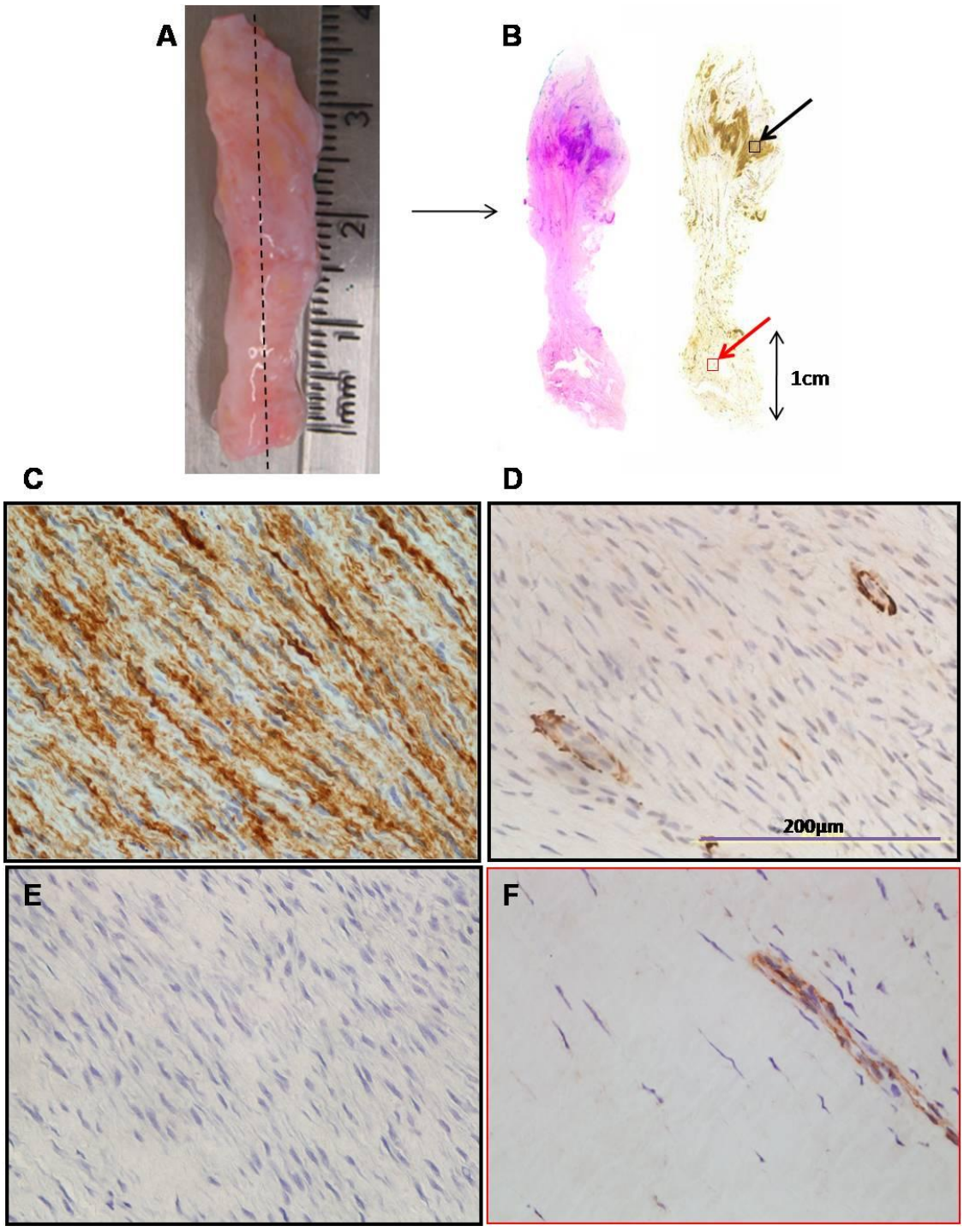


Figure 3.2. **Immunohistochemical analysis of Dupuytren's tissue.** (A) Digital cords were longitudinally bisected as shown by the dotted line. (B) Serial sections taken from the cut surface stained for H&E (left panel), α-SMA (right panel). (C) Magnified view of the box highlighted with a black arrow in panel B stained for α-SMA. (D) View of the same area depicted by the box highlighted with a black arrow in panel B but from a serial section stained for desmin. (E) View of the same area depicted by the box highlighted with a black arrow in panel B but from a serial section stained as a negative control with mouse serum only. (F) Positive control of α-SMA staining in blood vessel wall in an area of cord with little α-SMA staining (magnified view of box in B corresponding to red arrow). Magnification: (B) x4 and (C-F) x40.

3.2.3 Histological nodularity

Histologically a nodule is defined as a collection of cells in a whorled pattern (McGrouther, 2005). Many areas of cellular activity in diseased Dupuytren's tissue have been reported and these histological nodules have been reported to vary significantly in size from tiny foci of cells to larger well defined nodules (Chiu and McFarlane, 1978; Luck, 1959). Some reports suggest that few nodules are large enough to be palpated clinically but that most are microscopic in size (Chiu and McFarlane, 1978), whilst other studies suggest that most histological nodules can be palpated (Luck, 1959).

I systematically characterised the distribution of α- SMA positive cells throughout longitudinal sections of 103 excised Dupuytren's cords. Patient samples were grouped by the presence or absence of "histological nodules" which were defined microscopically as a focal 'condensation of cells' that could also be seen on the histological section as a macroscopically distinct area of α-SMA staining (Skalli et al., 1986).

Using these criteria, I found that 66% of all samples had histological nodules. The size and number of nodules was extremely variable, with marked heterogeneity between samples. Nodular cords were divided into 3 categories (1, 2 or 3+ nodules) (Fig. 3.3). Of the nodular samples, 55% had 1 nodule, 33% had 2 discrete nodules and 12% had 3 or more nodules. In total, 90% of samples from London were nodular compared to 55% from Edinburgh. Nodular cords were seen in 70% of men and 52% of women.

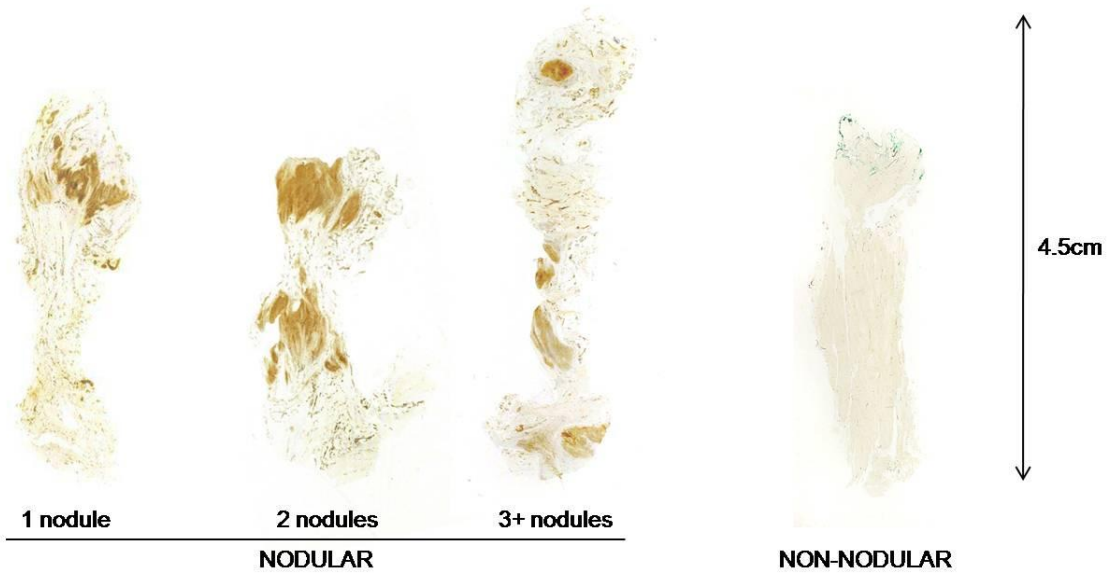


Figure 3.3. Quantification of nodules in excised digital cords. Histological sections were taken from the cut surface of excised Dupuytren's cord and stained for α-SMA. Digital cords were either nodular or non-nodular. A nodule was defined as a macroscopically distinct area of α-SMA staining. Nodular cords were further subdivided according to the number of nodules (1, 2, 3+).

The total nodule surface area and total cord surface area were traced and calculated using a Windows based histomorphometry system (OsteoMetrics, Decatur, USA). A pilot study was carried out with myself and two other independent observers to ensure the methodology was reliable and reproducible. Histological sections, enlarged on a computer screen were traced by hand around the perimeter of each nodule and the surface area calculated in mm^2. In total 10 different patient samples were examined and good correlation between observers was observed. Having established this, I then carried out the analysis on the remaining samples.

The mean total nodular surface area was $23mm^2$ (range: 1.3-$105mm^2$) and the mean total cord surface area was $143mm^2$ (range: 20-$388mm^2$). There was no difference in nodule

(p=0.3) or cord (p=0.4) surface area between gender, (men mean nodule, 24 mm^2; mean cord, 147 mm^2), and (women mean nodule, 19 mm^2; mean cord, 130 mm^2). Between geographical sites there was also no significant difference in the total nodular surface area (p=0.9) and total cord surface area (p=0.6): Edinburgh (mean nodule: 25mm^2; mean cord: 146mm^2), and London (mean nodule: 20mm^2; mean cord: 137mm^2). There was no significant difference (p=0.3) in mean cord surface area between nodular samples (149mm^2) and non-nodular samples (129mm^2).

Together these data show that cord is not acellular, approximately two-thirds of excised digital cords had α-SMA rich nodules, which in almost half of all cases existed as multiple nodules and were extremely variable in size. More men presented with nodular cords as compared to females and there was geographical variation with proportionally more nodular cords seen in London as compared to Scotland. However, there was no difference in the total nodule or cord surface areas between geographical areas and with gender. Furthermore, the total surface area of cord was not different in nodular or non-nodular samples.

3.2.4 Relationship between α-SMA rich nodules and the proximal interphalangeal joint

Previously it has been reported that clinical nodules occur along lines of tension in the hand and in some cases have been observed in the vicinity of interphalangeal joints of the digits (Chiu and McFarlane, 1978; Luck, 1959). Therefore, excised digital cords were examined to quantify whether histological nodules also co-localise with the interphalangeal joints.

Of the 103 excised digital cords, only in the latter 53 samples was the PIPJ identified intra-operatively and its position marked relative to cord prior to excision of the cord and with the digit flexed. 38 of these 53 samples were nodular and in 36 (95%) of these, a nodule was found in the vicinity of the the PIPJ. Two samples were also marked intra-operatively for the MCPJ and both showed a nodule in relation to the MCPJ. Six of the 10 patient samples with DIPJ contractures were nodular, of which 3 had multiple nodules. However, only one cord sample was marked intra-operatively for the DIPJ that showed a nodule near the joint. An example of PIPJ co-localisation is shown in Figure 3.4

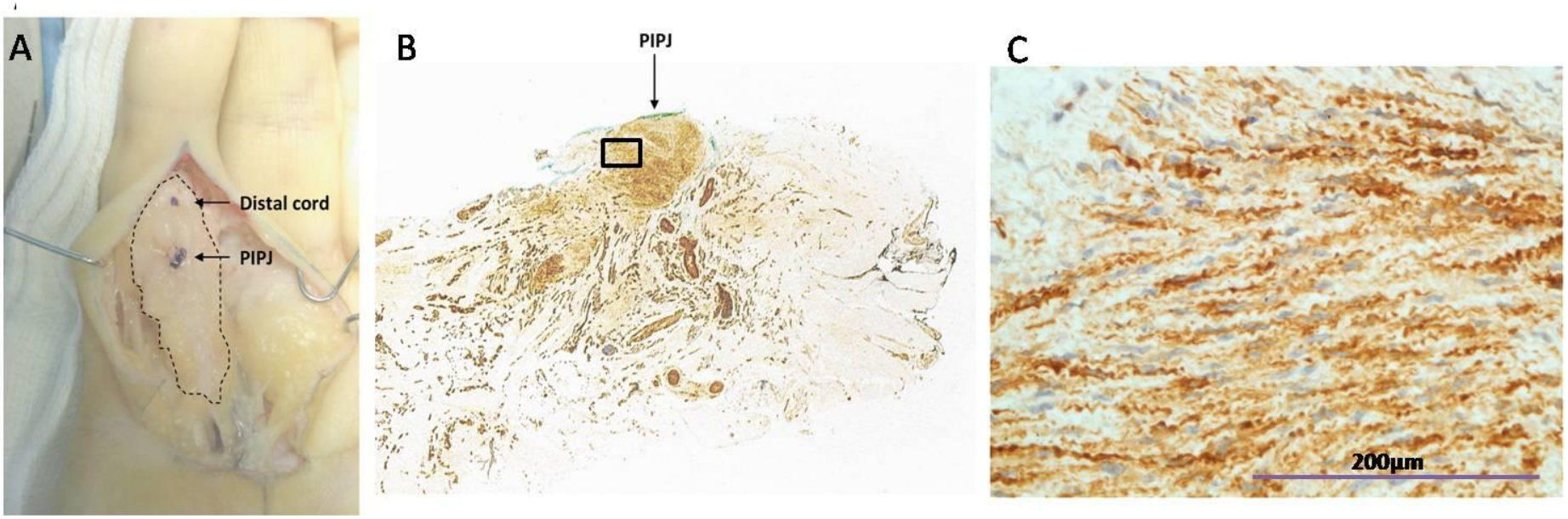


Figure 3.4. Relationship between α-SMA rich nodules and the PIPJ. (A) Dupuytren's fasciectomy with PIPJ and the distal end of digital cord marked intra-operatively with ink. Marking of the cord at the level of the PIPJ was done with the digit flexed prior to excision of the affected fascia. The dotted line outlines the excised digital cord. (B) Histological section stained for α-SMA with ink marked at the level of the PIPJ (green ink marking). (C) Magnified views of the α-SMA positive cells seen in the box highlighted in panel B.

3.2.5 Analysis of α-SMA distribution throughout Dupuytren's tissue

Immunohistochemical analysis of excised Dupuytren's cord samples from 8 patients has shown hypercellular zones within nodules comprised up to 40% α-SMA positive cells, compared to 20% in less cellular regions of the same specimen (Hindman et al., 2003). In addition, analysis of Dupuytren's tissue by immunohistochemistry has reported that 12 out 15 patient dermofasciectomy samples had α-SMA positive hypercellular Dupuytren's tissue extended into the dermis. The pattern of staining varied from intensely stained foci to weakly stained and dispersed patches of these cells (McCann et al., 1993).

To determine the distribution of α-SMA positive cells throughout Dupuytren's tissue, a number of different areas were systematically analysed in excised digital cords. In nodular cord, three areas were analysed for α-SMA positive cell distribution: the nodule(s), peri-nodule (adjacent to the nodule) and cord distal to nodule (fibrous tissue furthest from any nodule) (Fig 3.5A). In non-nodular cord, two areas were analysed: distal cord and proximal cord (Fig 3.5B). These areas were agreed upon in collaboration with Dr. Ann Sandison (consultant histopathologist) and a pilot study was conducted with myself and two other independent observers. In total 10 different patient samples were examined to establish a good correlation between observers and that the methodology was reliable and reproducible. Once this was established, I then analysed the remaining histological sections. In each sample individual cells were counted in 6 fields of view within each defined region of interest at 20 times magnification. For each region of interest, the total number of cells and the number of α-SMA positive cells were counted. From this, the percentage of the cells stained positive for α-SMA was calculated. Vascular areas were excluded from the α-SMA

positive cell count, as smooth muscle cells in vessel walls also stain positive for α-SMA. Therefore, in nodules with dense α-SMA staining, corresponding H&E sections were used to count the total number of cells and desmin was used to help delineate vasculature seen on sequential sections stained with H&E and for α-SMA (Christen et al., 2001).

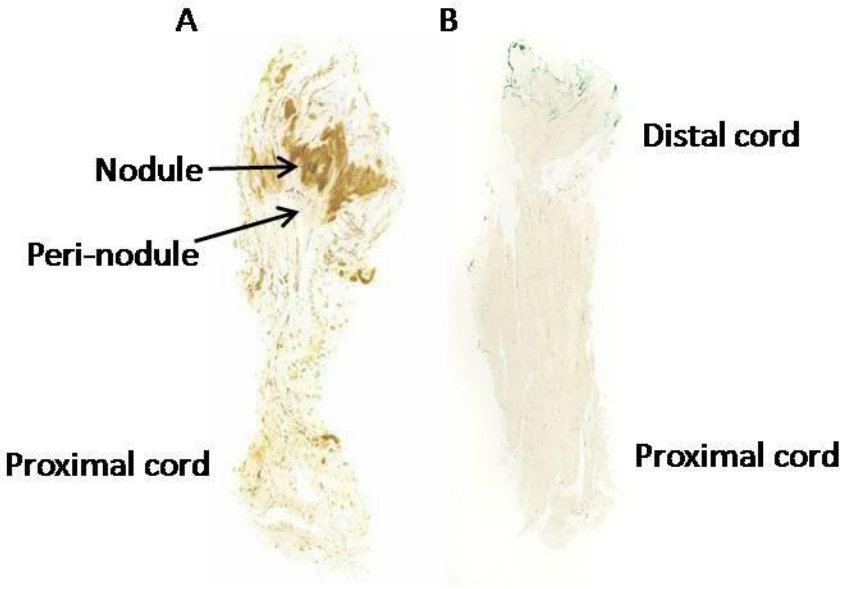


Figure 3.5. Systematic regional analysis of histological sections of nodular and non-nodular cord. (A) Areas analysed for nodular cord were: the nodule(s), peri-nodule (adjacent to the nodule) and cord-distal to nodule (fibrous tissue furthest from any nodule). (B) In non-nodular cord, two areas were analysed: distal cord and proximal cord.

Table 2 shows examples of the total number of cells and the number of α-SMA positive cells counted in systematically selected regions of interest in 5 nodular and 5 non-nodular cords. Counts are also expressed as the percentage α-SMA positive cells (myofibroblasts).

These data show at a cellular level Dupuytren's tissue is also very heterogenous (Fig. 3.6A-G). In nodular cords, the nodules (Fig. 3.6A) were consistently hyper-cellular (mean: 2374 ±1021 cells/mm^2), with cells densely packed together in 'whorls' and a mean of 97% cells staining positive for α-SMA. In the peri-nodular area (Fig. 3.6B), there were relatively fewer cells (mean: 763 ±313 cells/mm^2) and, on average, 32% of these were positive for α-SMA. Cord distal from any nodule (Fig. 3.6C) was least cellular (mean: 495 ±246 mm^2), with a mean of 8% α-SMA positive cells. Cells in cord distal from a nodule were aligned with the collagen fibres. Non-nodular cord was relatively cellular throughout (mean distal cord: 663 ±392 cells/mm^2 and mean proximal cord: 475 ±221 cells/mm^2) and more α-SMA positive cells (17%) were seen at the distal end (Fig. 6D) compared to 9% in proximal cord (Fig. 3.6E). Data from all samples including the mean total cell counts and mean percentage α-SMA positive cells (myofibroblasts) are shown for each region of analysis in nodular and non-nodular cords (Fig. 3.6F, G).

Table 3.2. Examples of cell counts in excised Dupuytren's tissue. The total number of cells and the number of α-SMA positive cells were counted in systematically selected regions of interest in nodular and non-nodular cords. Five examples of non-nodular and nodular cords are shown below. For nodular cord, examples are shown for a single nodule, +1 nodule, +2 nodules, and +3nodules. Six random fields of view were counted within each region (at x20 magnification), and expressed as the average number of α-SMA positive cells (SMA), the average number of total cells (Total) and % α-SMA positive cells (% SMA).

NON-NODULAR

Total cell count per mm^2 (%SMA)

	Distal cord			Proximal cord		
Lab no	**SMA**	**Total**	**% SMA**	**SMA**	**Total**	**% SMA**
ED025	40	884	5%	8	643	1%
ED040	12	500	2%	10	343	3%
ED042	40	488	8%	13	703	2%
ED042	10	400	3%	14	668	2%
ED057	363	1069	34%	0	502	0%

NODULAR

Total cell count per mm^2 (%SMA)

	Distal nodule			Nodule +1			Nodule +2			Nodule +3			Peri-nodule			Distal to nodule		
Lab no	**SMA**	**Total**	**% SMA**	**SMA**	**Total**	**% SMA**	**SMA**	**Total**	**% SMA**	**SMA**	**Total**	**% SMA**	**SMA**	**Total**	**% SMA**	**SMA**	**Total**	**% SMA**
ED018	1358	1388	98%										116	294	39%	35	142	25%
ED025	1434	1434	100%										146	918	16%	20	556	4%
ED026	1722	1722	100%	1394	1504	93%							64	728	9%	12	536	2%
ED046	3720	3720	100%	2104	2104	100%	1992	1992	100%				144	672	21%	8	356	2%
ED050	1696	1696	100%	4032	4032	100%	3400	3400	100%	3296	3296	100%	623	1287	48%	4	592	1%

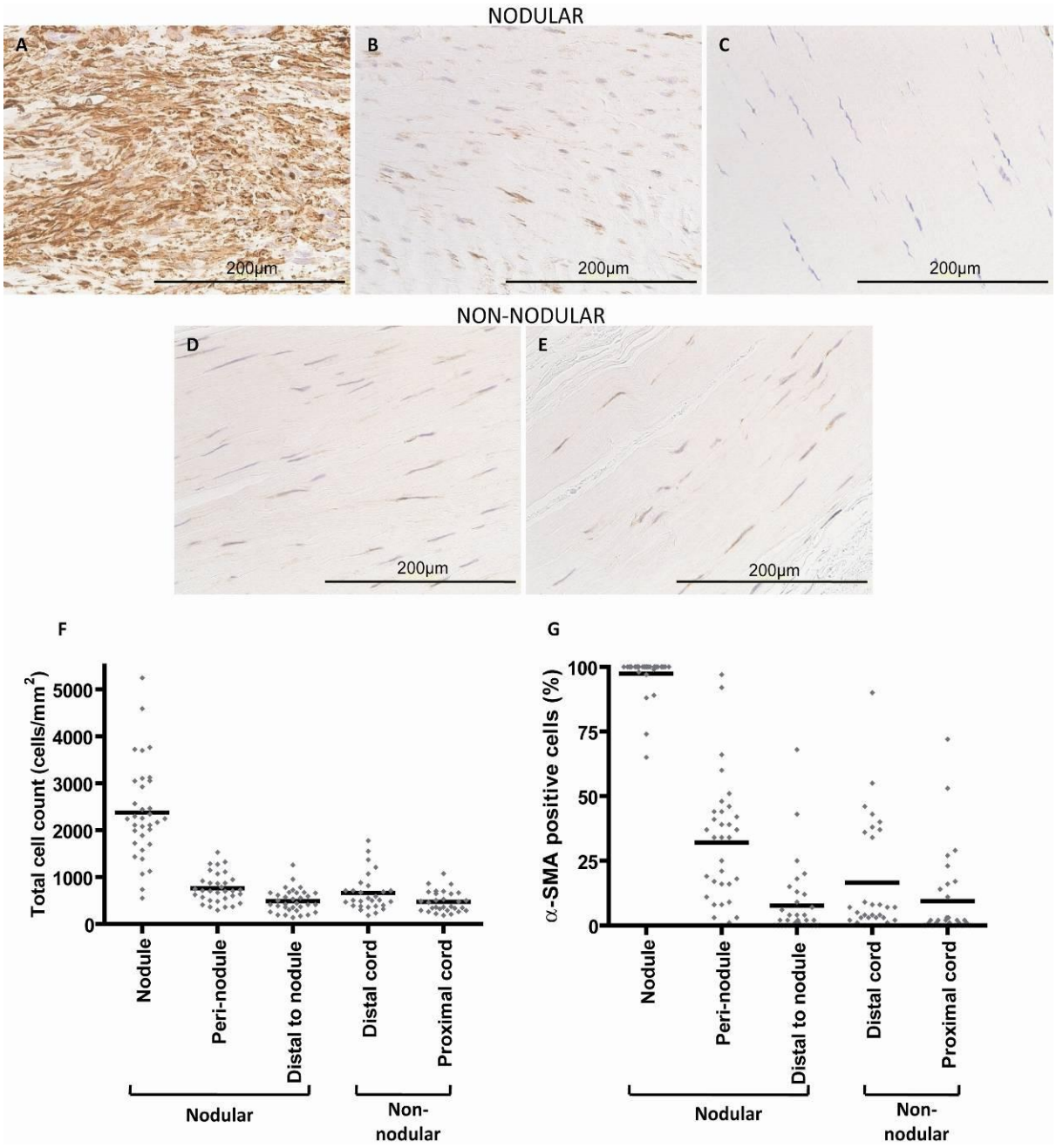


Figure 3.6. α-SMA distribution in Dupuytren's tissue. Histological sections of Dupuytren's tissue were stained with α-SMA. Representative panels (at x40 magnification) from systematically analysed regions of nodular cord: (A) nodule, (B) peri-nodule and (C) cord-distal to nodule. Representative panels from non-nodular cord: (D) distal cord, (E) proximal cord. (F) Total cell counts from analysed regions of nodular and non-nodular cord. (G) Corresponding percentages of α-SMA positive cells (G). Bars represent mean values.

3.2.6 Histological nodularity correlated with digital contracture

Ultrastructural examination of Dupuytren's tissue has also implied that myofibroblasts may be transient throughout the course of Dupuytren's tissue (Schurch et al., 1990), and an abundance of myofibroblasts has also been reported in active disease with decreased numbers of these cells in advanced disease (Chiu and McFarlane, 1978).

Therefore, I examined the relationship between my histological findings with the degree of pre-operative digital flexion contracture. There was a significant correlation (p<0.0001) between non-nodular cords and digital contracture (mean flexion deformity: 114±39°) compared to nodular cords (mean flexion deformity: 70±31°) (Fig. 3.7A). As post-operative cutaneous scarring may contribute to flexion deformity in recurrent disease, it was important to establish that this significant difference was maintained with samples from primary disease alone (p=0.01) (Fig. 3.7B).

Pre-operatively, women had a significantly greater (p=0.002) mean total flexion contracture than men (women: 107±39°, men: 75±36°). A greater flexion contracture was seen in both male (p<0.01) and female (p<0.05) non-nodular cords when compared to nodular cords. In men, the mean flexion contracture was 102±39° in non-nodular, and 67±32° in nodular samples. In women, the mean non-nodular flexion contracture was 132±34° in non-nodular, and 81±25° in nodular samples (Fig. 3.7C).

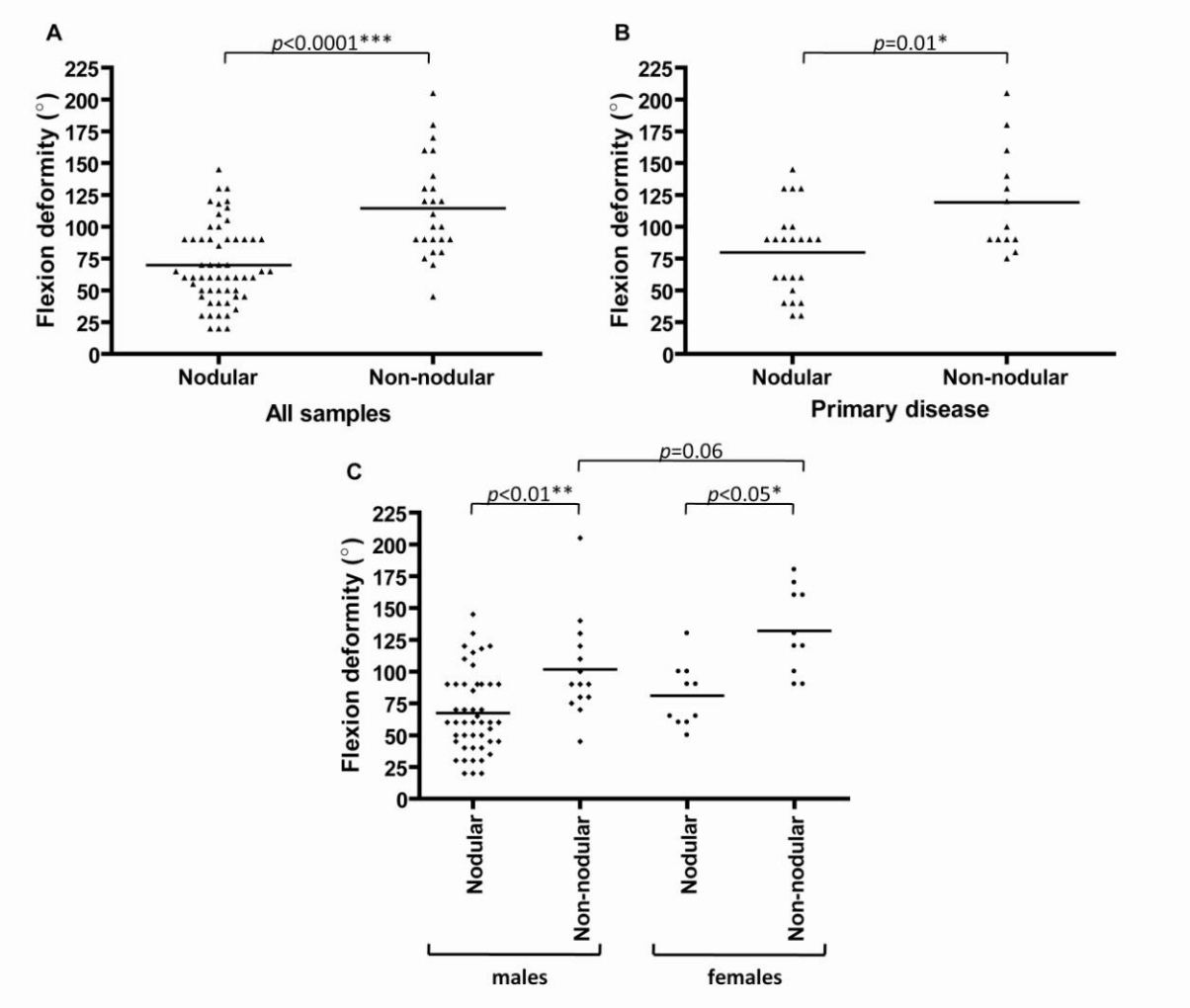


Figure 3.7. Dupuytren's tissue nodularity correlated with flexion contracture. (A) Flexion deformity for all nodular and non-nodular samples. (B) Flexion deformity for nodular and non-nodular samples from primary disease alone. (C) Flexion deformity for both men and women in all nodular and non-nodular samples. Bars represent mean values.

Nodular cords showed no difference (p=0.11) in degree of contracture between geographical sites (Edinburgh: 76±33°, London: 62±26°), whereas non-nodular cords were almost exclusively from Edinburgh (n= 33/36).

Analysis was also carried out to examine if there was any further correlation between nodule size and digital flexion contracture. However, there was no correlation between digital contracture and either total nodule surface area (p=0.2) or total cord surface area (p=0.3) (Fig. 3.8).

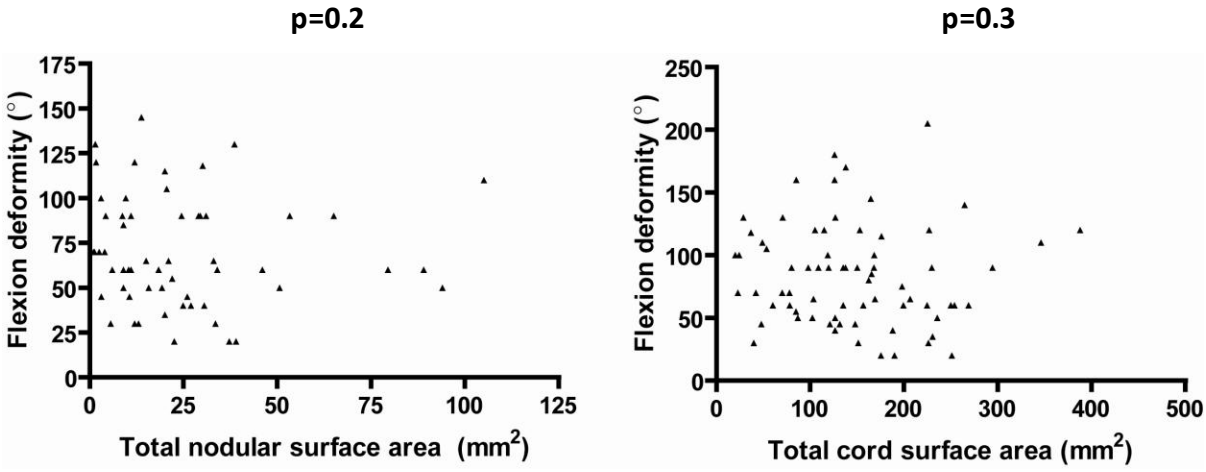


Figure 3.8. Nodule and cord surface area compared with flexion deformity. (A) Flexion deformity and total nodular surface area. (B) Flexion deformity and total cord surface area.

Together these data show that non-nodular cord samples were associated with significantly greater digital flexion contracture than nodular samples. This difference was maintained with gender and following surgery for either primary or recurrent disease. However, with nodular samples alone, no further correlation was found between the total nodule size and degree of flexion contracture.

3.2.7 Histological nodularity correlated with primary or recurrent disease

Previous studies have shown that highly cellular Dupuytren's tissue seen histologically in primary disease samples correlates significantly with disease recurrence when compared to less cellular tissue samples (Balaguer et al., 2009; Rombouts et al., 1989). Therefore, I set out to examine if myofibroblast-rich histological nodules were seen more commonly in primary or recurrent disease samples and whether nodularity was associated with the type of previous surgical procedure.

Nodules were seen as frequently in fasciectomy samples (67%) as they were in dermofasciectomy samples (66%). When further subdivided into primary or recurrent disease, approximately two thirds in both groups were still classified as nodular (Table 3.3). Two dermofasciectomy samples were excluded as the surgery was performed for cutaneous scar contracture and not true recurrence. Importantly, there was no significant difference (p=0.09) in flexion deformity between samples from primary (mean: 76±41°) and recurrent disease (mean: 88±37°).

Table 3.3. Nodular and non-nodular cords grouped by primary procedure or secondary procedure (for recurrent disease). Mean nodule surface areas (SA) for primary and recurrent disease are also included

	Total (n)	Non-nodular	Nodular	Nodular SA (mm^2)
Fasciectomy	**72**	**33%**	**67%**	
Primary	58	19 (33%)	39 (67%)	23±21
Secondary, following previous:	14	5 (36%)	9 (64%)	17±16
Fasciotomy	7	2	5	
Fasciectomy	7	3	4	
Dermofasciectomy	**31**	**34%**	**66%**	
Primary	13	5 (38%)	8 (62%)	33±29
Secondary, following previous:	18	5 (31%)	11 (69%)	22±30
Fasciotomy	6	3	3	
Fasciectomy	8	2	6	
Dermofasciectomy – scar tissue*	2	2		
Dermofasciectomy – firebreak	2		2	
Total no. samples	**103**	**34%**	**66%**	**24±23**

*excluded from non-nodular count

The overall mean total nodular surface area (sum of the surface area of all the nodules in a single specimen) was not significantly different (p=0.5) between primary (mean: 24±23mm^2) and recurrent disease (mean: 20±24mm^2). Total cord surface area was also not significantly different (p=0.5) between primary (mean: 144±71mm^2) and recurrent disease (mean: 140±98mm^2).

The total nodular surface area was not significantly different (p=0.54) in primary dermofasciectomy samples (mean: 33±29mm^2) as compared to either primary fasciectomy (mean: 23±21mm^2), secondary fasciectomy (mean: 17±16mm^2) and dermofasciectomy following recurrent disease (mean: 22±30mm^2) (Table 3.3).

These data suggest that nodules were seen equally in Dupuytren's samples following primary or recurrent surgery. Furthermore, nodular recurrence was seen following fasciotomy, fasciectomy, firebreak dermofasciectomy but not following radical dermofasciectomy.

3.3 DISCUSSION

The characterisation and systematic analysis of Dupuytren's tissue showed that two thirds of the 103 excised digital cords had histological nodules defined as a focal condensation of cells that was rich in α-SMA. These nodules varied in size and were found throughout Dupuytren's tissue. Nodules were also often seen within the vicinity of the PIPJ. I found cord tissue was cellular and also had variable numbers of myofibroblasts dispersed in amongst collagen bundles. Interestingly, non-nodular cords correlated significantly with greater digital contracture and this difference was maintained with primary disease samples alone. Non-nodular cords were mainly seen in Edinburgh, where patients presented with more advanced digital contractures. I observed no difference between nodularity in either primary or recurrent disease.

Clinical nodules have been reported to exist as solitary or multiple nodules and occur at various sites in the hand including the palm (Chiu and McFarlane, 1978; Luck, 1959). However, even in the absence of clinical nodules, small clusters of cells containing myofibroblasts have been reported in advanced tendon-like cords (Chiu and McFarlane, 1978). In agreement with Chiu (Chiu and McFarlane, 1978), I observed numerous hypercellular α-SMA-rich areas throughout Dupuytren's tissue that did not coincide with palpable clinical nodules.

I defined histological nodules based on their appearance under a light microscope as α-SMA rich focal condensations of cells. Overall, I found a single histological nodule (55%), 2 nodules (33%) and often multiple nodules (12%) within mature cords. Two thirds of cords had nodules that often existed as tiny foci of cells or as larger single or even multiple

nodules. The total nodular surface area range varied from 1.3 – 105mm^2. Nodular cords were also not significantly different in size compared to non-nodular cords. It is likely that multiple nodules may act in concert to contribute to digital contraction and, in response to increased tension, normal bands hypertrophy and thicken to form cords. The development of a longitudinal cord as a result of hypertrophy of several anatomical bands has been suggested previously (McFarlane, 1974).

Next I quantifed α-SMA expression in Dupuytren's tissue. Although α-SMA is the most frequently employed marker for myofibroblasts, bundles of contractile actin microfilaments alone cannot reliably distinguish between myofibroblasts and vascular smooth muscle cells (SMCs), especially in the nodule where mixed populations exist. The two cell populations can be distinguished at an ultrastructural level by the presence of fibronexi (Tomasek and Haaksma, 1991) specialised areas on the surface of myofibroblasts. However, as my objective was to assess myofibroblast distribution throughout cord tissue, ultrastructural imaging would have limited analysis to very small areas of tissue. Desmin is an established marker for SMCs in blood vessel walls (Christen et al., 2001) although a proportion of desmin-positive myofibroblasts have also been shown to be present around capillaries and blood vessels in proliferating Dupuytren's nodules (Schurch et al., 1990; Shum and McFarlane, 1988). I used desmin staining to delineate vascular areas seen on sequential sections stained with H&E and for α-SMA, and therefore, stromal α-SMA positive myofibroblasts were more reliably indentified and counted.

At a cellular level, I found that nodules were hypercellular (2374 cells/mm^2), with a mean of 97% α-SMA positive cells. These results are in line with previous ultrastructural studies that

have reported nodules comprise mainly of myofibroblasts (Chiu and McFarlane, 1978; Gabbiani and Majno, 1972; Iwasaki et al., 1984). The immunohistochemical analysis of myofibroblast distribution in Dupuytren's tissue using α-SMA to identify myofibroblasts has also been carried out in a small study of 8 patient samples (Hindman et al., 2003). However, in this study the nodular areas with one or more blood vessels were excluded from analysis in this study and may account for why a lower percentage in α-SMA positive cells (40%) was seen in hypercellular areas such as nodules, which are often vascular.

Non-nodular cord was also cellular throughout, with on average 9% (proximal) and 17% (distal) cells positive for α-SMA. I have also confirmed that α-SMA positive cells were distributed in amongst collagen fibres, aligned along a longitudinal axis in line with previous findings (Chiu and McFarlane, 1978). This heterogeneity is of some methodological importance, as comparisons between nodule and cord have been made in previous studies only on the basis of gross tissue morphology (Bisson et al., 2003; Bisson et al., 2004; Dave et al., 2001; Rayan and Tomasek, 1994; Townley et al., 2009).

When comparing histological findings and the patients clinical status, we found that non-nodular cords were associated with greater digital contractures, compared to nodular cords (p<0.0001). This significantly greater digital contracture in non-nodular cords was also evident when only considering primary disease samples and in both men and women. This implies that non-nodular cords may reflect the end stage process following extracellular matrix remodelling, whereas the presence of myofibroblast rich nodules may represent more active and less contracted digital cords. However, in nodular samples, no further correlation was found between nodule size and digital contracture and this may represent

different stages of disease in patients at time of surgery. Unfortunately, it is not possible to verify the progression of myofibroblast numbers and distribution in a given patient over time.

I also found that 95% (36/38) of nodules were in the vicinity of the PIPJ and nodules were also observed over the MCPJ in the only two cases marked intra-operatively for the MCPJ and one case marked for the DIPJ. The presence of clinical nodules in line with digital rays and in close proximity to the PIPJ and MCPJ has been previously described (Chiu and McFarlane, 1978; Luck, 1959). One explanation for the relative proximity of the PIPJ and histological nodules is based on the understanding that myofibroblasts perceive and thrive on tension (Gabbiani, 2003; Goffin et al., 2006; Hinz, 2006, 2007; Tomasek et al., 2002). In early or active disease, tension may act intermittently on Dupuytren's tissue as active extension of the PIPJ offers resistance against the thickened, contracted palmar fascia. The increased tension sensed by cells may promote myofibroblast differentiation through recruitment of α-SMA to stress fibres and specialised attachment site formation under strict control of TGF-β1 (Desmouliere et al., 1993) and fibronectin-EDA (Serini et al., 1998). This in turn leads to greater force generation. A densely packed cellular nodule could then theoretically exert sufficient force to promote or sustain digital contracture. The cells then remodel the surrounding matrix to a more shortened configuration. This would be supported by the increased expression of matrix metalloproteinases in Dupuytren's nodules and cord (Johnston et al., 2007; Johnston et al., 2008; Tarlton et al., 1998; Ulrich et al., 2003). The resulting increased flexion deformity would impair function and the reduced movement at the joint would in turn lead to a reduction in tension sensed by nodular myofibroblasts. This can be considered as a form of 'stress-shielding', which in wound

healing has been shown by morphometry using electron microscopy and in situ end-labelling of fragmented DNA to result in myofibroblast apoptosis after re-epithelialisation (Desmouliere et al., 1995). Furthermore, in a rat model where the wound was splinted with a sutured metal template, thereby preventing tension release, myofibroblast apoptosis as determined by TUNEL assay was inhibited and subsequent splint removal was followed by a reduction in myofibroblast numbers (Carlson et al., 2003). It is, therefore, conceivable that with advanced digital contractures, reduced tension through limited active joint extension may similarly lead to myofibroblast apoptosis, whereby myofibroblast rich nodules fail to persist. This may explain the progression from nodular to non-nodular cords and would also explain why patients with non-nodular cords tended to have more severe flexion deformities.

Studies have previously shown that recurrence following fasciectomy is correlated with electron microscopy findings of myofibroblasts present in histologically nodules (Gelberman et al., 1980; Rudolph and Vande Berg, 1991). Recurrence following primary fasciectomy has also been correlated with increased tissue cellularity as shown by light microscopy (Balaguer et al., 2009; Rombouts et al., 1989). In this study I have shown that histological nodules were seen as frequently in samples from both primary and recurrent disease (two-thirds of cords in each case) and there was also no significant difference in digital contracture between primary and recurrent disease. Recurrence was seen following previous fasciectomy (n=15), fasciotomy (n=13) and in 2 cases, following firebreak dermofasciectomy for previous recurrence, both cords being nodular. There was also no difference in nodular surface area between primary dermofasciectomy samples, primary fasciectomy, secondary fasciectomy or dermofaciectomy following recurrent disease (p=0.5). These histological

findings suggest similar pathogenesis in both primary and recurrent disease and that nodularity is not down-regulated following previous surgery. Indeed, the increased motion following initial surgery may facilitate myofibroblast differentiation and persistence. It is possible that residual unexcised Dupuytren's tissue following fasciotomy, fasciectomy and firebreak dermofasciectomy, may serve as a trigger for recurrence. This may also explain why radical dermofasciectomy has a lower rate of recurrence (1-5%) (Brotherston et al., 1994; Hall et al., 1997; Tonkin et al., 1984) than 'firebreak' dermofasciectomy (12%) (Ullah et al., 2009) or fasciectomy (40-50%) (Foucher et al., 1992; Hueston, 1961; Tonkin et al., 1984). It would be interesting to compare the myofibroblast distribution in the cords of any of our fasciectomy patients who develop recurrence in the future with the primary excision specimens.

In conclusion, the quantification of total cell numbers and α-SMA positive cells throughout excised Dupuytren's cord tissue confirms that myofbroblasts are mainly distributed in hypercellular nodules and are less numerous, but also present in variable numbers outside nodules and within cellular cord tissue. Myofibroblast aggregation in nodules in the vicinity of joints may lead to digital contracture and with subsequent matrix remodelling result in shortening of the affected fascia. Eventually fixed flexion deformity develops leading to an altered mechanical environment with loss of tension, myofibroblast apoptosis and thus may explain residual non-nodular cords.

Chapter Four

Establishing an *in vitro* model to study Dupuytren's disease

4.1 INTRODUCTION

The pathogenesis of Dupuytren's disease is poorly understood. Currently, the commonest treatment for patients with significant Dupuytren's contracture is surgery, although recurrence rates following fasciectomy are approximately 40-50% (Foucher et al., 1992; Hueston, 1961; Tonkin et al., 1984). However, recurrence following dermofasciectomy has been reported to be as low as 1-8% (Brotherston et al., 1994; Hall et al., 1997; Tonkin et al., 1984). The mechanism of reduced recurrence following dermofasciectomy also remains unexplained. To investigate further these features of this common disease requires a reliable disease model. The lack of an animal model for Dupuytren's disease underlines the necessity for a good *in vitro* system. Methodological considerations that must be addressed include the Dupuytren's myofibroblast source, choice of control cell types and assays to measure myofibroblast mediated collagen lattice contraction.

Many investigators have studied myofibroblasts derived from rat cutaneous and lung fibroblasts treated with TGF-β1. It is widely accepted that myofibroblasts are characterised by the presence of highly contractile α-SMA (Hinz, 2007; Tomasek et al., 2002). Compared to untreated control rat fibroblasts, these groups observed recruitment of α-SMA to stress fibres by immunofluoresence staining and increased expression of α-SMA protein by western blot analysis in the TGF-β1 treated myofibroblasts (Dugina et al., 2001; Follonier et al., 2008; Goffin et al., 2006). Dupuytren's cells derived from clinical nodules have been shown in monolayer cultures to express high levels of α-SMA protein compared to Dupuytren's cord cells and a human foreskin fibroblast cell line (Dave et al., 2001) and also, when compared to normal fibroblasts from mesenchymal tissues, epithelial cells and cardiac

and skeletal muscle cells (Benzonana et al., 1988). However, α-SMA expression in cells derived from genetically matched samples of Dupuytren's tissue and normal palmar and non-palmar dermal fibroblasts have not been compared.

A number of assays have been used to assess myofibroblast contractility. Attempts to correlate α-SMA expression and contraction using an isotonic collagen-gel contraction system have yielded inconsistent findings. Some authors reported no differences in contraction between Dupuytren's nodule, cord and carpal ligament-derived cells (Rayan and Tomasek, 1994; Tarpila et al., 1996), whilst others suggested increased contraction only with early passage nodule-derived cells (Moyer et al., 2002) or in nodule-derived cells expressing higher levels of α-SMA (Tomasek and Rayan, 1995). Isometric contractile forces within constrained FPCLs have also been studied using a culture force monitor (CFM) (Eastwood et al., 1994; Eastwood et al., 1996). Using this model, dermal fibroblasts reached a plateau of contraction (Brown et al., 1998) whilst neither Dupuytren's nodules or cord-derived cells reached a plateau and generated significantly greater isometric contractile force than control carpal ligament fibroblasts over a 20 hour test period (Bisson et al., 2004). However, comparisons of genetically matched Dupuytren's nodule-derived cells and normal dermal fibroblasts in both isotonic and isometric model systems have not been done. Furthermore, correlation of α-SMA expression with isometric contractility has not been undertaken in any cell type.

Therefore, this part of the study compares the isotonic and isometric contractile profiles of genetically matched cells isolated from Dupuytren's tissue, non-palmar and palmar skin samples in three dimensional collagen lattices. α-SMA mRNA levels, α-SMA protein

expression and α-SMA distribution are assessed in these lattices. Finally, based on the established surgical observation that recurrence rates are significantly reduced following dermofasciectomy, Dupuytren's cells were co-cultured with dermal fibroblasts to investigate whether the contractility of Dupuytren's cells is down regulated by non-palmar dermal fibroblasts.

4.2 RESULTS

My first aim was to identify a reliable source of myofibroblasts in order to study Dupuytren's disease. I also wanted to use human cells that would provide information most relevant to human disease and avoid confounding effects of species differences.

4.2.1 Human myofibroblast cell lines

I investigated which human myofibroblasts cell lines were available. There are limited well characterised human myofibroblast cell lines available commercially and of these none are isolated from Dupuytren's tissue. Myofibroblast cell lines that are available are derived from prostate tissue (WPMY-1 from ATCC) and fetal lung tissue (MRC-5 from Riken). However, three myofibroblast cell lines derived from Dupuytren's nodules are described in the literature (Tanaka et al., 2007; Yuba et al., 2007). They are reported as having been derived by sub-culturing Dupuytren's cord-derived cells over 2 years and to comprise a homogenous population of myofibroblasts. Ultrastructural analysis of these cell lines also reported that the myofibroblast characteristics are maintained and the karyotype analysis remained unchanged. These established cell lines also maintain the production of α-SMA mRNA and

protein and TGF-β1 . This study also showed that when xenografted into 5-week old null mice (BALB/c nu), these cell lines produced a palpable nodule, which developed at the site of inoculation (Yuba et al., 2007). I, therefore, set up collaboration with Dr Tanaka and was supplied with these cell lines for use in this project.

To characterise these cells and confirm they were a homogenous population of myofibroblasts, cells were cultured on glass coverslips for 24 hours and then analysed by immunofluorescence for α-SMA rich stress fibres. Cells were stained with α-SMA followed by Alexa Fluor 568 secondary antibody. F-actin was probed with Phalloidin-Alexa Fluor 488 and DNA with DAPI. The number of cells with positive α-SMA stress fibres were counted and expressed as a percentage of total cells (Hinz et al., 2001a). F actin staining was apparent in all cells (Fig. 1A) and α-SMA was seen in the peri-nuclear cytosol but only localised to stress fibres in a proportion of cells (Fig. 4.1A-C). Although the 3 cell lines did not consist of a homogenous population of myofibroblasts, a relatively high mean of 43% of cells had α-SMA positive stress fibres.

However, when these 3 cell lines were cultured using the same culture media and conditions as recommended (Yuba et al), none of them reached confluence after 5 months, with sub-populations of cells dying within each culture flask. *Mycoplasma* infection was tested for by pcr and excluded from all 3 cell-lines. It was due to their slow growth that I concluded these cells could not be used for further experiments.

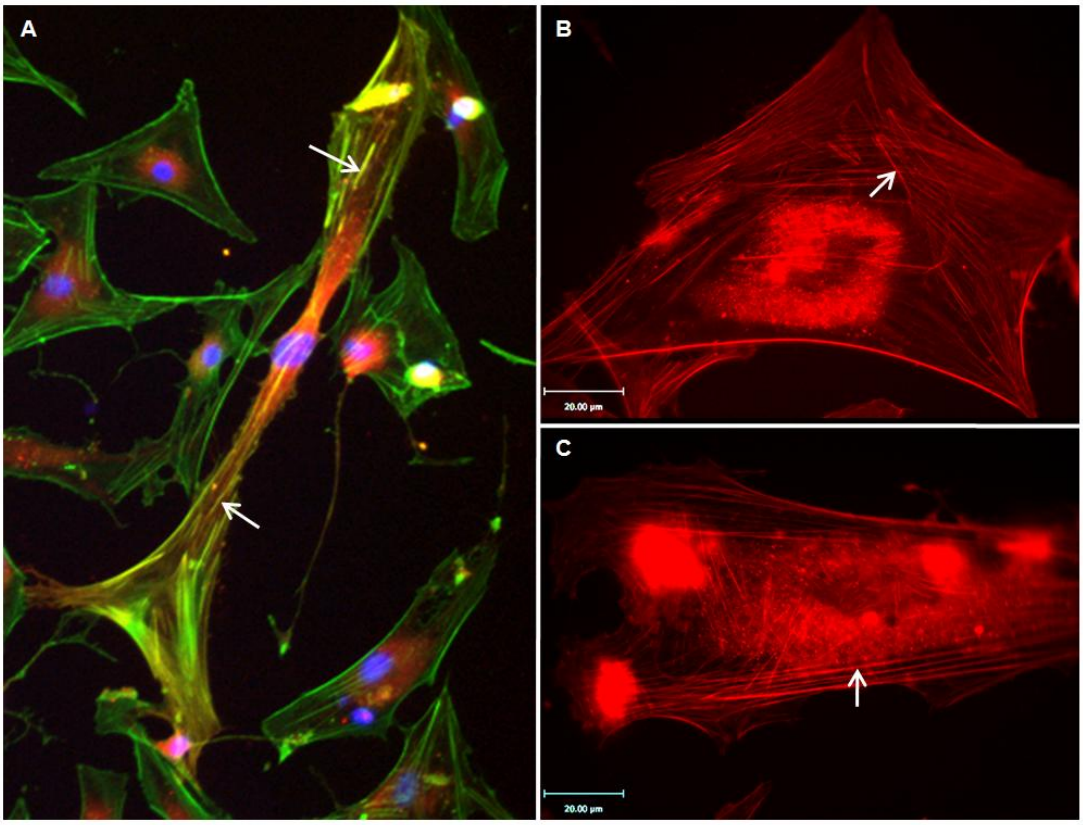


Figure 4.1. α-SMA distibution in Dupuytren's nodule-derived cell lines. Cells were cultured on glass coverslips for 24 hours, fixed and then immunofluorescently labelled using α-SMA antibodies (red), phalloidin (green) and DAPI (blue). (A) Representative images shown for triple stained Dupuytren's nodule-derived cell lines. (B,C) α-SMA (red) alone is shown to demonstrate cells with α-SMA positive stress fibres. Scale bar: 20µm. White arrows indicate cells with α-SMA positive stress fibres (merged staining of phalloidin (green) and α-SMA (red) in panel A, and α-SMA alone seen as red stress fibres in B and C)).

I next investigated primary human myofibroblasts from Dupuytren's patients for which I had access to abundant samples from Edinburgh and London. Dupuytren's cord samples processed for histology as seen in the previous chapter showed an abundance of nodules with α-SMA rich cells.

4.2.2 Cells from Dupuytren's patient samples

Tissue samples used for experiments in this chapter were obtained from 10 patients undergoing dermofasciectomy for Dupuytren's disease. The mean age of these patients was 58 yrs (range: 38-72yrs) and the male-to-female ratio was 7:3. Three types of tissue were obtained from each patient: Dupuytren's cord, palmar skin (uninvolved skin overlying Dupuytren's tissue) and non-palmar skin (full-thickness skin harvested from the groin). Cells were isolated from tissue samples by collagenase digestion and maintained in culture with DMEM supplemented with 10% FBS and 1x penicillin-streptomycin at 37˚C in a humidified incubator with 5% CO_2.

4.2.3 Cells derived from whole Dupuytren's cord

In order to characterise the cells isolated from excised Dupuytren's cord and to determine what proportion of these cells are myofibroblasts, α-SMA distribution in stress fibres was examined by immunofluoresence in cells (passage 1 and 2) derived from whole Dupuytren's tissue (Hinz et al., 2001a). Non-palmar and palmar skin fibroblasts were used as genetically matched controls. Cells were stained with α-SMA followed by Alexa Fluor 568 secondary antibody and DNA with DAPI. In non-palmar and palmar fibroblasts, α-SMA was consistently seen in the peri-nuclear cytosol (Fig. 4.2A,B), whereas in Dupuytren's cord cells α-SMA was more frequently localised to stress fibres (Fig. 4.2C). The number of cells with α-SMA positive stress fibres was counted and expressed as a percentage of total cells (Hinz et al., 2001a). Using this methodology, the mean percentage of α-SMA positive cells in whole cord was 9% ±3, compared to 4% ±1.7 in non-palmar skin and 4% ± 1.7 in palmar skin (p=0.04) (Fig. 4.2D).

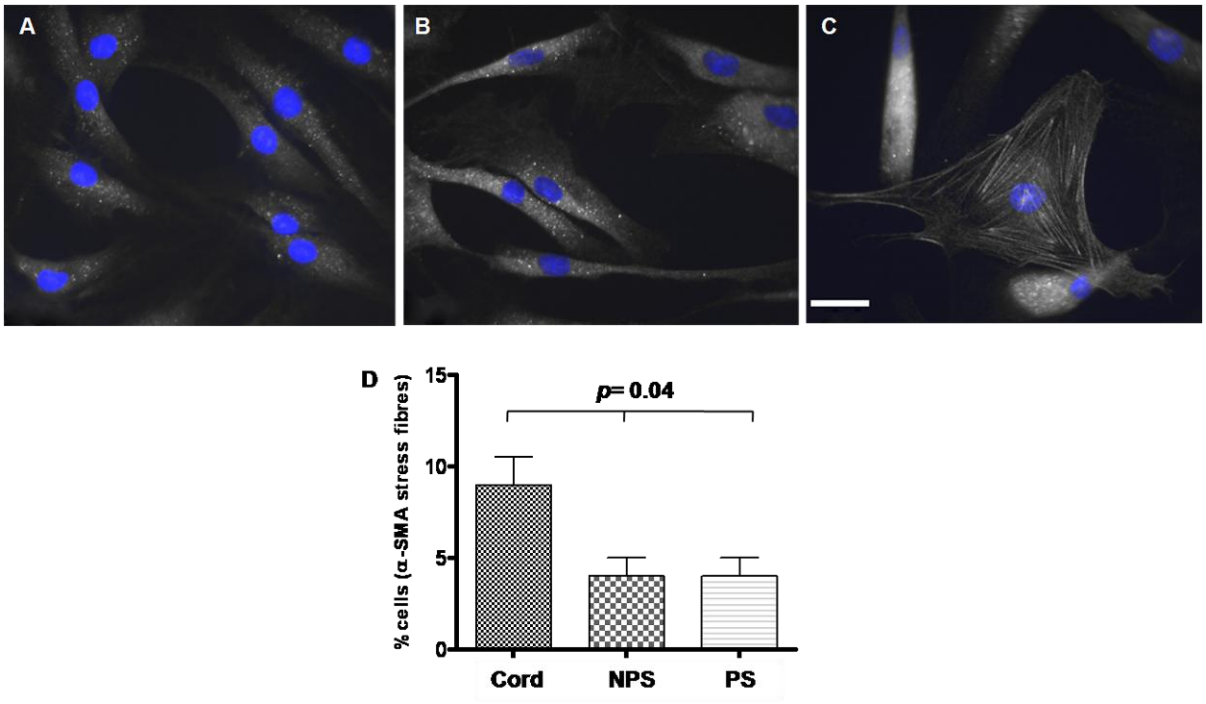


Figure 4.2. α-SMA distribution in cells from whole dupuytren's tissue and dermal fibroblasts. Cells were cultured on glass coverslips for 24 hours, fixed and then immunofluorescently labelled using α-SMA antibody (white) and DAPI (blue). Representative images are shown for (A) non-palmar skin fibroblasts, (B) palmar skin fibroblasts and, (C) Whole Dupuytren's cord cells. α-SMA localisation to stress fibres is seen in the central cell of panel (C). Scale bar: 30µm. (D) The numbers of cells with α-SMA positive stress fibres in non-palmar fibroblasts, palmar fibroblasts and whole Dupuytren's cord cells were counted on digital images and expressed as a percentage of total cells (original magnification x 60).

These data show that although there are more myofibroblasts in whole Dupuytren's tissue compared to control dermal fibroblasts, the overall percentage of myofibroblasts is still relatively low (Tomasek and Rayan, 1995).

4.2.4 Nodule-derived *versus* non-nodular fibroblasts

To ensure a reliable source of Dupuytren's cells with proportionally more α-SMA positive stress fibres, methodology using primary Dupuytren's tissue samples was developed. The previous chapter demonstrated that in longitudinal histology sections of cord a very high

percentage of samples had PIPJ nodules. Therefore, all PIPJ marked digital cords were routinely bisected. One half was subdivided and used to isolate cells specifically from the PIPJ area which I have shown to frequently contain α-SMA rich nodules, whilst the cut surface of the mirror half was processed by histology to confirm the presence of these α-SMA rich nodules (Verjee et al., 2009) (Fig. 4.3). Cells isolated from the PIPJ were also examined by immunofluorescence and the percentage of α-SMA positive stress fibres was correlated with the presence of histological nodules.

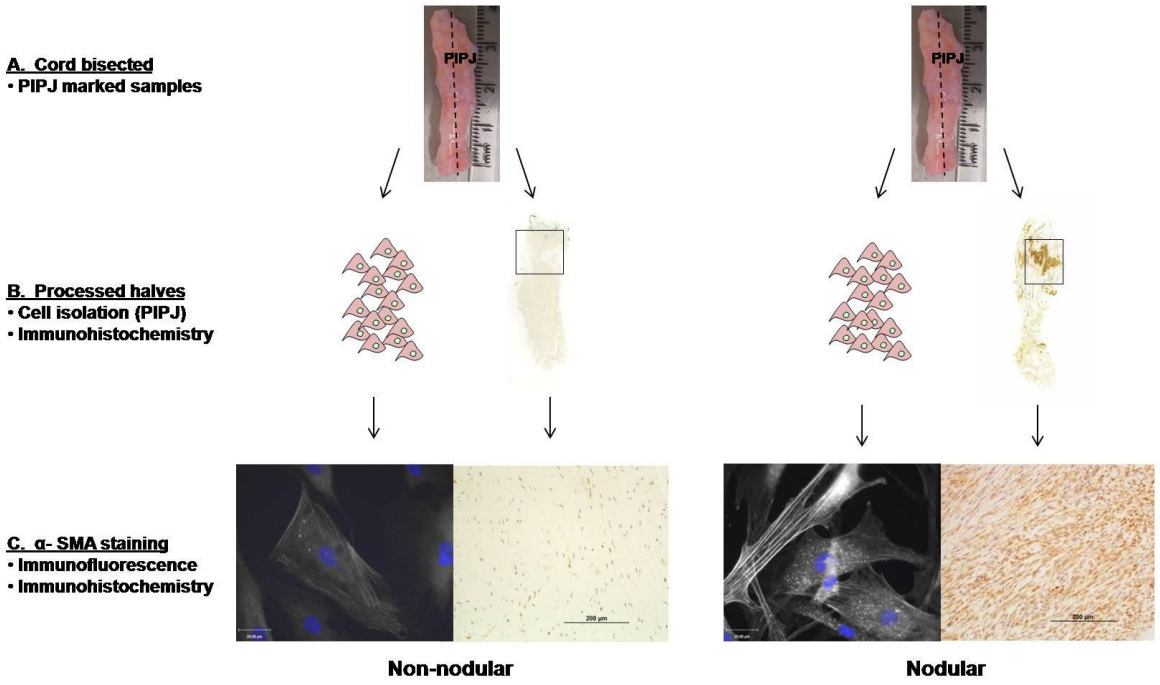


Figure 4.3. Methodology used to isolate Dupuytren's cells from nodular *versus* non-nodular cord. (A) Digital cords were longitudinally bisected as shown by the dotted line. (B) One half was fixed in formalin and histological sections taken from the cut surface were stained for α-SMA. Using the mirror half of the bisected cord, cells were also isolated specifically from the marked PIPJ region by collagenase digestion. (C) PIPJ cells were cultured on glass coverslips for 24 hours, fixed and then immunofluorescently labelled using α-SMA antibody (white) and DAPI (blue). Representative images are shown for non-nodular and nodular samples and compared to histological sections taken from the mirror half of the same excised cord sample.

In nodule-derived cells, α-SMA protein frequently localised to cytoskeletal stress fibres (Fig. 4.4A-C), whereas in dermal fibroblasts α-SMA protein was typically seen in the peri-nuclear cytoplasm (Fig. 4.4D,E). The percentage of cells with positive α-SMA stress fibres were counted in 3 nodular matched patient samples. Nodule-derived cells had significantly more cells with α-SMA stress fibres than dermal fibroblasts (mean α-SMA stress fibres: nodule-derived cells = 35% ± 13; dermal fibroblasts = 3% ± 0.5) (Fig. 4.4F). The percentage of cells with positive α-SMA stress fibres were also counted in 3 non-nodular matched patient samples (Fig. 4.4G). Non-nodular samples had 10% ±3% cells with α-SMA stress fibres. These data suggest that α-SMA is more frequently seen to localise to stress fibres in nodule-derived cells.

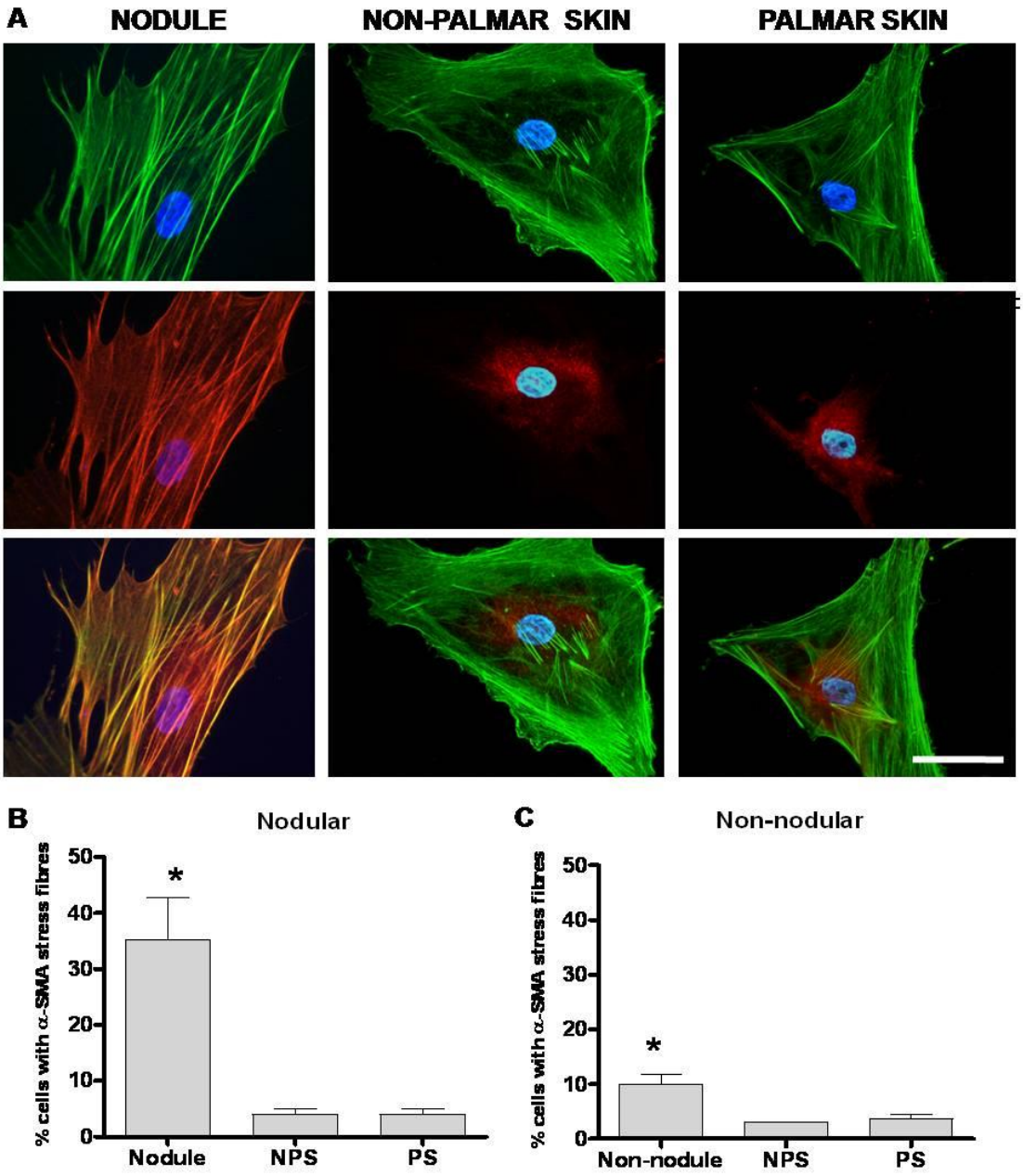


Figure 4.4. Quantification of α-SMA localisation to stress fibres in dermal fibroblasts, Dupuytren's nodule-derived and non-nodular cells. Cells were cultured on glass coverslips for 24 hours, fixed and then immunofluorescently labelled using α-SMA antibodies (red), phalloidin (green) and DAPI (blue). (A) Representative images are shown for Dupuytren's nodule-derived cell, non-palmar fibroblast and palmar fibroblast. The higher panels show staining for phalloidin (green) and DAPI (blue). The middle panels show α-SMA (red) and DAPI (blue), and the lower panels represent merged images with α-SMA (red), phalloidin (green) and DAPI (blue) staining. Scale bar: 20µm. (B, C) The numbers of cells with α-SMA positive stress fibres from nodular and non-nodular samples, palmar and non-palmar skin were counted on digital images (over 300 cells counted per cell type) and expressed as a percentage of total cells (original magnification x 60). * p = 0.03 (nodule-derived vs. non-nodular cells). Experiments were performed in triplicate and data are shown as the mean (±SEM) from a total of 3 different nodular and non-nodular matched patient samples.

4.2.5 Cell passage

It is recognised that cells change phenotype when cultured *in vitro* (Bell et al., 1979; Moyer et al., 2002). Therefore, to determine the optimal cell passage at which to examine Dupuytren's derived myofibroblasts, I analysed the effect of passage on the number of α-SMA positive stress fibres in both nodule-derived cells and dermal fibroblasts. Cells between passage 1 and 5 were cultured on glass coverslips and immunofluoresently labelled. Nodule-derived cells demonstrated a consistent decrease in α-SMA stress fibres over time, whereas no change was seen with dermal fibroblasts (Fig. 4.5).

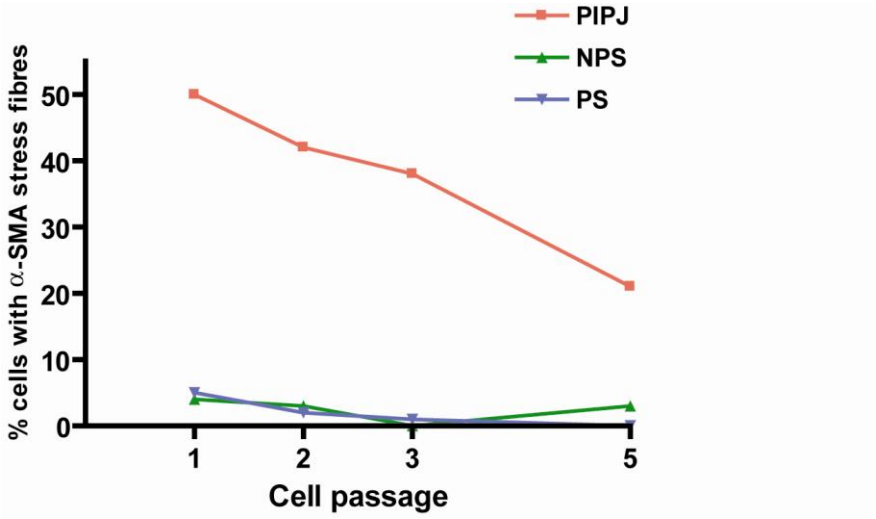


Figure 4.5. The effect of cell passage on α-SMA stress fibres in Dupuytren's nodule-derived cells and dermal fibroblasts. 20,000 nodule-derived cells and dermal fibroblasts from passage 1, 2, 3 and 5 were cultured on glass coverslips for 24 hours, fixed and then immunofluorescently labelled using α-SMA antibody and DAPI. The numbers of cells with α-SMA positive stress fibres in nodule-derived cells (nodule), palmar (PS) and non-palmar skin fibroblasts (NPS) were expressed as a percentage of total cells (deterimined by DAPI). Cells were counted in 10 fields of view at x40 magnification. Experiments were performed in triplicate and data are shown from one representativepatient as the mean (± SD).

In summary, these data show that isolating cells from Dupuytren's nodules is reliable technique for obtaining a higher percentage of myofibroblasts, which maintain their phenotype at lower cell passage.

4.2.6 FPCL contraction

Next I proceeded to determine the optimal *in vitro* contraction model for Dupuytren's myofibroblasts.

4.2.6.1 Isotonic contraction of FPCLs

Attempts to compare contractility of Dupuytren's nodule-derived cells, cord and carpal ligament-derived cells using isotonic contraction have in the past yielded inconsistent findings (Moyer et al., 2002; Rayan and Tomasek, 1994; Tomasek and Rayan, 1995). Therefore, initial experiments were carried out to examine the differences in isotonic contraction between Dupuytren's cells, non-palmar and palmar fibroblasts from matched patient samples using a simple stress-release model of FPCL contraction (Grinnell, 1994; Tomasek et al., 1992).

Following trypsinisation, 1 x 10^5 cells were seeded in 250µl of collagen. FPCLs were allowed to polymerise at 37°C for 30 minutes in 24-well tissue culture plates and then cultured with 1ml DMEM (with 10% FBS) at 37°C in 5% CO_2 for 24 hours. After 24 hours, FPCLs were mechanically released from the plate edges using a sterile needle, and FPCL surface area contraction measured using digital images at regular intervals over 48 hours. Polymerised collagen alone without cells consistently demonstrated only minimal surface area contraction (<3%) (Fig. 4.6A, B). Cells isolated from Dupuytren's tissue, non-palmar and palmar skin contracted rapidly over time to the same extent (Fig. 6A), and no significant difference in contraction was observed between these cells at 48 hours (Fig. 4.6C-E).

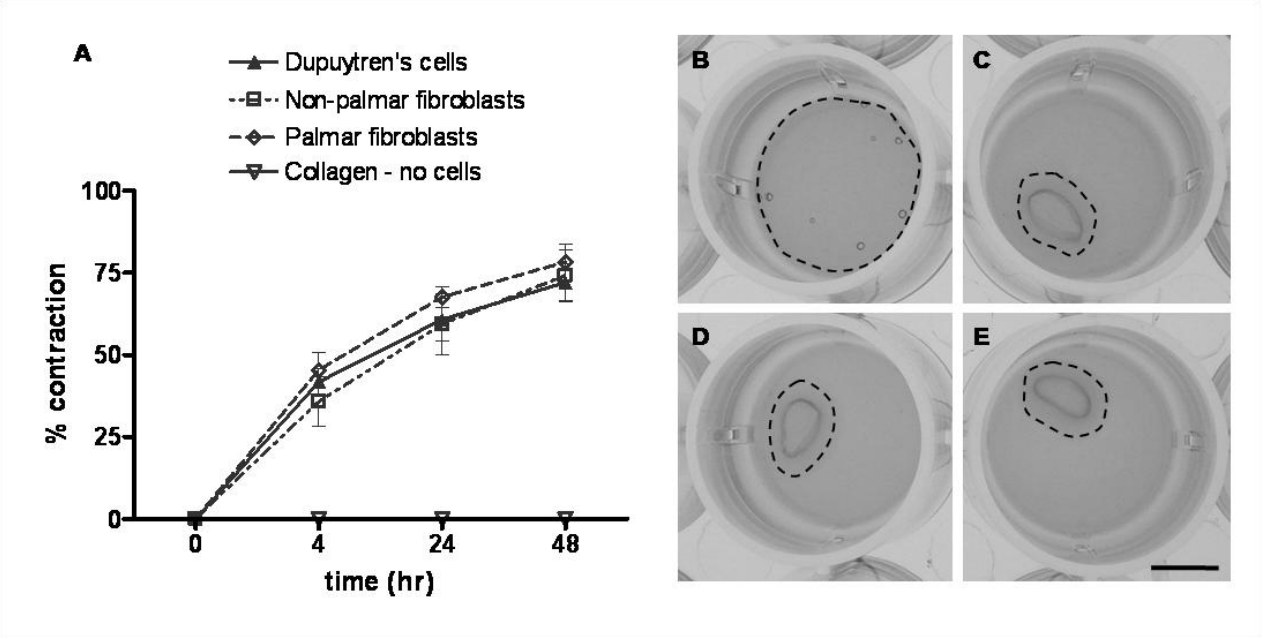


Figure 4.6. Isotonic contraction of collagen gels by dermal fibroblasts and Dupuytren's nodule-derived cells. Collagen gels were seeded with non-palmar fibroblasts, palmar fibroblasts or Dupuytren's nodule cells and cultured for 24h. Control gels were cultured for 24h in the absence of any cell type. (A) After 24h collagen gels were released from the edge of the culture dish and gel contraction was assessed by quantifying change in gel surface area over time up to 48h. Data are shown as the mean % contraction (± SEM) from triplicate experiments using cells derived from one patient and are representative of values from a total of 5 different patients. (B-D) Representative images of collagen gels without cells (B) or seeded with non-palmar fibroblasts (C), palmar fibroblasts (D) or Dupuytren's nodule cells (E) after 48h of contraction. The dashed black line indicates the outer edge of each collagen gel. Scale bar = 5mm.

These data suggest that despite there being significantly more α-SMA stress fibres in Dupuytren's cells and dermal fibroblasts, their isotonic force contraction is not significantly different at 48 hours.

4.2.6.2 Isometric contraction of FPCLs

One limitation of isotonic FPCL contraction is that in detaching the constructs, matrix stiffness is lost and this has been shown to result in loss of α-SMA stress fibres within 10 minutes (Tomasek et al., 1992). This in turn would disguise any differential contraction between populations of fibroblasts and myofibroblasts. Therefore, I next used the culture force monitor (CFM) to measure isometric contractile forces generated by constrained FPCLs as previously described (Fig. 4.7) (Eastwood et al., 1996).

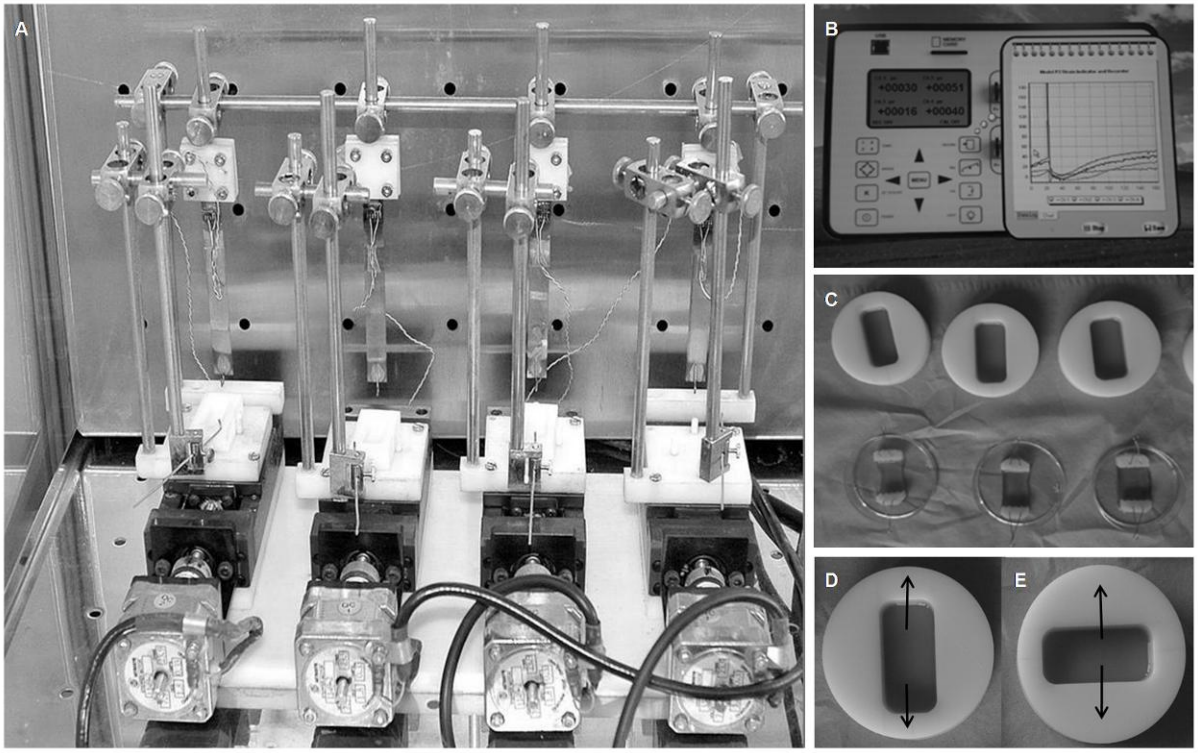


Figure 4.7. The culture force monitor (CFM). (A) Rectangular seeded collagen gels were cast and floated in medium, tethered between two flotation bars one of which is held stationary whilst the other is attached to a force transducer. (B) Cell-generated tensional forces in the collagen gel are detected by the force transducer, and live data are logged every 15 seconds providing a continuous output of force (dynes, $1x10^5$ *N*) generated. (C) After 24 hour contraction, gels are harvested and processed for α-SMA mRNA, protein and immunofluorescence. (D) Cells were routinely seeded in gels with a high aspect-ratio collagen lattice, although low aspect-ratio lattices (E) were also used in experiments to compare effects of less strain on cell contractility.

Dupuytren's nodule-derived cells, non-palmar and palmar fibroblasts from matched patient samples were seeded in high aspect-ratio FPCLs, attached to a CFM force transducer and isometric force generated was quantified in real time. FPCLs seeded with 1.5 million non-palmar fibroblasts (Fig. 4.8A) or palmar fibroblasts (Fig. 4.8B) initially contracted (mean: 0.5 ± 0.2 dynes/hr) and reached a plateau on average after 15hr (range: 4-20hrs), with a maximum force of 52 dynes. The same number of nodule-derived cells continued to contract to a maximum of 173 dynes (mean: 3.5 ± 1.1 dynes/hr) and did not reach tensional homeostasis (Fig. 4.8C).

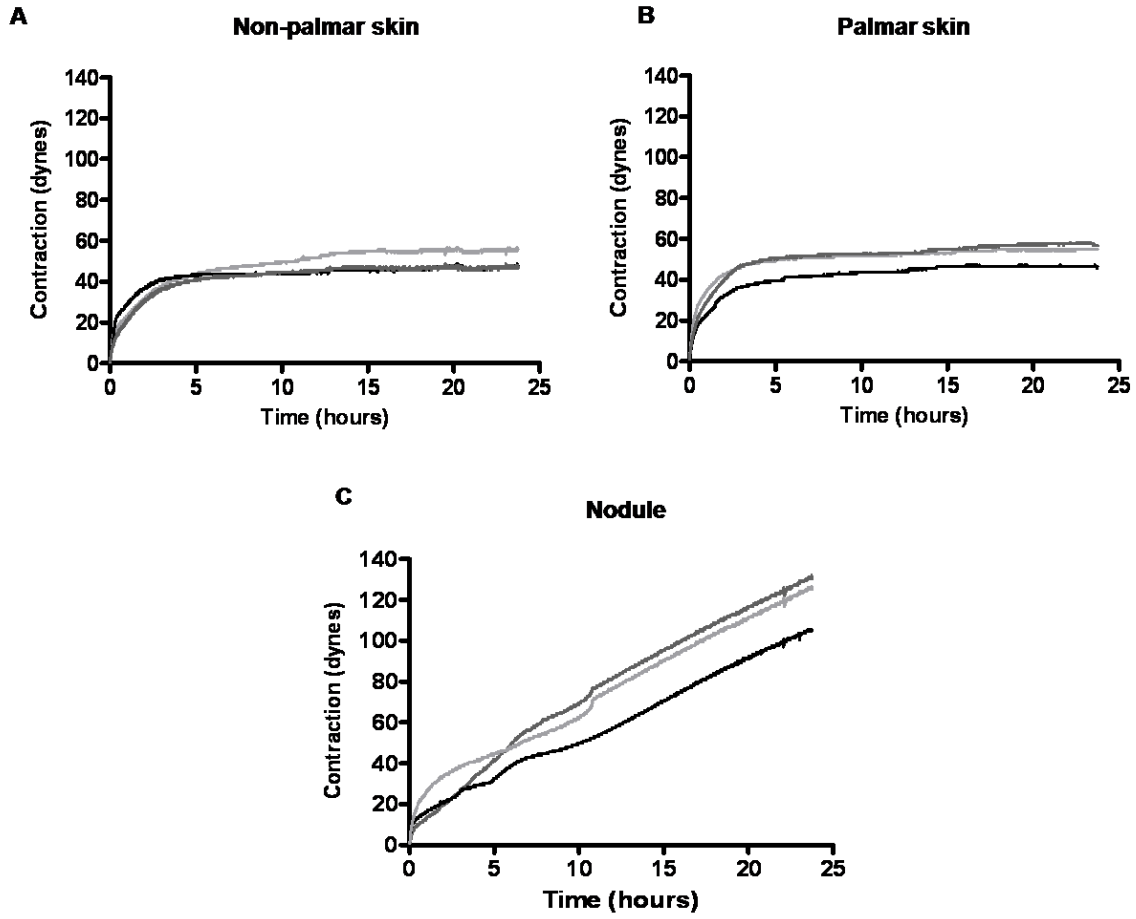


Figure 4.8. Isometric contraction of collagen gels by dermal fibroblasts and Dupuytren's nodule-derived cells. (A-C) Collagen gels were seeded with 1.5 million non-palmar fibroblasts (A), palmar fibroblasts (B) or Dupuytren's nodule-derived cells (C), cultured for 24h in the CFM and real-time isometric force contraction was quantified. Data shown represent triplicate experiments using cells derived from one patient.

To compare isometric force generated by cells isolated from α-SMA rich nodules (Fig. 4.9A) and non-nodular tissue samples (Fig. 4.9D), FPCLs were seeded with either nodule-derived cells or non-nodular cells and attached to the CFM for 24 hours. Nodule-derived cells and non-nodular cells were compared to collagen gels seeded with matched non-palmar and palmar skin fibroblasts (Fig. 4.9B,E). Whilst both nodule-derived cells and non-nodular cells continued to contract over 24 hours and neither reached a plateau, nodule-derived cells contracted at a greater rate than non-nodular cells (Fig. 4.9C, F).

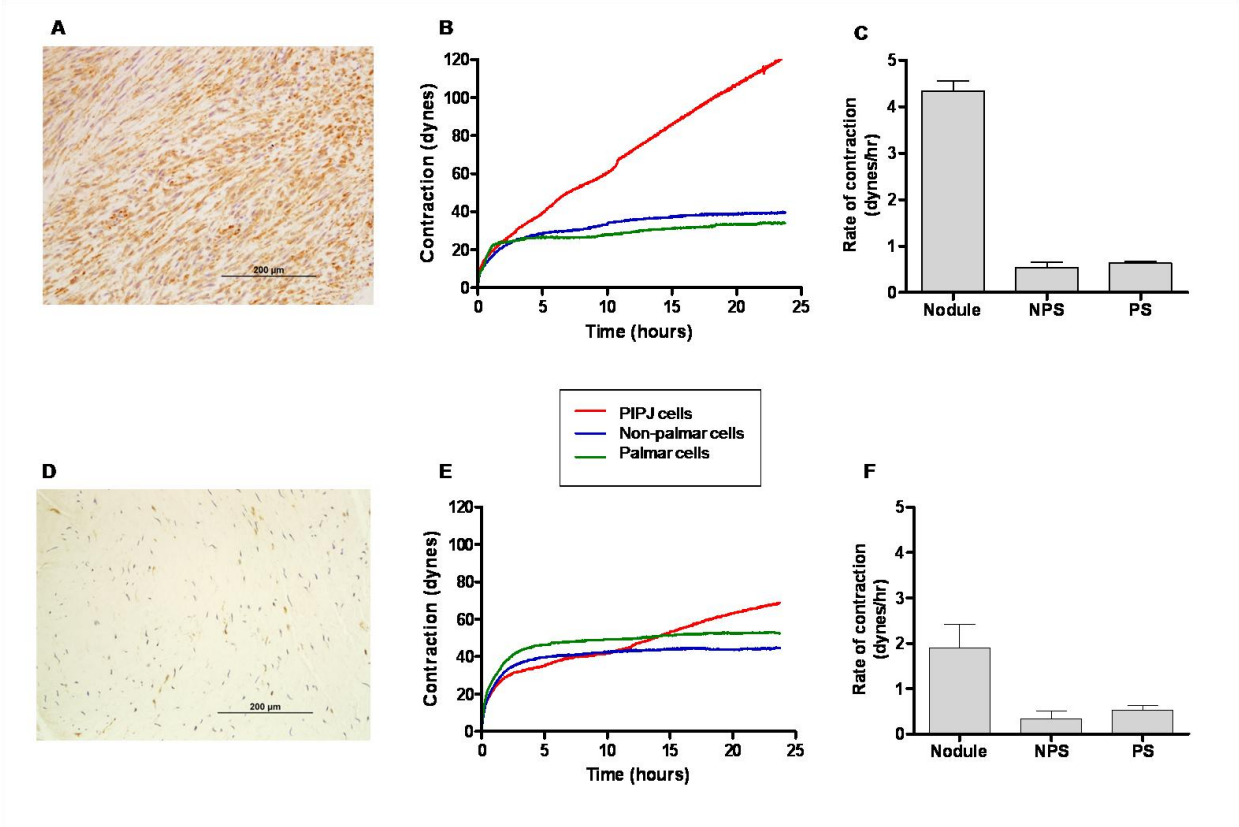


Figure 4.9. Isometric force generated by PIPJ nodular (A-C) and non-nodular (D-F) cells. (A) Histological section from a nodular sample stained for α-SMA. (B) Matched nodule-derived cells, non-palmar skin and palmar skin fibroblasts were seeded in collagen gels and isometric force contraction measured over 24 hours and, (C) measured as the average rate of contraction between 6 and 24 hours. (D) Histological section from a non-nodular sample stained for α-SMA. (E) Matched non-nodular cells, non-palmar skin and palmar skin fibroblasts were seeded in collagen gels and isometric force contraction measured over 24 hours and, (F) measured as the average rate of contraction between 6 and 24 hours. Values represent the mean of 3 experiments (± SEM) from one nodular and non-nodular patient sample (C+F).

These experiments were repeated in 5 nodular (nodule-derived) and 3 non-nodular matched patient samples. Although the absolute rate of force contraction varied between patients, nodule-derived cells consistently generated significantly higher force than non-nodular cells ($p = 0.03$) and neither reached a plateau over the 24h test period. In all matched samples, both nodule-derived and non-nodular cells also generated significantly higher force than dermal fibroblasts (Fig. 4.10).

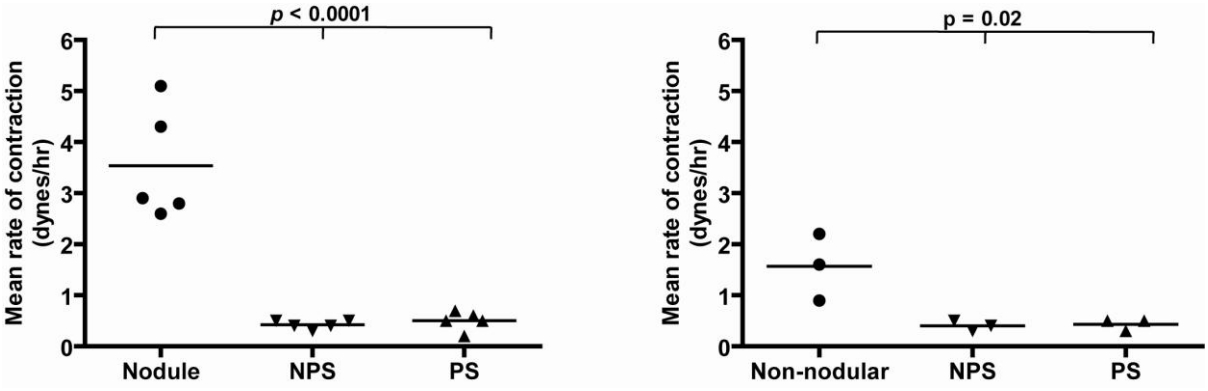


Figure 4.10. Isometric contraction in FPCLs from 5 nodular and 3 non-nodular matched patient samples. The average rate of contraction between 6 and 24 hours for nodule-derived cells (nodular), non-nodular Dupuytren's cells (non-nodular), non-palmar (NPS) and palmar fibroblasts (PS) is shown. (A) Five different "nodular" matched patient samples. (B) Three different "non-nodular" matched samples. Horizontal bars represent mean rates of contraction (dynes/hr).

To ensure nodule-derived cells were within the linear range of contraction and to verify at what cell density they reached a plateau, FPCLs were also seeded with reducing cell densities (1.125, 0.75, 0.375 and 0.15×10^6 million cells) in the same final volume of collagen gel (2.5ml). The rate of nodule-derived cell contraction was proportional to cell number (Fig. 4.11).

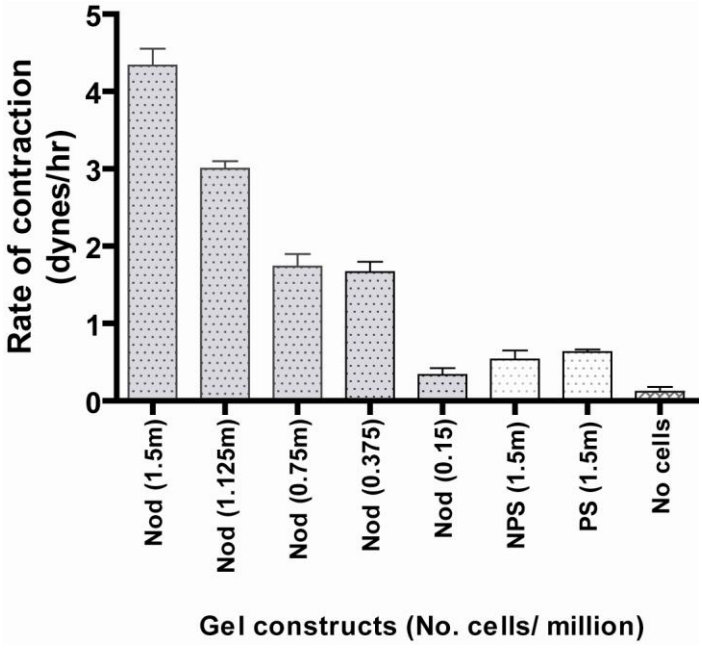


Figure 4.11. Isometric force contraction in collagen gels seeded with decreasing numbers of Dupuytren's nodule-derived cells. Collagen gels were seeded with decreasing numbers of nodule-derived cells (1.5m, 1.125m, 0.75m, 0.375m, 0.15m) and either non-palmar (NPS) or palmar fibroblasts (PS) (1.5m each). Collagen alone with no cells was included as a control. The average rate of contraction (dynes/hr) between 6 and 24 hours was quantified. Data are shown as the mean of triplicate experiments (± SEM) using cells derived from one patient and representative of results from 3 different patient samples.

Earlier monolayer studies demonstrated that decrease in α-SMA stress fibres by immunofluoresence over time in culture (Fig. 4.5). Therefore, using isometric force contraction as a read-out, the effect of passage on cell contractility was analysed in both nodule-derived cells and dermal fibroblasts. Collagen gels seeded with cells at passage 1 and 5 were attached to the CFM for 24 hours. Using nodule-derived cells, isometric force generation significantly decreased between passage 1 and 5, whereas mean isometric force generation increased with non-palmar skin fibroblasts (Fig. 4.12).

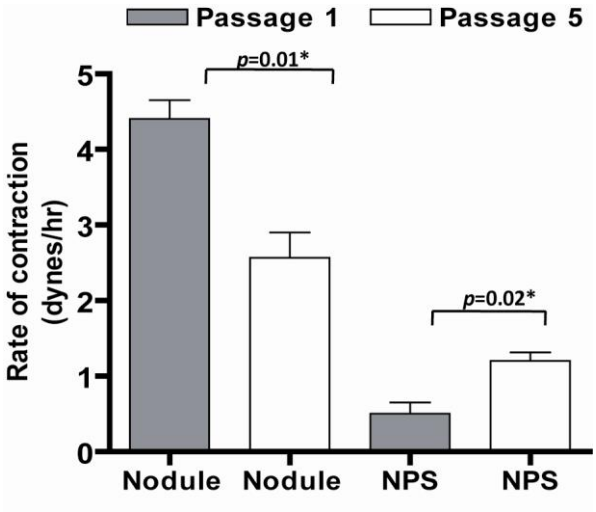


Figure 4.12. The effect of cell passage on the contractility of Dupuytren's nodule-derived cells and dermal fibroblasts. (A) 1.5 million nodule-derived cells (nodule) and dermal fibroblasts (NPS) from cell passage 1 and 5 were seeded in collagen gels and analysed for isometric force contraction. Data are shown as mean (± SEM) from triplicate experiments using cells derived from one patient.

These data show that differences in contraction between nodule-derived cells and dermal fibroblasts at 24 hours are only seen under isometric and not isotonic conditions. Compared with dermal fibroblasts, nodule-derived cells continued to contract in a dose dependent manner and did not reach a plateau. These contractile differences were seen consistently between different patients. Furthermore, with increasing cell passage, nodule-derived cells lost their contractility whereas dermal fibroblasts became more contractile.

4.2.7 Post-transcriptional regulation of α-SMA drives myofibroblast contractility

To correlate α-SMA expression in nodule-derived cells and dermal fibroblasts from matched patient samples with contraction, collagen gels seeded with each cell type underwent isometric contraction for 24h. Nodule-derived cells contracted at a significantly greater rate over the 24h test period than dermal fibroblasts (mean rate of contraction, nodule-derived cells = 4.3 dynes/hr; non-palmar fibroblasts= 0.5 dynes/hr; palmar fibroblast = 0.6 dynes/hr) (Fig. 4.13A). After 24 hours contraction, cells were then harvested from FPCLs and α-SMA mRNA levels and α-SMA protein levels determined by pcr and western blot respectively; α-SMA localisation was assessed by immunofluoresence.

No significant difference (p=0.9) was seen in total α-SMA mRNA levels when compared to RPLPO (Fig. 4.13B) and GAPDH (Fig. 4.13C). However, nodule-derived cells expressed more α-SMA protein than dermal fibroblasts compared to vimentin. Vimentin was used as a control as it is expressed equally in myofibroblasts and fibroblasts (Hinz et al., 2001a) (Fig. 4.13D). The ratio of α-SMA-to-vimentin was 1.74: 0.66: 0.42 (nodule-derived cells: non-palmar fibroblasts: palmar fibroblasts) as assessed by densitometry. Furthermore, whilst non-palmar and palmar fibroblasts frequently demonstrated α-SMA staining in a cytosolic peri-nuclear arrangement, in nodule cells α-SMA was typically distributed throughout the cell processes in stress fibres up to the sites of cell-matrix attachment (Fig. 4.13E). These data suggest change that post-transcriptional changes in α-SMA regulate contractility of Dupuytren's nodule-derived cells.

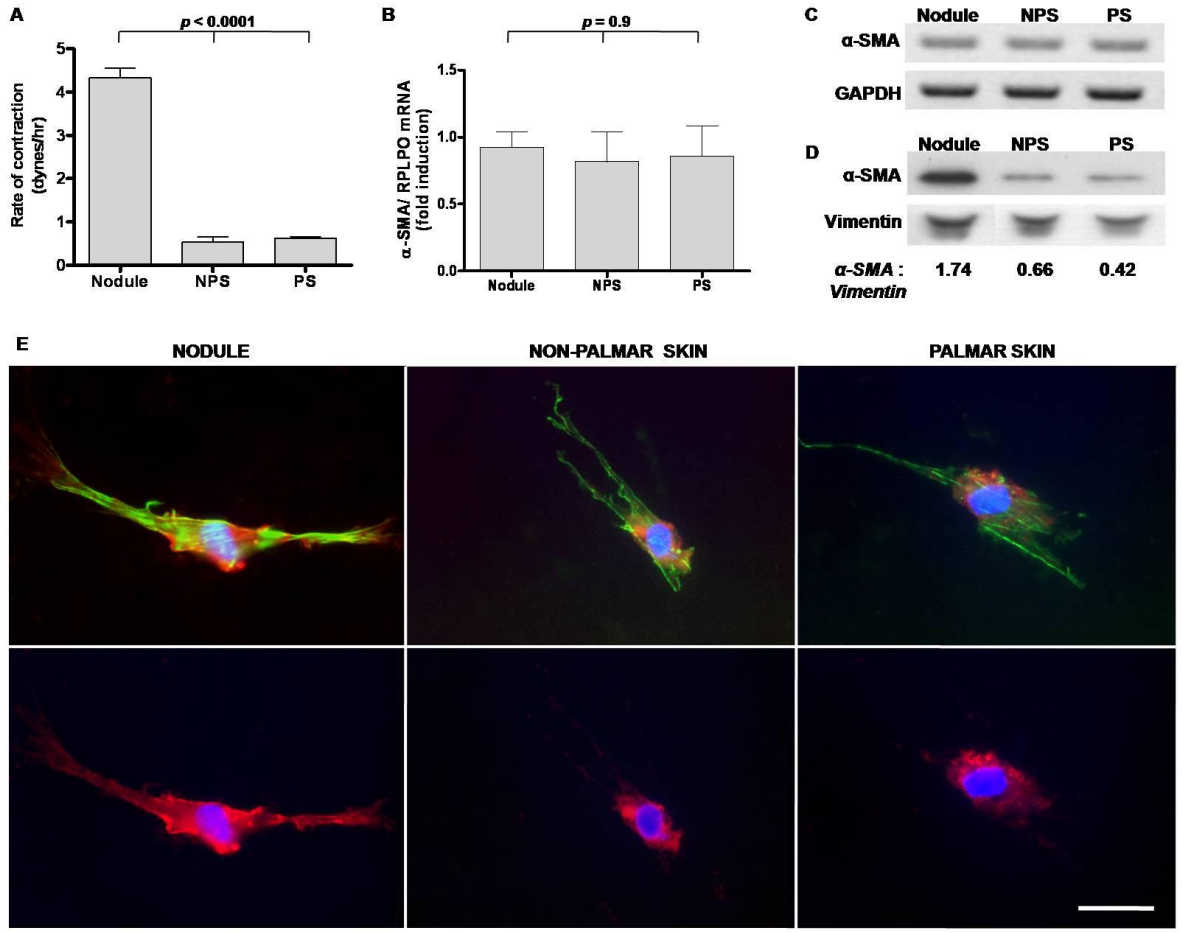


Figure 4.13. Contractility of Dupuytren's nodule-derived cells is regulated by post-transcriptional changes in α-SMA. (A) Isometric force contraction in collagen gels seeded with nodule-derived cells (nodule), non-palmar (NPS) and palmar fibroblasts (PS) over 24 hours. Experiments were performed in triplicate and values represent the mean ± SEM. After 24 hours cells were isolated from gels and levels of (B) α-SMA mRNA compared to RPLPO by quantitative RT-pcr (C) α-SMA mRNA compared to GAPDH, (D) levels of α- SMA protein compared with vimentin and, (E) α-SMA protein localisation analysed by immunofluorescence. (E) Representative immunofluorescence images of nodule-derived cells, palmar and non-palmar fibroblasts are taken from 7µm thick sections fixed and stained with α SMA antibodies (red), phalloidin (green) and DAPI (blue) are shown in the higher panels. The lower panels are images of the same cells showing only α-SMA staining (red) and DAPI (blue). Scale bar: 30µm. Data are shown from experiments using cells derived from one matched patient sample and are representative of a total of 3 different patients.

4.2.8 Dermal fibroblasts co-cultured with nodule-derived cells show no difference in isometric force contraction

Recurrence following dermofasciectomy has been reported to be as low as 1% (Tonkin et al., 1984). However, the mechanism of reduced recurrence following dermofasciectomy remains unexplained. Therefore, co-culture experiments were performed to test the hypothesis that the contractility of Dupuytren's nodule-derived cells is negatively regulated by non-palmar dermal fibroblasts. A co-culture system was used to investigate how dermal components regulate the behaviour of Dupuytren's myofibroblasts. Initially, using the stress-released model, collagen gels containing Dupuytren's cells from patient D13 were then overlaid with matched non-palmar dermal fibroblasts contracted significantly less than gels overlaid with palmar skin fibroblasts (figure 4.14A). However, the gel contraction assays using D13 cells was repeated a further three times. In these experiments no significant differences were observed in the rate or level of contraction of cord cells in co-culture with palmar or non palmar dermal fibroblasts (Fig. 4.14B).

These gel contraction experiments have been repeated in three further matched patient samples (D18, ED011 and ED013). Again no significant differences were observed in the rate or level of contraction of cord cells in co-culture with matched palmar or non palmar dermal fibroblasts (Fig. 4.14C-E).

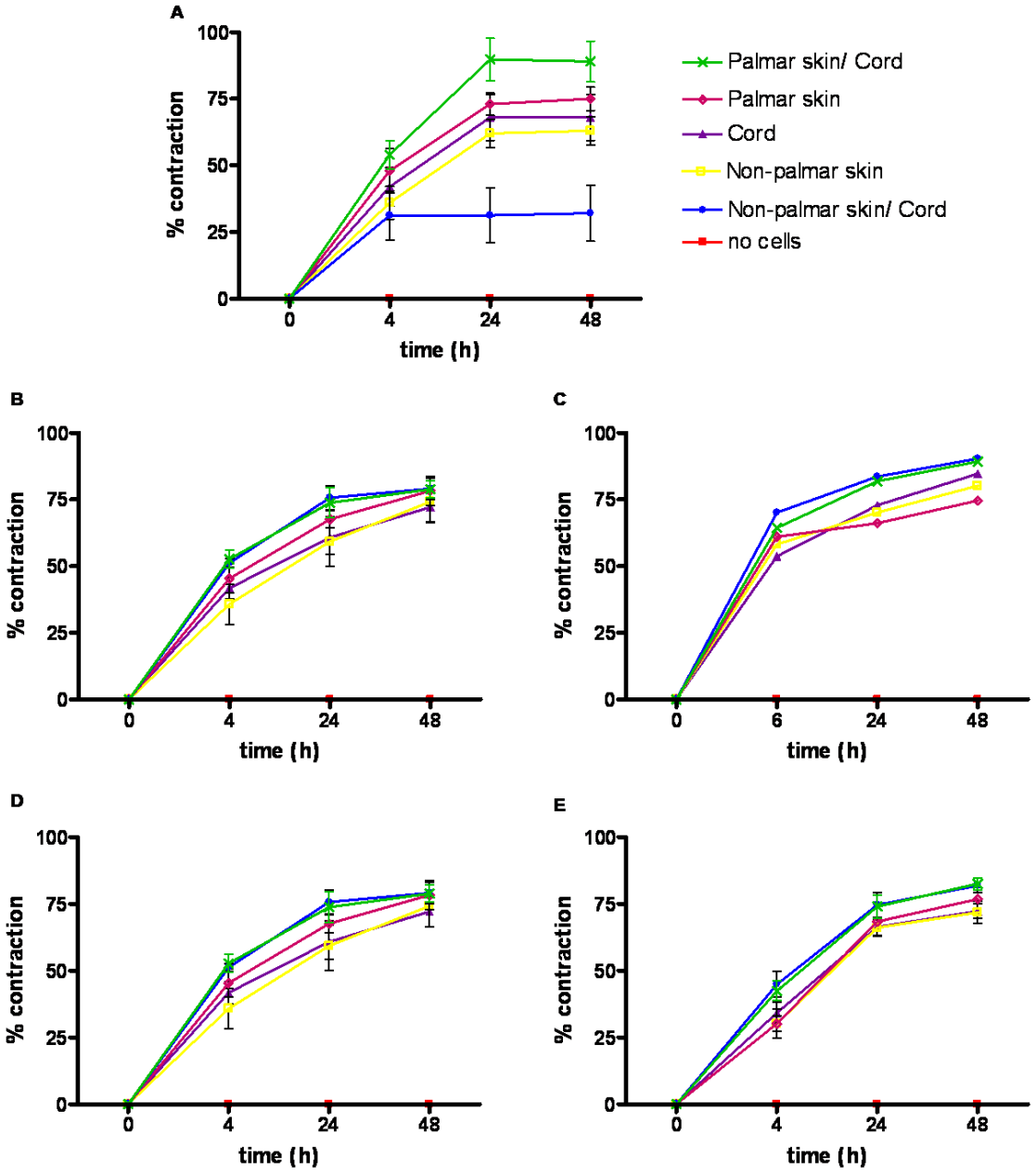


Figure 4.14. Isotonic contraction of stress released FPCLs using matched cells isolated from 4 patients. FPCLs containing Dupuytren's cells overlaid with non-palmar dermal fibroblasts contracted significantly less than Dupuytren's cells overlaid with palmar fibroblasts isolated from the same patient (A). However, in repeat experiments from the same patient FPCLs containing Dupuytren's cells overlaid with non-palmar dermal fibroblasts contracted to an equal extent to cord cells overlaid with palmar fibroblasts isolated from patient (B). Data shown are the average values from 3 independent experiments +/-SEM. Isotonic contraction of FPCLs was assessed in 3 further matched patient samples: D18 (C), ED013 (D) or ED011 (E), and again no differences in contraction were seen. Data shown are the average values from 3 independent experiments +/-SEM (D18), values from 2 independent experiments +/-SEM (ED011), or the average values from a single experiment (ED013).

The inhibitory effect of non palmar fibroblasts on cord contraction seen initially with co-culture contraction (Fig. 4.14A) has not been reproducible in 4 different patient samples. These experiments were repeated exhaustively controlling for user variability, collagen type, cell passage number, pH and cell number and the results remain variable: in some experiments using cells from patient D13 non-palmar fibroblasts inhibited contraction, in others they did not. The inhibition by non-palmar fibroblasts was never observed with cells from patients: D18, ED011 and ED013.

Isometric force contraction was also used as a read-out to examine co-cultures of nodule-derived cells and dermal fibroblasts. FPCLs were seeded with co-cultures of 1.5 million nodule-derived cells and dermal fibroblasts, with different cell proportions (75% nodule-derived cells+ 25% non-palmar or palmar fibroblasts; 25% nodule-derived cells+ 75% non-palmar or palmar fibroblasts) and attached to the CFM for 24 hours. As nodule cells were the contractile cell type, isometric forces generated from co-culture FPCLs were compared with control FPCLs seeded with equivalent densities of nodule cells (ie. 25% nodule cells co-culture was compared with 375,000 PIPJ nodule cells and 75% with 1.125m cells). No significant difference was observed in isometric force contraction with different ratios of the matched cells over 24 hours (Fig. 4.15A).

To further investigate the potential effects of longer term co-cultures, cells were co-cultured together for 5 days at the same cell ratios as described above. After 5 days, isometric forces generated were measured over 24 hours (Fig. 4.15B). No significant difference was observed with these co-cultures (75% nodule-derived cells+25% dermal fibroblasts; 25% nodule-derived cells+75% dermal fibroblasts).

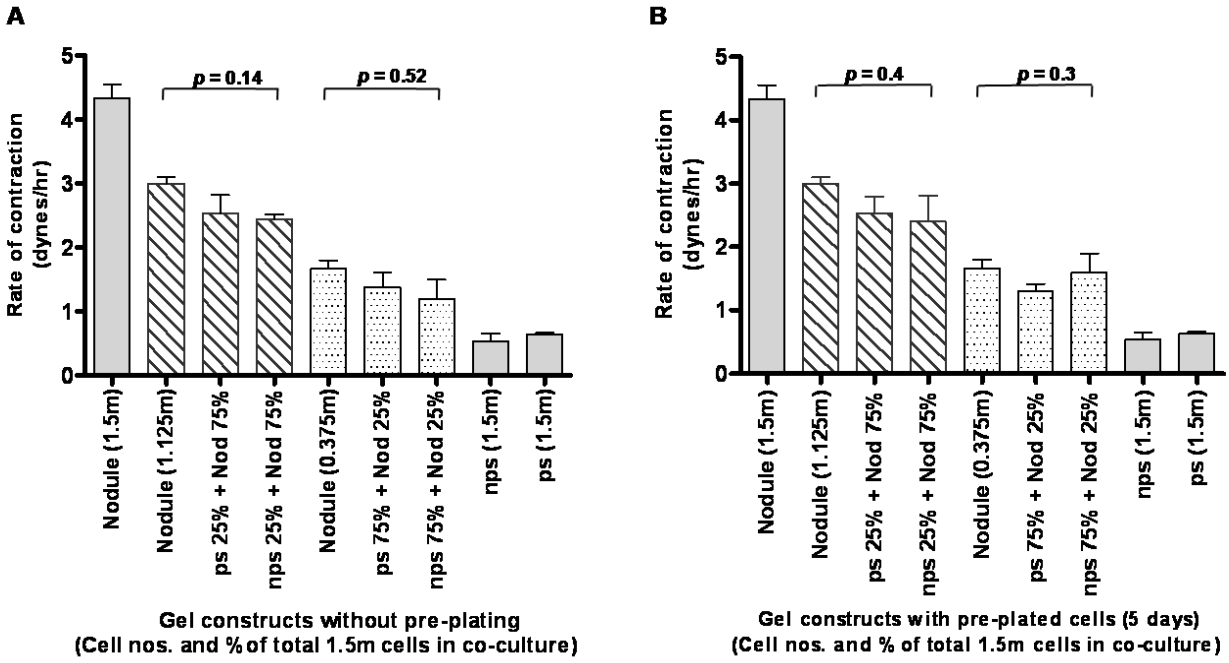


Figure 4.15. Isometric contraction of collagen gels seeded with co-cultures of dermal fibroblasts and Dupuytren's nodule-derived cells. (A) Co-cultures of nodule-derived cells and dermal fibroblasts (either palmar or non-palmar) were seeded in collagen gels at different cell ratios of nodule to dermal fibroblasts. A total of 1.5m cells were seeded in gels with co-cultures or dermal fibroblasts alone. Nodule-derived cells were seeded at equivalent cell densities to nodule-derived cells in co-culture (1.125m nodule cells = 75% nodule cells in co-culture; 0.375m nodule cells = 25% nodule cells in co-culture). Contractile profiles of co-cultures were then compared to nodule-derived cells of equivalent cell densities. (B) Co-cultures were also pre-plated for 5 days using the same cell ratios, then seeded in collagen gels and isometric force contraction measured over 24 hours. Data are shown as the mean (± SEM) from triplicate experiments using cells derived from one patient, and are representative of values from a total of 3 different patients

To ensure that each cell type proliferated at the same rate, parallel experiments were carried out with fluorescently labelled nodule-derived cells (Vybrant CFDA cell tracer kit, Invitrogen). In these experiments 20,000 cells were co-cultured on 18mm glass coverslips for 5 days and then fixed and stained with DAPI. Total cell numbers were determined by DAPI staining and fluorescent labelled nodule-derived cells were calculated as a percentage of the total. There was no difference in both proliferation rates of the individual cell types

(p=0.6) and the relative proportion of nodule cells to dermal fibroblasts in each co-culture construct (p=0.2, p=0.7) (Fig. 4.16A).

To support the data, a MTT based assay using the same proportion of cells as described above, demonstrated no difference in metabolic activity with co-culture constructs (p=0.3) (Fig. 4.16B).

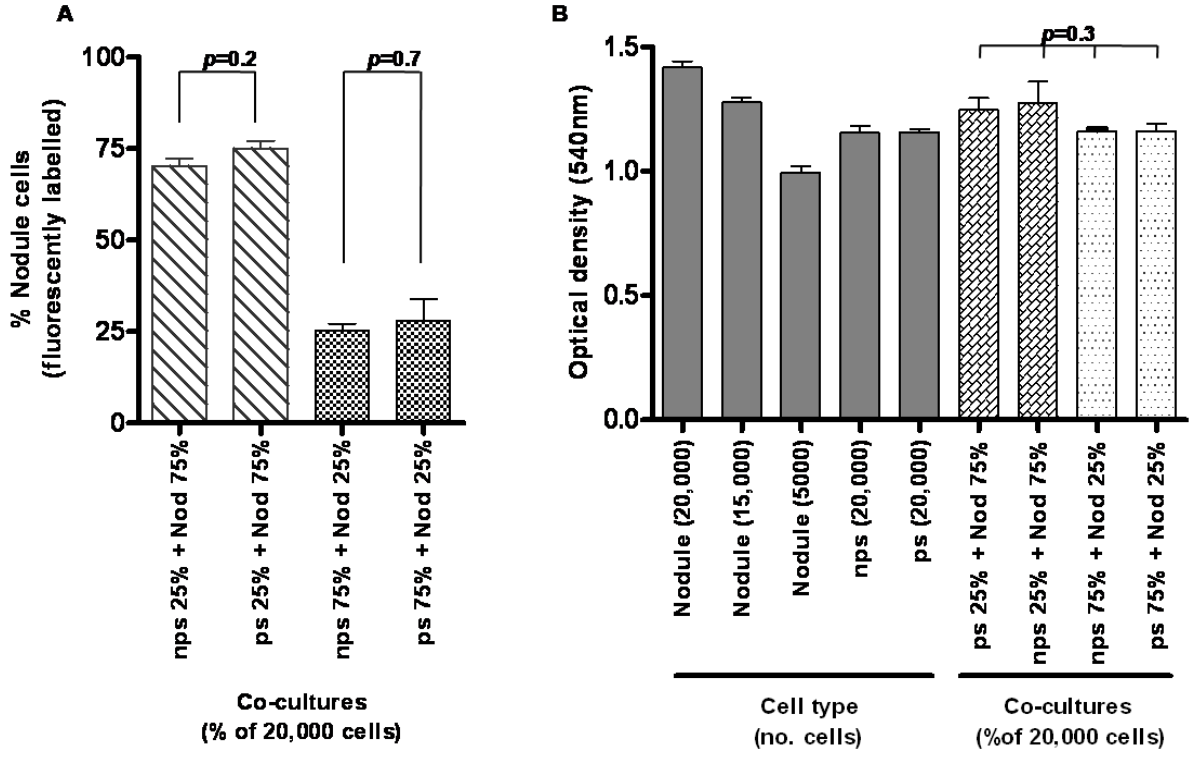


Figure 4.16. Five day co-culture proliferations studies and cell viability assay: (A) Monolayer experiments with 2,500 cells cultured on coverslips were performed with fluorescently labelled nodule cells and stained with DAPI to determine proliferation rates of cells when in co-culture. Fluorescently labelled nodule-derived cells were counted and are presented as a percentage of total cells (B) Using 5000 cells in 96 well plates, cell viability was analysed after 5 days in co-culture using a MTT assay (optical density at 540 nm). Experiments were performed in triplicate. Data are shown as mean ±SEM.

Co-cultures in both low and high aspect-ratio FPCLs were also compared to examine the dependence of strain on cell contractility as, high aspect-ratio FPCLs (Fig. 1D) have been shown to generate high strain patterns and better reflect cellular activity of Dupuytren's tissue (Eastwood et al., 1998). Identical co-cultures of 50% dermal fibroblasts and 50% nodule cells were seeded in collagen gels and compared with high and low aspect-ratio lattices. No significant difference in the rate of isometric force generation (p=0.1) was observed between FPCLs with different aspect-ratios (high aspect-ratio=2 ± 0.2 dynes/h; low aspect-ratio=1.6 ± 0.1 dynes/h) (Fig. 4.17). However, overall force generation was significantly greater (p=0.005) with high aspect-ratio FPCLs after 24 hours contraction (mean high aspect-ratio= 91±1 dynes/24h, and mean low aspect-ratio mean=77±4 dynes/24h).

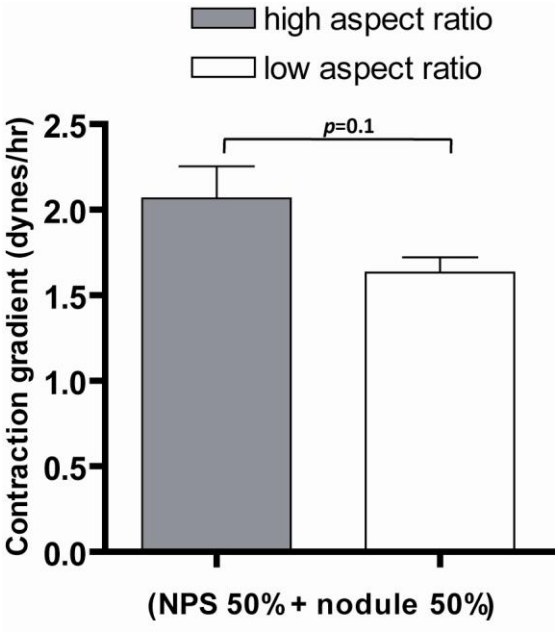


Figure 4.17. Rate of contraction and maximum isometric force contraction with different FPCL aspect-ratios. High and Low aspect-ratio FPCLs were seeded with identical co-cultures of 1.5 million cells (NPS 50% + nodule cells 50%). The rate of contraction in dynes/hr is shown for 24h.

4.3 DISCUSSION

Myofibroblasts are best studied in 3D collagen lattices under isometric conditions. Although several authors have studied myofibroblasts, cells have often been derived from rat subcutaneous and lung tissue (Follonier et al., 2008; Goffin et al., 2006; Hinz et al., 2001a; Hinz, 2007) with or without treatment with TGF-β1 (Arora et al., 1999; Dugina et al., 2001). Whilst previous studies have compared Dupuytren's nodule and cord cells, they have also used non-matched carpal ligament cells as controls (Bisson et al., 2003; Bisson et al., 2004; Brickley-Parsons et al., 1981; Murrell, 1991; Rayan and Tomasek, 1994; Tomasek and Rayan, 1995). This study has for the first time compared genetically matched cells from Dupuytren's nodules, non-palmar and palmar skin with regards to their contractile phenotypes in 3D collagen lattices. I also chose to compare nodule-derived cells with control dermal fibroblasts because it has been demonstrated that dermal fibroblasts are capable of transition to myofibroblasts (Hinz, 2007). Furthermore, it was possible to isolate numerous dermal fibroblasts from tissue samples making experiments in the CFM that required large numbers of cells possible.

In the previous chapter I showed that excised Dupuytren's cords often contained multiple α-SMA-rich histological nodules, which were variable in size and that a proportion of myofibroblasts were also found distributed throughout cord tissue outside nodules (Verjee et al., 2009). Whilst this heterogeneity may account for differences in contractility observed between samples with variable proportions of α-SMA-rich cells, it also represents a significant methodological issue in Dupuytren's cell-culture based studies as no reliable myofibroblast cell lines are available. Therefore, in this study, novel methodology was

established to ensure that proportionally more α-SMA-rich cells were isolated from tissue samples. Digital cords were bisected and half processed for cell culture, whilst the cut surface of the mirror half was processed to identify samples with α-SMA-rich nodules (condensation of cells) by immunohistochemistry. Subsequent quantification by immunofluorescence demonstrated on average 35% of cells express α-SMA stress fibres in histology confirmed nodular samples, as compared to 10% α-SMA stress fibres in non-nodular samples. Although this still does not constitute a homogenous population of myofibroblasts, this method of sampling α-SMA-rich cells represents a significant improvement on previous studies, which have reported on average between 9.7% and 15% α-SMA-positive cells isolated from clinical and not histologically defined nodules (Bisson et al., 2003; Tomasek and Rayan, 1995). Worth noting is that my immunohistochemical data from the previous chapter demonstrated that approxiamtely 97% cells within the nodule and 32% in the peri-nodular region were α-SMA positive. In contrast my immunofluorescence data in this chapter has shown a mean of 35% nodule-derived cells contained α-SMA positive stress fibres. It is difficult to compare these immunofluorescence results with previous immunohistochemical studies as the characteristics of cells grown on glass coverslips and maintained in culture are likely to have changed from their *in vivo* environment. Also tissue sampling must be considered whereby despite isolating cells from histologically confirmed tissue, cells from less α-SMA rich peri-nodular tissue may have also been included.

My findings also demonstrated that between 1-4% of dermal fibroblasts had α-SMA positive stress fibres. This is in line with previous monolayer immunofluoresecence studies that used control cells isolated from flexor retinaculum and showed 1.3% α-SMA positive cells (Bisson

et al., 2003) and 1-9% α-SMA positive cells (Tomasek and Rayan, 1995). Again, this difference may be explained by the phenotypic characteristics acquired by these cells as a result of cell culture on a rigid plastic substrate.

Initially, I analysed isotonic contraction in stress-released circular collagen lattices and found no differences in contraction between Dupuytren's cells and dermal fibroblasts. Several authors have used this model to examine Dupuytren's cells and similar findings to ours have been reported (Rayan and Tomasek, 1994). Although others have demonstrated increased contraction with nodule cells compared to cord cells or control carpal ligament fibroblasts (Moyer et al., 2002; Tomasek and Rayan, 1995), these differences were only maintained in earlier cell passage (Moyer et al., 2002) and when nodule derived cells were subdivided in to high α-SMA expression groups (Tomasek and Rayan, 1995). Interestingly, one study demonstrated increased contraction by dermal fibroblasts compared to nodule-derived cells (Tarpila et al., 1996) and attributed this to late stage Dupuytren's disease samples that had lost their contractile phenotype.

It is well recognised that in 3D collagen lattices, migrating fibroblasts develop tractional forces that increase matrix stiffness by reorganising the loose collagen matrix (Grinnell, 2003). The presence of TGF-β1 (Desmouliere et al., 1993), ED-A fibronectin (Serini et al., 1998) and continued high levels of extracellular stress (Arora et al., 1999; Hinz et al., 2001a) in constrained FPCLs leads to the incorporation of α-SMA in to stress fibres, development of prominent matrix focal adhesions and myofibroblast differentiation (Hinz, 2007). However, upon release of FPCLs, cell-generated tension within the lattice is immediately lost, with subsequent change in fibroblast morphology as rapid isotonic contraction occurs (Grinnell,

2003; Tomasek et al., 1992). This has been likened to wound healing and granulation tissue contraction (Grinnell, 1994) and more importantly, the loss of tension has been shown to result in rapid disassembly of stress fibres and degradation of α-SMA (Hinz et al., 2001a). Such changes in stress fibres following release have been observed within 2 minutes and after 10 minutes almost all stress fibres have disappeared (Tomasek et al., 1992).

In contrast, the culture force monitor permits real-time quantification of uniaxial isometric forces generated in constrained high aspect-ratio rectangular FPCLs (Bisson et al., 2004; Eastwood et al., 1996). This more representative model should also preserve the myofibroblast phenotype and hence more closely emulate the *in vivo* situation whereby Dupuytren's myofibroblasts perceive strain along lines of longitudinal tension. Therefore, I used this system to compare Dupuytren's nodule-derived cells with matched dermal fibroblasts. In line with previous studies, dermal fibroblasts reached a plateau, whereas nodule-derived cells continued to contract in a dose-dependent manner over a 24 hour test period (Bisson et al., 2004; Brown et al., 1998). In addition, by harvesting FPCLs following 24 hours contraction in the CFM, comparisons were made between α-SMA mRNA levels, α-SMA protein expression and α-SMA protein localisation by immunofluorescence in the matched cell types. Interestingly, no differences in α-SMA mRNA levels were seen between nodule-derived cells and dermal fibroblasts, although approximately 3-fold greater α-SMA protein levels were seen in nodule-derived cells compared with matched dermal fibroblasts. Furthermore, using immunofluorescence I found that in dermal fibroblasts, α-SMA was typically distributed in a 'halo' within the peri-nucleur cytoplasm, whereas in nodule-derived cells, α-SMA was frequently localised in stress fibres throughout the cell processes up to cell-matrix attachment sites. The presence of cytosolic α-SMA in fibroblasts is not seen in

vivo, although when fibroblasts are cultured on rigid plastic substrate in the presence of foetal bovine serum they have been described to acquire proto-myofibroblast features with transitory expression of cytosolic α-SMA (Hinz, 2007; Tomasek et al., 2002). My monolyer immunofluoresence studies also demonstrate that palmar and non-palmar fibroblasts when cultured in monolayer acquired a proto-myofibroblast phenotype with the expression of de novo cytosolic α-SMA. In contrast, significantly more differentiated myofibroblasts with α-SMA incorporated to stress fibres were seen in nodule-derived cells (Fig. 4.3). These differences seen with nodule-derived, non-palmar and palmar skin cells from matched samples have not been previously reported. Previous studies have reported only differences in α-SMA protein expression and localization between nodule- or cord-derived Dupuytren's cells when compared to non-matched control carpal ligament cells. The comparative levels of α-SMA mRNA in these cell types have not been analysed (Benzonana et al., 1988; Dave et al., 2001). Here we simultaneously examined α-SMA protein levels, protein localization and mRNA levels in cells isolated from the same patient. Our findings suggest post transcriptional changes in α-SMA occur in genetically matched cells to mediate the Dupuytren's myofibroblast cell phenotype. Recent studies on cellular mechanisms of local protein synthesis have now also suggested that, not only is mRNA subject to translation, but that cells can instruct the cytoskeleton and translation apparatus where to transport and when to translate the intended protein (Rodriguez et al., 2008). Therefore, post-transcriptional changes in α-SMA expression may include mRNA stability, mRNA localisation, translation, cytoskeletal localisation and stress fibre formation. Further studies using Dupuytren's matched cells are required to investigate these possibilities.

It has been reported in previous studies that nodule-derived cells maintain significant contractile differences up to cell passage 4-5 when compared to control fibroblasts (Bisson et al., 2004; Moyer et al., 2002). However, the data from this study suggests that contractility of nodule cells significantly decreases by cell passage 5. It was demonstrated that increasing cell passage was correlated with a consistent decrease in α-SMA stress fibres. The opposite was observed in dermal fibroblasts, with a significant increase in contractility with cell passage although no change was seen in α-SMA stress fibres. This suggests that culturing dermal fibroblasts on rigid plastic substrates may over time lead to increased cell-generated tension and promote the development of a more contractile protomyofibroblast phenotype (Hinz, 2007; Tomasek et al., 2002). The tendency towards a similar contractile phenotype between nodule-derived cells and dermal fibroblasts may reflect contractile adjustments by these cells as a consequence of the identical *in vitro* culture conditions. Therefore experiments were performed with cells from cell passage 1 or 2, unless stated otherwise.

Finally, based on the surgical observation that recurrence following dermofasciectomy is much lower than after fasciectomy (Tonkin et al., 1984), the hypothesis that non-palmar dermal fibroblasts may downregulate Dupuytren's myofibroblasts was tested. No differences were found in isometric force contraction with co-cultures when compared to controls of equivalent numbers of nodule cells alone, either over 24 hours or with longer-term cultures. No differences in contractility were observed with different ratios of nodule-derived cells to dermal fibroblasts and controlling for cell proliferation rates in co-culture. Ideally these co-cultures would be observed in the CFM for a time course longer than 24 hours. Although in my experience there was an increased incidence of bacterial

contamination and pH disturbance beyond 24 hours culture and therefore, experiments were limited to 24 hour test periods. Our pre-plated co-cultures were only performed over a period of 5 days and the CFM co-culture system is limited in that it does not reflect the processes involved *in vivo* for dermofasciectomy and, recurrent disease may evolve over several months or years.

It has been demonstrated previously that isometric contraction of a 3D collagen lattice by resident fibroblasts causes strains to develop within the lattice and these strains can be increased or decreased by altering the FPCL aspect-ratio (ratio of length/ width/ thickness) (Eastwood et al., 1998) to modulate cellular activity. Dupuytren's cord tissue *in vivo* has a high aspect-ratio and is subjected to considerable tensile force that causes high strain gradients, and these may in turn dictate cellular alignment along the major axis of the cord. Consequently, iso-strains run parallel with the long axis, which in Dupuytren's cord is reflected by fibroblasts aligned longitudinally with collagen fibres (Luck, 1959; Verjee et al., 2009). Interestingly, it has been observed clinically that after simple division of Dupuytren's tissue (fasciotomy), cords which are no longer under tension soften and temporarily disappear (Hueston, 1992). Furthermore, it has also been suggested that reducing skin tension following fasciotomy by a single Z-plasty significantly reduced recurrence at 2 years (Citron and Hearnden, 2003). Therefore identical co-cultures in both low and high aspect-ratio FPCLs were compared to examine the dependence of tension and strain on cell contractility. Although no significant difference in the rate of contraction (dynes/ hour) was found between the different aspect-ratios, a significant decrease in overall force generation was observed with low aspect-ratio FPCLs. This implies that Dupuytren's cells remain significantly more contractile than dermal fibroblasts even in the absence of high strain

gradients, although nodule-derived cells may prefer an environment with higher baseline levels of tensile force. It may be that dermofasciectomy, with resurfacing of the cutaneous defect in the digit with a full-thickness skin graft, may alter myofibroblast activity through a combination of reduced tension and more complete excision, as it can be difficult to accurately differentiate the surgical plane between Dupuytren's cord and palmar skin at the time of fasciectomy.

Our histological findings in the previous chapter (Verjee et al., 2009) showed that α-SMA-rich nodules occurred with equal frequency in primary and recurrent disease samples and were also not significantly different in size. Recurrences were seen following previous fasciotomy, fasciectomy and firebreak dermofasciectomy but not radical dermofasciectomy. Similarly, from these results it is possible that residual unexcised Dupuytren's tissue following less radical surgery may serve as a trigger for recurrence and, indeed, the increased motion following initial surgery may facilitate myofibroblast differentiation and persistence. This may also explain why radical dermofasciectomy has a lower rate of recurrence (1-5%) (Brotherston et al., 1994; Hall et al., 1997; Tonkin et al., 1984) than 'firebreak' dermofasciectomy (12%) (Ullah et al., 2009) or fasciectomy (40-50%) (Foucher et al., 1992; Hueston, 1961; Tonkin et al., 1984).

In conclusion, isometric force contraction measured by the culture force monitor represents the best model available for the study of cell contractility in Dupuytren's disease. Using matched patient samples it has been demonstrated that post transcriptional changes of α-SMA expression mediate the contractile phenotype of Dupuytren's cells. The different possible mechanisms for post-transcriptional modification warrant further investigation. Co-

cultures data suggests that contractility of Dupuytren's cells is not influenced by dermal fibroblasts. Reduced recurrence rate following dermofasciectomy may be due to other factors, such as more complete excision of affected tissue combined with reduced tension following application of full-thickness skin grafts.

CHAPTER FIVE

Inflammatory mediators and Dupuytren's disease

5.1 INTRODUCTION

Dupuytren's disease is a fibroproliferative condition, the pathophysiology of which remains unclear. Whilst Dupuytren's tissue is populated with highly contractile myofibroblasts that mediate digital contracture, the presence of inflammatory cells indicates that inflammation may be important in the pathogenesis of Dupuytren's disease. Studies using immunohistochemistry, light and electron microscopy have demonstrated a correlation between the numbers of macrophages and myofibroblasts in Dupuytren's nodules (Andrew et al., 1991). Furthermore, large numbers of macrophages were found at the interface between skin and excised Dupuytren's nodule (VandeBerg et al., 1982) and increased Langerhans cells, T-lymphocytes and macrophages have also been reported in nodules and at the dermo-epidermal junction with palmar skin (Qureshi et al., 2001). Mast cells have also been reported to be increased in Dupuytren's tissue compared to control carpal ligament (Schubert et al., 2006). Using FACS analysis, CD3-positive T-lymphocytes have also been shown to be present in 25% of Dupuytren's cells isolated from whole cord compared to 0.5% in control palmar fascia (Baird et al., 1993).

Growth factors and cytokines derived from inflammatory have been shown to regulate the myofibroblast phenotype. These cytokines and growth factors include IL-1beta, bFGF, TGF-β1 , TGF-β2, EGF, PDGF and CTGF (Baird et al., 1993; Bunker et al., 2000; Igarashi et al., 1996; Kuhn et al., 2001; Terek et al., 1995). High levels of TNF-α mRNA have been reported in Dupuytren's cord tissue compared to tissue from frozen shoulder and control shoulder tissue (Bunker et al., 2000) and, more recently, TNF-α has been shown to suppress α-SMA expression in human non-palmar dermal fibroblasts using both western blot analysis and

RT-PCR. Furthermore, a decrease in collagen matrix stiffness and isotonic contraction was seen after 5 days in culture of myofibs with TNF-α (Goldberg et al., 2007). Similar findings have been reported using myofibroblasts derived from hip joint tissue (Mattyasovszky et al., 2010), although in this study TNF-α was also shown to promote cell proliferation and viability. TNF-α has also been suggested to induce the transformation of human dermal microvascular endothelial cells to myofibroblasts (Chaudhuri et al., 2007). Therefore, the effect of TNF-α may vary depending on the cell type and conditions and has not been studied in Dupuytren's tissue.

Advanced glycation end-products (AGEs) and the receptor for advanced glycation end-products (RAGE) have recently been implicated in cell dysfunction, fibrosis and mechanisms of inflammatory disease (Sims et al., 2010; van Beijnum et al., 2008). The interaction between AGEs and their binding proteins have been shown to lead to the activation of a range of secondary messenger systems and the increased production of cytokines including TGF-β1 and PDGF (Throckmorton et al., 1995), TNF-α and IL-1 (Vlassara et al., 1988). In a rat proximal tubular cell line, the interaction of AGEs with RAGE has been shown to induce a dose-dependent epithelial-myofibroblast transdifferentiation determined by morphological changes, de novo α-SMA expression determined by mRNA and protein levels, and loss of E-cadherin staining (Li et al., 2004; Oldfield et al., 2001). The expression of RAGE in Dupuytren's tissue and the possible role of AGE-RAGE dependent induction of myofibroblasts in Dupuytren's disease have not been previously examined.

Therefore, in the final chapter of this study I analysed matched Dupuytren's nodule and cordsamples by immunohistochemistry for the presence of inflammatory cells

(macrophages, T cells, neutrophils, and mast cells) and RAGE expression. RAGE expression levels in matched fibroblasts were analysed using FACS. Co-localisation of inflammatory cells and RAGE with α-SMA was also examined. Finally, based on the observation that the earliest signs of Dupuytren's disease may seen in the palmar skin (Hueston, 1985; Hueston, 1963; Rayan, 1999), I went on to assess the role of TNF-α and AGEs in promoting the myofibroblast contractile phenotype in palmar dermal fibroblasts.

5.2 RESULTS

5.2.1 Inflammatory cells in Dupuytren's tissue are distributed predominantly within nodules

Inflammatory cells have been previously described in Dupuytren's tissue and a correlation between the numbers of macrophages and myofibroblasts in Dupuytren's nodules has been reported (Andrew et al., 1991). Approximately 25% of cells isolated from whole Dupuytren's cord were shown by FACS analysis to be CD3-positive T-lymphocytes (Baird et al., 1993). I undertook systematic analysis of histological sections of Dupuytren's tissue to confirm and quantify the distribution of inflammatory cells throughout Dupuytren's tissue.

Excised digital cord samples were longitudinally bisected, fixed in formalin and 7µm histological sections from the cut surface processed for immunohistochemistry. Sequential sections were stained with α-SMA antibody and inflammatory cell markers including, mast cell tryptase, neutrophil elastase, CD3 positive T-lymphocytes, CD4 positive T cells and macrophages (CD68 positive cells). Serum from the appropriate species in which the antibodies were raised was used at the same protein concentration as the monoclonal antibody solution for negative controls. Histological sections from inflammatory tissue (tonsil for CD3 T cells, CD4 T cells, CD68 positive macrophages, mast cell tryptase and bone marrow for neutrophil elastase) were used as positive controls (Fig. 5.1). Immunohistochemical staining for inflammatory cells showed good specificity and was reproducible, although staining for CD4 positive T cells produced consistently less intense staining despite optimisation in other tissues and at different antibody concentrations.

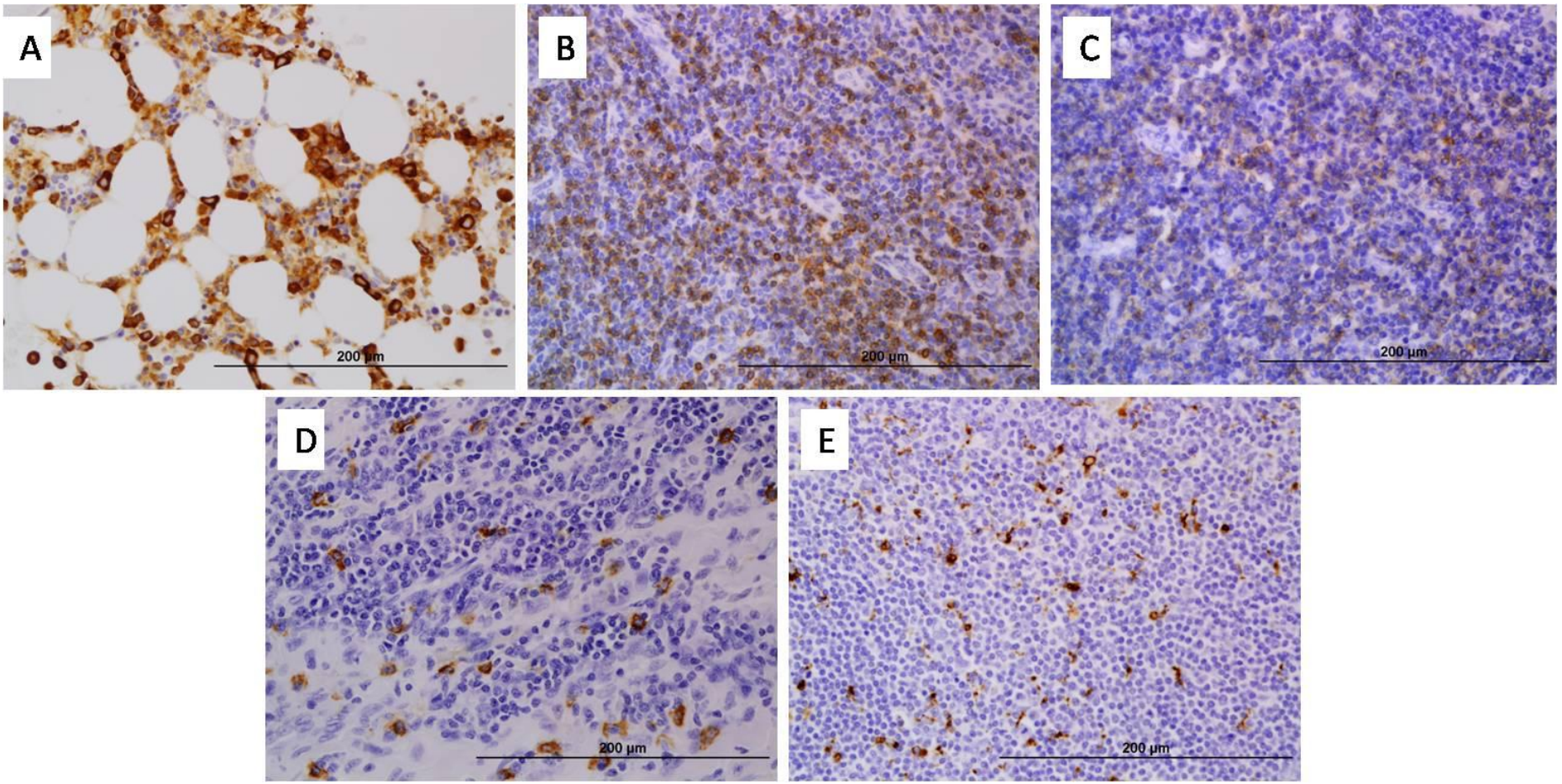


Figure 5.1. Positve controls - Immunohistochemistry staining for inflammatory cells. Histological sections were taken from bone marrow and stained for (A) neutrophil elastase. Histological sections were also taken from tonsil tissue and stained for (B) CD3 positive T cells, (C) CD4 positive T cells, (D) mast cell tryptase and (E) CD68 positive macrophages.

5.2.1.1 Nodules

Nodules rich in α-SMA were examined from 15 patient samples and in all of these sections numerous cells stained positive for mast cell tryptase, CD3 positive T-lymphocytes, and CD68 positive macrophages. Staining was seen both around blood vessels and within the stromal tissue. However, there was minimal staining for neutrophil elastase and CD4 positive T-lymphocytes in nodules (Fig. 5.2).

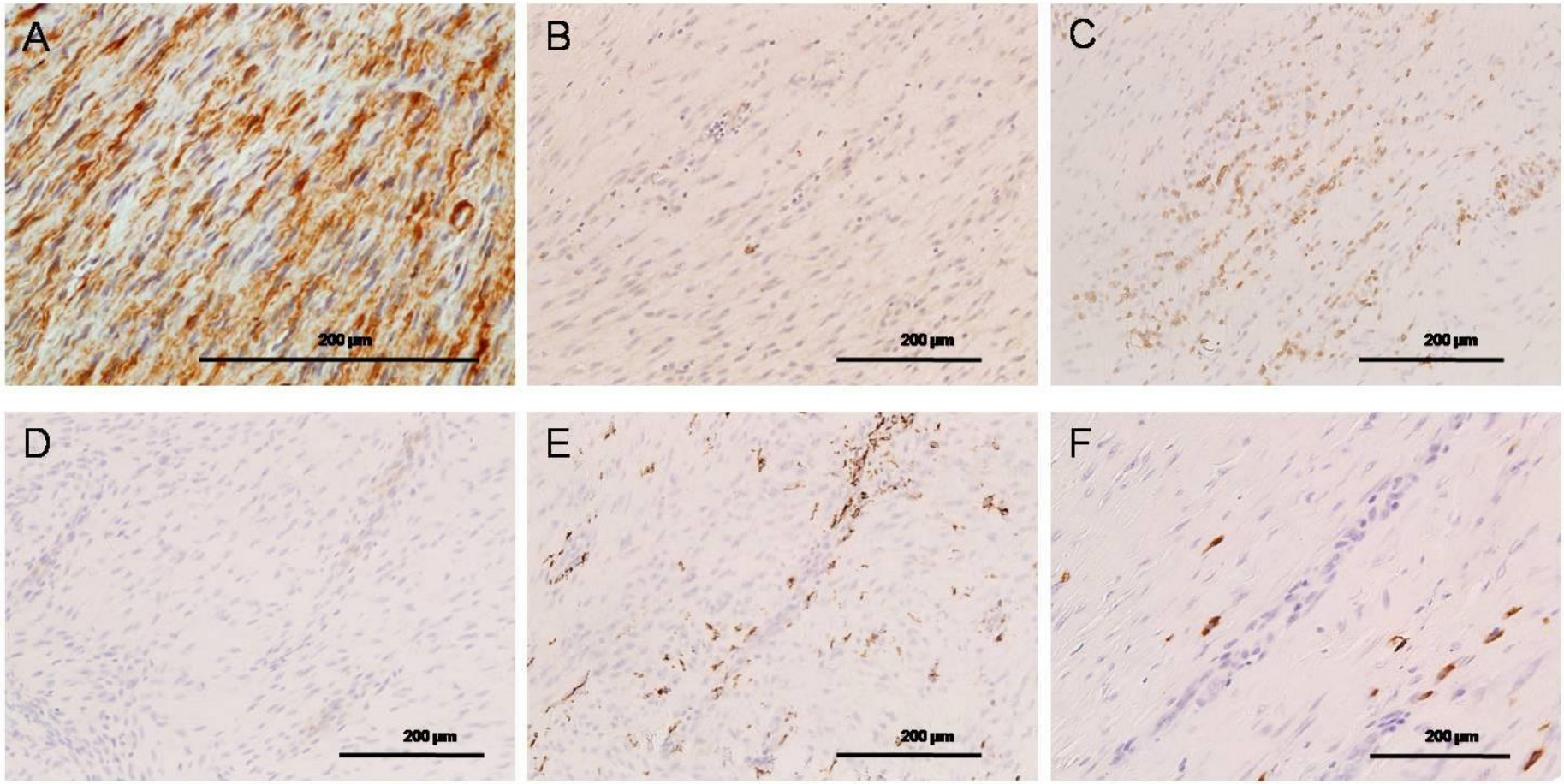


Figure 5.2. Immunohistochemistry staining for inflammatory cells in Dupuytren's nodule. Digital cord samples were longitudinally bisected and fixed in formalin. Histological sections were taken from the cut surface of cord and serial sections stained for (A) α-SMA, (B) neutrophil elastase, (C) CD3 positive T cells, (D) CD4 positive T cells, (E) CD68 positive macrophages and (F) mast cell tryptase. Images are representative from 15 patient samples.

5.2.1.2 Cord tissue distal from the nodule

Cord tissue distal from the nodule was also examined in the 15 nodular patient samples and although some cells did stain positive for α-SMA (Fig. 5.3A), in all patient samples minimal positive staining was observed for neutrophil elastase , CD3 and CD4 positive T cells and CD68 positive macrophages and mast cell tryptase (Fig. 5.3B-F).

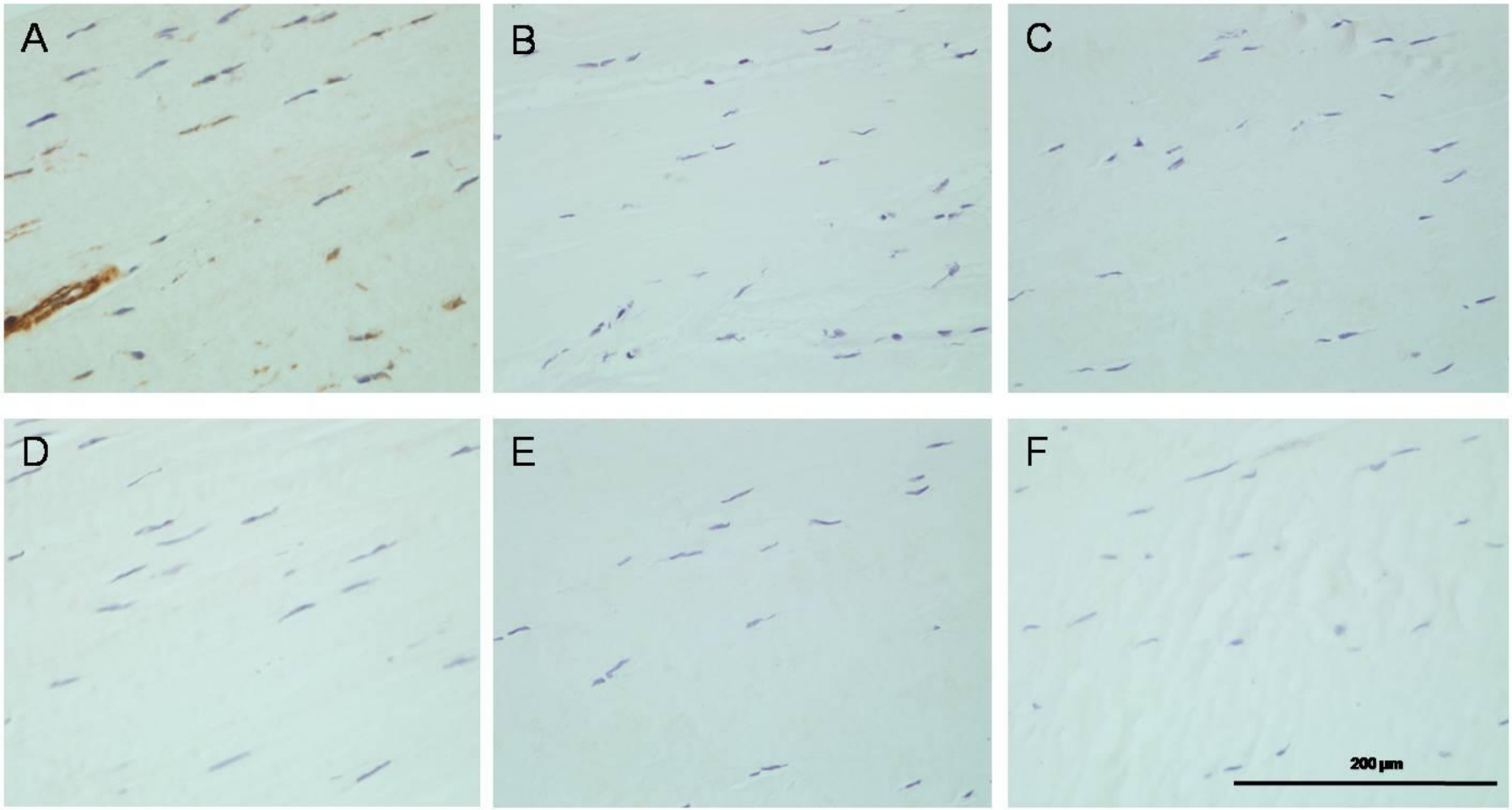


Figure 5.3. Immunohistochemistry staining for inflammatory cells in Dupuytren's cord distal to nodule. Digital cord samples were longitudinally bisected and fixed in formalin. Histological sections were taken from the cut surface of cord and serial sections stained for (A) α-SMA (with positive control blood vessel staining, (B) neutrophil elastase, (C) CD3 positive T cells, (D) CD4 positive T cells, (E) CD68 positive macrophages and (F) mast cell tryptase. Images are representative from 15 patient samples.

5.2.1.3 Non-nodular cord tissue

Non-nodular cord tissue was also examined in 10 patient samples. As with cord distal from the nodule, some cells stained positive for α-SMA (Fig. 5.4A) and very few cells stained positive for any of the panel of inflammatory markers including neutrophil elastase, CD3 positive T-lymphocytes, CD4 positive T cells and CD68 positive macrophages, mast cell tryptase (Fig. 5.4B-F).

Serum from the appropriate species in which the antibodies were raised was used at the same protein concentration as the monoclonal antibody solution for negative controls. Histological sections from inflammatory tissue (tonsil for CD3 T cells, CD4 T cells, CD68 positive macrophages, mast cell tryptase and bone marrow for neutrophil elastase) were used as positive controls.

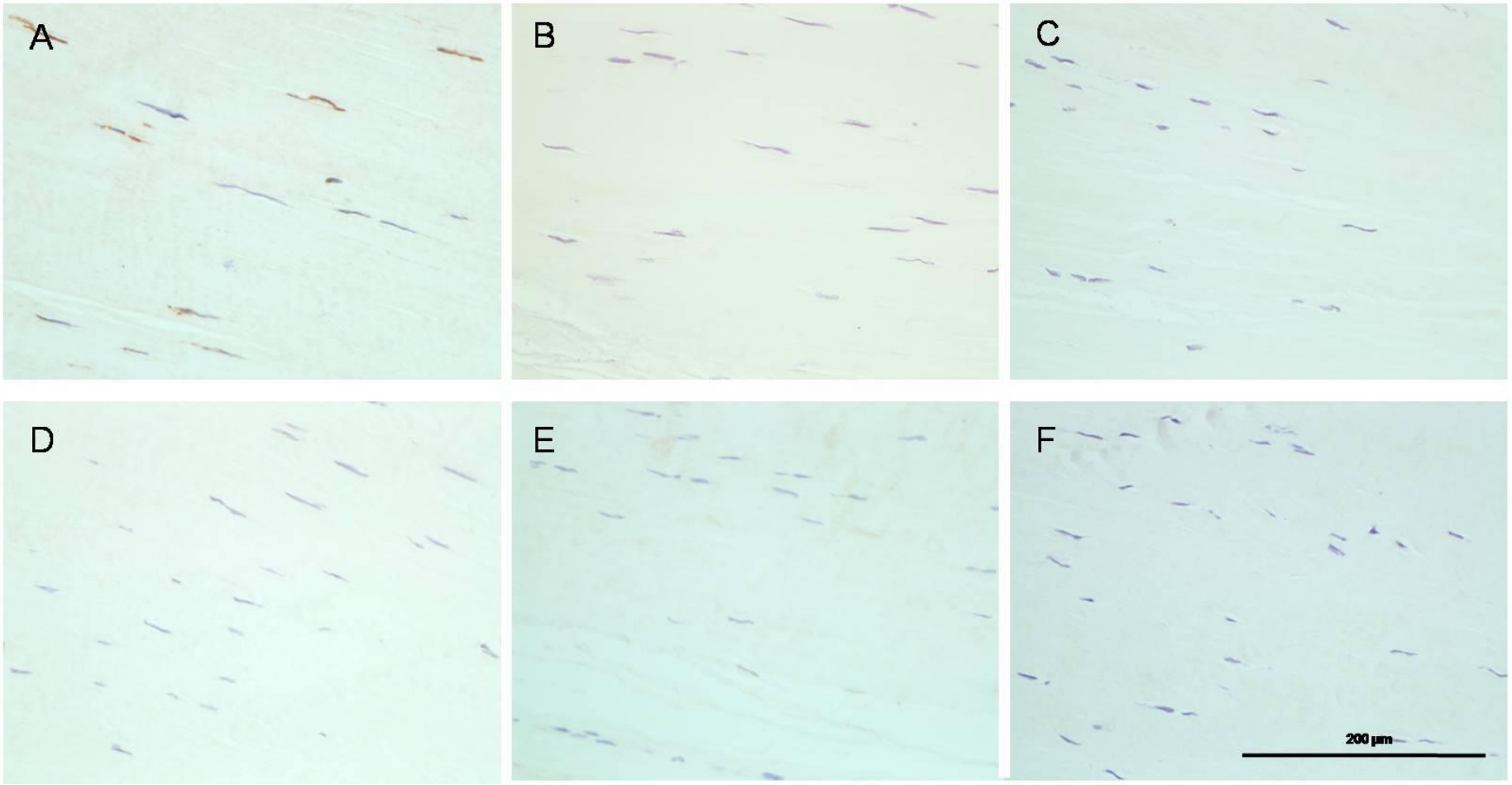


Figure 5.4. Immunohistochemistry staining for inflammatory cells in non-nodular Dupuytren's cord. Digital cord samples were longitudinally bisected and fixed in formalin. Histological sections were taken from the cut surface of cord and serial sections stained for (A) α-SMA, (B) neutrophil elastase, (C) CD3 positive T cells, (D) CD4 positive T cells, (E) CD68 positive macrophages and (F) mast cell tryptase. Images are representative from 10 patient samples.

5.2.1.4 Quantification of inflammatory cells found throughout Dupuytren's tissue

Based on the immunohistochemical sections (Fig 5.2-4), systematic analysis was also carried out to quantify the number of inflammatory cells observed throughout excised Dupuytren's cord tissue in 10 patient samples. For each region (nodule, cord distal to nodule and non-nodular cord), the total number of cells, the number of α-SMA positive cells and cells stained for neutrophil elastase, mast cell tryptase, CD3positive T cells, CD 4 positive T cells, CD68 positive macrophages were counted (x20 magnification) (Table 5.1).

Table 5.1. Quantification of total cell number, α-SMA positive cells, CD3 positive T cells, CD4 positive T cells, CD68 positive macrophages, and cells positive for mast cell tryptase and neutrophil elastase throughout excised Dupuytren's cord. Nodules, cord distal to nodule and non-nodular cord were analysed (presented as mean count (±SDEV) per mm^2) Six fields of view were counted within each region.

IHC stain	Nodule		Distal to nodule		Non-nodular cord	
	mean	SDEV	mean	SDEV	mean	SDEV
Total cells	1515	181	416	104	504	163
α-SMA	1493	199	12	8	8	7
Neutrophil elastase	2	1	0	1	0	0
CD3 positive T cells	220	99	2	2	1	2
CD4 positive T cells	2	1	0	0	0	0
CD68 positive macrophages	282	54	1	1	1	1
Mast cell tryptase	48	11	1	1	0	1

In summary, these data suggest that CD68 positive macrophages, CD3 T-cells and mast cell tryptase positive cells are common within cellular nodules and sparse within cord tissue. Neutrophil elastase positive cells and CD4 positive T-cells were observed infrequently throughout Dupuytren's tissue. Whilst Dupuytren's nodular tissue is populated with highly contractile myofibroblasts, the presence here of inflammatory cells also implies that inflammation may be important in pathogenesis of the disease.

5.2.2 RAGE expression is observed predominantly in α-SMA rich Dupuytren's nodules

AGEs are found in plasma, accumulate in various tissues with ageing and at an accelerated rate in diabetes (Brett et al., 1993; Makita et al., 1991).The interaction of AGEs-RAGE has been implicated in cell dysfunction and mechanisms of inflammatory disease (Davies et al., 2009; De Vriese et al., 2006; Fehrenbach et al., 2001; Li et al., 2004; Oldfield et al., 2001; Tikellis et al., 2008; van Beijnum et al., 2008). There are some data to suggest that the AGE-RAGE interaction is implicated in regulating myofibroblast phenotype (Oldfield et al., 2001). However, RAGE expression has not previously been characterised in tissue from patients with Dupuytren's disease.

Therefore, I characterised RAGE expression throughout Dupuytren's tissue. Longitudinally bisected cord samples were fixed in formalin and processed for immunohistochemistry. Sequential histological sections were stained with α-SMA and RAGE antibodies as well as goat serum. The latter was used at the same protein concentration as the RAGE antibody solution for a negative control. RAGE staining of vascular endothelium was used as an internal positive control within Dupuytren's tissue and was also examined on histological sections of inflammatory liver tissue (Fig 5.5)

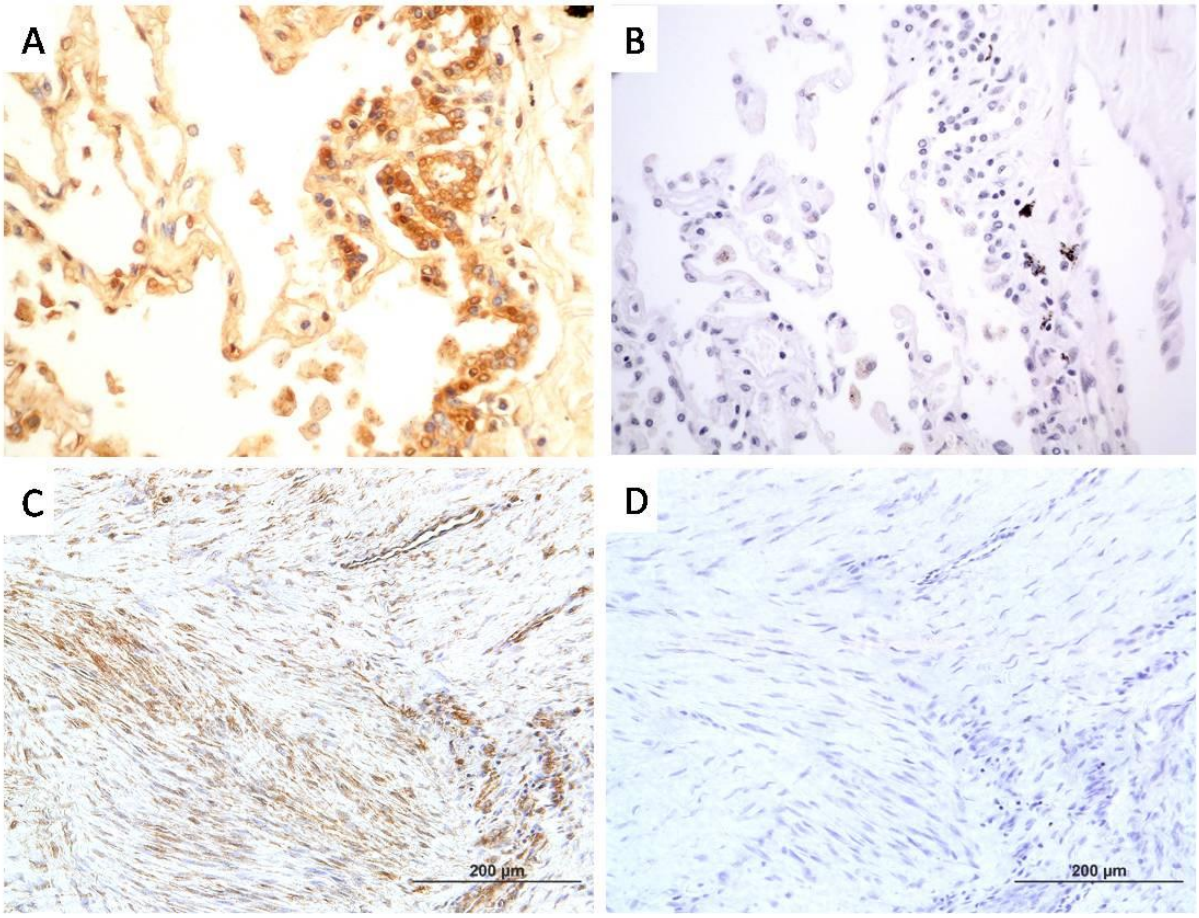


Figure 5.5. Positive/negative controls - Immunohistochemistry staining for RAGE. Histological sections were stained for RAGE (A and C) and with goat serum (B and D). Serial sections taken from lung tissue showing (A) positive control and (B) negative control. Serial sections taken from Dupuytren's tissue showing (C) positive control and (D) negative control.

Excised Dupuytren's tissue samples were systematically examined to determine patterns of α-SMA and RAGE distribution thoughout cord: within nodules (Fig. 5.6), within the peri-nodular region (Fig. 5.7), in cord distal to the nodules (Fig. 5.8) and in non-nodular cord (Fig. 5.9). These specific regions of cord tissue examined are outlined in chapter 3 (Dupuytren's morphology). In total, 15 nodular and 10 non-nodular samples were examined.

5.2.2.1 Nodules

Nodules rich in α-SMA were examined from 15 Dupuytren's patient samples. Histological sections in all the samples demonstrated abundant α-SMA and RAGE staining in nodules. Serial sections demonstrated RAGE co-localisation with α-SMA (Fig. 5.6). The staining for both α-SMA and RAGE demonstrated a distinct 'tide mark' that demarcated the interface between well circumscribed nodules and peri-nodular regions

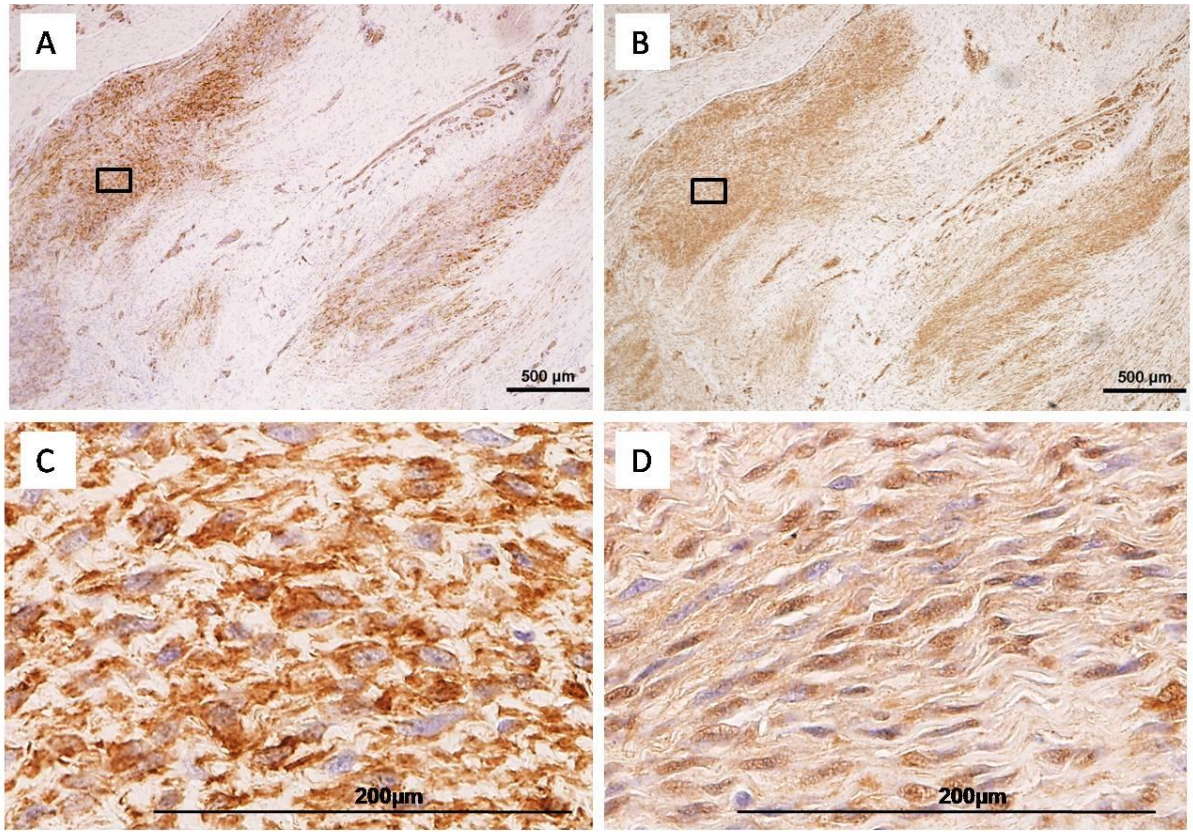


Figure 5.6. RAGE co-localises with α-SMA distribution in Dupuytren's nodule. Digital cord samples were longitudinally bisected and fixed in formalin. Histological sections were taken from the cut surface of cord and serial sections were stained for (A, C) α-SMA and (B, D) RAGE antibodies. Scale bars as shown. Images are representative from 15 patient samples.

5.2.2.2 Peri-nodular cord tissue

Next, peri-nodular regions were examined in serial sections from the same 15 nodular samples. In these areas cells also stained positive for RAGE and α-SMA. However, fewer cells stained positive for α-SMA and RAGE than in nodular regions. A similar distribution of α-SMA and RAGE staining was seen in the peri-nodular areas (Fig. 5.7).

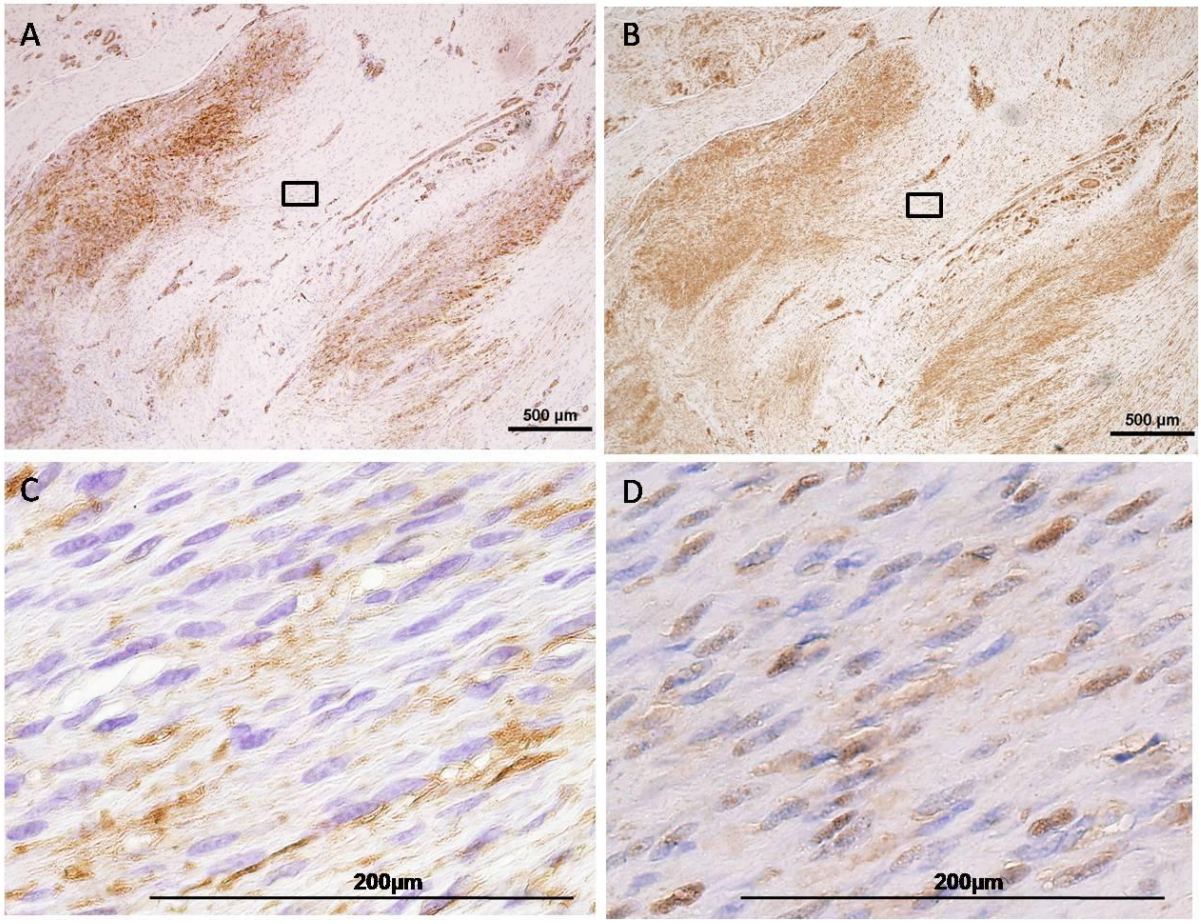


Figure 5.7. RAGE and α-SMA distribution in Dupuytren's peri-nodular region. Digital cord samples were longitudinally bisected and fixed in formalin. Histological sections were taken from the cut surface of cord and serial sections were stained for (A, C) α-SMA and (B, D) RAGE antibodies. Scale bars as shown. Images are representative from 15 patient samples.

5.2.2.3 Cord tissue distal from the nodule

Histological sections of cord tissue distal from the nodule were also stained with α-SMA and RAGE antibodies. These demonstrated relatively few cells that stained positive for α-SMA and only a small number of cells also stained positive for RAGE (Fig. 5.8).

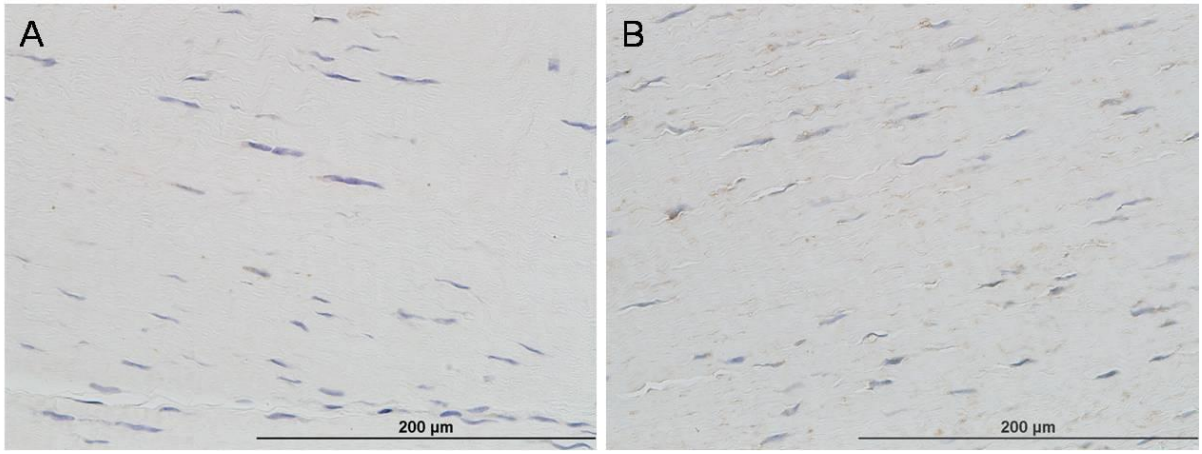


Figure 5.8. RAGE expression and α-SMA distribution in Dupuytren's cord distal from nodule. Digital cord samples were longitudinally bisected and fixed in formalin. Histological sections were taken from the cut surface of cord and serial sections were stained for (A) α-SMA and (B) RAGE antibodies. Scale bars are shown. Images are representative from 15 matched patient samples.

5.2.2.4 Non-nodular cord tissue

Histological sections of non-nodular cord tissue were also stained with α-SMA and RAGE antibodies. In total 10 patient samples were examined. These consistently demonstrated relatively few cells staining positive for α-SMA and RAGE (Fig. 5.9)

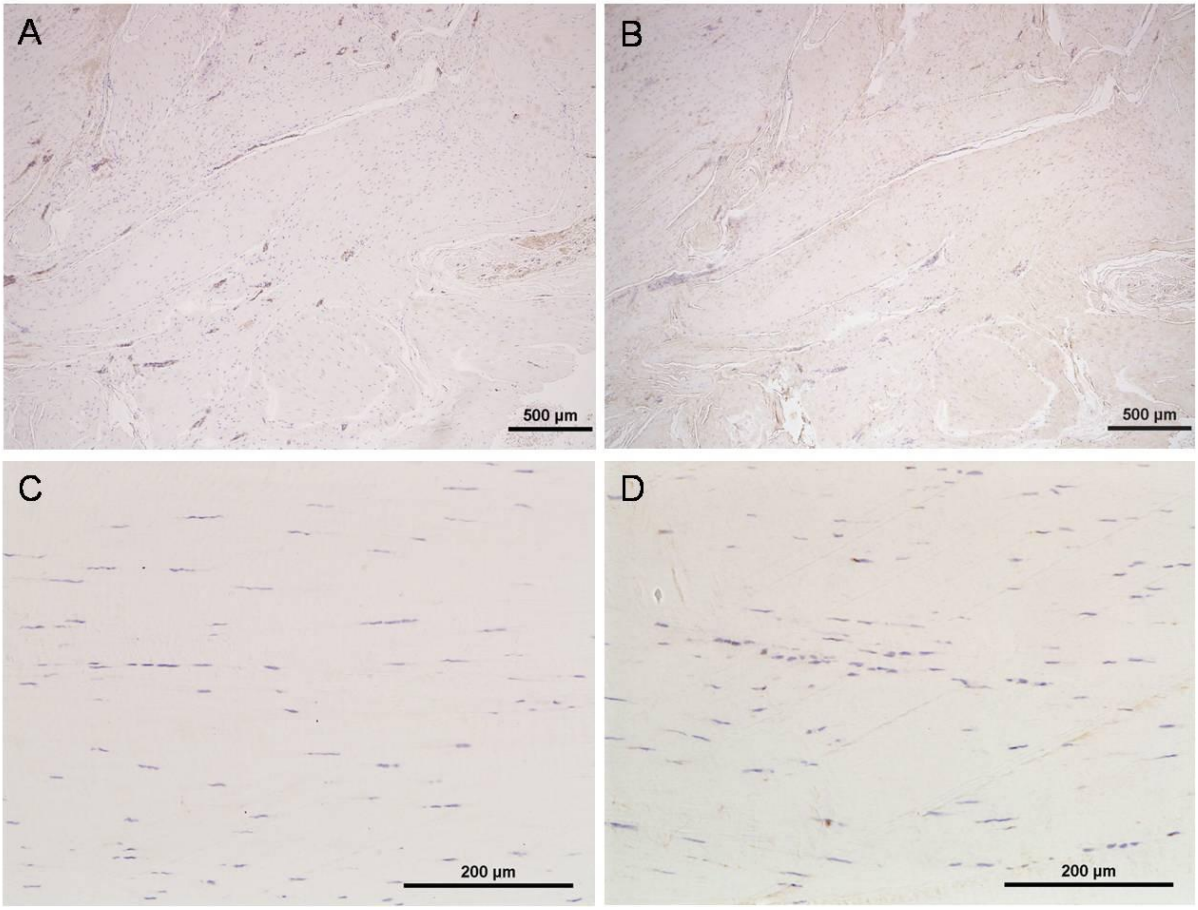


Figure 5.9. RAGE expression and α-SMA distribution in non-nodular Dupuytren's cord. Digital cord samples were longitudinally bisected and fixed in formalin. Histological sections were taken from the cut surface of cord and serial sections were stained for (A, C) α-SMA and (B, D) RAGE antibodies. Scale bars as shown. Images are representative from 10 matched patient samples.

5.2.3 Cell surface expression of RAGE is significantly greater in nodule-derived cells than non-nodular cells and in palmar skin fibroblasts compared to non-palmar skin fibroblasts.

To quantify the expression of RAGE on the surface of Dupuytren's nodule-derived cells, non-nodular cells, non-palmar and palmar fibroblasts, were cultured for 24 hours and then immunofluorescently labelled with RAGE antibody and analysed by FACS (Fig. 5.10). In total 4 nodular (Fig. 5.10A, C) and 4 non-nodular (Fig. 5.10B, D) matched patient samples were analysed. Cells alone, Alexa Fluor 488 secondary antibody alone and rabbit IgG were used as controls.

In nodular matched samples, nodule-derived cells expressed significantly more cell surface RAGE (p = 0.01) than non-palmar and palmar skin fibroblasts (Fig. 5.10A,C). In nodular samples the largest shift in mean RAGE fluorescence intensity (MFI) is seen in nodule-derived cells, then palmar skin fibroblasts and least in non-palmar skin fibroblasts compared to isotype antibody controls (Fig. 5.10C).

In contrast, no significant difference (p =0.4) was observed between Dupuytren's cord cells, non-palmar and palmar fibroblasts from non-nodular matched samples (Fig. 5.10B,D). However, a trend was observed with relatively increased RAGE expression in palmar skin fibroblasts. In non-nodular matched samples no shift was observed in mean fluorescence intensity between cells from non-nodular cells and dermal fibroblasts (Fig. 5.10F). A summary of the results for RAGE MFI, isotype control MFI and Δ MFI for all the 8 matched patient samples are shown in table 5.2.

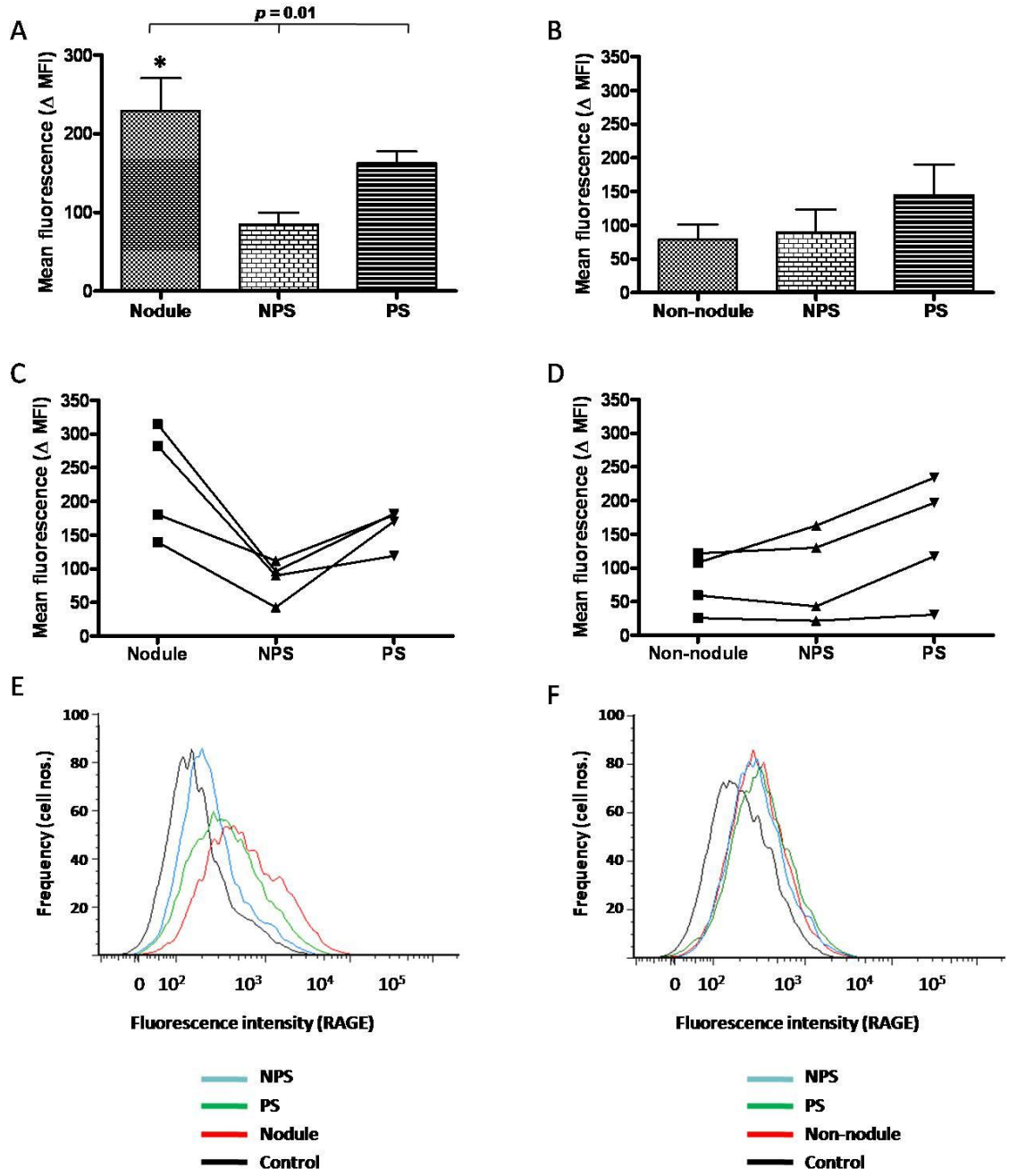


Figure 5.10. Nodule-derived cells express higher levels of cell surface RAGE than matched dermal fibroblasts. Nodule-derived cells, palmar and non-palmar fibroblasts ($1x10^4$ cells per experiment) were stained with RAGE antibody, fluorescently labelled and mean fluorescence intensity assessed by FACS analysis. **(A,C)** Cell surface RAGE expression levels in nodule-derived cells as compared with matched dermal fibroblasts. **(B,D)** Cell surface RAGE expression levels in non-nodular cells as compared with matched dermal fibroblasts. Results in A and B are shown for 4 matched nodular patient and non-nodular samples (± SEM). **(E)** RAGE fluorescent intensity trace showing nodule-derived cells, non-palmar fibroblasts, palmar fibroblasts and isotype control from 1 representative nodular matched patient sample, and **(F)** from 1 representative non-nodular matched patient sample.

Table 5.2. FACS analysis to determine RAGE cell surface expression (Δ mean fluorescence intensity) in 4 nodular and 4 non-nodular matched patient samples. Cells isolated from Dupuytren's nodule (PIPJ), non-nodular PIPJ, non-palmar skin (NPS) and palmar skin (PS).

Sample ID	Cell type	Isotype MFI	RAGE MFI	ΔMFI
Nodular				
ED035	PIPJ	783.59	934.23	150.64
	NPS	730.34	842.31	111.97
	PS	616.61	796.56	179.95
ED044	PIPJ	546.58	861.00	314.42
	NPS	239.81	335.98	96.17
	PS	342.52	524.17	181.65
ED045	PIPJ	453.12	592.55	139.43
	NPS	356.06	398.74	42.68
	PS	438.12	608.69	170.57
ED066	PIPJ	685.92	968.24	282.32
	NPS	464.68	608.48	90.06
	PS	463.01	582.30	119.29
Non-nodular				
ED063	PIPJ	264.55	290.24	25.69
	NPS	273.32	295.12	21.80
	PS	356.59	387.29	30.70
ED074	PIPJ	251.77	311.07	59.30
	NPS	169.95	212.94	42.99
	PS	210.14	327.65	117.51
ED091	PIPJ	594.17	702.33	108.16
	NPS	632.35	795.15	162.80
	PS	588.16	822.34	234.18
ED091	PIPJ	257.42	379.22	121.80
	NPS	258.51	388.65	130.14
	PS	262.97	459.71	196.74

Note: MFI= mean fluorescence intensity

Further analysis of the FACS data was undertaken to examine differences between RAGE cell surface expression in non-palmar and palmar skin. RAGE cell surface expression was significantly higher (p = 0.0012) in palmar skin fibroblasts than non-palmar skin fibroblasts (Fig. 11). This analysis was carried out using cells from 8 matched patient samples.

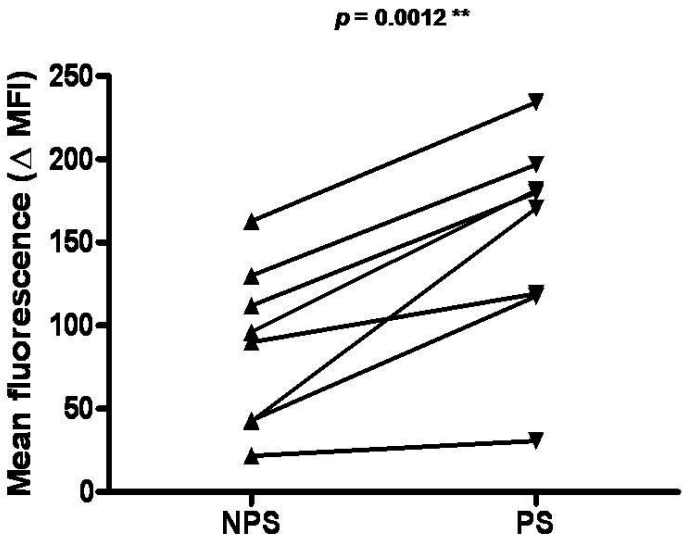


Figure 5.11. RAGE cell surface expression is greater in palmar than non-palmar fibroblasts. Fibroblasts ($1x10^4$) from matched palmar and non-palmar skin were stained with RAGE antibody, fluorescently labelled and the mean fluorescence intensity analysed by FACS. Cell surface RAGE expression levels were consistently higher in palmar fibroblasts than non-palmar fibroblasts. Data are shown from 8 matched patient samples.

In combination, the data from FACS analysis suggest that nodule-derived cells express significantly more RAGE at the cell surface compared to non-nodular derived cells and dermal fibroblasts. Furthermore, palmar skin fibroblasts express significantly more RAGE at the cell surface when compared with matched non-palmar skin fibroblasts.

5.2.4 Contractility of palmar fibroblasts is augmented with TNF-α, but not with AGEs

Previous authors have suggested that AGEs and RAGE are implicated in regulating myofibroblast phenotype in a proximal renal tubule cell line (Oldfield et al., 2001) and human dermal microvascular endothelial cells. TNF-α has been suggested to induce the transformation to myofibroblasts (Chaudhuri et al., 2007). High levels of TNF-α mRNA have been demonstrated in Dupuytren's nodules compared to control tissue (Bunker et al., 2000) and histological data in this study has demonstrated large number of mast cells, which are rich in TNF-α, in Dupuytren's nodules. However, TNF-α has also been shown to suppress α-SMA protein and mRNA expression in human dermal fibroblasts. This was associated with a decrease in collagen matrix stiffness and isotonic contraction after 5 days in culture (Goldberg et al., 2007). To date, the effects of AGEs on cells derived from Dupuytren's patients have not been previously examined and FACS data in this study suggests that RAGE is differentially expressed in skin fibroblasts. Therefore, based on the observation that early changes in Dupuytren's disease are seen in the palmar skin (Hueston, 1985; Hueston, 1963; Rayan, 1999), I tested the hypothesis that palmar skin fibroblasts develop a more contractile phenotype in the presence of TNF-α or AGEs. Furthermore, it has been suggested in a recent study that human endothelial cells pre-stimulated with AGEs demonstrated a significant inflammatory response with increased cytokine production (Ehlermann et al., 2006). Therefore, I also examined the effect of pre-stimulation with AGEs followed by TNF-α on palmar dermal fibroblasts.

I compared the differences in isometric force generated by collagen gels seeded with palmar fibroblasts and cultured in the presence of AGE-BSA or TNF-α. FPCLs were exposed to either control BSA (150µg/ml), AGE-BSA (150µg/ml), TNF-α (1ng/ml) or a combination of AGE-BSA (150µg/ml) and TNF-α (1ng/ml) and attached to the CFM for 24 hours. FPCLs were also stimulated with 10ng/ml TGF-β1 as a positive control to assess any increase in cell contractility. Measurement of isometric force contraction was limited to 24 hours as beyond this time changes in ionic concentration of the culture media were noted as a result of FPCL contraction (Fig. 5.12).

Furthermore, to investigate the potential effects of pre-stimulating palmar skin fibroblasts with AGEs, cells were also cultured for 5 days with AGE-BSA (150µg/ml), and after 5 days, cells were seeded in collagen gels and cultured in the presence of TNF-α (1ng/ml) or AGE-BSA (150µg/ml) in the CFM. Isometric force generated was measured over 24hours. Experiments were performed in duplicate and with cells isolated from 3 different patient samples. A two-fold increase in contractility was observed with palmar fibroblasts treated with TNF-α (1ng/ml) and a significant increase in contractility with TGF-β1 (10ng/m) ($p=0.0001$) was seen over 24 hours. However, no difference was observed with the addition of AGE-BSA for either 24 hours or with longer term culture in the presence of AGE-BSA. Pre-incubation with AGE-BSA for 5 days followed by 24 hours culture in the CFM with AGE-BSA also showed no difference in contractility. Furthermore, pre-incubation with AGE-BSA for 5 days followed by 24 hours culture in the CFM with TNF-α showed that the contractile effect of TNF-α was reduced to that of FPCLs incubated with AGE-BSA alone (Fig. 5.12).

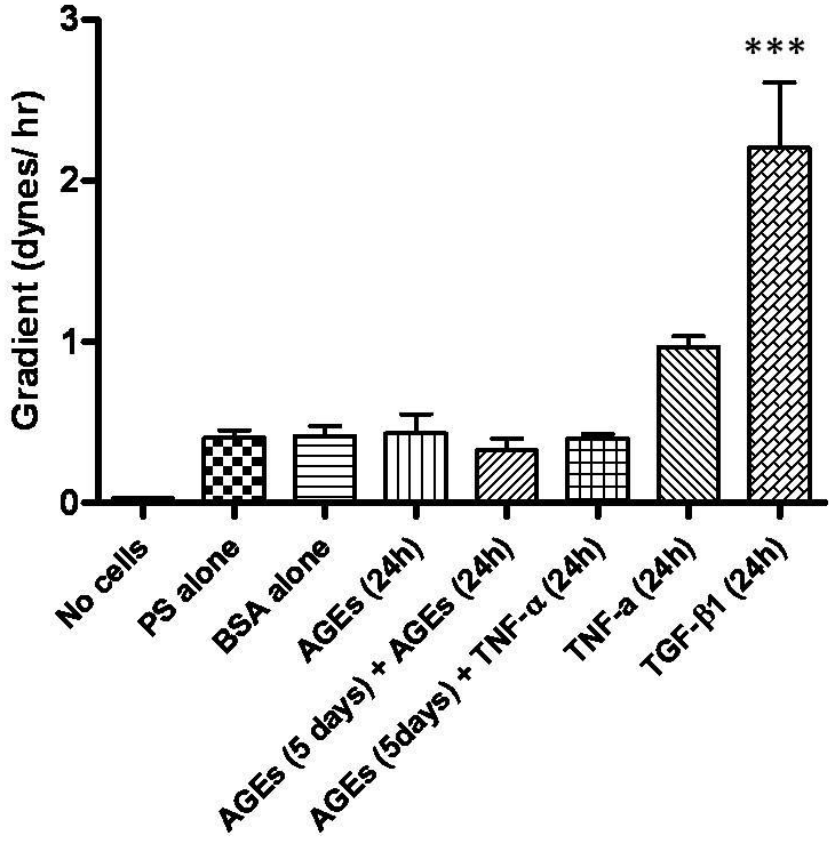


Figure 5.12. Contractility of palmar skin fibroblasts is augmented by TNF-α and TGF-β1. (A) Collagen gels seeded with 1.5 million palmar fibroblasts were cultured in the CFM for 24h with either DMEM (10%FBS) alone, control BSA (15µg/ml), AGE-BSA (150µg/ml), TNF-α (1ng/ml), or TGF-β1 (10ng/ml) and real-time isometric force contraction was quantified. Palmar fibroblasts were also pre-cultured for 5 days with AGE-BSA (150µg/ml) and following trypsinisation these cells were seeded in collagen gels (1.5 million), and then cultured for 24h in the CFM with either TNF-α (1ng/ml) or AGE-BSA (150µg/ml). Collagen alone was also used as a control. Data are shown for the mean rate of contraction from 3 different patient samples (±SEM). *** signifies *p*=0.0001.

In summary, these data suggest that a two-fold increase in contractility results following stimulation of palmar fibroblasts with TNF-α and a significant five-fold increase in isometric force contraction over 24 hours was seen with TGF-β1 (p=0.0001). No difference in isometric force contraction was observed with the addition of AGE-BSA to palmar skin fibroblasts in culture over 24 hours or with pre-exposure over 5 days.

5.3 DISCUSSION

In Dupuytren's nodules, highly contractile myofibroblasts mediate digital contracture. Whilst the stimulus for myofibroblast recruitment in Dupuytren's disease remains unclear, several studies have shown that fibroblast to myofibroblast differentiation is regulated by both cytokines and mechanical stress (Hinz, 2007; Tomasek et al., 2002). There are also data to suggest that inflammation might play a role in the pathogenesis of Dupuytren's disease based on their observations of inflammatory cells in nodules (Andrew et al., 1991; Qureshi et al., 2001; Schubert et al., 2006) and at the interface between nodules and palmar skin (VandeBerg et al., 1982). I systematically examined histological sections of Dupuytren's tissue stained for a panel of inflammatory cells and, using the CFM, analysed the effects of the pro-inflammatory cytokine TNF-α and AGE-RAGE ligand interaction on the contractility of dermal fibroblasts seeded in 3D collagen lattices. To date the effects of both TNF-α and AGE-RAGE ligand interaction have not been investigated in the context of Dupuytren's disease.

Inflammatory cells in nodular and non-nodular Dupuytren's tissue samples were examined in serial sections processed for immunohistochemistry and stained with a panel of inflammatory antibodies, including CD68 positive cells (macrophages), CD3 and CD4-positive T lymphocytes, neutrophil elastase and mast cell tryptase. In line with previous published findings (Andrew et al., 1991; Qureshi et al., 2001; Schubert et al., 2006) the histological sections demonstrated macrophages, mast cells and CD3-positive T lymphocytes amongst myofibroblasts within Dupuytren's nodules, and a proportion of these cells were also observed around blood vessels. Interestingly, Dupuytren's nodules were rich in mast cells,

which are a rich source of TNF-α (Krishnaswamy et al., 2006). In non-nodular cord, almost no inflammatory cells were observed and it is also of interest that virtually no cells stained positive for neutrophil elastase in either nodular or non-nodular cord. This is in contrast to inflammation during wound healing, where neutrophils are commonly seen in the wound where they are involved with clearance of debris and bacteria and initiating myofibroblast dependent wound contraction (Martin and Leibovich, 2005).

Whilst my data and those from previous publications indicate that inflammatory cells are present in nodules, suggesting a key role for inflammation in Dupuytren's disease, it is important to note that excised digital cord samples contain nodules from active disease but do not provide any information on the role of inflammation in early disease. Therefore, these histological findings may only pertain to established disease, when surgical intervention was indicated.

More recently, AGEs have been reported to accumulate in ageing tissues and build up at an accelerated rate in patients with diabetes, where they are also linked to their diet (Brett et al., 1993; Makita et al., 1991; Makita et al., 1992). There is increasing data implicating AGE-RAGE ligand-receptor interaction has been implicated in mechanisms of inflammatory disease through activation of multiple signal transduction pathways, up-regulation of adhesion molecules, secretion of inflammatory cytokines and the production of growth factors such as TGF-β1 (Throckmorton et al., 1995). Furthermore, AGE-RAGE interaction has been shown to induce a TGF-β1 dependent epithelial-myofibroblast transdifferentiation in a proximal renal tubule cell line (Oldfield et al., 2001). AGE exposure induced dose-dependent myofibroblast differentiation determined by morphological changes and de novo α-SMA

expression, and these effects wre blocked with antibodies against RAGE of TGF-β1 (Oldfield et al., 2001). This group further confirmed de novo α-SMA expression by immunoctochemistry , mRNA and protein levels (Li et al., 2004). However, these studies have been carried out on rat renal tubular cells and the role of AGEs or RAGE in Dupuytren's disease has not been examined yet..

Therefore, I characterised RAGE expression in Dupuytren's matched patient samples based on the hypothesis that AGEs through their interaction with RAGE may promote myofibroblast differentiation in Dupuytren's patients. My histological data showed that RAGE was expressed abundantly in myofibroblast-rich nodular and peri-nodular areas. FACS analysis data showed nodular cells have significantly higher levels of cell surface RAGE expression compared to non-nodular cells and dermal fibroblasts. Interestingly, palmar fibroblasts showed significantly more RAGE expression than non-palmar fibroblasts. Whilst the distribution of RAGE in nodules implies it may have a role in modulating myofibroblast activity, the significance of the different epidermal distribution and increased RAGE expression in palmar fibroblasts compared to non-palmar fibroblasts remains uncertain. However, increased RAGE expression in palmar skin and Dupuytren's nodules compared to non-palmar skin, would fit with the observation that early signs of Dupuytren's disease are seen in the palmar skin (Hueston, 1985; Hueston, 1963) and hence supports the hypothesis that the early changes seen in the palmar skin may drive the fibrotic process. Therefore, I used dermal fibroblasts derived from palmar skin and control matched non-palmar skin fibroblasts to test the hypothesis that TNF-α and the AGE-RAGE ligand interaction promote myofibroblast phenotype in Dupuytren's disease.

I went on to examine the effects of AGEs on palmar skin fibroblast contractility in 3D collagen lattices. No differences were seen in contractility over 24 hours in the CFM or with longer term 5 day pre-incubation in the presence of AGEs in culture flasks followed by 24 hours in the CFM. Previous studies using a rat kidney epithelial cell line have reported an increase in expression of α-SMA mRNA and protein expression in monolayer experiments over 24 hours and a linear increase in α-SMA positive cells over a 6 day period (Oldfield et al., 2001). Although I used similar doses of AGEs in my experiments, marked differences in methodology including the examination of cells in 3D lattices under isometric conditions, differences in cell type and cell source may account for the different results.

Several growth factors and cytokines derived from inflammatory cells have also been shown to regulate the myofibroblast phenotype in Dupuytren's disease, include IL-1, bFGF, PDGF, TGF-β1 , TGF-β2, EGF, PDGF and CTGF (Baird et al., 1993; Bunker et al., 2000; Igarashi et al., 1996; Kuhn et al., 2001; Terek et al., 1995). The best studied of these is TGF-β1, which has been shown to induce the myofibroblast phenotype at supra-physiological concentrations in 3D collagen lattices under isometric conditions (Bisson et al., 2009; Wong and Mudera, 2006). My data confirms these findings and showed significant increased palmar fibroblast contractility ($p=0.0001$) with 10ng/ml TGF-β1 compared to untreated palmar fibroblasts.

The effects of TNF-α have not been previously examined in palmar skin fibroblasts and this is the first report of TNF-α resulting in increased palmar fibroblast contractility under isometric conditions in 3D collagen lattices. Interestingly, I found that FPCLs treated with 1ng/ml TNF-α showed a 2-fold increase in contractility over 24 hours with similar findings when repeated in three different patient samples. Previously, TNF-α mRNA levels have been

shown to be increased in whole Dupuytren's cord samples when compared to control tissue taken from patients with frozen shoulder and also normal control shoulders (Bunker et al., 2000), further suggesting TNF-α may play a role in the pathogenesis of Dupuytren's disease.

However, in rat lung fibroblasts TNF-α has been shown to suppress α-SMA expression (Mariani et al., 1999) and decreased α-SMA mRNA expression with TNF-α has also been demonstrated in myofibroblasts from hip joint tissue (Mattyasovszky et al., 2010). In the inflammatory phase of wound healing TNF-α is expressed by inflammatory cells and, both inhibits ECM synthesis and activates MMPs (Singer and Clark, 1999). Previous authors have examined the effects of TNF-α (1ng/ml) in normal human dermal fibroblasts and used isotonic contraction model systems to measure FPCL contractility (Goldberg et al., 2007). This study showed a significant decrease in FPCL contraction upon stimulation with 1ng/ml TNF-α and a significant reduction in collagen 1A and α-SMA mRNA levels and protein levels were demonstrated in cells treated with TNF-α (Goldberg et al., 2007). Furthermore, they demonstrated that TNF-α suppressed TGF-β1 induced myofibroblast phenotypic changes. Similarly, TNF-α has also been shown to anatagonise TGF-β1-induced upregulation of type I and III collagen in fibroblasts through a JNK-dependent regulatory mechanism in mouse fibroblasts (Verrecchia et al., 2002). The anatgonsitic relationship between TGF-β1 and TNF-α warrants further investigation and may play an important role in maintaining tissue homeostasis and ECM turn-over. However, the precise effect of TNF-α may be variable depending on the cell type examined. Indeed, it is worth noting these studies have also shown that TNF-α stimulation can lead to increased proliferation and viability of

myofibroblasts (Mattyasovszky et al., 2010) and human dermal microvascular endothelial cells (HUVEC) (Chaudhuri et al., 2007).

Finally, I examined palmar skin fibroblast contractility following pre-stimulation with AGEs for 5 days, followed by 24 hour culture with TNF-α in the CFM. The rationale for these experiments was based on a study that suggested marked difference between AGE pre-stimulated and control human umbilical vein endothelial cells (HUVECs). Only HUVECs sensitized by AGEs showed a significant pro-inflammatory response as demonstrated by increased cytokine release, adhesion molecules, MAP kinase and NF-kappa B cRel activation (Ehlermann et al., 2006). However, my data showed that AGE pre-stimulation may suppress the contractile stimulus of TNF-α. An explanation for this may be that RAGE is a multi-ligand receptor that also responds to other pro-inflammatory proteins, such as high mobility group protein B1 (HMGB-1) and S100 proteins (van Beijnum et al., 2008). Different permutations of these ligands in combination with AGEs warrant further investigation.

In conclusion, my data suggest that in the presence of TNF-α palmar fibroblasts develop a more contractile phenotype. Possible sources of TNF-α are macrophages and mast cells in Dupuytren's nodules. Although RAGE is abundantly expressed in Dupuytren's nodules and palmar skin, the role of AGEs in Dupuytren's disease remains uncertain. Most importantly, data from this chapter suggests that TNF-α may play a key role in the pathogenesis of Dupuytren's disease.

CHAPTER SIX

Concluding discussion

6.1 Concluding discussion and future plans

Many aspects of the pathophysiology of Dupuytren's disease are still poorly understood. Surgery remains the mainstay of treatment and the problem of recurrence has not been resolved. An improved understanding of the recruitment, differentiation and contraction of myofibroblasts will offer the potential for less invasive means of addressing primary disease. Similar mechanisms may also control the activity of myofibroblasts in other fibrotic diseases. Any therapeutic modality developed for treating Dupuytren's disease may, therefore, also have a role in the general management of fibrosis.

I began by characterising Dupuytren's tissue morphology with a detailed histological analysis of cell and myofibroblast distribution throughout Dupuytren's tissue. I examined over 100 excised digital cord samples and demonstrated that cord tissue is cellular even in non-nodular cords. Nodules were often hypercellular and comprised of a focal condensation of cells. I also showed that Dupuytren's tissue is very heterogenous. A variable proportion of cells observed outside histological nodules and throughout non-nodular cord were also myofibroblasts (9-17%) (Verjee et al., 2009). Myofibroblasts were often seen in non-nodular cord as microscopic pockets of cells aligned longitudinally with collagen fibres. In nodular cords, myofibroblast distribution was also variable and almost half of the cords examined had multiple histological nodules that varied significantly in size.

In agreement with literature describing clinical nodules in relation to the interphalangeal joints of the hand (Chiu and McFarlane, 1978; Luck, 1959), I found that in 95% of nodular samples, a nodule was observed within the vicinity of this joint. A histological nodule was

also seen overlying the MCPJ in 2 further cases where the relationship was specifically sought. The close proximity of myofibroblast rich nodules with joints in the hand may be explained by tension, which can act intermittently on Dupuytren's tissue as movement at the PIPJ offers resistance against the thickened, contracted palmar fascia. Increased tension through the joint, the presence of cytokines and ED-A fibronectin induce myofibroblast differentiation, which in turn would lead to greater force generation. A nodule, densely packed with myofibroblasts, could then theoretically generate and maintain greater contractile force, as myofibroblasts have been shown to have the ability to sustain co-ordinated micro-contractions over a long period of time (Castella et al., 2010; Follonier et al., 2008). Continuous contraction, combined with remodelling of the surrounding ECM by MMPs (Johnston et al., 2007; Johnston et al., 2008; Tarlton et al., 1998; Ulrich et al., 2003), will result in shortening of the affected fascia and over time lead to digital contracture. With advanced disease and the development of fixed flexion deformity, associated loss of movement at the joint is likely to result in "stress shielding", with subsequent loss of tension and myofibroblast apoptosis. Myofibroblast apoptosis following stress-shielding and loss of tension was seen after re-epithelialisation (Desmouliere et al., 1995) and following release of tension in splinted wounds in a rat model (Carlson et al., 2003). It is, therefore, conceivable that with advanced digital contractures, reduced tension through limited active joint extension may similarly lead to myofibroblast apoptosis and resolution of the nodule. This may explain the progression from nodular to non-nodular cords, and why I found that patients with non-nodular cords from advanced disease had significantly more severe flexion deformities. In contrast, nodules containing highly contractile myofibroblasts were present in patients with less digital flexion contractures and active disease.

Many studies have used animal models to examine myofibroblast recruitment, contractility and apoptosis. However, whilst these models emulate the activity of myofibroblasts in wound healing, there is no animal model for the study of Dupuytren's disease. Therefore, to examine Dupuytren's myofibroblasts *in vitro*, I first compared 3D models of contractility using stress-released FPCLs to measure isotonic contraction and restrained FPCLs to measure uniaxial isometric force contraction using the culture force monitor (CFM). These models have previously been used to examine the contractility of Dupuytren's nodule-derived cells compared with non-matched carpal ligament control fibroblasts (Bisson, Tomasek). Using matched sets of Dupuytren's nodule-derived cells and control non-palmar and palmar skin fibroblasts from patients, I examined cell contractility in both systems and also correlated contractility with α-SMA. These comparisons established that Dupuytren's myofibroblasts are best examined under isometric conditions using the CFM. Stress-released FPCLs demonstrated no significant difference between matched cells in terms of isotonic force contraction. However, using the CFM control dermal fibroblasts reached a plateau, unlike Dupuytren's nodule-derived cells that generated continually increasing isometric force. Variability was reduced by comparing the three types of cells from the same patient and inter-patient variability was accounted for by selecting nodular samples, with proportionally more α-SMA as determined by immunohistochemistry.

Whilst establishing this model I also had to address certain methodological issues. The first concern was Dupuytren's tissue heterogeneity. Initial attempts at isolating myofibroblasts from Dupuytren's tissue yielded low percentages of cells with α-SMA positive stress fibres. In order to source Dupuytren's nodule-derived cells with proportionally more

myofibroblasts for use in cell culture, I set up collaboration with Dr. Tanaka (University of Osaka, Japan), who has reported 4 Dupuytren's nodule cell lines comprising a homogenous population of myofibroblasts (Tanaka et al., 2007). However, when examined for α-SMA stress fibres these cells were not a homogenous population of myofibroblasts and a similar proportion of cells with α-SMA positive stress fibres were also seen with nodule-derived cells from patient samples. Therefore, I established new methodology using patient samples to reliably ensure I selected samples with proportionally more myofibroblasts. This was done by bisecting each cord sample and processing one half for histology and the other for cell isolation. For cell isolation, bisected cord samples were further sub-divided with tissue marked for the PIPJ processed separately. This enabled me to use cells from samples with α-SMA positive nodules proven by histology, thereby providing a reliable source of Dupuytren's nodule-derived cells expressing α-SMA. Next, using the matched cells in the CFM, I also determined that the myofibroblast contractile phenotype was only maintained in early cell passage (passage 1 or 2), beyond which nodule-derived cells start to show a decrease in contractility and in the proportion of cells with α-SMA stress fibres. In contrast, I found that dermal fibroblasts develop a more contractile phenotype. These changes may reflect contractile adjustments by these cells as a consequence of the identical *in vitro* culture conditions.

By using genetically matched sets of Dupuytren's nodule-derived cells and control non-palmar and palmar fibroblasts from patients, I also correlated cell contractility with α-SMA distribution, as well as α-SMA mRNA and protein levels. I found that in dermal fibroblasts, α-SMA was typically distributed in a 'halo' within the peri-nucleur cytoplasm, whereas in

nodule-derived cells, α-SMA was frequently localised in stress fibres throughout the cell processes up to cell-matrix attachment sites. The presence of α-SMA in fibroblasts is not seen in vivo, although when fibroblasts are cultured on a rigid plastic substrate in the presence of foetal bovine serum they acquire proto-myofibroblast features with de novo expression of cytosolic α-SMA (Hinz, 2006; Tomasek et al., 2002). Upon reaching a certain threshold of stress in the ECM, α-SMA is incorporated in to stress fibres and this defines a differentiated myofibroblast (Goffin et al., 2006; Hinz, 2007). I found that higher contractility of Dupuytren's myofibroblasts was reflected by increased α-SMA protein levels with recruitment of α-SMA to stress fibres, whilst no differences in α-SMA mRNA levels were seen. These findings suggest that post-transcriptional changes in α-SMA lead to the development of the Dupuytren's myofibroblast phenotype (Verjee et al., 2010). Previous studies have only reported only differences in α-SMA protein expression and localization between nodule- and cord-derived Dupuytren's cells compared to non-matched control carpal ligament cells. The relative levels of α-SMA mRNA in these cell types were not assessed (Benzonana et al., 1988; Dave et al., 2001). Here I simultaneously examined α-SMA protein levels, protein localization and mRNA levels in cells isolated from the same patient. Recent studies on cellular mechanisms of local protein synthesis have also suggested that not only is mRNA subject to translation, but that cells can instruct the cytoskeleton and translation apparatus where to transport and when to translate the intended protein (Rodriguez et al., 2008). Therefore, post-transcriptional changes in α-SMA expression may include mRNA stability, mRNA localisation, translation, cytoskeletal localisation and stress fibre formation. Further studies using Dupuytren's matched cells are required to investigate the relative contribution of each of these.

Based on the surgical observation that recurrence is significantly reduced following dermofasciectomy, I then tested the hypothesis that non-palmar dermal fibroblasts down-regulate the contractility of Dupuytren's nodule derived cells. In these experiments, either palmar or non-palmar dermal fibroblasts were co-cultured with Dupuytren's nodule-derived cells. However, no difference in contractility by Dupuytren's nodule-derived cells was observed, despite controlling for different co-culture cell ratios and with longer term co-cultures. Furthermore, no significant difference in contractility was observed between FPCLs set up with different aspect ratios to generate high and low strain gradients, implying that Dupuytren's myofibroblasts are inherently contractile under isometric conditions (Verjee et al., 2010). These co-culture data suggests that contractility of Dupuytren's cells is not influenced by dermal fibroblasts and that reduced recurrence rate following dermofasciectomy may be due a more complete excision of affected tissue, combined with the possibility of reduced tension following application of full-thickness skin grafts.

Furthermore, the clinical data I collected along with patient samples suggested that recurrence was seen following previous fasciotomy, fasciectomy and firebreak dermosfasciectomy, but not following radical dermofasciectomy. The histological data from these patient samples also showed that nodules occurred with equal frequency in primary and recurrent disease samples. Taken together with my co-culture data, these data suggest that following less radical surgery, residual unexcised Dupuytren's tissue may serve as a nidus for recurrence. The increased motion achieved following initial surgery may facilitate further myofibroblast differentiation and persistence. This may also explain why radical dermofasciectomy has a lower rate of recurrence (1-8%) (Brotherston et al., 1994; Hall et

al., 1997; Tonkin et al., 1984) than 'firebreak' dermofasciectomy (12%) (Ullah et al., 2009) or fasciectomy (40-50%) (Foucher et al., 1992; Hueston, 1961; Tonkin et al., 1984).

The stimulus for myofibroblast recruitment in Dupuytren's disease remains unclear, although inflammation might play a role in the pathogenesis of Dupuytren's disease. This hypothesis has been proposed based on observations of inflammatory cells in nodules (Andrew et al., 1991; Qureshi et al., 2001; Schubert et al., 2006) and at the interface between nodules and palmar skin (VandeBerg et al., 1982). My histological data support these findings and further provide systematic analysis of inflammatory cells throughout excised Dupuytren's tissue. CD3 positiveT-lymphocytes were observed in nodules as well as large numbers of mast cells and macrophages, which can produce pro-inflammatory cytokines, including TNF-α. In contrast, almost no inflammatory cells were seen in non-nodular cord tissue.

High levels of TNF-α have previously been reported in Dupuytren's cord tissue compared to control tissue from normal and frozen shoulders (Bunker et al., 2000). In the inflammatory phase of wound healing TNF-α is expressed by inflammatory cells and, both inhibits ECM synthesis and activates MMPs (Singer and Clark, 1999). In rat lung fibroblasts TNF-α has been shown to suppress α-SMA expression (Mariani et al., 1999) and decreased α-SMA mRNA expression with TNF-α has also been demonstrated in myofibroblasts from hip joint tissue (Mattyasovszky et al., 2010). Previous authors have measured isotonic contraction using human non-palmar fibroblasts and also demonstrated decreased contractility and reduced α-SMA mRNA and protein expression with TNF-α (Goldberg et al., 2007). In contrast, my data showed that under isometric conditions, TNF-α promotes a 2-fold

increase in palmar fibroblast contractility over 24 hours, although not to the same order of magnitude as with TGF-β1 which generated a 5-fold increase in contractility. Therefore, the precise effect of TNF-α may be variable, depending on the model system used and the cell type examined. It is also worth noting that TNF-α stimulation can lead to increased proliferation and viability of myofibroblasts from joint capsule tissue {Mattyasovszky, 2010 #302) and human dermal microvascular endothelial cells (HUVEC) (Chaudhuri et al., 2007). A dose response for TNF-α will also show if this cytokine has the same effect at supra-physiological levels, as previously demonstrated with TGF-β1 (Bisson et al., 2009; Wong and Mudera, 2006). Investigation of the effect of TNF-α on non-palmar skin fibroblasts under isometric conditions is required to determine if these effects are specific to palmar fibroblasts. Furthermore, it has also been shown that TNF-α suppressed TGF-β1 induced myofibrobalst phenotypic changes in normal dermal fibrobalsts (Goldberg et al., 2007). Similarly, TNF-α has also been shown to anatagonise TGF-β1-induced upregulation of type I and III collagen in fibroblasts through a JNK-dependent regulatory mechanism in mouse fibroblasts (Verrecchia et al., 2002). The anatgonsitic relationship between TGF-β1 and TNF-α also needs further investigation and may play an important role in maintaining tissue homeostasis and ECM turn-over. The combined stimulation of palmar skin fibroblasts with TNF-α and TGF-β1 in the CFM may result in synergistic or inhibitory effects on contractility and remains to be examined.

AGE interaction with RAGE has been shown to induce a TGF-β1 dependent epithelial-myofibroblast transdifferentiation in a proximal renal tubule cell line as observed by morphology, de novo expression of α-SMA mRNA and protein (Li et al., 2004; Oldfield et al.,

2001). AGEs have been shown to accumulate in ageing tissues and in patients with diabetes, where they are also linked to their diet (Makita et al., 1991). I hypothesised that AGEs in the tissues of genetically susceptible individuals could directly stimulate the conversion of fibroblasts in the palmar fascia to myofibroblasts. RAGE expression in Dupuytren's tissue has not been examined previously and my data showed RAGE expression co-localised with α-SMA in nodules as well as significant differences in RAGE expression in palmar and non-palmar skin fibroblasts. However, stimulation of palmar skin fibroblasts for 24 hours or after 5 days with AGEs did not increase their contractility. Furthermore, my data showed that pre-stimulation of palmar fibroblasts with AGEs may also suppress the contractile stimulus seen by then adding TNF-α. An explanation for this may be that RAGE is a multi-ligand receptor that also responds to other pro-inflammatory proteins, such as high mobility group protein B1 (HMGB-1) and S100 proteins (van Beijnum et al., 2008). Therefore, different permutations of these ligands in combination with AGEs warrant further investigation and will involve futre work planned beyond this thesis.

Other areas of future work include, examining in more detail the post-transcriptional changes in α-SMA that occur in genetically matched cells to mediate the Dupuytren's myofibroblast cell phenotype. These post-transcriptional changes in α-SMA expression may include mRNA stability, mRNA localisation, translation, cytoskeletal localisation and stress fibre formation. Further studies using Dupuytren's matched cells are required to investigate each of these possibilities in turn.

Finally, work will be carried out to analyse the ability of TNF-α to induce palmar skin fibroblasts to develop into a more contractile phenotype will be carried out. The dose

response to TNF-α on palmar skin fibroblasts will determine if higher doses induce or suppress contractility of palmar skin fibroblasts. These experiments will also be done in combination with TGF-β1 to determine if the combined effects are synergistic or inhibitory on palmar skin fibroblast contractility and on α-SMA expression in stress fibres, mRNA and protein levels. The optimal concentration of TNF-α from these experiments will then be used to examine contractility in control matched non-palmar skin fibroblasts, and to determine if the increased contractility observed so far is only specific to palmar skin fibroblasts.

6.2 Conclusion

In conclusion, I have examined in detail the distribution of α-SMA positive cells and the cellularity throughout excised Dupuytren's cord. I confirmed that myofibroblasts are mainly found in histological nodules. These nodules were often hypercellular and comprised a focal condensation of cells. Myofibroblasts were also found in variable numbers outside nodules and in amongst collagen bundles of Dupuytren's cord. Histological nodules were found in the vicinity of the PIPJ of the hand and α-SMA rich nodules were associated with lesser digital contracture, whereas cords without α-SMA rich nodules from advanced disease correlated significantly with greater fixed flexion deformity. This implies that α-SMA expression may be transient through Dupuytren's disease. Reduced movement at the joint in advanced disease may result in a form of stress-shielding with loss of tension and subsequent myofibroblast apoptosis that leaves behind residual stage non-nodular cords.

Using cells derived from α-SMA rich nodules, and genetically matched non-palmar skin and palmar skin I have shown that nodule-derived cells generate higher levels of isometric force that continue to increased over 24h, unlike dermal fibroblasts which generate less force and characteristically plateau. Most significantly, I have demonstrated that myofibroblast differentiation in Dupuytren's nodule-derived cells is characterised by recruitment of α-SMA to stress fibres and reflected by increased α-SMA protein levels, but not α-SMA mRNA levels. Whilst contractility of Dupuytren's nodule-derived cells was not influenced by dermal fibroblasts, I found in palmar fibroblasts a two-fold increase in isometric force contraction with TNF-α and a significant five-fold increase with TGF-β1. In Dupuytren's disease, TNF-α may have a role to play in modulating the myofibroblast phenotype.

Bibliography

References

Abbott K, Denney J, Burke FD and McGrouther DA (1987). A review of attitudes to splintage in Dupuytren's contracture. J Hand Surg Br 12:326-328.

Abe R, Donnelly SC, Peng T, Bucala R and Metz CN (2001). Peripheral blood fibrocytes: differentiation pathway and migration to wound sites. J Immunol 166:7556-7562.

Abe Y, Rokkaku T, Ofuchi S, Tokunaga S, Takahashi K and Moriya H (2004a). Surgery for Dupuytren's disease in Japanese patients and a new preoperative classification. J Hand Surg Br 29:235-239.

Abe Y, Rokkaku T, Ofuchi S, Tokunaga S, Takahashi K and Moriya H (2004b). An objective method to evaluate the risk of recurrence and extension of Dupuytren's disease. J Hand Surg Br 29:427-430.

Abe Y, Rokkaku T, Ofuchi S, Tokunaga S, Takahashi K and Moriya H (2004c). Dupuytren's disease on the radial aspect of the hand: report on 135 hands in Japanese patients. J Hand Surg Br 29:359-362.

Alberts B, Johnson A, Lewis J, Raff M, Roberts K and Walter P (2002). Molecular Biology of the Cell, 4th edition edn (New York, Garland Science).

Alioto RJ, Rosier RN, Burton RI and Puzas JE (1994). Comparative effects of growth factors on fibroblasts of Dupuytren's tissue and normal palmar fascia. J Hand Surg Am 19:442-452.

Andrew JG, Andrew SM, Ash A and Turner B (1991). An investigation into the role of inflammatory cells in Dupuytren's disease. J Hand Surg Br 16:267-271.

Andrew JG and Kay NR (1991). Segmental aponeurectomy for Dupuytren's disease: a prospective study. J Hand Surg Br 16:255-257.

Arkkila PE, Kantola IM, Viikari JS, Ronnemaa T and Vahatalo MA (1996). Dupuytren's disease in type 1 diabetic patients: a five-year prospective study. Clin Exp Rheumatol 14:59-65.

Arora PD and McCulloch CA (1994). Dependence of collagen remodelling on alpha-smooth muscle actin expression by fibroblasts. J Cell Physiol 159:161-175.

Arora PD, Narani N and McCulloch CA (1999). The compliance of collagen gels regulates transforming growth factor-beta induction of alpha-smooth muscle actin in fibroblasts. Am J Pathol 154:871-882.

Badalamente MA, Stern L and Hurst LC (1983). The pathogenesis of Dupuytren's contracture: contractile mechanisms of the myofibroblasts. J Hand Surg Am 8:235-243.

Badalamente MA, Hurst LC and Sampson SP (1988). Prostaglandins influence myofibroblast contractility in Dupuytren's disease. J Hand Surg Am 13:867-871.

Badalamente MA, Hurst LC, Grandia SK and Sampson SP (1992). Platelet-derived growth factor in Dupuytren's disease. J Hand Surg Am 17:317-323.

Badalamente MA, Sampson SP, Hurst LC, Dowd A and Miyasaka K (1996). The role of transforming growth factor beta in Dupuytren's disease. J Hand Surg [Am] 21:210-215.

Badalamente MA and Hurst LC (2007). Efficacy and safety of injectable mixed collagenase subtypes in the treatment of Dupuytren's contracture. J Hand Surg Am 32:767-774.

Bailey AJ, Tarlton JF, Van der Stappen J, Sims TJ and Messina A (1994). The continuous elongation technique for severe Dupuytren's disease. A biochemical mechanism. J Hand Surg Br 19:522-527.

Baird KS, Crossan JF and Ralston SH (1993). Abnormal growth factor and cytokine expression in Dupuytren's contracture. J Clin Pathol 46:425-428.

Balaguer T, David S, Ihrai T, Cardot N, Daideri G and Lebreton E (2009). Histological Staging And Dupuytren'S Disease Recurrence or Extension after Surgical Treatment: A Retrospective Study of 124 Patients. J Hand Surg Eur Vol.

Bayat A, Alansar A, Hajeer AH, Shah M, Watson JS, Stanley JK, Ferguson MW and Ollier WE (2002a). Genetic susceptibility in Dupuytren's disease: lack of association of a novel transforming growth factor beta(2) polymorphism in Dupuytren's disease. J Hand Surg Br 27:47-49.

Bayat A, Watson JS, Stanley JK, Alansari A, Shah M, Ferguson MW and Ollier WE (2002b). Genetic susceptibility in Dupuytren's disease. TGF-beta1 polymorphisms and Dupuytren's disease. J Bone Joint Surg Br 84:211-215.

Bayat A, Stanley JK, Watson JS, Ferguson MW and Ollier WE (2003). Genetic susceptibility to Dupuytren's disease: transforming growth factor beta receptor (TGFbetaR) gene polymorphisms and Dupuytren's disease. Br J Plast Surg 56:328-333.

Bell E, Ivarsson B and Merrill C (1979). Production of a tissue-like structure by contraction of collagen lattices by human fibroblasts of different proliferative potential in vitro. Proc Natl Acad Sci U S A 76:1274-1278.

Benzonana G, Skalli O and Gabbiani G (1988). Correlation between the distribution of smooth muscle or non muscle myosins and alpha-smooth muscle actin in normal and pathological soft tissues. Cell Motil Cytoskeleton 11:260-274.

Berndt A, Kosmehl H, Mandel U, Gabler U, Luo X, Celeda D, Zardi L and Katenkamp D (1995). TGF beta and bFGF synthesis and localization in Dupuytren's disease (nodular palmar fibromatosis) relative to cellular activity, myofibroblast phenotype and oncofetal variants of fibronectin. Histochem J 27:1014-1020.

Betz N, Ott OJ, Adamietz B, Sauer R, Fietkau R and Keilholz L (2010). Radiotherapy in early-stage Dupuytren's contracture. Long-term results after 13 years. Strahlenther Onkol 186:82-90.

Bisson MA, McGrouther DA, Mudera V and Grobbelaar AO (2003). The different characteristics of Dupuytren's disease fibroblasts derived from either nodule or cord: expression of alpha-smooth muscle actin and the response to stimulation by TGF-beta1. J Hand Surg Br 28:351-356.

Bisson MA, Mudera V, McGrouther DA and Grobbelaar AO (2004). The contractile properties and responses to tensional loading of Dupuytren's disease--derived fibroblasts are altered: a cause of the contracture? Plast Reconstr Surg 113:611-621; discussion 622-614.

Bisson MA, Beckett KS, McGrouther DA, Grobbelaar AO and Mudera V (2009). Transforming growth factor-beta1 stimulation enhances Dupuytren's fibroblast contraction in response to uniaxial mechanical load within a 3-dimensional collagen gel. J Hand Surg Am 34:1102-1110.

Brett J, Schmidt AM, Yan SD, Zou YS, Weidman E, Pinsky D, Nowygrod R, Neeper M, Przysiecki C, Shaw A and et al. (1993). Survey of the distribution of a newly characterized receptor for advanced glycation end products in tissues. Am J Pathol 143:1699-1712.

Brickley-Parsons D, Glimcher MJ, Smith RJ, Albin R and Adams JP (1981). Biochemical changes in the collagen of the palmar fascia in patients with Dupuytren's disease. J Bone Joint Surg Am 63:787-797.

Brinckerhoff CE and Matrisian LM (2002). Matrix metalloproteinases: a tail of a frog that became a prince. Nat Rev Mol Cell Biol 3:207-214.

Brotherston TM, Balakrishnan C, Milner RH and Brown HG (1994). Long term follow-up of dermofasciectomy for Dupuytren's contracture. Br J Plast Surg 47:440-443.

Brown RA, Prajapati R, McGrouther DA, Yannas IV and Eastwood M (1998). Tensional homeostasis in dermal fibroblasts: mechanical responses to mechanical loading in three-dimensional substrates. J Cell Physiol 175:323-332.

Brown RA, Sethi KK, Gwanmesia I, Raemdonck D, Eastwood M and Mudera V (2002). Enhanced fibroblast contraction of 3D collagen lattices and integrin expression by TGF-beta1 and -beta3: mechanoregulatory growth factors? Exp Cell Res 274:310-322.

Bryan AS and Ghorbal MS (1988). The long-term results of closed palmar fasciotomy in the management of Dupuytren's contracture. J Hand Surg Br 13:254-256.

Bulstrode NW, Bisson M, Jemec B, Pratt AL, McGrouther DA and Grobbelaar AO (2004). A prospective randomised clinical trial of the intra-operative use of 5-fluorouracil on the outcome of dupuytren's disease. J Hand Surg Br 29:18-21.

Bulstrode NW, Jemec B and Smith PJ (2005). The complications of Dupuytren's contracture surgery. J Hand Surg Am 30:1021-1025.

Bunker TD, Reilly J, Baird KS and Hamblen DL (2000). Expression of growth factors, cytokines and matrix metalloproteinases in frozen shoulder. J Bone Joint Surg Br 82:768-773.

Burge P (1999). Genetics of Dupuytren's disease. Hand Clin 15:63-71.

Burridge K and Chrzanowska-Wodnicka M (1996). Focal adhesions, contractility, and signaling. Annu Rev Cell Dev Biol 12:463-518.

Carlson MA, Longaker MT and Thompson JS (2003). Wound splinting regulates granulation tissue survival. J Surg Res 110:304-309.

Caroli A, Zanasi S, Marcuzzi A, Guerra D, Cristiani G and Ronchetti IP (1991). Epidemiological and structural findings supporting the fibromatous origin of dorsal knuckle pads. J Hand Surg Br 16:258-262.

Castella LF, Buscemi L, Godbout C, Meister JJ and Hinz B (2010). A new lock-step mechanism of matrix remodelling based on subcellular contractile events. J Cell Sci 123:1751-1760.

Chambers RC, Leoni P, Kaminski N, Laurent GJ and Heller RA (2003). Global expression profiling of fibroblast responses to transforming growth factor-beta1 reveals the induction of inhibitor of differentiation-1 and provides evidence of smooth muscle cell phenotypic switching. Am J Pathol 162:533-546.

Chaudhuri V, Zhou L and Karasek M (2007). Inflammatory cytokines induce the transformation of human dermal microvascular endothelial cells into myofibroblasts: a potential role in skin fibrogenesis. J Cutan Pathol 34:146-153.

Chiquet-Ehrismann R and Chiquet M (2003). Tenascins: regulation and putative functions during pathological stress. J Pathol 200:488-499.

Chiu HF and McFarlane RM (1978). Pathogenesis of Dupuytren's contracture: a correlative clinical-pathological study. J Hand Surg Am 3:1-10.

Christen T, Verin V, Bochaton-Piallat M, Popowski Y, Ramaekers F, Debruyne P, Camenzind E, van Eys G and Gabbiani G (2001). Mechanisms of neointima formation and remodeling in the porcine coronary artery. Circulation 103:882-888.

Citron N and Messina JC (1998). The use of skeletal traction in the treatment of severe primary Dupuytren's disease. J Bone Joint Surg Br 80:126-129.

Citron N and Hearnden A (2003). Skin tension in the aetiology of Dupuytren's disease; a prospective trial. J Hand Surg Br 28:528-530.

Classen DA and Hurst LN (1992). Plantar fibromatosis and bilateral flexion contractures: a review of the literature. Ann Plast Surg 28:475-478.

Dalkowski A, Schuppan D, Orfanos CE and Zouboulis CC (1999). Increased expression of tenascin C by keloids in vivo and in vitro. Br J Dermatol 141:50-56.

Darby I, Skalli O and Gabbiani G (1990). Alpha-smooth muscle actin is transiently expressed by myofibroblasts during experimental wound healing. Lab Invest 63:21-29.

Dave SA, Banducci DR, Graham WP, 3rd, Allison GM and Ehrlich HP (2001). Differences in alpha smooth muscle actin expression between fibroblasts derived from Dupuytren's nodules or cords. Exp Mol Pathol 71:147-155.

Davies CA, Herrick AL, Cordingley L, Freemont AJ and Jeziorska M (2009). Expression of advanced glycation end products and their receptor in skin from patients with systemic sclerosis with and without calcinosis. Rheumatology (Oxford) 48:876-882.

De Vriese AS, Tilton RG, Mortier S and Lameire NH (2006). Myofibroblast transdifferentiation of mesothelial cells is mediated by RAGE and contributes to peritoneal fibrosis in uraemia. Nephrol Dial Transplant 21:2549-2555.

Derynck R and Zhang YE (2003). Smad-dependent and Smad-independent pathways in TGF-beta family signalling. Nature 425:577-584.

Desmouliere A, Rubbia-Brandt L, Abdiu A, Walz T, Macieira-Coelho A and Gabbiani G (1992). Alpha-smooth muscle actin is expressed in a subpopulation of cultured and cloned fibroblasts and is modulated by gamma-interferon. Exp Cell Res 201:64-73.

Desmouliere A, Geinoz A, Gabbiani F and Gabbiani G (1993). Transforming growth factor-beta 1 induces alpha-smooth muscle actin expression in granulation tissue myofibroblasts and in quiescent and growing cultured fibroblasts. J Cell Biol 122:103-111.

Desmouliere A, Redard M, Darby I and Gabbiani G (1995). Apoptosis mediates the decrease in cellularity during the transition between granulation tissue and scar. Am J Pathol 146:56-66.

Desmouliere A, Darby IA and Gabbiani G (2003). Normal and pathologic soft tissue remodeling: role of the myofibroblast, with special emphasis on liver and kidney fibrosis. Lab Invest 83:1689-1707.

Desmouliere A, Chaponnier C and Gabbiani G (2005). Tissue repair, contraction, and the myofibroblast. Wound Repair Regen 13:7-12.

Dias JJ and Braybrooke J (2006). Dupuytren's contracture: an audit of the outcomes of surgery. J Hand Surg Br 31:514-521.

Direkze NC, Forbes SJ, Brittan M, Hunt T, Jeffery R, Preston SL, Poulsom R, Hodivala-Dilke K, Alison MR and Wright NA (2003). Multiple organ engraftment by bone-marrow-derived myofibroblasts and fibroblasts in bone-marrow-transplanted mice. Stem Cells 21:514-520.

Dudas J, Mansuroglu T, Batusic D, Saile B and Ramadori G (2007). Thy-1 is an in vivo and in vitro marker of liver myofibroblasts. Cell Tissue Res 329:503-514.

Dugina V, Fontao L, Chaponnier C, Vasiliev J and Gabbiani G (2001). Focal adhesion features during myofibroblastic differentiation are controlled by intracellular and extracellular factors. J Cell Sci 114:3285-3296.

Eastwood M, McGrouther DA and Brown RA (1994). A culture force monitor for measurement of contraction forces generated in human dermal fibroblast cultures: evidence for cell-matrix mechanical signalling. Biochim Biophys Acta 1201:186-192.

Eastwood M, Porter R, Khan U, McGrouther G and Brown R (1996). Quantitative analysis of collagen gel contractile forces generated by dermal fibroblasts and the relationship to cell morphology. J Cell Physiol 166:33-42.

Eastwood M, Mudera VC, McGrouther DA and Brown RA (1998). Effect of precise mechanical loading on fibroblast populated collagen lattices: morphological changes. Cell Motil Cytoskeleton 40:13-21.

Eddy RJ, Petro JA and Tomasek JJ (1988). Evidence for the nonmuscle nature of the "myofibroblast" of granulation tissue and hypertropic scar. An immunofluorescence study. Am J Pathol 130:252-260.

Egawa T (1985). Dupuytren's contracture in Japan. In: Heuston J, T and Tubiana R, eds. Dupuytren's disease (Edinburgh, Churchill Livingstone), pp. 100-103

Ehlermann P, Eggers K, Bierhaus A, Most P, Weichenhan D, Greten J, Nawroth PP, Katus HA and Remppis A (2006). Increased proinflammatory endothelial response to S100A8/A9 after preactivation through advanced glycation end products. Cardiovasc Diabetol 5:6.

Ehrlich HP, Desmouliere A, Diegelmann RF, Cohen IK, Compton CC, Garner WL, Kapanci Y and Gabbiani G (1994). Morphological and immunochemical differences between keloid and hypertrophic scar. Am J Pathol 145:105-113.

Elliot D (1999). The early history of Dupuytren's disease. Hand Clin 15:1-19, v.

Elsdale T and Bard J (1972). Collagen substrata for studies on cell behavior. J Cell Biol 54:626-637.

Eyden B (2003). Electron microscopy in the study of myofibroblastic lesions. Semin Diagn Pathol 20:13-24.

Eyden B (2005). The myofibroblast: a study of normal, reactive and neoplastic tissues, with an emphasis on ultrastructure. Part 1--normal and reactive cells. J Submicrosc Cytol Pathol 37:109-204.

Fehrenbach H, Weiskirchen R, Kasper M and Gressner AM (2001). Up-regulated expression of the receptor for advanced glycation end products in cultured rat hepatic stellate cells during transdifferentiation to myofibroblasts. Hepatology 34:943-952.

Folger PA, Zekaria D, Grotendorst G and Masur SK (2001). Transforming growth factor-beta-stimulated connective tissue growth factor expression during corneal myofibroblast differentiation. Invest Ophthalmol Vis Sci 42:2534-2541.

Follonier L, Schaub S, Meister JJ and Hinz B (2008). Myofibroblast communication is controlled by intercellular mechanical coupling. J Cell Sci 121:3305-3316.

Forbes SJ, Russo FP, Rey V, Burra P, Rugge M, Wright NA and Alison MR (2004). A significant proportion of myofibroblasts are of bone marrow origin in human liver fibrosis. Gastroenterology 126:955-963.

Foucher G, Cornil C and Lenoble E (1992). Open palm technique for Dupuytren's disease. A five-year follow-up. Ann Chir Main Memb Super 11:362-366.

Foucher G, Medina J and Navarro R (2003). Percutaneous needle aponeurotomy: complications and results. J Hand Surg Br 28:427-431.

Gabbiani G, Ryan GB and Majne G (1971). Presence of modified fibroblasts in granulation tissue and their possible role in wound contraction. Experientia 27:549-550.

Gabbiani G and Majno G (1972). Dupuytren's contracture: fibroblast contraction? An ultrastructural study. Am J Pathol 66:131-146.

Gabbiani G, Kapanci Y, Barazzone P and Franke WW (1981). Immunochemical identification of intermediate-sized filaments in human neoplastic cells. A diagnostic aid for the surgical pathologist. Am J Pathol 104:206-216.

Gabbiani G (2003). The myofibroblast in wound healing and fibrocontractive diseases. J Pathol 200:500-503.

Geiger B, Bershadsky A, Pankov R and Yamada KM (2001). Transmembrane crosstalk between the extracellular matrix--cytoskeleton crosstalk. Nat Rev Mol Cell Biol 2:793-805.

Gelberman RH, Amiel D, Rudolph RM and Vance RM (1980). Dupuytren's contracture. An electron microscopic, biochemical, and clinical correlative study. J Bone Joint Surg Am 62:425-432.

Gholami SS and Lue TF (2002). Correction of penile curvature using the 16-dot plication technique: a review of 132 patients. J Urol 167:2066-2069.

Goffin JM, Pittet P, Csucs G, Lussi JW, Meister JJ and Hinz B (2006). Focal adhesion size controls tension-dependent recruitment of alpha-smooth muscle actin to stress fibers. J Cell Biol 172:259-268.

Goldberg MT, Han YP, Yan C, Shaw MC and Garner WL (2007). TNF-alpha suppresses alpha-smooth muscle actin expression in human dermal fibroblasts: an implication for abnormal wound healing. J Invest Dermatol 127:2645-2655.

Goto T, Yanaga F and Ohtsuki I (1998). Studies on the endothelin-1-induced contraction of rat granulation tissue pouch mediated by myofibroblasts. Biochim Biophys Acta 1405:55-66.

Grinnell F (1994). Fibroblasts, myofibroblasts, and wound contraction. J Cell Biol 124:401-404.

Grinnell F, Zhu M, Carlson MA and Abrams JM (1999). Release of mechanical tension triggers apoptosis of human fibroblasts in a model of regressing granulation tissue. Exp Cell Res 248:608-619.

Grinnell F and Ho CH (2002). Transforming growth factor beta stimulates fibroblast-collagen matrix contraction by different mechanisms in mechanically loaded and unloaded matrices. Exp Cell Res 273:248-255.

Grinnell F (2003). Fibroblast biology in three-dimensional collagen matrices. Trends Cell Biol 13:264-269.

Grinnell F and Petroll WM (2010). Cell Motility and Mechanics in Three-Dimensional Collagen Matrices. Annu Rev Cell Dev Biol.

Gudmundsson KG, Arngrimsson R, Sigfusson N, Bjornsson A and Jonsson T (2000). Epidemiology of Dupuytren's disease: clinical, serological, and social assessment. The Reykjavik Study. J Clin Epidemiol 53:291-296.

Hall PN, Fitzgerald A, Sterne GD and Logan AM (1997). Skin replacement in Dupuytren's disease. J Hand Surg Br 22:193-197.

Halliday NL and Tomasek JJ (1995). Mechanical properties of the extracellular matrix influence fibronectin fibril assembly in vitro. Exp Cell Res 217:109-117.

Harris AK, Wild P and Stopak D (1980). Silicone rubber substrata: a new wrinkle in the study of cell locomotion. Science 208:177-179.

Harris AK, Stopak D and Wild P (1981). Fibroblast traction as a mechanism for collagen morphogenesis. Nature 290:249-251.

Hashimoto N, Jin H, Liu T, Chensue SW and Phan SH (2004). Bone marrow-derived progenitor cells in pulmonary fibrosis. J Clin Invest 113:243-252.

Hindman HB, Marty-Roix R, Tang JB, Jupiter JB, Simmons BP and Spector M (2003). Regulation of expression of alpha-smooth muscle actin in cells of Dupuytren's contracture. J Bone Joint Surg Br 85:448-455.

Hindocha S, Stanley JK, Watson S and Bayat A (2006). Dupuytren's diathesis revisited: Evaluation of prognostic indicators for risk of disease recurrence. J Hand Surg [Am] 31:1626-1634.

Hindocha S, McGrouther DA and Bayat A (2009). Epidemiological Evaluation of Dupuytren's Disease Incidence and Prevalence Rates in Relation to Etiology. Hand (N Y) 4:256-269.

Hinz B, Celetta G, Tomasek JJ, Gabbiani G and Chaponnier C (2001a). Alpha-smooth muscle actin expression upregulates fibroblast contractile activity. Mol Biol Cell 12:2730-2741.

Hinz B, Mastrangelo D, Iselin CE, Chaponnier C and Gabbiani G (2001b). Mechanical tension controls granulation tissue contractile activity and myofibroblast differentiation. Am J Pathol 159:1009-1020.

Hinz B, Dugina V, Ballestrem C, Wehrle-Haller B and Chaponnier C (2003). Alpha-smooth muscle actin is crucial for focal adhesion maturation in myofibroblasts. Mol Biol Cell 14:2508-2519.

Hinz B and Gabbiani G (2003). Mechanisms of force generation and transmission by myofibroblasts. Curr Opin Biotechnol 14:538-546.

Hinz B, Pittet P, Smith-Clerc J, Chaponnier C and Meister JJ (2004). Myofibroblast development is characterized by specific cell-cell adherens junctions. Mol Biol Cell 15:4310-4320.

Hinz B (2006). Masters and servants of the force: the role of matrix adhesions in myofibroblast force perception and transmission. Eur J Cell Biol 85:175-181.

Hinz B (2007). Formation and function of the myofibroblast during tissue repair. J Invest Dermatol 127:526-537.

Honner R, Lamb DW and James JI (1971). Dupuytren's contracture. Long term results after fasciectomy. J Bone Joint Surg Br 53:240-246.

Hu FZ, Nystrom A, Ahmed A, Palmquist M, Dopico R, Mossberg I, Gladitz J, Rayner M, Post JC, Ehrlich GD and Preston RA (2005). Mapping of an autosomal dominant gene for Dupuytren's contracture to chromosome 16q in a Swedish family. Clin Genet 68:424-429.

Hueston J (1985). The role of the skin in Dupuytren's disease. Ann R Coll Surg Engl 67:372-375.

Hueston J, T (1963). Dupuytren's Contracture. (Edinburgh, E & S Livingstone), pp. 51-120.

Hueston JT (1961). Limited fasciectomy for Dupuytren's contracture. Plast Reconstr Surg Transplant Bull 27:569-585.

Hueston JT (1984). 'Firebreak' grafts in Dupuytren's contracture. Aust N Z J Surg 54:277-281.

Hueston JT (1992). Regression of Dupuytren's contracture. J Hand Surg Br 17:453-457.

Hurst LC and Badalamente MA (1999). Nonoperative treatment of Dupuytren's disease. Hand Clin 15:97-107, vii.

Hurst LC, Badalamente MA, Hentz VR, Hotchkiss RN, Kaplan FT, Meals RA, Smith TM and Rodzvilla J (2009). Injectable collagenase clostridium histolyticum for Dupuytren's contracture. N Engl J Med 361:968-979.

Hutchinson JW, Tierney GM, Parsons SL and Davis TR (1998). Dupuytren's disease and frozen shoulder induced by treatment with a matrix metalloproteinase inhibitor. J Bone Joint Surg Br 80:907-908.

Huttunen HJ, Fages C and Rauvala H (1999). Receptor for advanced glycation end products (RAGE)-mediated neurite outgrowth and activation of NF-kappaB require the cytoplasmic domain of the receptor but different downstream signaling pathways. J Biol Chem 274:19919-19924.

Hwang K, Sim HB, Huan F and Kim DJ (2010). Myofibroblasts and Capsular Tissue Tension in Breast Capsular Contracture. Aesthetic Plast Surg.

Hynes R, O. (1990). Fibronectins (New York, Springer-Verlag).

Igarashi A, Nashiro K, Kikuchi K, Sato S, Ihn H, Fujimoto M, Grotendorst GR and Takehara K (1996). Connective tissue growth factor gene expression in tissue sections from localized scleroderma, keloid, and other fibrotic skin disorders. J Invest Dermatol 106:729-733.

Iwasaki H, Muller H, Stutte HJ and Brennscheidt U (1984). Palmar fibromatosis (Dupuytren's contracture). Ultrastructural and enzyme histochemical studies of 43 cases. Virchows Arch A Pathol Anat Histopathol 405:41-53.

Jemec B, Linge C, Grobbelaar AO, Smith PJ, Sanders R and McGrouther DA (2000). The effect of 5-fluorouracil on Dupuytren fibroblast proliferation and differentiation. Chir Main 19:15-22.

Johnston P, Chojnowski AJ, Davidson RK, Riley GP, Donell ST and Clark IM (2007). A complete expression profile of matrix-degrading metalloproteinases in Dupuytren's disease. J Hand Surg Am 32:343-351.

Johnston P, Larson D, Clark IM and Chojnowski AJ (2008). Metalloproteinase gene expression correlates with clinical outcome in Dupuytren's disease. J Hand Surg Am 33:1160-1167.

Kaarteenaho-Wiik R, Lakari E, Soini Y, Pollanen R, Kinnula VL and Paakko P (2000). Tenascin expression and distribution in pleural inflammatory and fibrotic diseases. J Histochem Cytochem 48:1257-1268.

Kamm KE and Stull JT (1989). Regulation of smooth muscle contractile elements by second messengers. Annu Rev Physiol 51:299-313.

Kaufman LJ, Brangwynne CP, Kasza KE, Filippidi E, Gordon VD, Deisboeck TS and Weitz DA (2005). Glioma expansion in collagen I matrices: analyzing collagen concentration-dependent growth and motility patterns. Biophys J 89:635-650.

Keilholz L, Seegenschmiedt MH and Sauer R (1996). Radiotherapy for prevention of disease progression in early-stage Dupuytren's contracture: initial and long-term results. Int J Radiat Oncol Biol Phys 36:891-897.

Ketchum LD and Donahue TK (2000). The injection of nodules of Dupuytren's disease with triamcinolone acetonide. J Hand Surg Am 25:1157-1162.

Kischer CW and Speer DP (1984). Microvascular changes in Dupuytren's contracture. J Hand Surg Am 9A:58-62.

Kloen P, Jennings CL, Gebhardt MC, Springfield DS and Mankin HJ (1995). Transforming growth factor-beta: possible roles in Dupuytren's contracture. J Hand Surg Am 20:101-108.

Kosmehl H, Berndt A, Katenkamp D, Mandel U, Bohle R, Gabler U and Celeda D (1995). Differential expression of fibronectin splice variants, oncofetal glycosylated fibronectin and laminin isoforms in nodular palmar fibromatosis. Pathol Res Pract 191:1105-1113.

Koumas L, Smith TJ, Feldon S, Blumberg N and Phipps RP (2003). Thy-1 expression in human fibroblast subsets defines myofibroblastic or lipofibroblastic phenotypes. Am J Pathol 163:1291-1300.

Krishnaswamy G, Ajitawi O and Chi DS (2006). The human mast cell: an overview. Methods Mol Biol 315:13-34.

Kuhn MA, Payne WG, Kierney PC, Pu LL, Smith PD, Siegler K, Ko F, Wang X and Robson MC (2001). Cytokine manipulation of explanted Dupuytren's affected human palmar fascia. Int J Surg Investig 2:443-456.

Kuhn MA, Wang X, Payne WG, Ko F and Robson MC (2002). Tamoxifen decreases fibroblast function and downregulates TGF(beta2) in dupuytren's affected palmar fascia. J Surg Res 103:146-152.

Larson D and Jerosch-Herold C (2008). Clinical effectiveness of post-operative splinting after surgical release of Dupuytren's contracture: a systematic review. BMC Musculoskelet Disord 9:104.

Lee LC, Zhang AY, Chong AK, Pham H, Longaker MT and Chang J (2006). Expression of a novel gene, MafB, in Dupuytren's disease. J Hand Surg [Am] 31:211-218.

Levinson H, Moyer KE, Saggers GC and Ehrlich HP (2004). Calmodulin-myosin light chain kinase inhibition changes fibroblast-populated collagen lattice contraction, cell migration, focal adhesion formation, and wound contraction. Wound Repair Regen 12:505-511.

Li J, Qu X and Schmidt AM (1998). Sp1-binding elements in the promoter of RAGE are essential for amphoterin-mediated gene expression in cultured neuroblastoma cells. J Biol Chem 273:30870-30878.

Li JH, Wang W, Huang XR, Oldfield M, Schmidt AM, Cooper ME and Lan HY (2004). Advanced glycation end products induce tubular epithelial-myofibroblast transition through the RAGE-ERK1/2 MAP kinase signaling pathway. Am J Pathol 164:1389-1397.

Ling RS (1963). The Genetic Factor in Dupuytren's Disease. J Bone Joint Surg Br 45:709-718.

Liu XD, Umino T, Ertl R, Veys T, Skold CM, Takigawa K, Romberger DJ, Spurzem JR, Zhu YK, Kohyama T, Wang H and Rennard SI (2001). Persistence of TGF-beta1 induction of increased fibroblast contractility. In Vitro Cell Dev Biol Anim 37:193-201.

Loos B, Puschkin V and Horch RE (2007). 50 years experience with Dupuytren's contracture in the Erlangen University Hospital--a retrospective analysis of 2919 operated hands from 1956 to 2006. BMC Musculoskelet Disord 8:60.

Luck JV (1959). Dupuytren's contracture; a new concept of the pathogenesis correlated with surgical management. J Bone Joint Surg Am 41-A:635-664.

Lyall HA (1993). Dupuytren's disease in identical twins. J Hand Surg [Br] 18:368-370.

Maccallum P and Hueston JT (1962). The pathology of Dupuytren's contracture. Aust N Z J Surg 31:241-253.

Makita Z, Radoff S, Rayfield EJ, Yang Z, Skolnik E, Delaney V, Friedman EA, Cerami A and Vlassara H (1991). Advanced glycosylation end products in patients with diabetic nephropathy. N Engl J Med 325:836-842.

Makita Z, Vlassara H, Rayfield E, Cartwright K, Friedman E, Rodby R, Cerami A and Bucala R (1992). Hemoglobin-AGE: a circulating marker of advanced glycosylation. Science 258:651-653.

Malmstrom J, Lindberg H, Lindberg C, Bratt C, Wieslander E, Delander EL, Sarnstrand B, Burns JS, Mose-Larsen P, Fey S and Marko-Varga G (2004). Transforming growth factor-beta 1 specifically induce proteins involved in the myofibroblast contractile apparatus. Mol Cell Proteomics 3:466-477.

Marenzana M, Wilson-Jones N, Mudera V and Brown RA (2006). The origins and regulation of tissue tension: identification of collagen tension-fixation process in vitro. Exp Cell Res 312:423-433.

Mariani TJ, Arikan MC and Pierce RA (1999). Fibroblast tropoelastin and alpha-smooth-muscle actin expression are repressed by particulate-activated macrophage-derived tumor necrosis factor-alpha in experimental silicosis. Am J Respir Cell Mol Biol 21:185-192.

Martin P and Leibovich SJ (2005). Inflammatory cells during wound repair: the good, the bad and the ugly. Trends Cell Biol 15:599-607.

Mattyasovszky SG, Hofmann A, Brochhausen C, Ritz U, Kuhn S, Wollstadter J, Schulze-Koops H, Muller LP, Watzer B and Rommens PM (2010). The effect of the pro-inflammatory cytokine tumor necrosis factor-alpha on human joint capsule myofibroblasts. Arthritis Res Ther 12:R4.

McCann BG, Logan A, Belcher H, Warn A and Warn RM (1993). The presence of myofibroblasts in the dermis of patients with Dupuytren's contracture. A possible source for recurrence. J Hand Surg Br 18:656-661.

McCarthy DM (1992). The long-term results of enzymic fasciotomy. J Hand Surg Br 17:356.

McFarlane RM (1974). Patterns of the diseased fascia in the fingers in Dupuytren's contracture. Displacement of the neurovascular bundle. Plast Reconstr Surg 54:31-44.

McGrouther DA (1982). The microanatomy of Dupuytren's contracture. Hand 14:215-236.

McGrouther DA (2005). Dupuytren's Contracture. In: Green DP, Hotchkiss RN, Pederson WC and Wolfe SW, eds. Green's Operative Hand Surgery, Vol one (Philadelphia, Churchill Livingstone), pp. 159-185.

McIndoe A and Beare RL (1958). The surgical management of Dupuytren's contracture. Am J Surg 95:197-203.

Meek RM, McLellan S and Crossan JF (1999). Dupuytren's disease. A model for the mechanism of fibrosis and its modulation by steroids. J Bone Joint Surg Br 81:732-738.

Meek RM, McLellan S, Reilly J and Crossan JF (2002). The effect of steroids on Dupuytren's disease: role of programmed cell death. J Hand Surg Br 27:270-273.

Messina A and Messina J (1993). The continuous elongation treatment by the TEC device for severe Dupuytren's contracture of the fingers. Plast Reconstr Surg 92:84-90.

Mikkelsen OA, Hoyeraal HM and Sandvik L (1999). Increased mortality in Dupuytren's disease. J Hand Surg Br 24:515-518.

Moermans JP (1991). Segmental aponeurectomy in Dupuytren's disease. J Hand Surg Br 16:243-254.

Moyer KE, Banducci DR, Graham WP, 3rd and Ehrlich HP (2002). Dupuytren's disease: physiologic changes in nodule and cord fibroblasts through aging in vitro. Plast Reconstr Surg 110:187-193; discussion 194-186.

Murrell GA (1991). The role of the fibroblast in Dupuytren's contracture. Hand Clin 7:669-680; discussion 681.

Murrell GA, Francis MJ and Bromley L (1991). The collagen changes of Dupuytren's contracture. J Hand Surg Br 16:263-266.

Mykkanen OM, Gronholm M, Ronty M, Lalowski M, Salmikangas P, Suila H and Carpen O (2001). Characterization of human palladin, a microfilament-associated protein. Mol Biol Cell 12:3060-3073.

Naugle JE, Olson ER, Zhang X, Mase SE, Pilati CF, Maron MB, Folkesson HG, Horne WI, Doane KJ and Meszaros JG (2006). Type VI collagen induces cardiac myofibroblast differentiation: implications for postinfarction remodeling. Am J Physiol Heart Circ Physiol 290:H323-330.

Neeper M, Schmidt AM, Brett J, Yan SD, Wang F, Pan YC, Elliston K, Stern D and Shaw A (1992). Cloning and expression of a cell surface receptor for advanced glycosylation end products of proteins. J Biol Chem 267:14998-15004.

Niu Y, Xie T, Ge K, Lin Y and Lu S (2008). Effects of extracellular matrix glycosylation on proliferation and apoptosis of human dermal fibroblasts via the receptor for advanced glycosylated end products. Am J Dermatopathol 30:344-351.

Norotte G, Apoil A and Travers V (1988). A ten years follow-up of the results of surgery for Dupuytren's disease. A study of fifty-eight cases. Ann Chir Main 7:277-281.

Norris RA, Damon B, Mironov V, Kasyanov V, Ramamurthi A, Moreno-Rodriguez R, Trusk T, Potts JD, Goodwin RL, Davis J, Hoffman S, Wen X, Sugi Y, Kern CB, Mjaatvedt CH, Turner DK, Oka T, Conway SJ, Molkentin JD, Forgacs G and Markwald RR (2007). Periostin regulates collagen fibrillogenesis and the biomechanical properties of connective tissues. J Cell Biochem 101:695-711.

Oldfield MD, Bach LA, Forbes JM, Nikolic-Paterson D, McRobert A, Thallas V, Atkins RC, Osicka T, Jerums G and Cooper ME (2001). Advanced glycation end products cause epithelial-myofibroblast transdifferentiation via the receptor for advanced glycation end products (RAGE). J Clin Invest 108:1853-1863.

Pan D, Watson HK, Swigart C, Thomson JG, Honig SC and Narayan D (2003). Microarray gene analysis and expression profiles of Dupuytren's contracture. Ann Plast Surg 50:618-622.

Parizi M, Howard EW and Tomasek JJ (2000). Regulation of LPA-promoted myofibroblast contraction: role of Rho, myosin light chain kinase, and myosin light chain phosphatase. Exp Cell Res 254:210-220.

Pittet B, Rubbia-Brandt L, Desmouliere A, Sappino AP, Roggero P, Guerret S, Grimaud JA, Lacher R, Montandon D and Gabbiani G (1994). Effect of gamma-interferon on the clinical and biologic evolution of hypertrophic scars and Dupuytren's disease: an open pilot study. Plast Reconstr Surg 93:1224-1235.

Prockop DJ and Kivirikko KI (1995). Collagens: molecular biology, diseases, and potentials for therapy. Annu Rev Biochem 64:403-434.

Qian A, Meals RA, Rajfer J and Gonzalez-Cadavid NF (2004). Comparison of gene expression profiles between Peyronie's disease and Dupuytren's contracture. Urology 64:399-404.

Qureshi FI, Hornigold R, Spencer JD and Hall SM (2001). Langerhans cells in Dupuytren's contracture. J Hand Surg [Br] 26:362-367.

Raizman JE, Komljenovic J, Chang R, Deng C, Bedosky KM, Rattan SG, Cunnington RH, Freed DH and Dixon IM (2007). The participation of the Na+-Ca2+ exchanger in primary cardiac myofibroblast migration, contraction, and proliferation. J Cell Physiol 213:540-551.

Rajkumar VS, Howell K, Csiszar K, Denton CP, Black CM and Abraham DJ (2005). Shared expression of phenotypic markers in systemic sclerosis indicates a convergence of pericytes and fibroblasts to a myofibroblast lineage in fibrosis. Arthritis Res Ther 7:R1113-1123.

Rayan GM and Tomasek JJ (1994). Generation of contractile force by cultured Dupuytren's disease and normal palmar fibroblasts. Tissue Cell 26:747-756.

Rayan GM (1999). Clinical presentation and types of Dupuytren's disease. Hand Clin 15:87-96, vii.

Reddig PJ and Juliano RL (2005). Clinging to life: cell to matrix adhesion and cell survival. Cancer Metastasis Rev 24:425-439.

Richards HJ (1952). Dupuytren's contracture treated with vitamin E. Br Med J 1:1328.

Riikonen T, Koivisto L, Vihinen P and Heino J (1995). Transforming growth factor-beta regulates collagen gel contraction by increasing alpha 2 beta 1 integrin expression in osteogenic cells. J Biol Chem 270:376-382.

Rodrigo JJ, Niebauer JJ, Brown RL and Doyle JR (1976). Treatment of Dupuytren's contracture. Long-term results after fasciotomy and fascial excision. J Bone Joint Surg Am 58:380-387.

Rodriguez AJ, Czaplinski K, Condeelis JS and Singer RH (2008). Mechanisms and cellular roles of local protein synthesis in mammalian cells. Curr Opin Cell Biol 20:144-149.

Rombouts JJ, Noel H, Legrain Y and Munting E (1989). Prediction of recurrence in the treatment of Dupuytren's disease: evaluation of a histologic classification. J Hand Surg [Am] 14:644-652.

Ross DC (1999). Epidemiology of Dupuytren's disease. Hand Clin 15:53-62, vi.

Rudolph R and Vande Berg J (1991). The myofibroblast in Dupuytren's contracture. Hand Clin 7:683-692; discussion 693-684.

Sambrook J, Fritsch EF and Maniatis T (1989). Molecular cloning: a laboratory manual, 2nd edition edn (New York, Cold Spring Harbor Laboratory Press).

Satish L, Laframboise WA, O'Gorman DB, Johnson S, Janto B, Gan BS, Baratz ME, Hu FZ, Post JC, Ehrlich GD and Kathju S (2008). Identification of differentially expressed genes in fibroblasts derived from patients with Dupuytren's Contracture. BMC Med Genomics 1:10.

Schmidt AM, Yan SD, Brett J, Mora R, Nowygrod R and Stern D (1993). Regulation of human mononuclear phagocyte migration by cell surface-binding proteins for advanced glycation end products. J Clin Invest 91:2155-2168.

Schubert TE, Weidler C, Borisch N, Schubert C, Hofstadter F and Straub RH (2006). Dupuytren's contracture is associated with sprouting of substance P positive nerve fibres and infiltration by mast cells. Ann Rheum Dis 65:414-415.

Schurch W, Skalli O and Gabbiani G (1990). Cellular biology. In: McFaralane RM, McGrouther DA and Flint MH, eds. Dupuytren's disease: biology and treatment (London, Churchill Livingstone), pp. 31-47.

Schurch W, Seemayer T, A., Hinz B and Gabbiani G (2006). The myofibroblast. In: Mills S, E., ed. Histology for pathologists (Philadelphia, Lipincott-Williams & Wilkins Pub).

Seegenschmiedt MH, Olschewski T and Guntrum F (2001). Radiotherapy optimization in early-stage Dupuytren's contracture: first results of a randomized clinical study. Int J Radiat Oncol Biol Phys 49:785-798.

Sennwald GR (1990). Fasciectomy for treatment of Dupuytren's disease and early complications. J Hand Surg Am 15:755-761.

Serini G, Bochaton-Piallat ML, Ropraz P, Geinoz A, Borsi L, Zardi L and Gabbiani G (1998). The fibronectin domain ED-A is crucial for myofibroblastic phenotype induction by transforming growth factor-beta1. J Cell Biol 142:873-881.

Serini G and Gabbiani G (1999). Mechanisms of myofibroblast activity and phenotypic modulation. Exp Cell Res 250:273-283.

Shephard P, Martin G, Smola-Hess S, Brunner G, Krieg T and Smola H (2004). Myofibroblast differentiation is induced in keratinocyte-fibroblast co-cultures and is antagonistically regulated by endogenous transforming growth factor-beta and interleukin-1. Am J Pathol 164:2055-2066.

Shih B, Brown JJ, Armstrong DJ, Lindau T and Bayat A (2009a). Differential Gene Expression Analysis of Subcutaneous Fat, Fascia, and Skin Overlying a Dupuytren's Disease Nodule in Comparison to Control Tissue. Hand (N Y) 4:294-301.

Shih B, Wijeratne D, Armstrong DJ, Lindau T, Day P and Bayat A (2009b). Identification of biomarkers in Dupuytren's disease by comparative analysis of fibroblasts versus tissue biopsies in disease-specific phenotypes. J Hand Surg Am 34:124-136.

Shoukrey NM and Tabbara KF (1993). Ultrastructural study of a corneal keloid. Eye (Lond) 7 (Pt 3):379-387.

Shum DT and McFarlane RM (1988). Histogenesis of Dupuytren's disease: an immunohistochemical study of 30 cases. J Hand Surg [Am] 13:61-67.

Sims GP, Rowe DC, Rietdijk ST, Herbst R and Coyle AJ (2010). HMGB1 and RAGE in inflammation and cancer. Annu Rev Immunol 28:367-388.

Singer AJ and Clark RA (1999). Cutaneous wound healing. N Engl J Med 341:738-746.

Skalli O, Ropraz P, Trzeciak A, Benzonana G, Gillessen D and Gabbiani G (1986). A monoclonal antibody against alpha-smooth muscle actin: a new probe for smooth muscle differentiation. J Cell Biol 103:2787-2796.

Skalli O, Schurch W, Seemayer T, Lagace R, Montandon D, Pittet B and Gabbiani G (1989). Myofibroblasts from diverse pathologic settings are heterogeneous in their content of actin isoforms and intermediate filament proteins. Lab Invest 60:275-285.

Srivastava S, Nancarrow JD and Cort DF (1989). Dupuytren's disease in patients from the Indian sub-continent. Report of ten cases. J Hand Surg [Br] 14:32-34.

Starkweather KD, Lattuga S, Hurst LC, Badalamente MA, Guilak F, Sampson SP, Dowd A and Wisch D (1996). Collagenase in the treatment of Dupuytren's disease: an in vitro study. J Hand Surg Am 21:490-495.

Stiles PJ (1966). Ultrasonic therapy in Dupuytren's contracture. J Bone Joint Surg Br 48:452-454.

Stupack DG and Cheresh DA (2002). Get a ligand, get a life: integrins, signaling and cell survival. J Cell Sci 115:3729-3738.

Tamariz E and Grinnell F (2002). Modulation of fibroblast morphology and adhesion during collagen matrix remodeling. Mol Biol Cell 13:3915-3929.

Tanaka K, Sano K, Nakano T, Yuba K and Kinoshita M (2007). Suppression of alpha smooth muscle actin expression by IFN-gamma in established myofibroblast cell lines. J Interferon Cytokine Res 27:835-839.

Tarlton JF, Meagher P, Brown RA, McGrouther DA, Bailey AJ and Afoke A (1998). Mechanical stress in vitro induces increased expression of MMPs 2 and 9 in excised Dupuytren's disease tissue. J Hand Surg Br 23:297-302.

Tarpila E, Ghassemifar MR, Wingren S, Agren M and Franzen L (1996). Contraction of collagen lattices by cells from Dupuytren's nodules. J Hand Surg Br 21:801-805.

Terek RM, Jiranek WA, Goldberg MJ, Wolfe HJ and Alman BA (1995). The expression of platelet-derived growth-factor gene in Dupuytren contracture. J Bone Joint Surg Am 77:1-9.

Throckmorton DC, Brogden AP, Min B, Rasmussen H and Kashgarian M (1995). PDGF and TGF-beta mediate collagen production by mesangial cells exposed to advanced glycosylation end products. Kidney Int 48:111-117.

Tikellis C, Thomas MC, Harcourt BE, Coughlan MT, Pete J, Bialkowski K, Tan A, Bierhaus A, Cooper ME and Forbes JM (2008). Cardiac inflammation associated with a Western diet is mediated via activation of RAGE by AGEs. Am J Physiol Endocrinol Metab 295:E323-330.

Tomasek J and Rayan GM (1995). Correlation of alpha-smooth muscle actin expression and contraction in Dupuytren's disease fibroblasts. J Hand Surg Am 20:450-455.

Tomasek JJ, Schultz RJ and Haaksma CJ (1987). Extracellular matrix-cytoskeletal connections at the surface of the specialized contractile fibroblast (myofibroblast) in Dupuytren disease. J Bone Joint Surg Am 69:1400-1407.

Tomasek JJ and Haaksma CJ (1991). Fibronectin filaments and actin microfilaments are organized into a fibronexus in Dupuytren's diseased tissue. Anat Rec 230:175-182.

Tomasek JJ, Haaksma CJ, Eddy RJ and Vaughan MB (1992). Fibroblast contraction occurs on release of tension in attached collagen lattices: dependency on an organized actin cytoskeleton and serum. Anat Rec 232:359-368.

Tomasek JJ, Vaughan MB and Haaksma CJ (1999). Cellular structure and biology of Dupuytren's disease. Hand Clin 15:21-34.

Tomasek JJ, Gabbiani G, Hinz B, Chaponnier C and Brown RA (2002). Myofibroblasts and mechano-regulation of connective tissue remodelling. Nat Rev Mol Cell Biol 3:349-363.

Tomasek JJ, Vaughan MB, Kropp BP, Gabbiani G, Martin MD, Haaksma CJ and Hinz B (2006). Contraction of myofibroblasts in granulation tissue is dependent on Rho/Rho kinase/myosin light chain phosphatase activity. Wound Repair Regen 14:313-320.

Tomita K, van Bokhoven A, van Leenders GJ, Ruijter ET, Jansen CF, Bussemakers MJ and Schalken JA (2000). Cadherin switching in human prostate cancer progression. Cancer Res 60:3650-3654.

Tonkin MA, Burke FD and Varian JP (1984). Dupuytren's contracture: a comparative study of fasciectomy and dermofasciectomy in one hundred patients. J Hand Surg Br 9:156-162.

Townley WA, Cambrey AD, Khaw PT and Grobbelaar AO (2008). Matrix metalloproteinase inhibition reduces contraction by dupuytren fibroblasts. J Hand Surg [Am] 33:1608-1616.

Townley WA, Cambrey AD, Khaw PT and Grobbelaar AO (2009). The role of an MMP inhibitor in the regulation of mechanical tension by Dupuytren's disease fibroblasts. J Hand Surg Eur Vol 34:783-787.

Ullah AS, Dias JJ and Bhowal B (2009). Does a 'firebreak' full-thickness skin graft prevent recurrence after surgery for Dupuytren's contracture?: a prospective, randomised trial. J Bone Joint Surg Br 91:374-378.

Ulrich D, Hrynyschyn K and Pallua N (2003). Matrix metalloproteinases and tissue inhibitors of metalloproteinases in sera and tissue of patients with Dupuytren's disease. Plast Reconstr Surg 112:1279-1286.

Urban M, Feldberg L, Janssen A and Elliot D (1996). Dupuytren's disease in children. J Hand Surg Br 21:112-116.

van Beijnum JR, Buurman WA and Griffioen AW (2008). Convergence and amplification of toll-like receptor (TLR) and receptor for advanced glycation end products (RAGE) signaling pathways via high mobility group B1 (HMGB1). Angiogenesis 11:91-99.

van Rijssen AL and Werker PM (2006). Percutaneous needle fasciotomy in dupuytren's disease. J Hand Surg Br 31:498-501.

VandeBerg JS, Rudolph R, Gelberman R and Woodward MR (1982). Ultrastructural relationship of skin to nodule and cord in Dupuytren's contracture. Plast Reconstr Surg 69:835-844.

Vaughan MB, Howard EW and Tomasek JJ (2000). Transforming growth factor-beta1 promotes the morphological and functional differentiation of the myofibroblast. Exp Cell Res 257:180-189.

Verjee LS, Midwood K, Davidson D, Essex D, Sandison A and Nanchahal J (2009). Myofibroblast distribution in Dupuytren's cords: correlation with digital contracture. J Hand Surg Am 34:1785-1794.

Verjee LS, Midwood K, Davidson D, Eastwood M and Nanchahal J (2010). Post-transcriptional regulation of alpha-smooth muscle actin determines the contractile phenotype of Dupuytren's nodular cells. J Cell Physiol.

Verrecchia F, Wagner EF and Mauviel A (2002). Distinct involvement of the Jun-N-terminal kinase and NF-kappaB pathways in the repression of the human COL1A2 gene by TNF-alpha. EMBO Rep 3:1069-1074.

Vi L, Feng L, Zhu RD, Wu Y, Satish L, Gan BS and O'Gorman DB (2009). Periostin differentially induces proliferation, contraction and apoptosis of primary Dupuytren's disease and adjacent palmar fascia cells. Exp Cell Res 315:3574-3586.

Vlassara H, Brownlee M, Manogue KR, Dinarello CA and Pasagian A (1988). Cachectin/TNF and IL-1 induced by glucose-modified proteins: role in normal tissue remodeling. Science 240:1546-1548.

Vlassara H, Striker LJ, Teichberg S, Fuh H, Li YM and Steffes M (1994). Advanced glycation end products induce glomerular sclerosis and albuminuria in normal rats. Proc Natl Acad Sci U S A 91:11704-11708.

Vogel V and Sheetz M (2006). Local force and geometry sensing regulate cell functions. Nat Rev Mol Cell Biol 7:265-275.

Watt AJ, Curtin CM and Hentz VR (2010). Collagenase injection as nonsurgical treatment of dupuytren's disease: 8-year follow-up. J Hand Surg Am 35:534-539, 539 e531.

Weinzierl G, Flugel M and Geldmacher J (1993). [Lack of effectiveness of alternative non-surgical treatment procedures of Dupuytren contracture]. Chirurg 64:492-494.

Weiss SW and Goldblum JR (2008). Enzinger and Weiss's Soft Tissue Tumours, Fifth edn (St. Louis, Missouri, Mosby).

Werner S and Grose R (2003). Regulation of wound healing by growth factors and cytokines. Physiol Rev 83:835-870.

Wilbrand S, Ekbom A and Gerdin B (2000). Cancer incidence in patients treated surgically for Dupuytren's contracture. J Hand Surg Br 25:283-287.

Wong M and Mudera V (2006). Feedback inhibition of high TGF-beta1 concentrations on myofibroblast induction and contraction by Dupuytren's fibroblasts. J Hand Surg Br 31:473-483.

Yamada E, Mizutani H, Yoshida T, Isoda K and Shimizu M (1999). Tocoretinate inhibited the contraction of collagen gel matrices by human dermal fibroblasts with tenascin-C expression. J Dermatol Sci 22:45-53.

Yi S, Johnson G and Moneim M, S. (1999). Etiology of Dupuytren's Disease. Hand Clinics:43-52.

Yuba K, Sano K, Nakano T, H. M, Tanaka K, Tanaka K, E. D, Y. O, M. K and M. A (2007). Frequent establishment of long-term cultured myofibroblast cell lines derived from Dupuytren's nodules, which are implantable into nude mice. Bulletin of The Osaka Medical College 53:123-132.

Appendix

Publications

Suleman Verjee LN, Midwood K, Davidson D, Eastwood M, Nanchahal J. Post-transcriptional regulation of α-smooth muscle actin determines the contractile phenotype of Dupuytren's nodular cells. J Cell Physiol. 2010. (Epub ahead of print).

Suleman Verjee LN, Midwood K, Davidson D, Essex,D, Sandison A, Nanchahl J. Myofibroblasts distribution in Dupuytren's cords: correlation with digital contracture. J Hand Surg Am. 2009 Dec: 34(10):1785-94

Presentations

Suleman Verjee L, Kim Midwood K, Jagdeep Nanchahal J. The myofibroblast in Dupuytren's disease. Abstract accepted for presentation at The International Federation of Societies for Surgery of the Hand (IFSSH) 2010. To be presented by Professor Jagdeep Nanchahal as an invited guest speaker.

Suleman Verjee LN, Midwood K, Nanchahal J. Myofibroblasts distribution in Dupuytren's cords: correlation with digital contracture. Presented to the London Matrix Group meeting. University College London. July 2009

Suleman Verjee LN, Midwood K, Davidson D, Nanchahal J. Myofibroblasts distribution in Dupuytren's cords: correlation with digital contracture. Presented at the ASSH & BSSH combined meeting. London. March 2009

Suleman Verjee LN, Midwood K, Nanchahal J. Tenascin-C and the pathogenesis of Dupuytren's disease. Healing Foundation Research & Development council meeting. Royal College of Surgeons. London. June 2008

Regulating myofibroblasts in Dupuytren's disease. Kennedy Institute of Rheumatology seminar series – visiting Professor Robert Hotchkiss. London. October 2008

Suleman Verjee LN, Midwood K, Nanchahal J. Tenascin-C and the pathogenesis of Dupuytren's disease. Presented at the Healing Foundation clinical research fellow's seminar. University of Manchester. September 2008